



UNIVERSITY OF
BIRMINGHAM

**NOVEL TRANSFORMATIONS OF GOLD CARBENE AND VINYL
GOLD CARBENOID INTERMEDIATES FROM THE ADDITION OF
OXYGEN NUCLEOPHILES TO ALKYNES**

by

PAIGE AMANDA RIST

A thesis submitted to the University of Birmingham for the degree of
DOCTOR OF PHILOSOPHY

College of Engineering and Physical Sciences
School of Chemistry
The University of Birmingham June 2021

UNIVERSITY OF
BIRMINGHAM

University of Birmingham Research Archive

e-theses repository

This unpublished thesis/dissertation is copyright of the author and/or third parties. The intellectual property rights of the author or third parties in respect of this work are as defined by The Copyright Designs and Patents Act 1988 or as modified by any successor legislation.

Any use made of information contained in this thesis/dissertation must be in accordance with that legislation and must be properly acknowledged. Further distribution or reproduction in any format is prohibited without the permission of the copyright holder.

Abstract

The work described in this thesis focuses on novel transformations of gold carbene and vinyl gold carbenoid intermediates, generated via the addition of oxygen nucleophiles to alkynes.

Gold-catalysed oxyarylation of alkynes with benzothiophene S-oxides has been demonstrated for C-3 selective alkylation of benzothiophenes. Current methods for the direct C-3 functionalisation of benzothiophenes are limited. This thesis describes a mild and efficient method, incorporating a novel substitution pattern that allows for further elaboration of the functionalised benzothiophene products. Alongside reaction scope exploration, several studies have been performed to investigate the mechanistic pathway, catalyst degradation, and substrate inhibition. These studies provide further understanding into the reactivity of sulfoxides in gold-catalysed transformations and the stability of phosphite-based cationic gold catalysts, that may aid future research.

The second part of this thesis explores the novel transformations of sulfenylated propargyl carboxylates to investigate the influence of sulfur substitution on the gold-catalysed transformations of alkynes. This work demonstrates the first examples of sulfenylated propargyl carboxylates reacting under gold catalysis; a range of compounds have been synthesised from nucleophilic addition reactions and gold-catalysed rearrangements of these novel substrates. In addition, a stereoselective gold-catalysed oxidative rearrangement is demonstrated, to afford a range of captodative olefin products.

Acknowledgements

I would like to thank my supervisors Dr. Paul Davies and Dr. Richard Grainger for their support throughout my PhD, and for always being available to provide help and guidance.

I would also like to thank all of the Davies group members, both past and present, for their continued support and friendship over the years. I would particularly like to thank Peter, Ana and Laura, who have always been there to give me advice and join me on much needed coffee breaks.

I am grateful to the University of Birmingham and the ESPRC for their financial support.

I would also like to acknowledge all of the staff in the analytical services team for all of their hard work. I would especially like to thank Dr. Cécile Le Duff for all of her help with the spectroscopic studies and Dr. Louise Male for her X-ray crystallography work.

Lastly, I would like to thank my family and friends. I could not have done this without all of you keeping my spirits up and always making me laugh after a long day in the lab. My little nephew Ted never fails to put a smile on my face and my parents have always been my greatest supporters. I especially want to thank my boyfriend Matt for all of his encouragement over the years, and for not complaining too much when the brightness of my laptop and the tapping of keys was keeping him awake until the early hours during the making of this thesis.

List of Abbreviations

	ngstr m(s)
Ac	acetyl
app	apparent
Ar	aryl
ASAP	atmospheric solids analysis probe
Au(Pic)Cl ₂	dichloro(2-pyridinecarboxylato)gold(III)
aq.	aqueous
Bn	benzyl
Bu	butyl
Bz	benzoyl
C	celsius
Cald	calculated
COSY	correlated spectroscopy
cPr	cyclopropyl
CI	chemical ionisation
Cy	cyclohexyl
δ	chemical shift
DMAP	dimethylaminopyridine
DMSO	dimethylsulfoxide
d.r.	diastereomeric ratio
DTBP	tris(2,4-di- <i>tert</i> -butylphenyl) phosphite
EDG	electron-donating group
ee	enantiomeric excess
E ⁺	electrophile
EI	electron impact

eq	equivalent(s)
Eq.	equation
ES	electron spray
Et	ethyl
EWG	electron-withdrawing group
Exp	experiment
g	grams
h	hour(s)
HMBC	heteronuclear multiple bond correlation
HOMO	highest occupied molecular orbital
HRMS	high resolution mass spectrometry
HSQC	heteronuclear single quantum coherence
Hz	hertz
<i>i</i> (italics)	iso
IPr	1,3-bis(2,6-diisopropylphenyl)imidazol-2-ylidene
IR	infrared
<i>J</i>	<i>coupling constant</i>
JohnPhos	2-(di- <i>tert</i> -butylphosphino)biphenyl
L	litre
LUMO	lowest unoccupied molecular orbital
HMDS	hexamethyldisilazide
m	metre(s)
<i>m</i>	meta
<i>m</i> CPBA	<i>meta</i> -chloroperbenzoic acid
Me	methyl
Mes	mesityl
M	molar

mol	moles
mmol	millimoles
mp	melting point
min	minute(s)
MS	mass spectrometry
<i>m/z</i>	mass/charge
n	normal
NMR	nuclear magnetic resonance
Nu	nucleophile
<i>o</i>	<i>ortho</i>
<i>p</i>	<i>para</i>
Pe	pentyl
Ph	phenyl
Pic	picolinate
Piv	pivaloyl
ppm	parts per million
Pr	propyl
Py	pyridine
q	quartet
rt	room temperature
s	singlet
sat.	saturated
SM	starting material
SPhos	2-Dicyclohexylphosphino-2',6'-dimethoxybiphenyl
t	triplet
t (<i>italics</i>)	tertiary
TFA	trifluoroacetic acid

TFAA	trifluoroacetic anhydride
THF	tetrahydrofuran
TLC	thin layer chromatography
TMS	trimethylsilyl
Tol	tolyl
TOF	time of flight
Tf	trifluoromethanesulfonyl
Ts	4-methylbenzenesulfonyl
T.S [‡]	transition state
v	volume
ν	wavenumber
wrt	with respect to
XPhos	2-dicyclohexylphosphino-2',4',6'-triisopropylbiphenyl

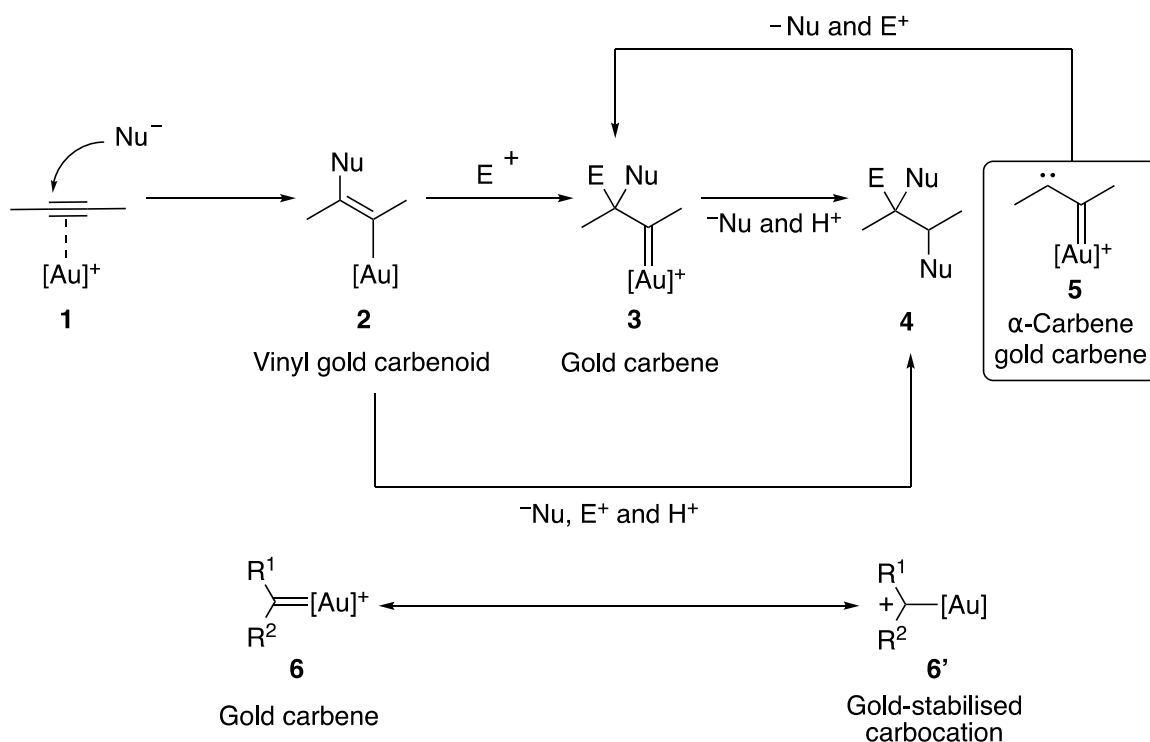
Contents

Chapter 1: Introduction into Homogeneous Gold Catalysis	10
Chapter 2: Gold-Catalysed Oxyarylation of Alkynes with Benzothiophene S-oxides	16
2.1 Introduction	17
2.1.1 Alkyne Oxyarylation with Sulfoxides	17
2.1.2 [3,3]-Sigmatropic Rearrangement vs Gold Carbene Formation	19
2.1.3 Acid-Catalysed Alkyne Oxyarylation with Sulfoxides	26
2.1.4 Methods for Benzothiophene Functionalisation	28
2.2 Results and Discussion	32
2.2.1 Aims and Objectives	32
2.2.2 Proposed Mechanism for Alkyne Oxyarylation with Benzothiophene S-oxides	33
2.2.3 Optimisation of the Gold-Catalysed Oxyarylation Reaction	34
2.2.4 Starting Material Preparation	38
2.2.5 Scope of the Gold-Catalysed Oxyarylation Reaction	40
2.2.6 Determining Regioselectivity	47
2.2.6.1 C-3 Regioisomer Determination	47
2.2.6.2 C-7 Regioisomer Determination	48
2.2.7 Rationale for Observed Regioselectivities in Oxyarylation Reactions	50
2.3 Mechanistic Studies	52
2.3.1 Evidence for [3,3]-Sigmatropic Rearrangement	52
2.3.2 Effect of Sulfoxides on the Rate of Oxyarylation	54
2.3.3 Same Excess Experiment	64
2.3.4 Product Inhibition Study	70
2.3.5 Catalyst Spectroscopic Studies	71
2.4 Conclusion and Outlook	76
Chapter 3: Gold-Catalysed Rearrangements of Sulfenylated Propargyl Carboxylates	78
3.1 Introduction	79
3.1.1 Gold-Catalysed Rearrangements of Propargyl Carboxylates	79
3.1.2 Intramolecular Cyclisation Reactions of Propargyl Carboxylates	82
3.1.2.1 Cycloisomerisation of Enyne Carboxylates	82
3.1.2.2 Nazarov Cyclisation Reactions of Enyne Carboxylates	84
3.1.2.3 Intramolecular Cyclisation Reactions: The Use of Nucleophilic Substituents	87
3.1.3 Intermolecular Gold-Catalysed Reactions of Propargyl Carboxylates with Nucleophiles	89
3.1.4 Gold-Catalysed Oxidation of Propargyl Carboxylates	93

3.1.5 Gold-Catalysed Rearrangements of Propargyl Carboxylates in the Absence of Nucleophiles	95
3.1.6 Conclusion	99
3.2 Aims and Objectives	100
3.3 Synthesis of Sulfenylated Propargyl Carboxylates	103
3.4 Gold-Catalysed Nucleophilic Addition Reactions with Sulfenylated Propargyl Carboxylates	117
3.4.1 Initial Studies into the Gold Catalysis of Sulfenylated Propargyl Carboxylates	117
3.4.2 Variation of Sulfur Substituents	125
3.4.3 Variation of Substituents at the Propargylic Position	127
3.5 Gold-Catalysed Rearrangements of Sulfenylated Propargyl Carboxylates	135
3.6 Gold-Catalysed Oxidation Reactions	139
3.6.1 Initial Studies into Oxidative Gold Catalysis	142
3.6.2 Optimisation Studies	143
3.6.3 Scope of the Gold-Catalysed Oxidation Reaction	148
3.6.3.1 Mechanism and Stereoselectivity	152
3.7 Conclusion and Outlook	157
Chapter 4: Experimental Section	160
4.1 General Experimental	161
4.2 Alkynes	163
4.3 Gold Complexes	168
4.4 Benzothiophene S-oxides	170
4.5 C-3 Substituted Benzothiophenes	173
4.6 Alkynyl Thioethers and Thiosulfonates	197
4.7 Pyridine N-Oxides	202
4.8 Propargyl Alcohols	205
4.9 Sulfenylated Propargyl Alcohols	210
4.10 Propargyl Carboxylates	222
4.11 Products from Propargyl Carboxylate Catalysis	235
5 Appendix	259
5.1 NOESY Spectra for Stereochemical Assignment of Captodative Olefins	259
5.2 Crystal Data and Structure Refinement for 412	266
6 References	270

Chapter 1: Introduction into Homogeneous Gold Catalysis

Vinyl gold carbenoids and gold carbenes are often proposed as key intermediates during the many transformations available to alkynes under gold catalysis. The generation of such intermediates from benign alkynes, without the need for hazardous and explosive diazo compounds, is an advantageous and diverse ability of gold catalysts.¹ Nucleophilic addition to the gold-activated alkyne generates a vinyl gold carbenoid intermediate **2**, which can react further with an electrophile to generate a gold carbene intermediate **3** (Scheme 1). The formation of the gold carbene **3** is equivalent to the addition of a nucleophile and an electrophile to a hypothetical α -carbene gold carbene **5** (Scheme 1). Depicting the formal process in this manner emphasises the synthetic potential of the transformation, with the strategy allowing the exploration of reactive intermediates that are otherwise difficult to obtain.



Scheme 1. Generation of gold carbene and vinyl gold carbenoid intermediates from alkynes

The gold carbene and vinyl gold carbenoid intermediates can be further exploited in several ways. The same processes can be drawn from the vinyl gold carbenoid and the gold carbene intermediates (Scheme 1, **2 - 4** vs **3 - 4**). However, in practice, each of these species may offer different reactive pathways to form different products. The gold carbene intermediate can also be drawn as a gold-stabilised carbocation, and the nature of this species is influenced by the substituents and the gold ligand (Scheme 1, **6** and **6'**).² For simplicity, in this thesis the species will be depicted as the gold carbene. Understanding the influence of the gold-catalyst and the substrate on reactivity is key for pathway control.

Fürstner isolated gold carbenes **7** and **8** and found that much of the carbene stabilisation comes from the organic framework, rather than the gold, when the organic framework harbours methoxy groups (Figure 1).³ The C-C bond length between the carbene and one of the aryl groups of **8** was markedly contracted compared to the other aryl group. In the solid state, the aryl group with the contracted C-C bond was nearly co-planar with the carbene centre. On the other hand, the Au-C bond does not significantly change compared to gold carbene **7**, which contains an adjacent methoxy group. These results indicate that most of the electronic stabilisation at the carbene centre is from the aryl group rather than gold. However, the methoxy groups are not innocent and donation of electron density from the organic framework may leave little opportunity for gold to stabilise the carbene centre. On the other hand, Straub demonstrated that gold can in fact stabilise the carbene centre, with the isolated gold carbene **9** exhibiting a contracted Au-C bond compared to the methoxy-substituted carbenes **7** and **8**.⁴

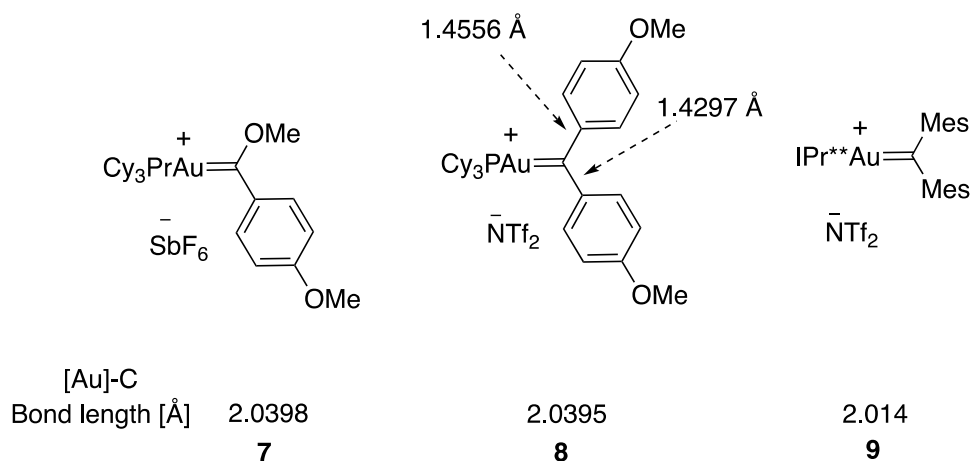
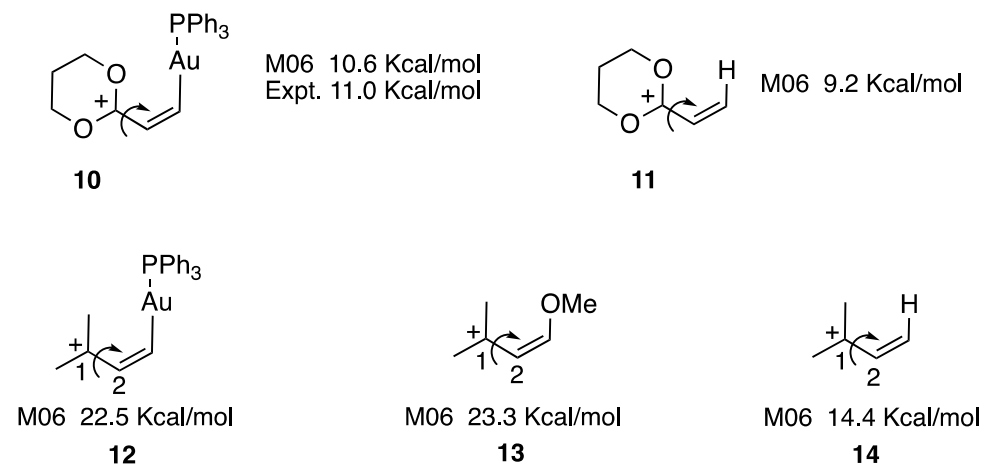


Figure 1. Bond lengths of isolated gold carbenes by Fürstner and Straub

Toste and co-workers found that the difference in the calculated rotational barriers of allyl cation **11** and gold-stabilised allyl cation **10** was negligible, indicating that there was no significant gold stabilisation of the allyl cation (Figure 2). However, it was also found that gold stabilisation of allyl cations was higher in the absence of stabilising heteroatoms vicinal to the carbocation (Figure 2, **10** vs **12**). For the gold-stabilised allyl cation **12**, the barrier of rotation for C1-C2 was calculated to be 22.5 kcal/mol, which is 8.1 kcal/mol higher than the allyl cation **14**. It was also discovered that in the case of **12**, the gold stabilises the allyl cation to a similar degree as a methoxy group (Figure 2, **12** vs **13**). In the same computational study, Toste's group show that π -donating ligands, such as a chloride, increase Au to carbene π back-bonding, resulting in shorter Au-C bonds whilst longer Au-C bond lengths were calculated for π -acidic ligands such as phosphites (Figure 2, **15** to **18**).⁵ Overall, these studies highlight that the nature of gold-bound intermediates is highly influenced by the organic framework and the ancillary ligands. It is important to understand how the organic framework and ligands can affect the nature of these intermediates in order to tune catalytic systems and influence reactive pathways. These factors will be discussed over the course of chapters 2 and 3.

Toste - Calculated rotational barriers of gold carbenoids



Toste - Calculated bond lengths of gold carbenoids

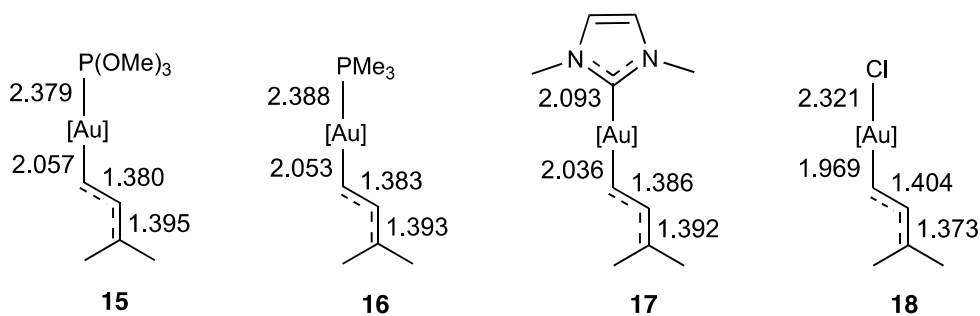
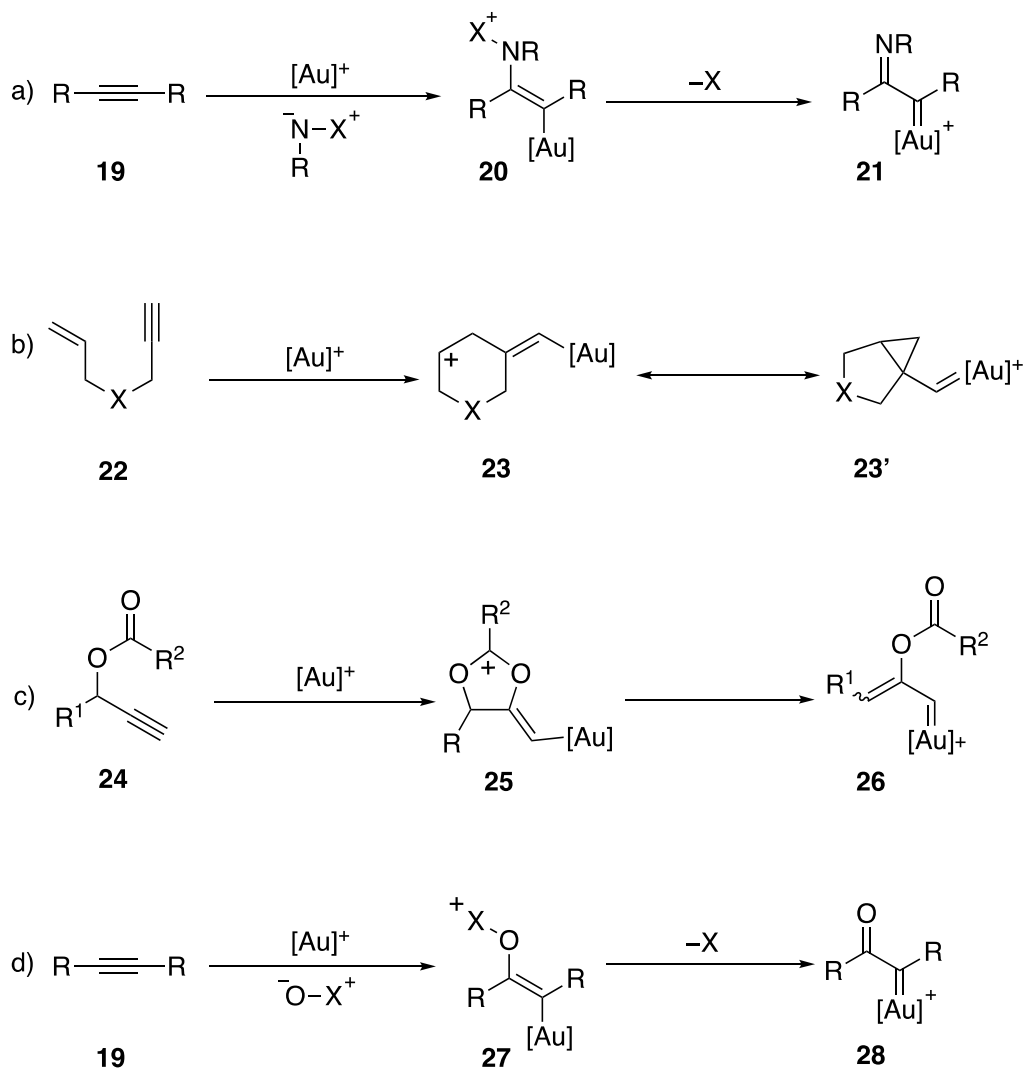


Figure 2. Ligand- and substituent-effects on the nature of gold carbenes and gold-stabilised allyl cations

There are many routes used to generate gold carbene and vinyl gold carbenoid intermediates from alkynes. The most common routes are shown in Scheme 2: a) addition of nitrenoids to alkynes, b) enyne cycloisomerisation, c) rearrangement of propargyl carboxylates and d) alkyne oxidation. This thesis will discuss the generation and subsequent reactivity of such intermediates through alkyne oxidation chemistry and the rearrangement of propargyl carboxylates (Scheme 2, c and d). There are also other reaction manifolds available to alkynes and propargyl carboxylates under gold catalysis that do not proceed through gold carbene intermediates, and these are also

explored in the following chapters. Gold-catalysed alkyne oxyarylation will be discussed in Chapter 2 as a method for C-3 selective benzothiophene functionalisation. Chapter 3 will explore the effect of sulfur substitution on the reactivity of propargyl carboxylates under gold catalysis, alongside the generation of novel compounds from nucleophilic addition and oxidation of the gold-bound intermediates.



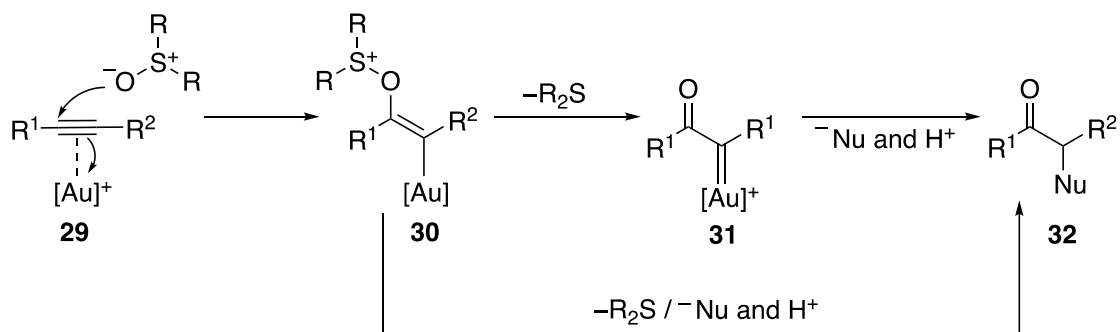
Scheme 2. Methods for gold carbene and vinyl gold carbenoid formation from alkynes

**Chapter 2: Gold-Catalysed
Oxyarylation of Alkynes with
Benzothiophene S-oxides**

2.1 Introduction

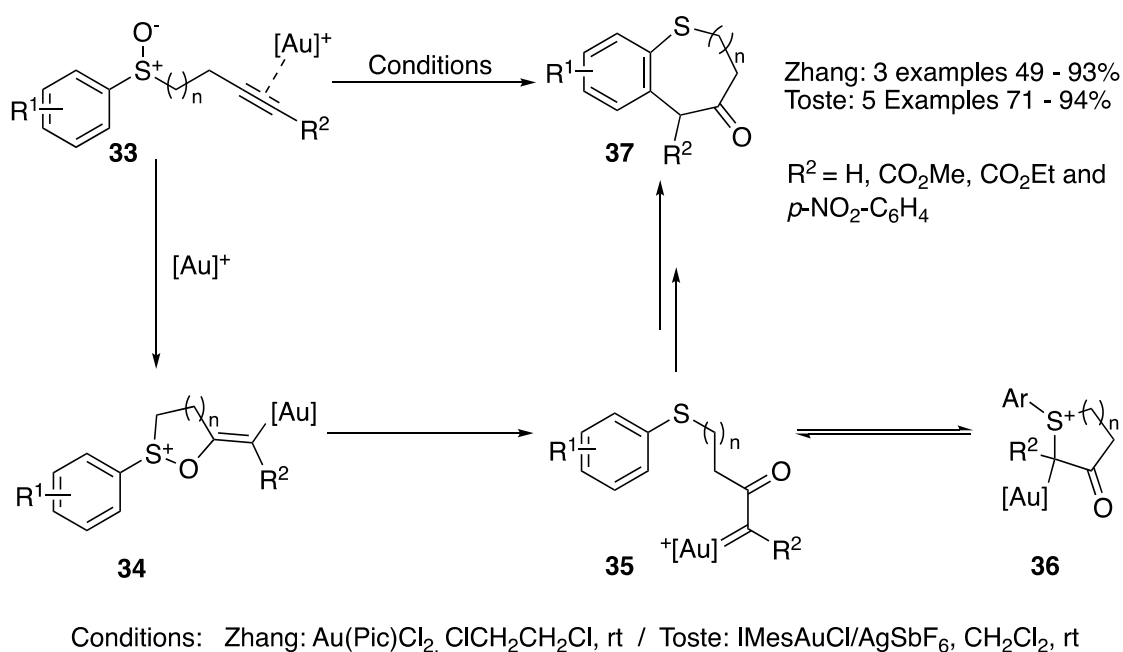
2.1.1 Alkyne Oxyarylation with Sulfoxides

The most common route towards α -oxo carbenes is through metal insertion to diazo carbonyl compounds. However, the preparation of highly energetic and potentially explosive diazo carbonyl compounds often requires the use of hazardous precursors. A common route towards diazo carbonyls involves the acylation of diazomethane which is highly toxic and explosive.⁶ An alternative gold-catalysed oxidation method provides a safe and effective way to generate the same useful intermediate through benign alkyne starting materials. Sulfoxides were proposed by the groups of Toste and Zhang as suitable oxidants for this process, with 'R₂S' expected to behave as an efficient leaving group after initial oxidation (Scheme 3).⁷ The overall gold-catalysed transformation involves nucleophilic addition of the oxidant to the gold-activated alkyne **29** to generate a vinyl gold carbenoid intermediate **30** (Scheme 3). Subsequent elimination of the tethered sulfide leaving group (nucleofuge) generates the reactive α -oxo gold carbene intermediate **31**. The vinyl gold carbenoid **30** and α -oxo gold carbene **31** can be manipulated further by trapping reactive nucleophiles or through insertion/migration pathways.



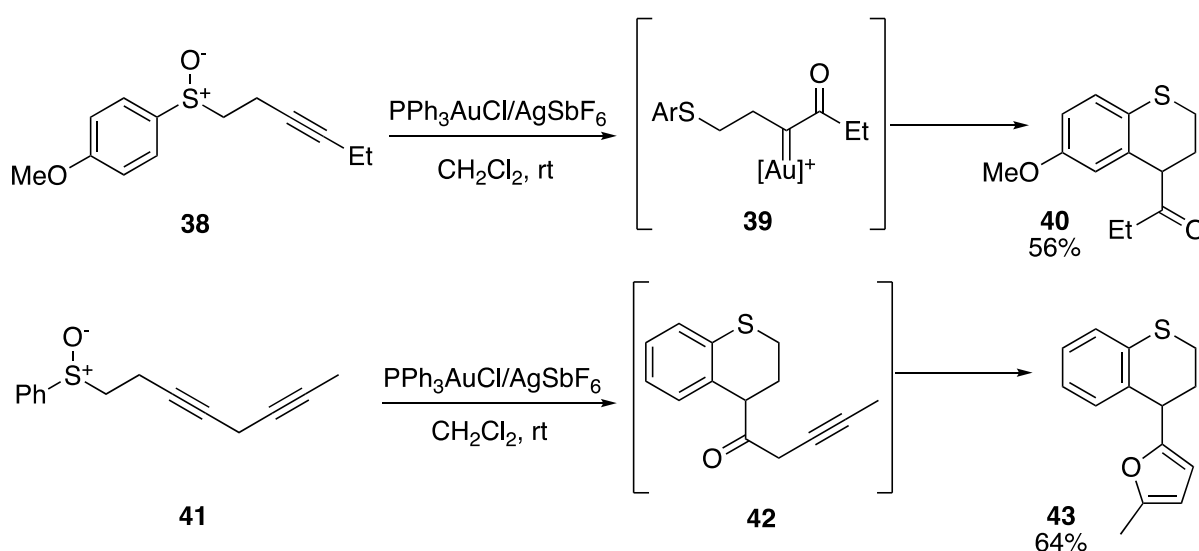
Scheme 3. Strategy for the generation of α -oxo gold carbenes from sulfoxides

In 2007, both Zhang and Toste separately reported the intramolecular oxyarylation of alkynes to yield products that are consistent with the formation of an α -oxo gold carbene intermediate (Scheme 4).⁷ It was later discovered that the transformation in fact by-passes the formation of a gold carbene intermediate; this will be discussed later in this section. The rearrangement of alkynyl sulfoxide **33** is initiated by gold electrophilic-activation of the alkyne, followed by a regioselective 5-exo-dig cyclisation (for $n=1$) of the tethered sulfoxide onto the alkyne. Loss of the sulfide leaving group from vinyl gold carbenoid **34** is proposed, to generate the α -oxo gold carbene **35** which is subsequently trapped by the nucleophilic phenyl substituent. Rearomatisation and protodeauration result in the final benzothiepinone **37**. In the publication by Zhang, it is suggested that the gold-coordinated sulfur ylide **36** may be formed reversibly during the transformation.



Scheme 4. Generation of benzothiepinones from gold-catalysed intramolecular oxyarylation of alkynyl sulfoxides

Toste found that the presence of an alkyl substituent on the alkyne resulted in the formation of benzothiopeine **40** through a gold-catalysed 6-*endo*-dig cyclisation mechanism. This discovery enabled the formation of furan-substituted benzothiopeine **43** through gold-catalysed oxyarylation followed by cycloisomerisation (Scheme 5).



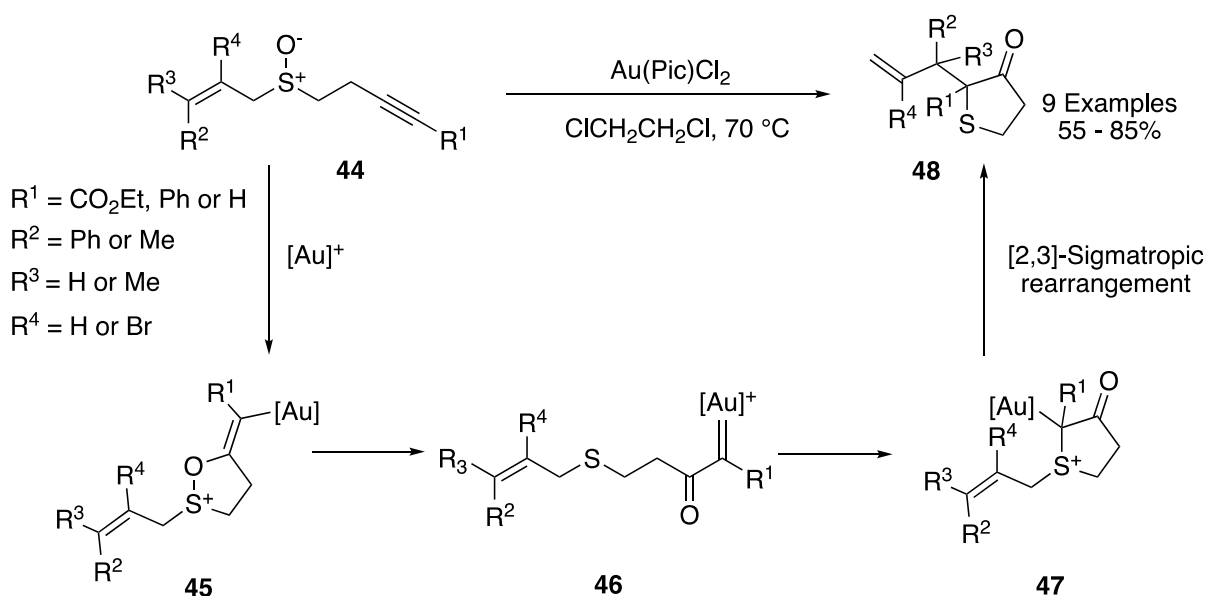
Scheme 5. Generation of benzothiopeines from gold-catalysed intramolecular oxyarylation of alkyl-substituted alkynes with sulfoxides

Following this work, several gold-catalysed C-C bond forming rearrangements between sulfoxides and alkynes have been demonstrated. The generation of α -oxo gold carbenes has also been significantly expanded to other types of oxidants. These findings have enabled a plethora of novel transformations to be developed; Friedel-Crafts addition, cyclopropanation, 1,2-migration and nucleophilic addition reactions are amongst the range of reactions available to α -oxo gold carbenes.⁸

2.1.2 [3,3]-Sigmatropic Rearrangement vs Gold Carbene Formation

Following the initial discoveries by Zhang and Toste, Davies employed this strategy for the in situ generation and subsequent rearrangement of sulfur ylides from alkynyl sulfoxides (Scheme 6).⁹ In this work, alkynyl sulfoxides **44** with an allyl substituent were

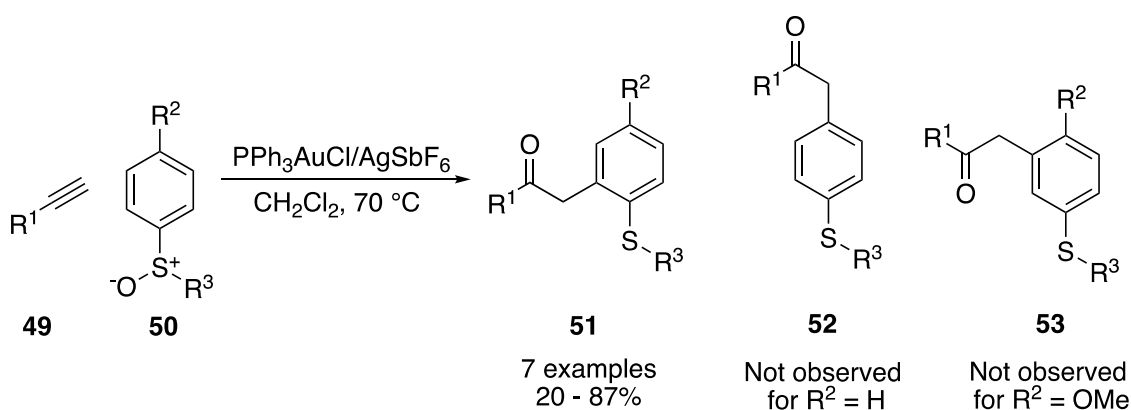
subjected to gold catalysis and yielded a range of sulfur heterocycles. The proposed mechanism follows that described by Toste and Zhang, where intramolecular oxidation of the alkyne by the sulfoxide results in the gold carbene intermediate **46** via the vinyl gold carbenoid **45**. The gold carbene is then trapped by the sulfur to generate a gold-coordinated sulfur ylide **47**, which subsequently undergoes a [2,3]-sigmatropic rearrangement to provide the final sulfur heterocycle **48**. This work supports Zhang's hypothesis that sulfur ylides are potential intermediates during the intramolecular oxidation reactions of alkynyl sulfoxides. When commenting on this work, Zhang stated that the only viable mechanism for the formation of **48** appears to be via an α -oxo gold carbene. Further work by the Davies group has since supported that sulfur ylides are formed simultaneously alongside C-O bond cleavage or promptly afterwards, rather than via a distinct gold carbene intermediate.¹⁰



Scheme 6. In situ generation of gold-coordinated sulfur ylides and subsequent [2,3]-sigmatropic rearrangement

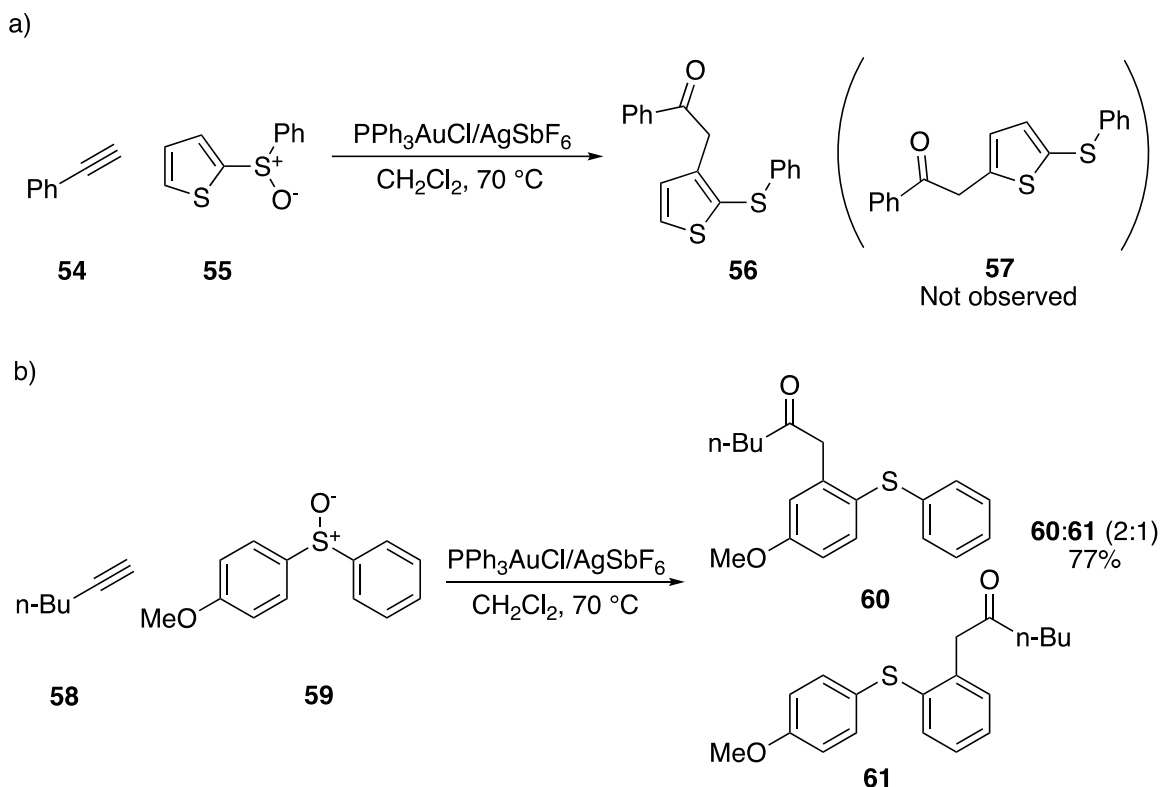
Ujaque and Asensio sought to develop an intermolecular method for alkyne oxyarylation with sulfoxides.¹¹ To this end, terminal alkynes **49** were reacted with

aromatic sulfoxides **50** under gold catalysis for the acylmethylation of the sulfoxide aryl-substituent (Scheme 7). Intriguingly, controlling the regioselectivity of acylmethylation on the aromatic ring was not problematic. According to the proposed mechanism, a mixture of regioisomers should be observed from intermolecular attack of the aryl ring to the gold carbene intermediate (Scheme 7, **51** - **53**). In contrast to what was expected, regioisomer **51** was the sole product observed.



Scheme 7. Unexpected regioselectivity from intermolecular oxyarylation of alkynes with aromatic sulfoxides

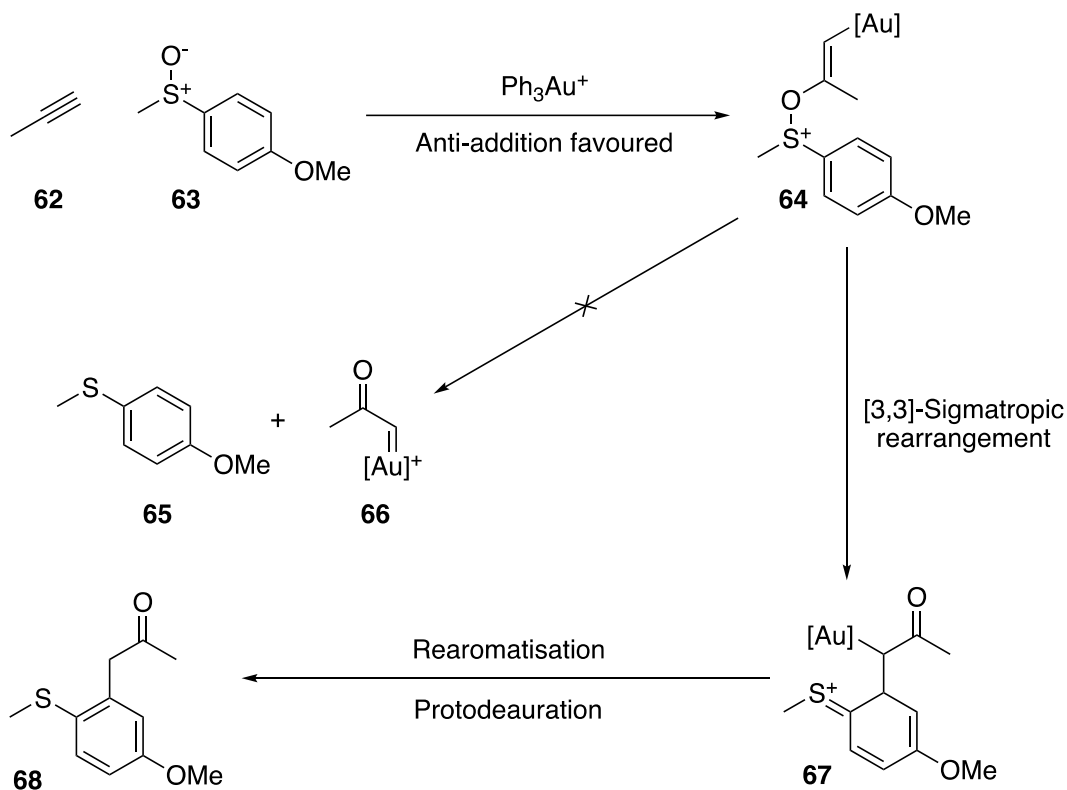
To further probe this unexpected result, asymmetric aromatic sulfoxides **55** and **59** were submitted to the reaction conditions (Scheme 8). In both cases, only products were observed from acylmethylation at the aryl positions adjacent to the sulfur substituent (Scheme 8a and 8b). With sulfoxide **55**, the formation of regioisomer **57** would also be expected according to the currently accepted mechanism of intermolecular nucleophilic capture of a gold carbene intermediate (Scheme 8a). For asymmetric sulfoxide **59**, acylmethylation of the phenyl substituent was also observed, to provide **61** alongside **60**, despite the increased nucleophilicity of the methoxy-substituted phenyl ring. In addition, no acylmethylation at the carbon adjacent to the methoxy directing-group was observed (Scheme 8b).



Scheme 8. Gold-catalysed alkyne oxyarylation with asymmetric aromatic sulfoxides

DFT calculations with propyne **62** and sulfoxide **63** were performed to clarify the unexpected regioselectivity observed during the investigations (Scheme 9). Attempts to computationally identify the α -oxo gold carbene **66** were unsuccessful, with all attempts evolving to the vinyl gold carbenoid intermediate **64** or providing irrational structures. Firstly, DFT calculations show that anti-addition of the sulfoxide and the gold catalyst across the alkyne was favoured, generating the *E* vinyl gold carbenoid intermediate **64**. From here, DFT calculations support an intramolecular [3,3]-sigmatropic rearrangement process for the regio-determining C-C bond forming step. The final product is formed following rearomatisation and protodeauration of intermediate **67**. A [3,3]-sigmatropic rearrangement mechanism is consistent with the observed regioselectivity, with acylmethylation occurring solely at the aryl position

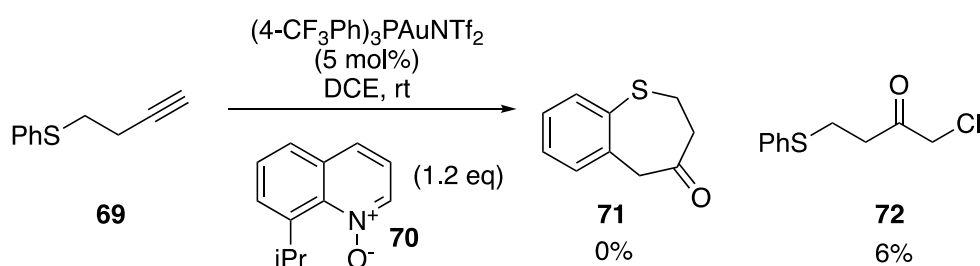
adjacent to the sulfur substituent. These results contrast the mechanism proposed by Zhang and Toste for the analogous intramolecular oxyarylation of alkynes.



Scheme 9. Proposed mechanism for the intermolecular oxyarylation of alkynes with aromatic sulfoxides supported by DFT calculations

The discovery of a [3,3]-sigmatropic rearrangement mechanism led Zhang to revisit the mechanistic proposal for the original work on intramolecular oxyarylation of alkynyl sulfoxides.¹² In addition, Zhang suggested that the facile preparation of benzothiepinones (see Scheme 4, **37**) via an intermediate gold carbene was dubious with the formation of sulfur ylides having been demonstrated in analogous work by Davies (see Scheme 6); the formation of a sulfur ylide may be expected to impede the cyclisation process. Zhang used pyridine and quinoline *N*-oxides to probe the reaction mechanism. Since the initial discovery with sulfoxides, Zhang, along with other groups including the Davies group, discovered such *N*-oxides were also suitable for gold-

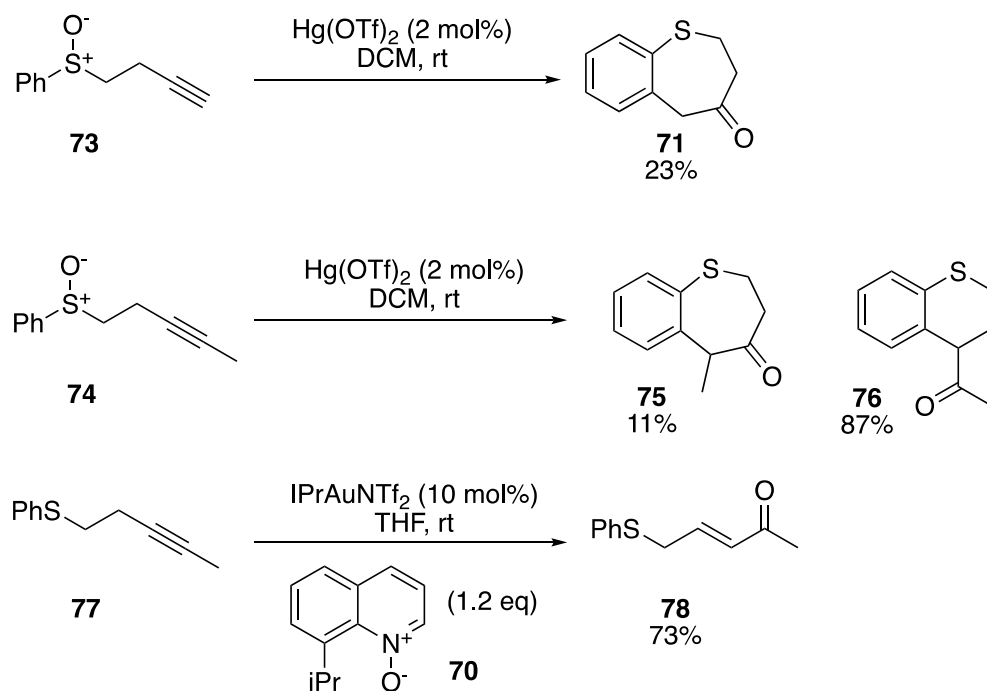
catalysed alkyne oxidation and it is strongly implied that gold carbenes are formed during these processes.¹³ Therefore, an intermolecular oxidation protocol was tested with alkynyl thioether **69** and oxidant **70**, however benzothiepinone **71** was not observed (Scheme 10). Instead, α -chloroketone **72** was formed from chloride abstraction of the solvent. Zhang states that chloride abstraction is consistent with the formation of a highly electrophilic gold carbene intermediate. Chloride abstraction of the solvent from an intermediate carbene was also observed by the Davies group during the formation of sulfur heterocycles **48** (see Scheme 6) when a PtCl₂ catalyst was used instead of Au(Pic)Cl₂. The absence of the benzothiepinone **71** during this intermolecular oxidation protocol opposes the formation of a gold carbene intermediate during the intramolecular oxyarylation of alkynyl sulfoxides.



Scheme 10. Attempted intermolecular oxidation protocol for oxyarylation of an alkynyl thioether via an intermediate gold carbene

If a [3,3]-sigmatropic rearrangement mechanism was operative, other metals should also catalyse the transformation if they can promote the initial cyclisation step. Hg(OTf)₂ does in fact catalyse the reaction with both terminal and internal alkynyl sulfoxides to form the benzothiepinone (Scheme 11, **71** and **75**) and benzothiopine (Scheme 11, **76**) products. Conversely, when internal alkynyl thioether **77** was reacted with quinoline *N*-oxide **70**, enone **78** was formed as the major product from 1,2 C-H migration at the gold carbene intermediate. The benzothiopine **76** was not observed

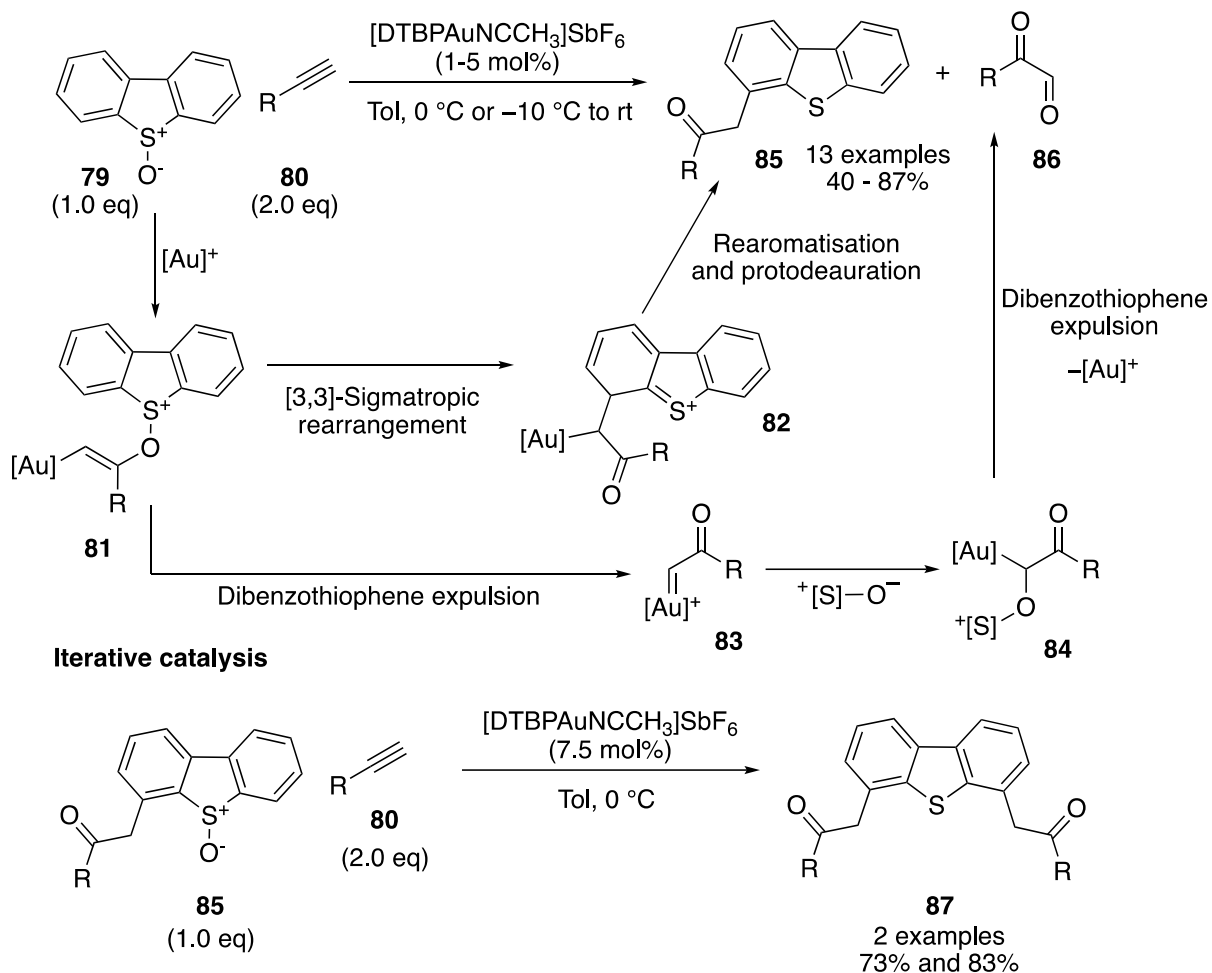
from the intermolecular oxidation protocol, corroborating the postulated [3,3]-sigmatropic rearrangement mechanistic pathway. To solidify experimental evidence, DFT studies were performed which calculated a higher energy barrier for Friedel-Crafts-type cyclisation at an intermediate gold carbene, whilst a [3,3]-sigmatropic rearrangement pathway was favoured.



Scheme 11. Intramolecular oxyarylation of alkynyl sulfoxides with Hg(OTf)_2 and an attempted intermolecular oxidation protocol for alkynyl thioether oxyarylation

Davies and Grainger described an intermolecular alkyne oxyarylation strategy for regioselective functionalisation of dibenzothiophenes (Scheme 12).¹⁴ Dibenzothiophene S-oxide **79** was reacted with terminal alkynes **80** under gold catalysis to provide the C-4-substituted dibenzothiophenes **85** exclusively. Iterative catalysis was also possible to form the di-substituted dibenzothiophenes **87**. During optimisation studies, it was realised that intermolecular interception of the vinyl gold carbenoid **81** or gold carbene **83** by a second sulfoxide was also possible to yield the over-oxidised alkyne **86** and the free dibenzothiophene. Undesirable pathways were

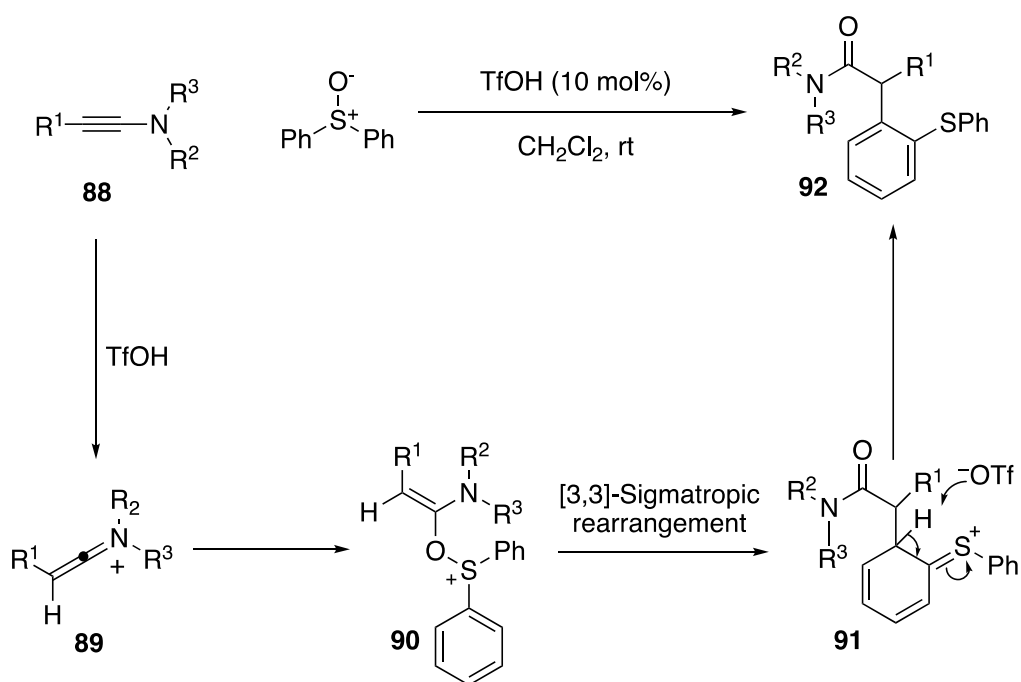
avoided by using an electron-deficient catalyst to discourage formation of the gold carbene; a gold carbene intermediate was less likely to undergo the desired transformation according to the previous mechanistic studies by Asensio and Zhang.



2.1.3 Acid-Catalysed Alkyne Oxyarylation with Sulfoxides

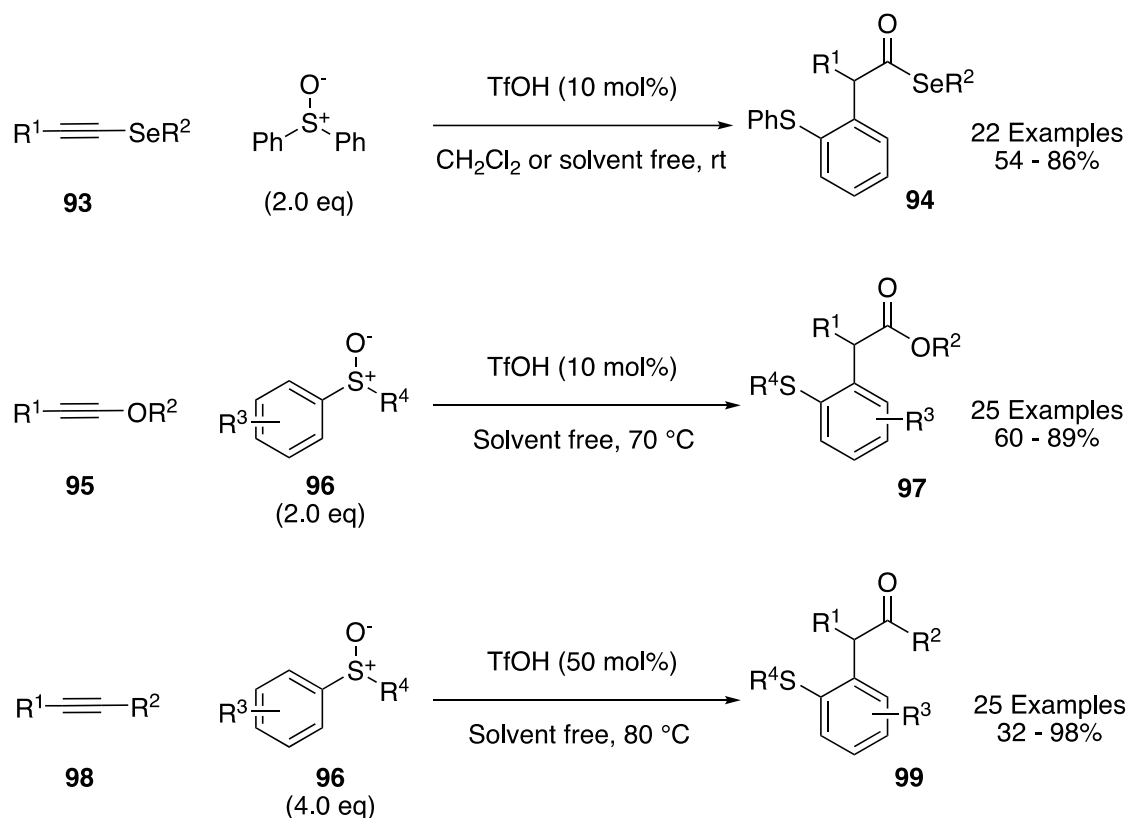
Inspired by previous work into gold-catalysed oxyarylation, Maulide developed a complimentary acid-catalysed process between alkynes and sulfoxides. Initial work involved the oxyarylation of ynamides **88** with triflic acid (Scheme 13).¹⁵ The proposed mechanism follows a similar pathway to that of the gold-catalysed process. The alkyne is activated by the acid and the nitrogen allows for regioselective protonation of the

alkyne by stabilising the positive charge through the keteniminium intermediate **89**. This results in regioselective addition of the oxidant to provide intermediate **90** which undergoes [3,3]-sigmatropic rearrangement to provide intermediate **91**. Rearomatisation of **91** provides the final acylmethylated product **92**.



Scheme 13. Acid-catalysed intermolecular oxyarylation of ynamides with sulfoxides

Maulide has also utilised acid-catalysis for the oxyarylation of selenoalkynes **93**, ynol ethers **95** and alkynes **98** (Scheme 14).¹⁶ For unactivated alkynes **98**, higher equivalents of the sulfoxide **96** and triflic acid were required for the transformation to proceed. The cationic intermediate formed after acid-activation of the triple bond is less stable than the analogous vinyl gold carbenoid. This intermediate is therefore prone to oligomerisation or interception from other nucleophiles such as water or triflate and performing the reaction neat aided oxyarylation. Higher equivalents of the sulfoxide were used to outcompete unproductive pathways. Competition studies confirmed that electron rich alkynes that were able to stabilise cationic intermediates performed better in the reaction, as did electron-rich sulfoxides.



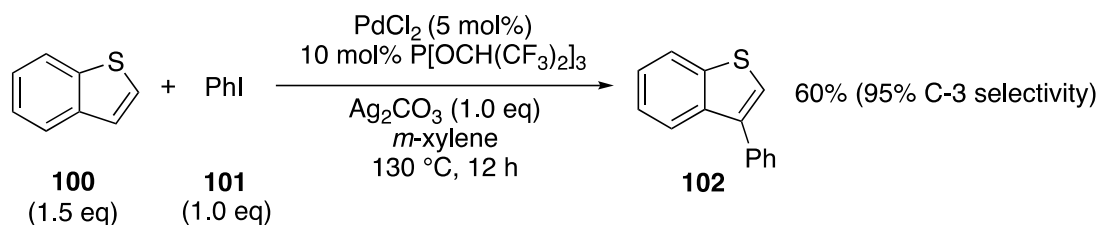
Scheme 14. Acid-catalysed intermolecular oxyarylation of selenoalkynes, ynol ethers and alkynes with sulfoxides

2.1.4 Methods for Benzothiophene Functionalisation

The research section of this chapter will discuss the use of gold-catalysed oxyarylation as a method for C-3 selective benzothiophene functionalisation. Benzothiophenes display unique photophysical and electronic properties and are prevalent in many pharmacologically active compounds.¹⁷ Direct functionalisation of benzothiophenes provides a synthetically appealing method for the preparation of differently-substituted species, however the current methods available for direct functionalisation of benzothiophenes are limited.

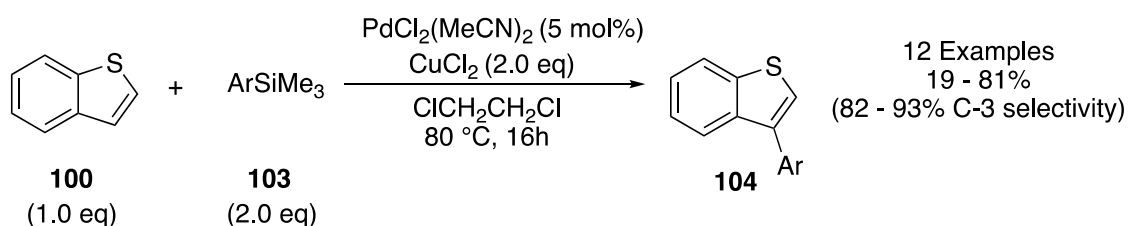
The recent surge in Pd-catalysed C-H functionalisation methodology has enabled the direct substitution of heteroaromatics without the need for directing groups or pre-

functionalised substrates. The metal-catalysed C-H functionalisation of benzothiophenes at the C-2 position is well established, whilst C-H functionalisation at the C-3 position is still relatively underdeveloped.¹⁸ Over the past decade, efforts have been made by various groups to develop methods for C-3 selective Pd-catalysed C-H functionalisation of benzothiophenes. Initial work, performed by Itami and co-workers, demonstrated the C-3 selective Pd-catalysed C-H functionalisation of thiophenes with aryl iodides. One example of C-3 selective benzothiophene arylation was also reported using this method (Scheme 15).¹⁹ This work initiated the exploration of Pd-catalysed C-3 benzothiophene functionalisation by various other groups.



Scheme 15. Pd-catalysed C-3 arylation of benzothiophene with phenyl iodide

In 2012, Funaki and Sato developed a library of C-3 arylated benzothiophenes from Pd-catalysed C-H functionalisation (Scheme 16).²⁰ This method involved aryl silane coupling partners **103** and copper chloride was used to regenerate the Pd(II) catalyst.

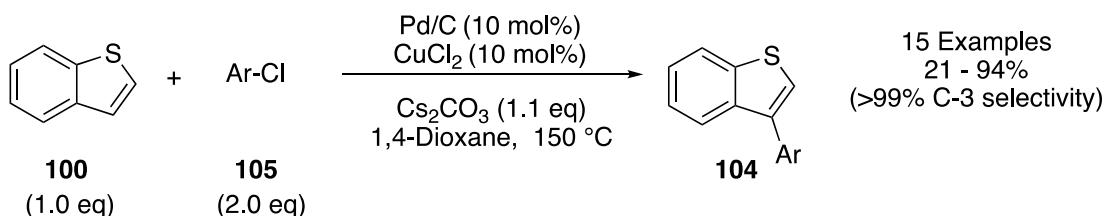


Scheme 16. Pd-catalysed C-3 arylation of benzothiophenes with aryl silanes

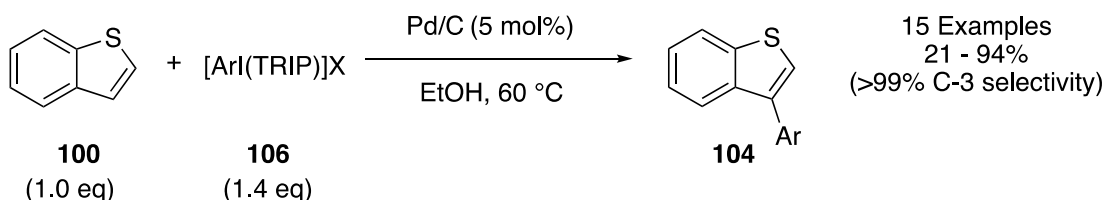
In 2014, Glorius reported selective C-3 benzothiophene functionalisation with aryl chlorides **105** under heterogeneous catalysis with Pd/C and a CuCl₂ co-catalyst (Scheme 17). Whilst regioselectivity was high, the reaction required a very high

temperature of 150 °C.²¹ Shortly after, Glorius reported an improved method under heterogeneous Pd/C catalysis with aryl iodonium salts **106** which could be performed at a much lower temperature of 60 °C with a lower catalyst loading (Scheme 17).²²

Glorius 2013:

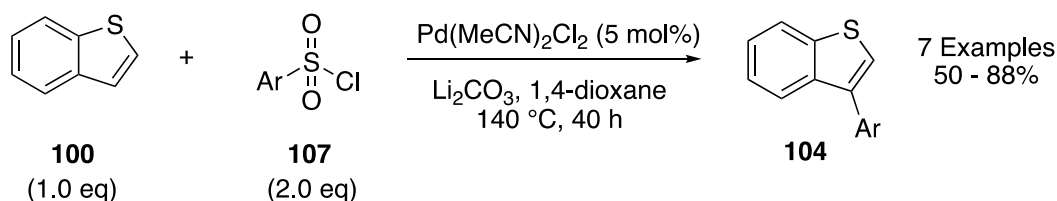


Glorius 2014:



Scheme 17. Heterogeneous Pd-catalysed C-3 arylation of benzothiophenes

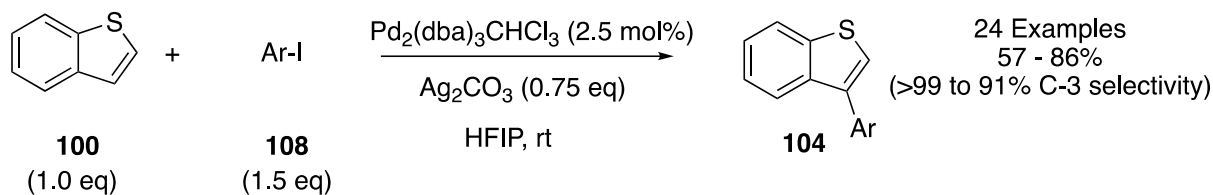
Another homogeneous approach by Doucet showed that aryl sulfonyl chlorides **107** were also appropriate coupling partners for Pd-catalysed C-3 functionalisation of benzothiophenes (Scheme 18).²³ Again, this method required an extremely high temperature of 140 °C and long reaction times.



Scheme 18. Pd-catalysed C-3 arylation of benzothiophenes with aryl sulfonyl chlorides

More recently, Larrosa developed a room-temperature protocol using sub-stoichiometric amounts of Ag₂CO₃ in the solvent hexafluoro-2-propanol (Scheme 19).²⁴

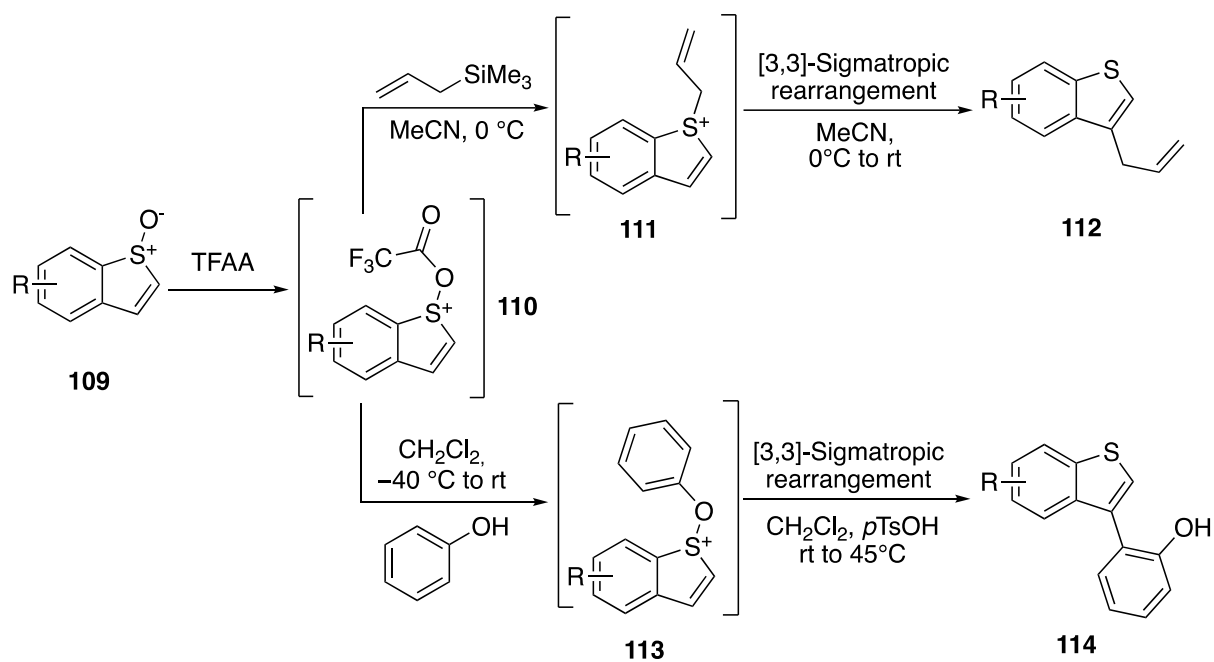
This method also enabled the use of readily available aryl iodide **108** coupling partners and produced C-3 regioselectivities of >99% in most cases.



Scheme 19. Pd-catalysed C-3 arylation of benzothiophenes with aryl iodides at rt

Whilst recent advancements in Pd-catalysed C-H functionalisation has enabled a highly selective method for C-3 functionalisation of benzothiophenes, there is still great demand for new and complimentary methods to be developed. For Pd-catalysed methods, vigorous reaction screening studies are essential as conditions are complex and often require excess base, high temperatures, specialised solvents and in some cases stoichiometric amounts of an oxidant. Furthermore, methods are currently limited to benzothiophene arylation.

More recently, Procter developed a method for C-3 benzothiophene functionalisation from benzothiophene S-oxides via an interrupted Pummerer-type reaction with phenols and allyl silanes (Scheme 20).²⁵ Activation of the benzothiophene S-oxide **109** with trifluoroacetic anhydride generates intermediate **110**. Nucleophilic addition of the allyl silane or phenol coupling partner to **110** forms intermediates **111** or **113** respectively, which undergo [3,3]-sigmatropic rearrangement at the C-3 benzothiophene position. Rearomatisation results in the desired C-3 benzothiophenes **112** or **114**. This method is metal free and allows for C-3 alkylation with allyl silane nucleophiles, a substitution pattern that is not currently available via Pd-catalysed methods.



Scheme 20. C-3 selective functionalisation of benzothiophenes via an interrupted Pummerer reaction and [3,3]-sigmatropic rearrangement of benzothiophene S-oxides

2.2 Results and Discussion

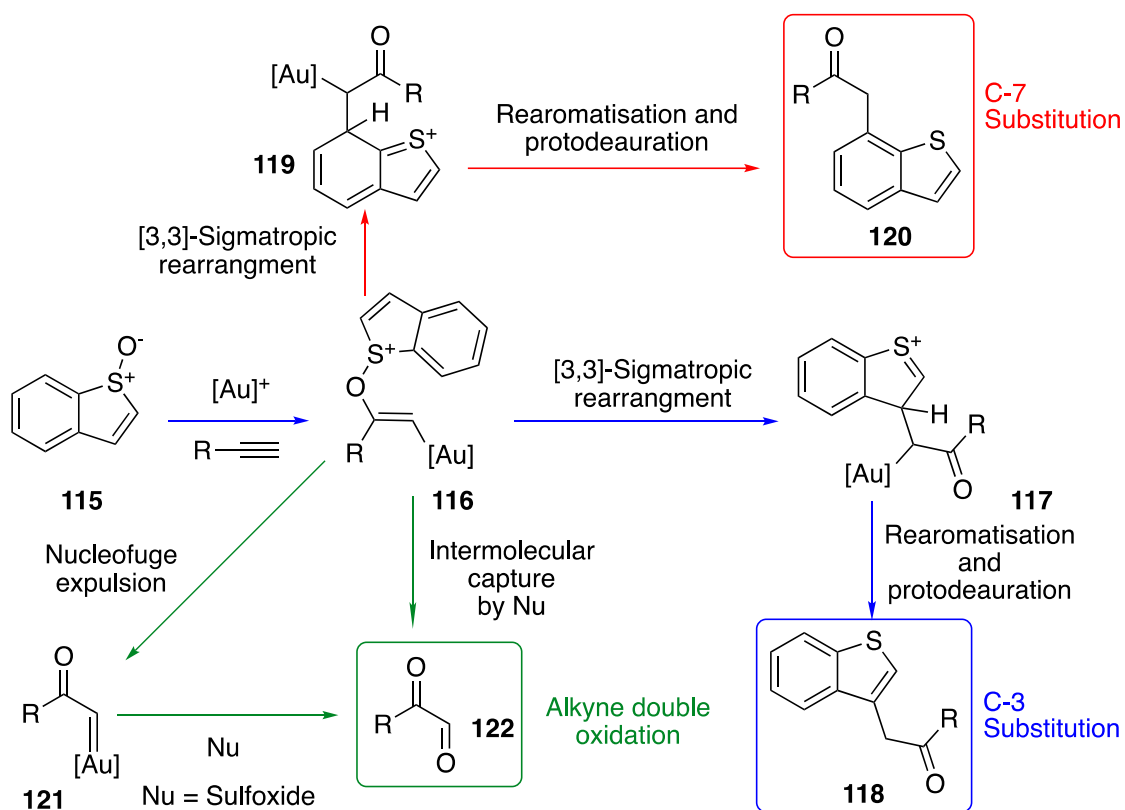
2.2.1 Aims and Objectives

The aim was to explore whether alkyne oxyarylation with benzothiophene S-oxides could provide a route into C-3 substituted benzothiophenes. This novel method would enable benzothiophene C-3 alkylation, which is not possible by existing Pd-catalysed C-H functionalisation methods. The proposed route via Csp²-Csp³ bond forming acylmethylation would also provide a functionalisation method with 100% atom efficiency. Alongside providing a novel route towards usefully-substituted benzothiophenes, the study would broaden the understanding of C-C bond forming rearrangements between sulfoxides and alkynes. The intent was to investigate the [3,3]-sigmatropic rearrangement mechanism alongside studying the behaviour of the

sulfoxide in the transformation. Exploring the mechanism in greater depth would provide a better understanding of gold-catalysed oxidation reactions with sulfoxides.

2.2.2 Proposed Mechanism for Alkyne Oxyarylation with Benzothiophene S-oxides

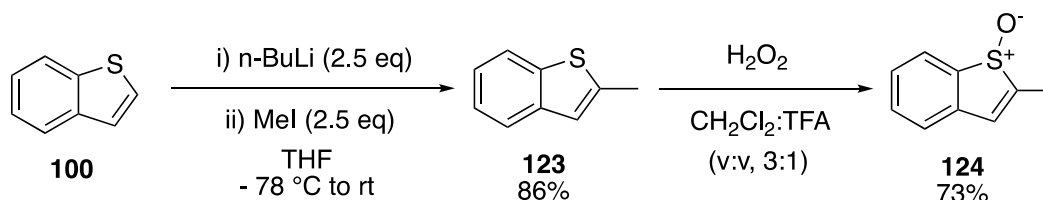
For this transformation, a regioselective vinyl gold carbenoid intermediate **116** should be formed by attack of the benzothiophene S-oxide **115** at the internal carbon of the terminal alkyne; the alkyne substituent should allow for regioselective oxidation by stabilising positive charge build up at this position (Scheme 21). For the desired process, selective [3,3]-sigmatropic rearrangement from the vinyl gold carbenoid intermediate **116** would occur at the C-3 position rather than the C-7 position (Scheme 21, **116** to **117** vs **119**). Following [3,3]-sigmatropic rearrangement, rearomatisation of the thiophene ring and protodeauration would result in the C-3 substituted benzothiophene (Scheme 21, **117** to **118**). As shown in the introduction, analogous [3,3]-sigmatropic rearrangements onto benzenoid rings are well established. However, it was hypothesised that the lower aromaticity of the thiophene in the fused ring system would favour C-3 over C-7 substitution.²⁶ Another competing pathway could see nucleofuge expulsion by intermolecular interception of the vinyl gold carbenoid **116** by a second benzothiophene S-oxide, releasing the free benzothiophene and the over-oxidised alkyne **122**.¹² Alkyne over-oxidation could also occur by intramolecular nucleofuge expulsion via formation of the gold carbene intermediate **121**, which is subsequently trapped by benzothiophene S-oxide to provide **122**. It was anticipated that favouring the reactivity towards oxyarylation vs alkyne over-oxidation could be tuned by varying the catalyst and reaction conditions.



Scheme 21. Proposed mechanistic pathways for the alkyne oxyarylation reaction

2.2.3 Optimisation of the Gold-Catalysed Oxyarylation Reaction

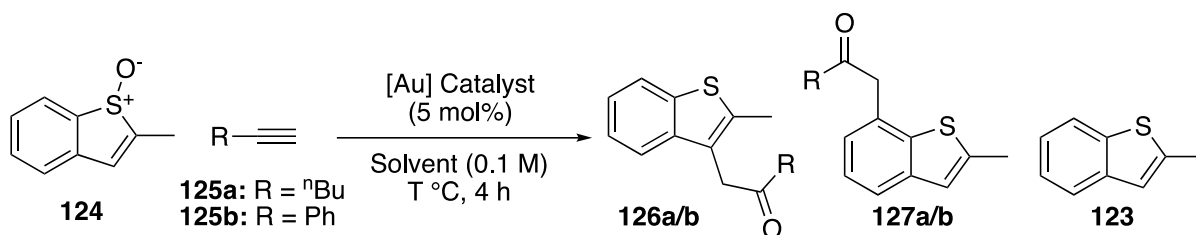
Benzothiophene S-oxide decomposes out of solution, thus 2-methylbenzothiophene S-oxide **124** was prepared for reaction screening studies.²⁷ Lithiation of benzothiophene **100** and subsequent trapping with methyl iodide afforded 2-methylbenzothiophene **123**, which was oxidised to **124** using H₂O₂ (Scheme 22).



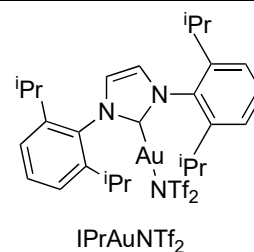
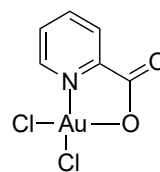
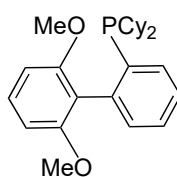
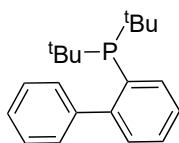
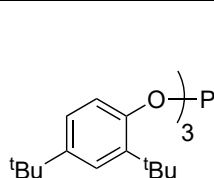
Scheme 22. Synthesis of 2-methylbenzothiophene S-oxide

Commercially available 1-hexyne (**125a**) and phenylacetylene (**125b**) were used alongside 2-methylbenzothiophene S-oxide for the initial screening studies (Table 1).

Table 1. Reaction screening studies for gold-catalysed alkyne oxyarylation



Entry	125a/b (eq.)	[Au] Catalyst	Solvent	T/°C	Yield/%			
					124	126a/b	127a/b	123
1	125a (2)	Au(Pic)Cl ₂ ^b	PhMe	rt	36	17	4	14
2	125a (2)	SPhosAuNTf ₂	PhMe	0	74	16	2	0
3	125a (2)	SPhosAuNTf ₂	PhMe	rt	56	18	2	0
4	125a (2)	[JohnPhosAuNCMe]SbF ₆	PhMe	0	46	34	3	6
5	125a (2)	IPrAuNTf ₂	PhMe	0	32	40	9	- ^d
6	125a (2)	(^p CF ₃ C ₆ H ₄) ₃ PAuCl/AgNTf ₂ ^c	PhMe	0	16	60	11	11
7	125a (2)	(^p CF ₃ C ₆ H ₄) ₃ PAuCl/AgSbF ₆ ^c	CH ₂ Cl ₂	0	0	65	16	- ^d
8	125a (2)	(^p CF ₃ C ₆ H ₄) ₃ PAuCl/NaBARF ^c	CH ₂ Cl ₂	0	96	3	1	0
9	125a (2)	DTBPAuCl/AgOTs ^c	PhMe	0	88	6	4	0
10	125a (2)	[DTBPAuNCPh]SbF ₆	CH ₂ Cl ₂	0	0	64	23	- ^d
11	125a (2)	[DTBPAuNCPh]SbF ₆	C ₆ H ₅ F	0	7	63	24	<6 ^e
12	125a (1)	[DTBPAuNCPh]SbF ₆	CH ₂ Cl ₂	0	7	50	17	4
13	125b (2)	[DTBPAuNCPh]SbF ₆	CH ₂ Cl ₂	0	- ^d	51	9	9
14	125b (2)	[DTBPAuNCPh]SbF ₆	C ₆ H ₅ F	0	0	80	10	<7 ^e
15	125b (2) ^f	[DTBPAuNCPh]SbF ₆	C ₆ H ₅ F	0	0	67	12	<10 ^e
16	125b (1)	[DTBPAuNCPh]SbF ₆	C ₆ H ₅ F	0	0	62	9	8
17	125b (1) ^g	[DTBPAuNCPh]SbF ₆	C ₆ H ₅ F	0	- ^d	50	9	- ^d



^aReactions were performed on a 0.1 mmol scale for 4 h (unless stated otherwise) and yields were determined by ¹H NMR spectroscopy using internal standard 1,2,4,5-tetramethylbenzene. ^bReaction was stirred for 40 h at rt. ^c[Au] = 5 mol%, AgX = 7.5 mol%. ^dYields could not be determined due to overlapping resonances in the ¹H NMR spectrum. ^eRepresents the maximum possible yield because of overlapping resonances. ^f2.5 mol% catalyst was used. ^g2 eq. of **124**.

It became apparent in early studies with 1-hexyne that [3,3]-sigmatropic rearrangement was viable to both the C-3 position and the C-7 position to provide both **126a** and **127a**. No other regioisomers were observed, and the C-3 functionalised product was the major regioisomer in all cases. In some cases, the free benzothiophene **123** was also observed from the alkyne over-oxidation pathway (See Scheme 21). The screening study began with Au(Pic)Cl₂, which led to no reaction by TLC at 0 °C. The reaction was warmed to rt after 2 h and stirred for a further 40 h to yield only 17% of the C-3 functionalised benzothiophene **126a** (Table 1, entry 1). A series of Au(I) catalysts were then tested. Electron-rich SPhos-, JohnPhos- and IPr-ligated gold catalysts displayed good C-3 regioselectivity but low reactivity towards oxyarylation (Table 1, entries 2-5). In most cases, improved reactivity was observed with electron-deficient phosphine and phosphite-ligated gold catalysts. Testing (pCF₃C₆H₄)PAuCl with several silver salts showed that weakly-coordinating SbF₆⁻ was the superior counterion, obtaining an 81% combined yield of oxyarylation products **126a** and **127a** (Table 1, entry 7), while a 71% combined yield of **126a** and **127a** was obtained with AgNTf₂ (Table 1, entry 6) and no significant reactivity was observed when NaBAR_F was used (Table 1, entry 8). Whilst high reactivity and reasonable C-3 regioselectivity was observed with the (pCF₃C₆H₄)PAuCl catalytic systems, an appreciable amount of the free benzothiophene **123** was also formed (Table 1, entries 6 and 7). It was proposed that electron-deficient gold catalysts were less capable of stabilising positive charge build-

up at the neighbouring carbon, decreasing the likelihood of nucleofuge expulsion from the vinyl gold-carbenoid intermediate (see Scheme 21, **116** to **121**). Accordingly, the electron-deficient phosphite catalyst [DTBPAuNCPPh]SbF₆ was tested and afforded a cleaner reaction, observed by ¹H NMR spectroscopic analysis of the crude reaction material, and an increase in the combined yields of **126a** and **127a** compared to (pCF₃C₆H₄)PAuCl/AgSbF₆ (Table 1, entries 10 vs 7). Reactions in either CH₂Cl₂ and fluorobenzene provided comparable results with [DTBPAuNCPPh]SbF₆, providing an 87% overall yield of oxyarylation products with ~2.8:1 C-3:C-7 regioselectivity (Table 1, entries 10 and 11). The use of a tosylate counterion with DTBPAuCl saw reduced reactivity (Table 1, entry 9).

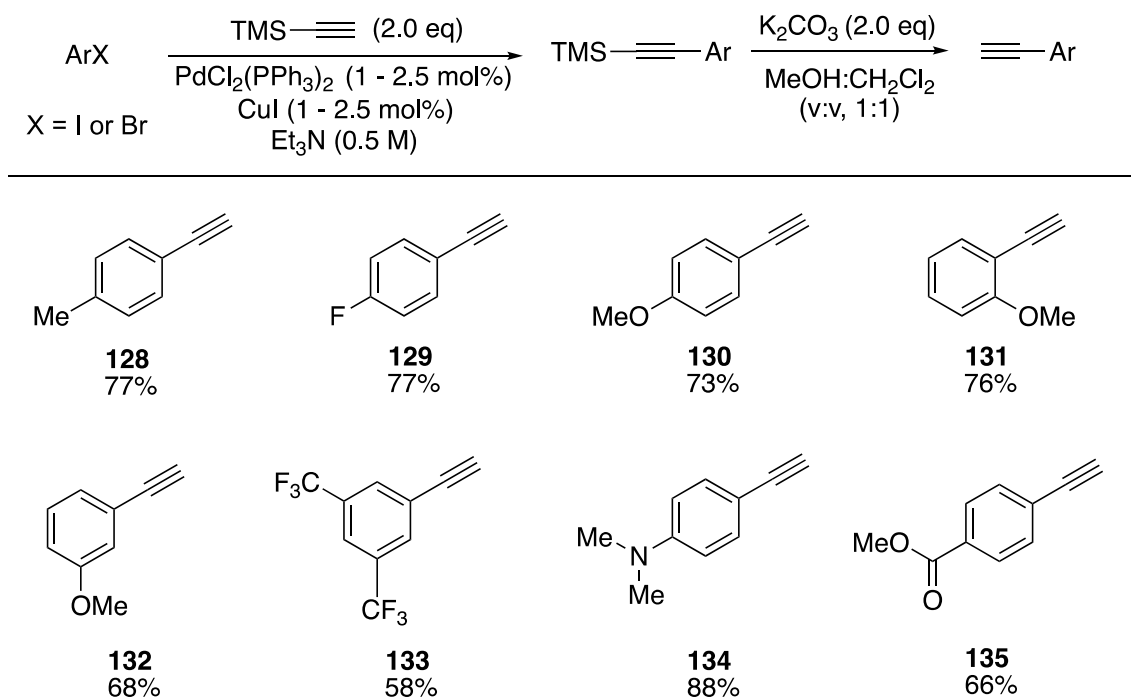
Reaction screening studies were then performed with commercially available phenylacetylene (**125b**) and [DTBPAuNCPPh]SbF₆ to test how well aromatic alkynes performed in the oxyarylation reaction. In comparison to what was observed with 1-hexyne, the use of fluorobenzene instead of CH₂Cl₂ greatly improved the yield of oxyarylation products **126b** and **127b** from 60% to 90% (Table 1, entry 13 vs 14). Additionally, the C-3 vs C-7 regioselectivity was much higher at 8:1 with phenyl acetylene compared to 2.8:1 with 1-hexyne. The catalyst loading was reduced to 2.5 mol% and a good, combined yield of 79% **126b** and **127b** was obtained (Table 1, entry 15).

The stoichiometry was also investigated. When the equivalents of alkyne were reduced from 2 eq to 1 eq there was a notable reduction in the yields of **126** and **127** with both alkynes (Table 1, entry 10 vs 12 and entry 14 vs 16). When the stoichiometry was

reversed and 1 eq of phenylacetylene was reacted with 2 eq of sulfoxide **124**, the yield was further decreased (Table 1, entry 17). A stoichiometry of 1 eq sulfoxide and 2 eq alkyne was therefore chosen for the optimised conditions, alongside the [DTBPAuNCPPh]SbF₆ catalyst and the solvent fluorobenzene.

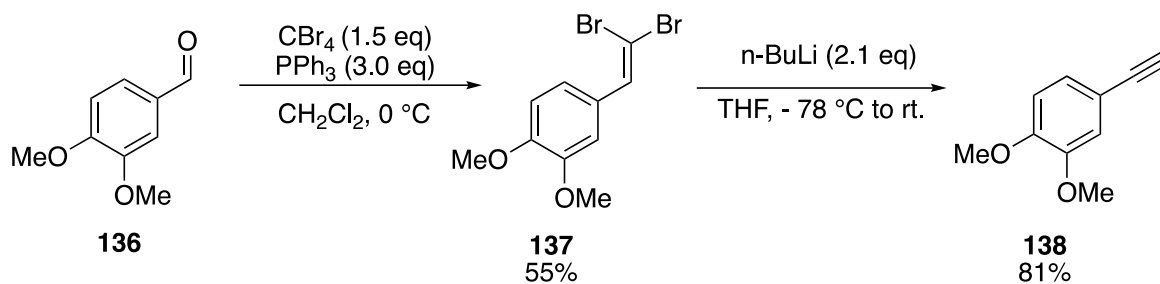
2.2.4 Starting Material Preparation

For substrate scope exploration, a variety of alkynes were synthesised. Sonagashira reactions of aryl halides with TMS acetylene, followed by TMS deprotection, afforded terminal alkynes **128** – **135** in good yield (Scheme 23).



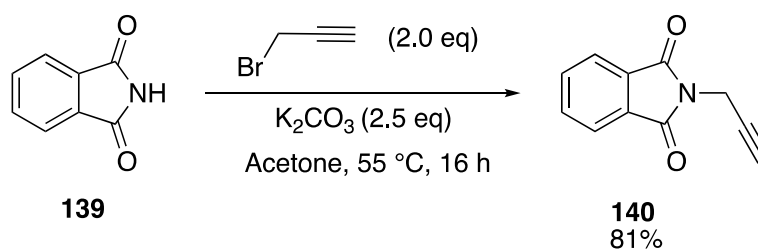
Scheme 23. Synthesis of alkynes via Sonagashira cross-coupling.

4-Ethynyl-1,2-dimethoxybenzene **138** was synthesised using the Corey-Fuchs reaction (Scheme 24). Firstly, the dibromoolefin **137** was made from the corresponding aldehyde **136**. A reaction between dibromoolefin **137** and n-BuLi afforded the terminal alkyne **138** in 81% yield.



Scheme 24. Corey-Fuchs synthesis of 4-Ethynyl-1,2-dimethoxybenzene

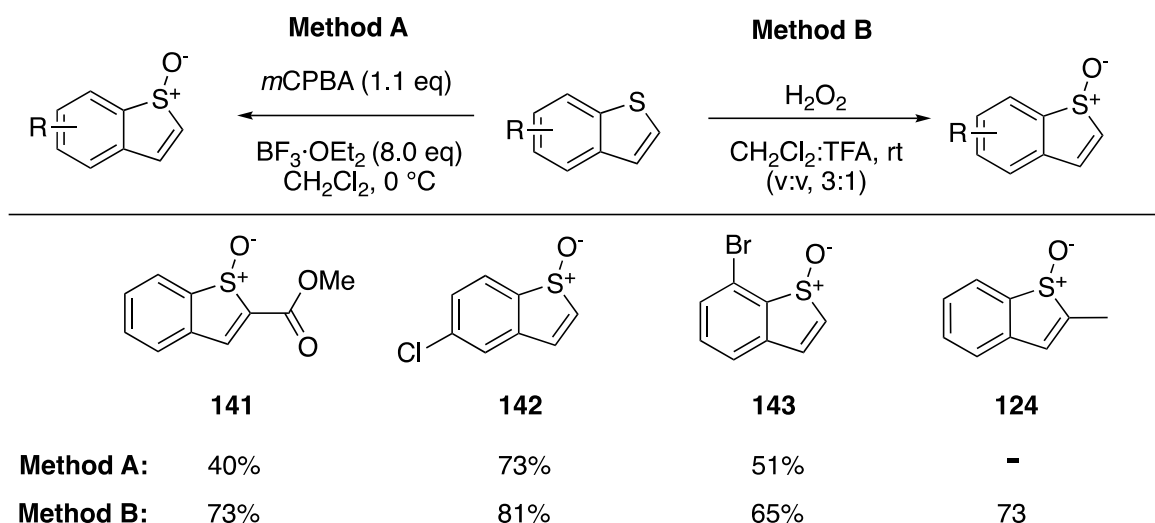
Finally, *N*-propargylphthalimide **140** was synthesised by a nucleophilic substitution reaction between phthalimide **139** and propargyl bromide with K_2CO_3 (Scheme 25).



Scheme 25. Synthesis of *N*-propargylphthalimide

All other alkynes used during the investigation of the reaction scope were commercially sourced.

Other than the previously described synthesis of 2-methylbenzothiophene, all other benzothiophene analogues were commercially sourced and oxidised to the corresponding benzothiophene *S*-oxides. Two different methods for benzothiophene oxidation were tested. The first method used *m*CPBA with the additive BF_3OEt_2 in large excess (Scheme 26, method A).²⁸ However, in all cases, remaining starting material was recovered, with only moderate yields of the benzothiophene *S*-oxides obtained. Using H_2O_2 as the oxidising agent in the presence of trifluoroacetic acid was found to afford the desired benzothiophene *S*-oxides in much higher yields (Scheme 26, method B).^{25, 29}

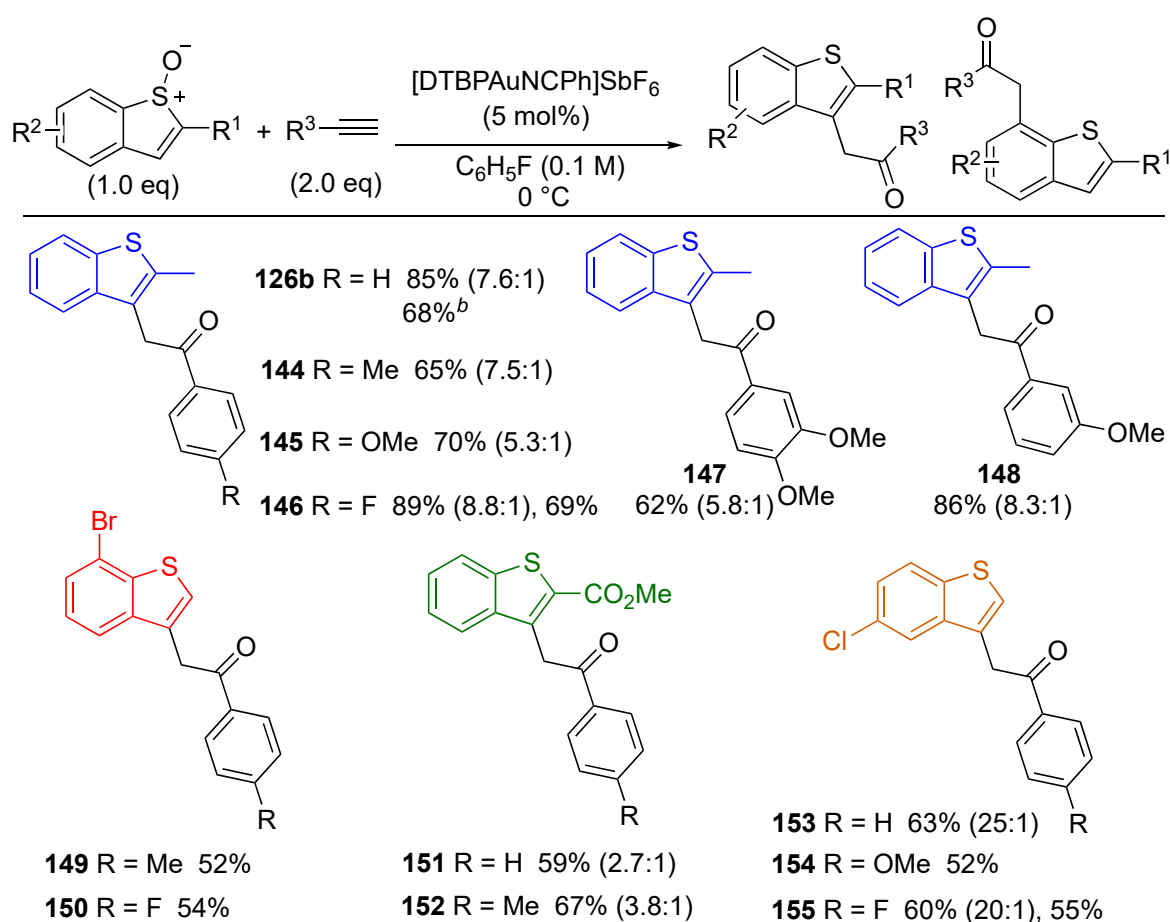


Scheme 26. Synthesis of benzothiophene S-oxides

2.2.5 Scope of the Gold-Catalysed Oxyarylation Reaction

The optimised conditions were then applied across the four differently substituted benzothiophene S-oxides with a range of aromatic and aliphatic terminal alkynes (Schemes 27 - 29). The reactions were typically performed on a 0.2 to 0.5 mmol scale. Electron-rich methoxy- and methyl-substituted aromatic alkynes afforded the oxyarylation products in good yields, however an appreciable amount of the free benzothiophene from the alkyne over-oxidation pathway was also observed for these reactions (Scheme 27, **144**, **145**, **147** and **154**). Electron-deficient and electronically unbiased aromatic alkynes produced good to excellent yields of the oxyarylation products (Scheme 27 **126b**, **146**, **148** and **153**). Benzothiophenes with different substitution patterns were also well tolerated (Scheme 27, **149** to **155**). 5-Chlorobenzothiophene S-oxide afforded very high C-3 regioselectivities with aromatic alkynes (Scheme 27, **153** to **155**). In some cases, a simple trituration with methanol yielded the C-3 regioisomer exclusively (Scheme 27, **154** and **155**). With the C-7 position inaccessible, 7-bromobenzothiophene S-oxide provided the pure C-3 alkylated products, and the remaining material was the free 7-bromobenzothiophene

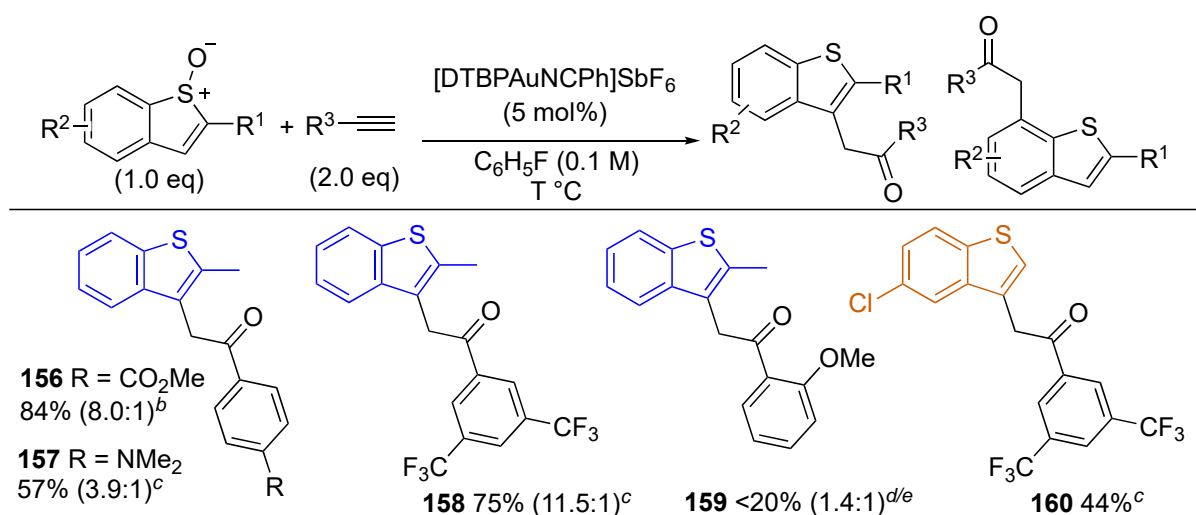
formed via the alkyne over-oxidation pathway (Scheme 27, **149** and **150**). Whilst the presence of a carboxylic ester at the C-2 position saw lower C-3 regioselectivities, it did not otherwise adversely affect the reactivity (Scheme 27, **151** and **152**). This is consistent with the proposed [3,3]-sigmatropic rearrangement mechanism, as a reduction in reactivity would be expected with an electron deficient C-2 substituent if the mechanism was to occur via intermolecular capture of an intermediate gold carbene. A large 1 mmol scale reaction was performed for the synthesis of **126b**, and the C-3 regioisomer was isolated exclusively in 68% yield.



^aIsolated yield of the C-3 regioisomer exclusively where ratio is not given. ^b1.00 mmol scale reaction.

Scheme 27. Scope of gold-catalysed aromatic alkyne oxyarylation reaction with benzothiophene S-oxides

Higher temperatures were required for the oxyarylation of some electron-deficient and nitrogen-containing alkynes (Scheme 28). It is believed that the electron-deficient alkynes have a lower binding affinity to the gold catalyst, thus alkyne electrophilic activation and subsequent attack of the benzothiophene S-oxide is challenging at lower temperatures. 4-Ethynyl-*N,N*-dimethylaniline did not undergo oxyarylation unless heated to 70 °C, and a lower regioselectivity was obtained compared to other electron-rich alkynes that were reacted at 0 °C (Scheme 28, **157**). On the other hand, high C-3 regioselectivities were observed for electron-deficient alkynes at higher temperatures (Scheme 28, **156**, **158** and **160**). In the case of **160**, a simple trituration with methanol provided the pure C-3 regioisomer. The presence of an aromatic ortho-substituent on the alkyne significantly reduced reactivity; <20% of **159** was obtained and an appreciable amount of starting material was observed by TLC after heating the reaction at 75 °C for 8 h.

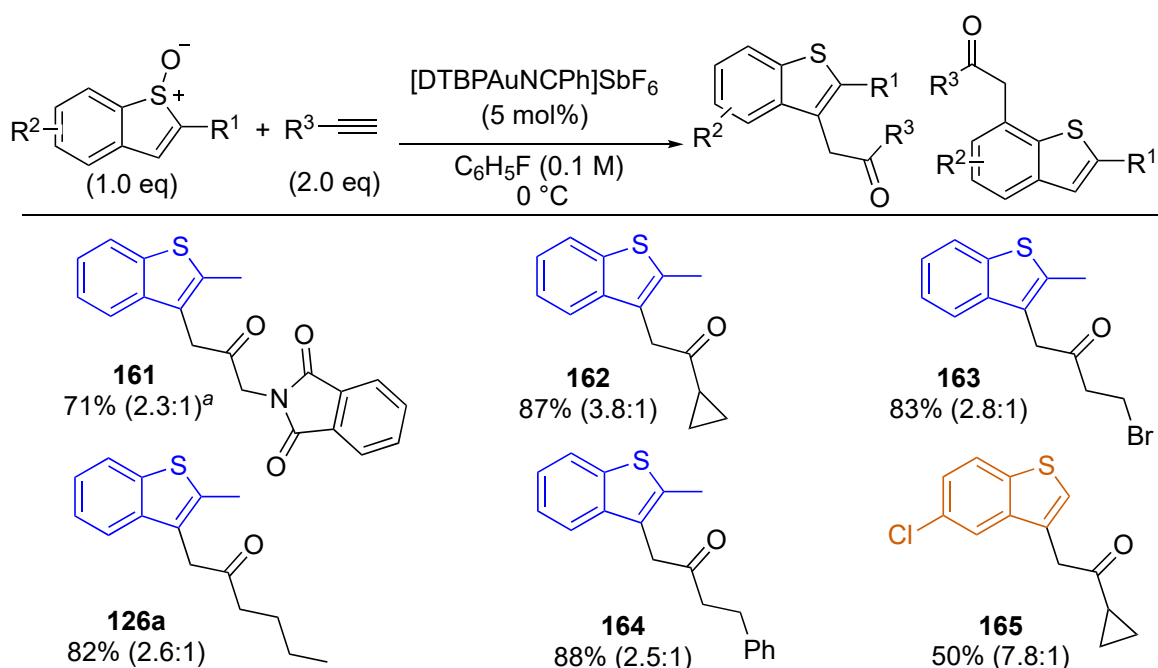


^aIsolated yield of the C-3 regioisomer exclusively where ratio is not given. ^bT = 50 °C. ^cT = 70 °C.

^dT = 75 °C. ^eMinor impurities observed in the ¹H NMR spectrum of the isolated product.

Scheme 28. Scope of gold-catalysed aromatic alkyne oxyarylation reaction with benzothiophene S-oxides at higher temperatures

Aliphatic alkynes also performed well in the gold-catalysed oxyarylation reaction, although the regioselectivities were lower than those attained with aromatic alkynes (Scheme 29). As observed with the aromatic alkynes, 5-chlorobenzothiophene S-oxide afforded a higher C-3 regioselectivity compared with 2-methylbenzothiophene S-oxide in the analogous reaction with cyclopropyl acetylene (Scheme 29, **165** vs. **162**). For the oxyarylation of *N*-propargylphthalimide with 2-methylbenzothiophene S-oxide, a temperature of 50 °C was required to achieve optimal reactivity. When 2.0 eq. of alkyne were used, hydration of *N*-propargylphthalimide took place and the hydration product was inseparable from the desired product **161** by column chromatography. Fortunately, no hydration product was attained when *N*-propargylphthalimide was reduced to 1.0 eq, obtaining **161** in 71% yield.



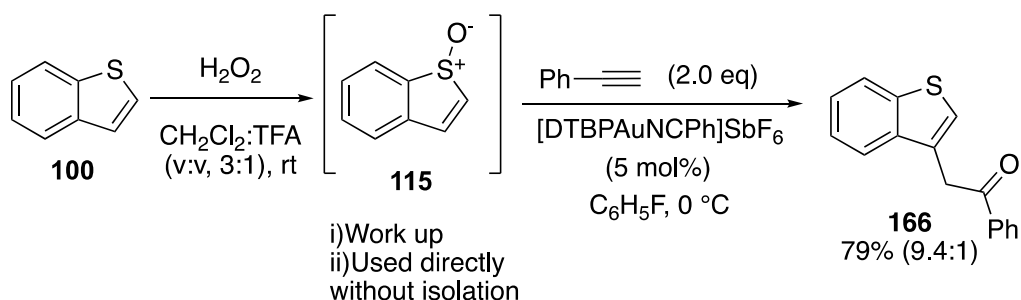
^aReaction was performed at 50 °C with 1.0 eq. of the alkyne.

Scheme 29. Scope of gold-catalysed aliphatic alkyne oxyarylation with benzothiophene S-oxides

In some cases, it was noticed that resonances corresponding to unknown phosphorus-containing impurities were present in small amounts in the ^1H NMR spectra of the oxyarylation products. This was also confirmed by the presence of unknown resonances in the ^{31}P NMR spectra of some of the catalysis products. It was apparent that these phosphorus-containing residues were not interacting with the silica phase during column chromatography and were being isolated alongside less polar catalysis products. To prevent isolating these unknown impurities, it was important to flush the column with 10% CH_2Cl_2 in hexane (~ 150 mL/mmol reaction scale over ~ 2 -3 mins) before increasing the solvent polarity to isolate the desired benzothiophenes. This technique allowed the impurities to be removed from the column prior to isolating the pure product.

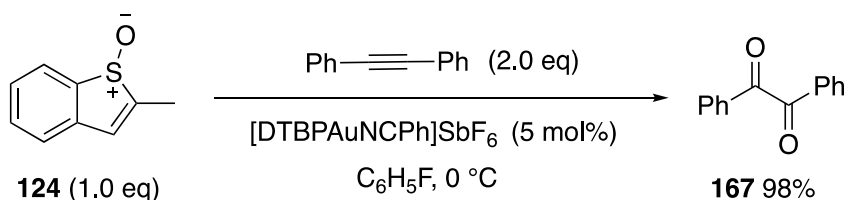
Unsubstituted benzothiophene S-oxide **115** decomposes out of solution and therefore could not be isolated. Accordingly, a telescoped oxidation-catalysis protocol was developed, demonstrating the feasibility of benzothiophene functionalisation from alkyne oxyarylation (Scheme 30). Firstly, the oxidation of benzothiophene **100** was regularly monitored by TLC to ensure there was no over-oxidation to the sulfone. Any unreacted benzothiophene or benzothiophene sulfone would be taken through to the catalysis reaction and ultimately reduce the overall yield of oxyarylation products. Following oxidation, a basic workup and extraction was performed with NaHCO_3 and CH_2Cl_2 . The CH_2Cl_2 was then removed under reduced pressure in a room temperature water bath (approx. 25 °C) to ensure there was no decomposition of benzothiophene S-oxide in solution. A minimum amount of CH_2Cl_2 was left unevaporated to ensure benzothiophene S-oxide always remained in solution (approx. 2 mL/mmol).

Fluorobenzene was then added to the solution before the remaining CH₂Cl₂ was removed. The solution was then cooled to 0 °C before the catalyst and alkyne were added. This method yielded the functionalised benzothiophene **166** in 79% isolated yield with a 9.4:1 ratio of C-3:C-7 regioisomers.



Scheme 30. Gold-catalysed oxyarylation of phenylacetylene with benzothiophene S-oxide

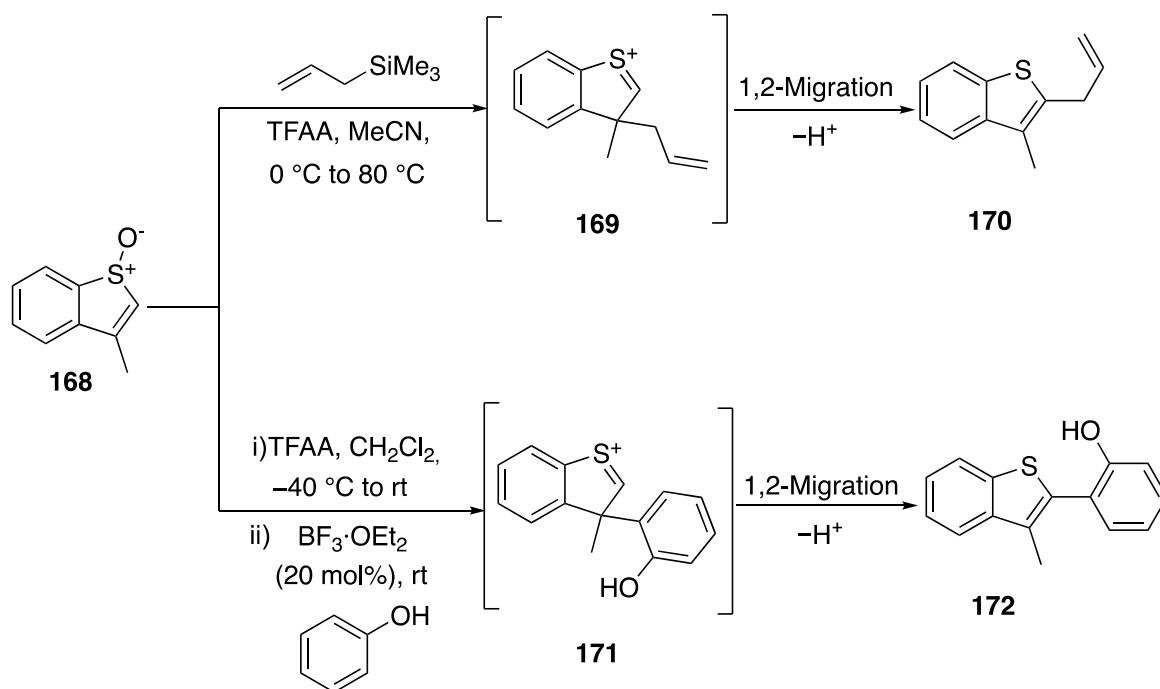
Benzothiophene substitution of internal alkynes was then investigated in the attempted oxyarylation of diphenylacetylene with 2-methylbenzothiophene S-oxide **124** (Scheme 31). If successful, a stereocentre would be introduced in the alkylated benzothiophene product, however no oxyarylation products were observed. Instead, the alkyne over-oxidation product **167** was obtained in a 98% yield (wrt the sulfoxide) indicating that 2-methylbenzothiophene S-oxide is an excellent oxidant for internal alkynes but [3,3]-sigmatropic rearrangement from the vinyl gold carbenoid is not favoured.



Scheme 31. Reaction of diphenylacetylene with 2-methylbenzothiophene S-oxide under standard reaction conditions

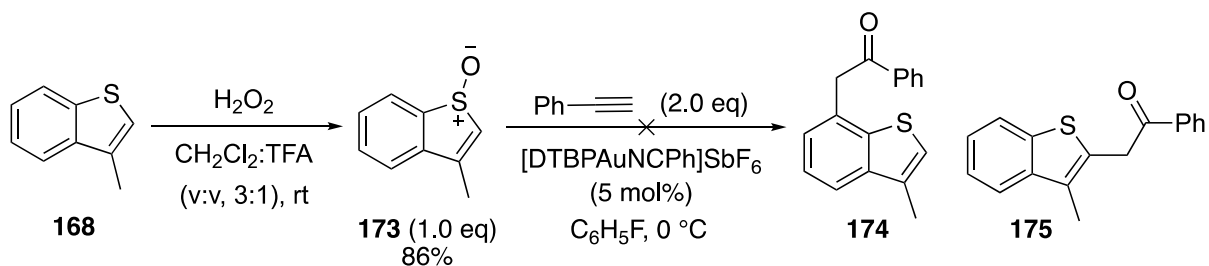
Procter's group has demonstrated C-2 benzothiophene functionalisation via an interrupted Pummerer reaction with C-3 substituted benzothiophene S-oxides.³⁰

Trifluoroacetic anhydride is used to activate benzothiophene S-oxide **168**. Nucleophilic addition of the allyl silane or phenol coupling partners to the activated sulfoxide, followed by [3,3]-sigmatropic rearrangement at the C-3 position provides intermediates **169** and **171** respectively. 1,2-Migration of the C-3 substituent occurs to yield the C-2 functionalised benzothiophenes **170** and **172** (Scheme 32).



Scheme 32. C-2 Benzothiophene functionalisation by Procter and co-workers

3-Methyl benzothiophene S-oxide **168** was explored under the optimised reaction conditions. On reaction with phenylacetylene, product **175** was anticipated if such migration pathways were available to C-3 substituted benzothiophene S-oxides in the gold-catalysed oxyarylation reaction (Scheme 33). With the C-3 position inaccessible, another pathway may see C-7 benzothiophene functionalisation to provide **174** from [3,3]-sigmatropic rearrangement at this position. Unfortunately, the reaction between 3-methyl benzothiophene S-oxide and phenylacetylene was intractable, and further studies are therefore required to investigate the reactivity of C-3 substituted benzothiophene S-oxides in the gold-catalysed oxyarylation reaction.



Scheme 33. Attempted oxyarylation of phenylacetylene with 3-methylbenzothiophene S-oxide

2.2.6 Determining Regioselectivity

2.2.6.1 C-3 Regioisomer Determination

Product **126b** was used to determine the regioselectivity of the major isomer and the same analysis was applied to all of the C-3 substituted benzothiophene products. In the ^1H NMR spectrum of 2-methylbenzothiophene **123**, the C-3 proton is represented by an aromatic singlet at 6.89 ppm that is distinct from the other aromatic protons of the benzenoid ring (Figure 3). Close analysis of the C-3 proton of 2-methyl benzothiophene shows fine splitting from coupling with the C-2 methyl group, however it is not a clearly resolved quartet. The C-2 methyl group is also represented by a doublet of $J = 1.2$ Hz in the ^1H NMR spectrum of 2-methylbenzothiophene. In the ^1H NMR spectrum of product **126b** (Figure 3), the absence of an aromatic singlet and no splitting of the C-2 methyl group are both indicative of C-3 substitution. Whilst fine splitting is not observed in the ^1H NMR spectrum, the 2D COSY experiment of **126b** shows long range coupling between the pendant CH_2 and the C-2 methyl group (Figure 3). In addition, the 2D HMBC experiment of product **126b** shows that the pendant CH_2 and the methyl group both interact with two of the same quaternary carbons, determined to be C-2 and C-3. These correlations would only be observed in the C-3 regioisomer (Figure 3).

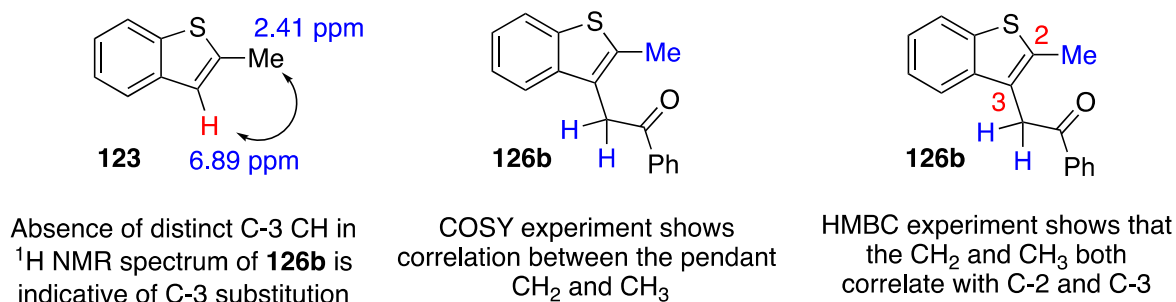


Figure 3. Determination of C-3 substituted benzothiophene 126b

2.2.6.2 C-7 Regioisomer Determination

Product **127b** was used to determine the regioselectivity of the minor C-7 regioisomer, and the same analysis was applied to all of the C-7 substituted benzothiophene products. In the ^1H NMR spectrum of **127b**, the presence of the characteristic C-3 proton that exhibits long range coupling to the C-2 methyl group confirmed that oxyarylation had occurred on the benzenoid ring. This long-range coupling between the C-3 proton and the C-2 methyl group was also observed in the 2D COSY spectrum (Figure 4).

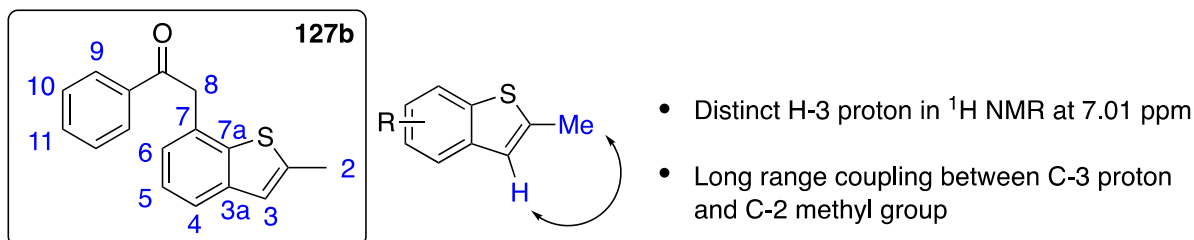


Figure 4. Confirmation of substitution at the benzenoid ring of product 127b

The ^1H NMR and 2D COSY spectra revealed that the splitting pattern of the benzenoid ring of product **127b** was consistent with either C-4 or C-7 benzothiophene substitution (Figure 4). In the ^1H NMR spectrum, H-4 was represented by doublet and saw coupling with only H-5 in the 2D COSY spectrum. H-6 was also represented by a doublet from coupling with H-5. H-5 exhibited coupling to both H-4 and H-6 and was therefore represented by an apparent triplet in the ^1H NMR spectrum.

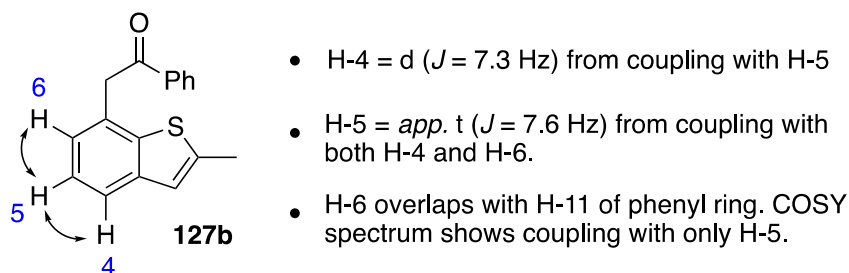


Figure 5. Splitting pattern of the benzenoid ring of 127b

Although, mechanistically, functionalisation at the C-4 position was not plausible by alkyne oxyarylation via sigmatropic rearrangement, HMBC and DEPT-135 experiments were performed to confirm that **127b** was the C-7 regioisomer (Figure 6). Identification of quaternary carbons C-3a and C-7a were critical for determining the regioselectivity, therefore all of the quaternary carbons in the product were sequentially identified. C-2 was identified by its correlation with the C-2 methyl protons and H-3. The quaternary carbon C-9a was confirmed by its correlation with the protons on the phenyl ring. C-9a did not correlate with any of the benzothiophene protons, thus ruling out C-9a as a quaternary carbon on the benzothiophene ring. The quaternary carbon C-7 was confirmed by its correlation with H-5, H-6 and H-8. The chemical shift of C-7 is also consistent with an alkylated carbon on the benzothiophene as it is further up-field than the other benzothiophene carbons. This was also observed with the analogous C-3 regioisomer **126b**, with C-3 experiencing an up-field shift compared to the other benzothiophene carbons. Quaternary carbon C-7a was confirmed by its correlation with H-6 and H-8. By process of elimination, the last quaternary carbon C-3a was confirmed and a correlation between C-3a and H-3 was observed in the HMBC spectrum. With the internal quaternary carbons C-3a and C-7a identified, the C-7 regioselectivity of **127b** could be confirmed. C-3a does not interact with the pendant

CH₂ at C-8 whilst the quaternary carbon C-7a does, thus confirming the benzothiophene is alkylated at the C-7 position.

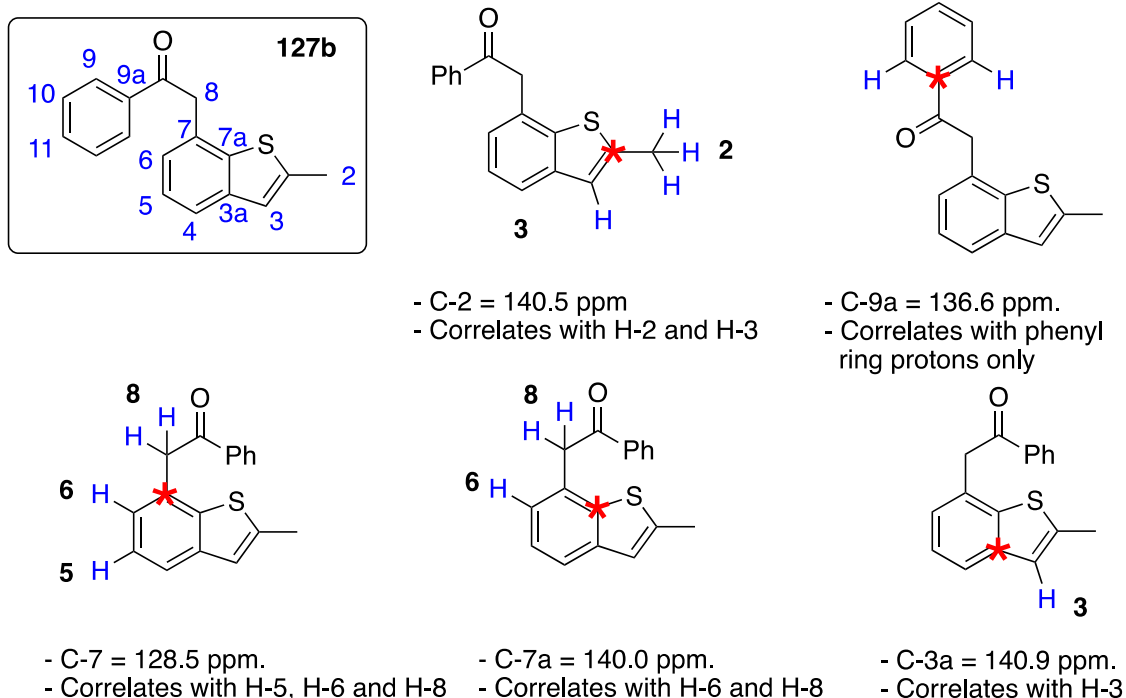


Figure 6. Selected HMBC correlations confirming the structure of 127b

2.2.7 Rationale for Observed Regioselectivities in Oxyarylation Reactions

C-3 substituted benzothiophenes were obtained as the major regioisomers across all of the products formed during this study. It is postulated that the lower aromaticity of the thiophene ring, compared to the benzenoid ring, results in a lower energy transition state for the [3,3]-sigmatropic rearrangement step; the aromaticity of the thiophene ring and benzenoid ring are disrupted for benzothiophene C-3 and C-7 functionalisation respectively. Although the C-3 regioisomers were formed as the major regioisomers in all cases, there were notable differences in the regioselectivity of oxyarylation with different alkynes. These differences can be rationalised by considering possible transition states for the [3,3]-sigmatropic rearrangement step from the vinyl gold carbenoid intermediate (Figure 7).

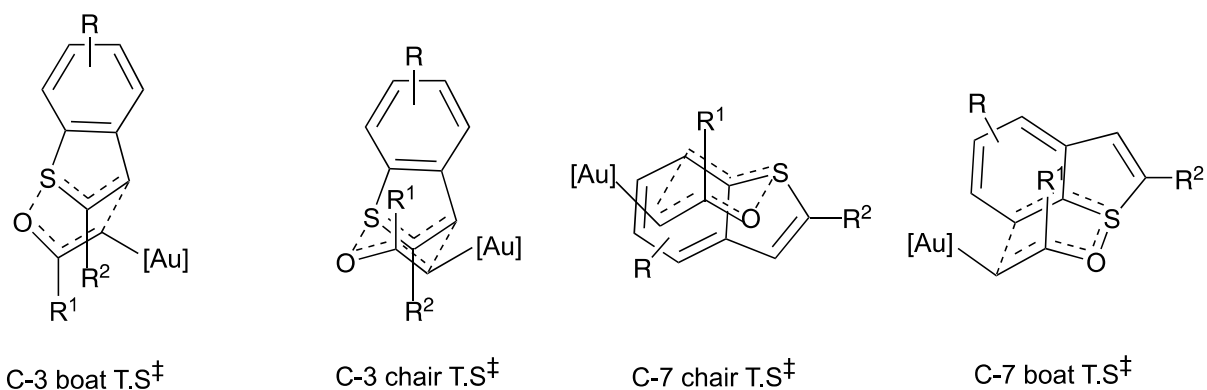


Figure 7. Proposed transition states for the [3,3]-sigmatropic rearrangement step

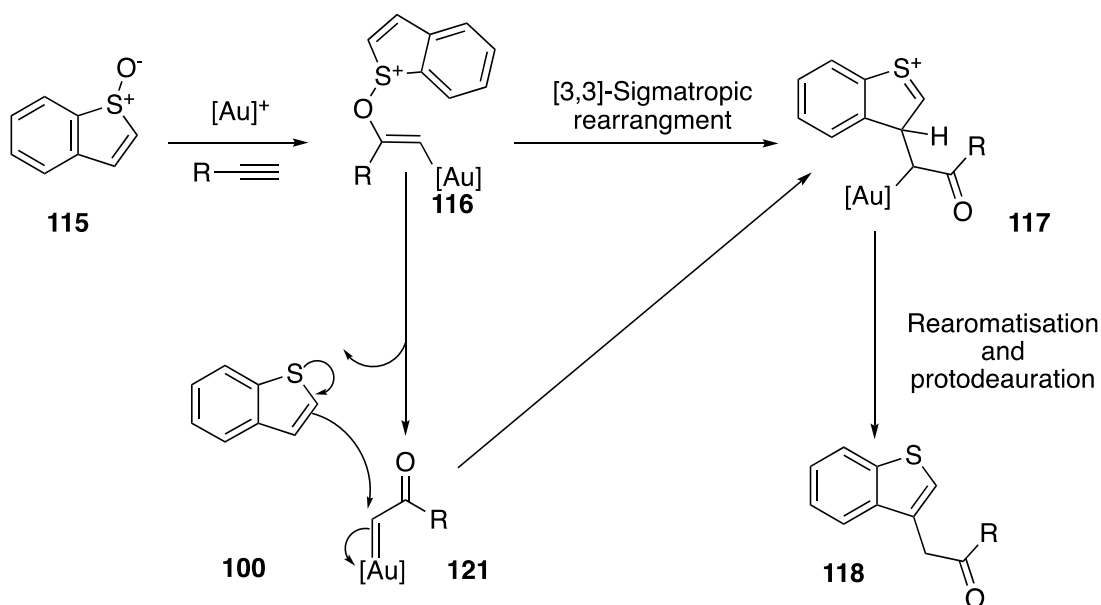
Aromatic alkynes gave higher C-3 regioselectivities compared to aliphatic alkynes in the oxyarylation reaction. It is proposed that for aromatic alkynes, a chair T.S[‡] is favoured for oxyarylation to the C-3 position as overlap of the alkyne substituent R¹ with the benzenoid ring of the benzothiophene may result in favourable π - π interactions (Figure 7, C-3 chair T.S[‡]).³¹ With an aromatic substituent, favourable π - π interactions may be responsible for a lower energy C-3 chair T.S[‡] compared to the transition states for C-7 substitution; in the C-7 chair T.S[‡] there is no overlay between the aromatic substituent and the benzenoid ring and limited overlay in the C-7 boat T.S[‡]. Favourable π - π interactions would account for the higher C-3 regioselectivities observed with aromatic alkynes compared to aliphatic alkynes. In addition, differently-substituted benzothiophene S-oxides provided different regioselectivities in the reaction. 5-chlorobenzothiophene S-oxide saw high C-3 regioselectivities compared to the other benzothiophene S-oxides studied, whilst methyl benzothiophene-2-carboxylate S-oxide saw lower C-3 regioselectivities. The benzothiophene substituents are likely to influence the regioselectivity of the oxyarylation reaction electronically, by affecting the HOMO-LUMO interactions during the [3,3]-sigmatropic rearrangement step. In addition, a large C-2 substituent R² may experience unfavourable steric

interactions during C-3 oxyarylation, with either the alkyne substituent R¹ (C-3 boat TS[‡]) or the gold catalyst (C-3 chair TS[‡]) depending on whether the transformation proceeds via a boat or chair TS[‡]. Such steric interactions may contribute to the lower the C-3 regioselectivity observed with methyl benzothiophene-2-carboxylate S-oxide compared to the other benzothiophene S-oxides studied.

2.3 Mechanistic Studies

2.3.1 Evidence for [3,3]-Sigmatropic Rearrangement

There were two plausible mechanistic pathways that would result in the formation of the C-3 substituted benzothiophenes: intramolecular [3,3]-sigmatropic rearrangement from the vinyl gold carbenoid intermediate **116** or intermolecular benzothiophene capture of a gold carbene intermediate **121** (Scheme 34).

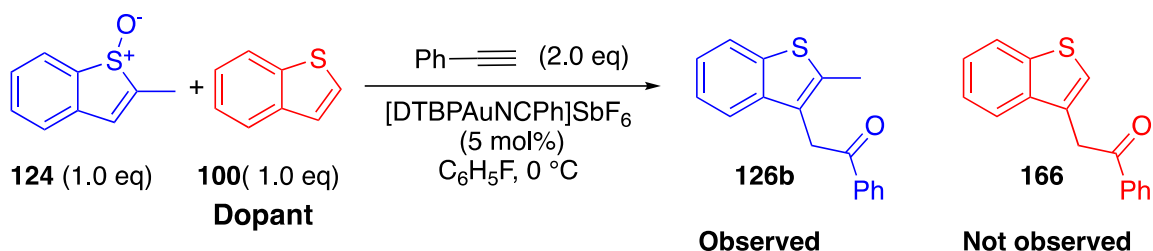


Scheme 34. Possible mechanistic pathways for the formation of C-3 alkylated benzothiophenes by alkyne oxyarylation

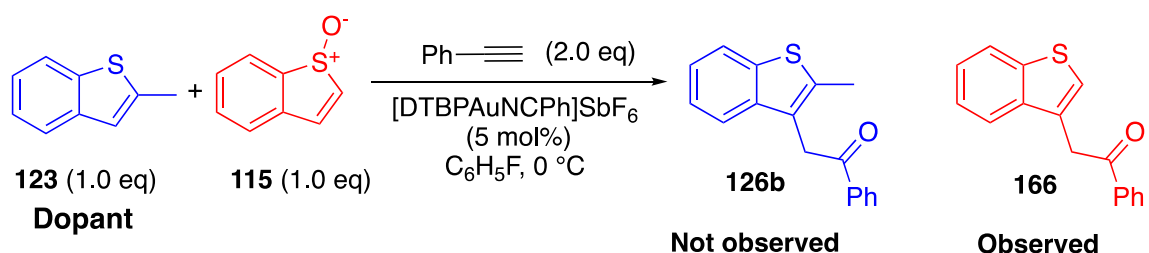
The formation of C-7 substituted benzothiophenes during gold-catalysed oxyarylation is consistent with a [3,3]-sigmatropic rearrangement mechanism. As discussed

previously, methylbenzothiophene-2-carboxylate S-oxide also displayed good reactivity in the oxyarylation reaction, which is consistent with a [3,3]-sigmatropic rearrangement mechanism. Moreover, mechanistic studies performed by other groups support a [3,3]-sigmatropic rearrangement mechanism for gold-catalysed alkyne oxyarylation with aromatic sulfoxides (see section 2.1.2).¹¹⁻¹² Although a [3,3]-sigmatropic rearrangement mechanism seemed likely, a cross-over experiment was performed to consolidate the existing evidence (Scheme 35).

Exp one



Exp two



Scheme 35. Cross-over experiments with benzothiophene dopants supporting a [3,3]-sigmatropic rearrangement mechanism

In experiment one, benzothiophene **100** was added as a dopant to the reaction between 2-methylbenzothiophene S-oxide **124** and phenylacetylene. Only product **126b**, from oxyarylation of 2-methylbenzothiophene S-oxide, was observed during this reaction. Product **166**, from oxyarylation of the benzothiophene dopant, was not formed. Alone, this does not entirely rule out a stepwise mechanism as it is possible that the 2-methylbenzothiophene nucleofuge **123** is more reactive towards a gold

carbene intermediate than the dopant benzothiophene **100**. Experiment two shows the reaction between benzothiophene S-oxide **115** and phenylacetylene in the presence of the dopant 2-methylbenzothiophene **123**. Again, no product was observed from oxyarylation of the dopant **123**. The results of both experiments collectively support an intramolecular mechanism via [3,3]-sigmatropic rearrangement.

2.3.2 Effect of Sulfoxides on the Rate of Oxyarylation

During reaction screening studies, it was discovered that reducing the equivalents of the alkyne decreased the yield of the desired substituted benzothiophene products (see Table 1, entry 12 and 16). In addition, switching the stoichiometry of the reaction and using 2 eq of sulfoxide **124** with 1 eq of alkyne further reduced the yield of oxyarylation products (see Table 1, entry 17). As there was no significant change in side product formation, it was hypothesised that increasing the relative concentration of the sulfoxide reduced the rate of oxyarylation. Therefore, the effect of sulfoxide concentration was investigated alongside whether benzothiophene S-oxides were capable of co-ordinating to the gold catalyst thus tempering its catalytic activity. If this was the case, higher concentrations of alkyne may be required to push the reaction equilibrium towards productive gold-alkyne complexes.

To test how sulfoxide concentration affected the rate of the oxyarylation reaction, Bures' Variable Time Normalisation Analysis (VTNA) visual technique was used. This technique allows the order of a reactant to be estimated by monitoring product concentration over time.³² This method involves 'normalising' the X-axis, so that the trajectories of the two reaction profiles are no longer dependent on the substrate that differs in concentration across the two reactions. Reaction profiles of two reactions,

that differ only in the initial concentration of the substrate being studied, will overlay after the normalisation has been performed. In the example reactions one and two, $[A]_i$ is the same whilst $[B]_i$ is different (Figure 8).

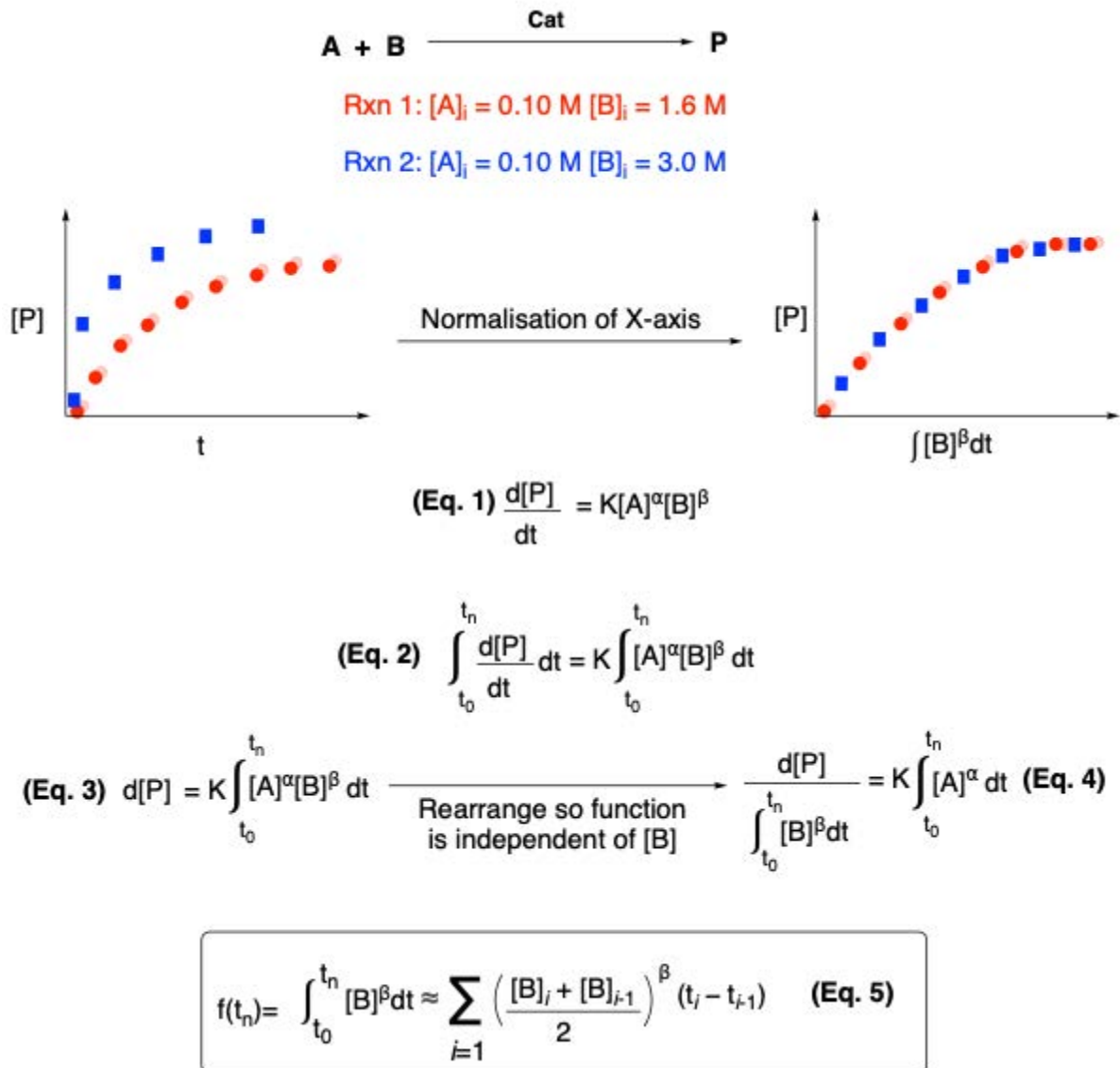


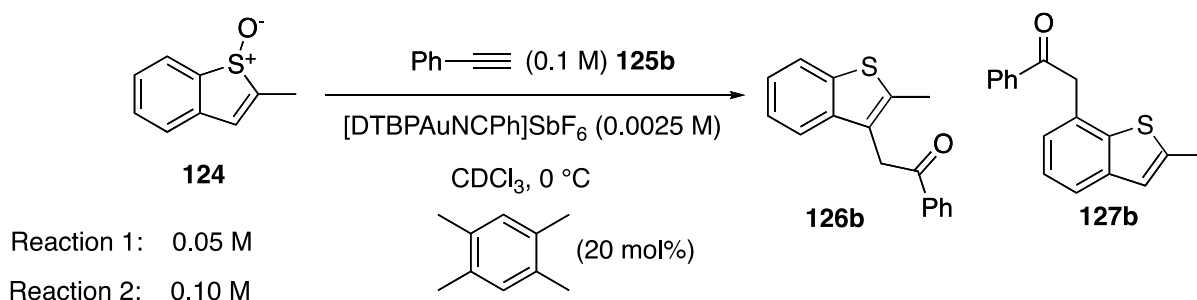
Figure 8. Derivation of the normalised abscissa for Bures' Variable Time Normalisation

Analysis to determine the order of reactants

The rate equation is integrated with respect to time, as the product concentration will be measured over a period of time t_0 to t_n (Figure 8, Eq. 1 to Eq. 2). The new normalized axis can be determined by performing a simple rearrangement of the integrated rate

equation (Figure 8, Eq. 3 to Eq. 4). $[P]$ is now plotted against $\int[B]^\beta dt$ on the X-axis, and the function is now independent of $[B]$. The component $\int[B]^\beta dt$ can be estimated using the trapezoid rule (Figure 8, Eq. 5) from experimentally determined $[B]$. The functions for experiments one and two should overlap when the order with respect to B is set to the correct value in the X-axis component. Therefore, the correct order with respect to B can be determined by trial and error until the functions for both reactions overlap.

This method was used to estimate the order of reaction with respect to 2-methylbenzothiophene S-oxide **124** in the gold-catalysed oxyarylation of phenyl acetylene. Two reactions were performed that differed only in the concentration of sulfoxide **124** (Scheme 36). The reactions were performed in an NMR tube and product concentration was monitored by 1H NMR spectroscopy using 1,2,4,5-tetramethylbenzene as internal standard. The presence of the internal standard was shown to have no effect on product formation prior to performing the VTNA studies.



Scheme 36. Reactions for VTNA measured by in situ 1H NMR spectroscopy (500 MHz)

One way of determining the order was to use the combined concentration of the C-3 and C-7 regioisomers (**126b** and **127b**) in the analysis. Performing the analysis in this way would assume that the order with respect to sulfoxide **124** was the same for the formation of both regioisomers. Another way would be to focus solely on the major C-3 regioisomer **126b**. However, this could be problematic as the measured change in

[sulfoxide **124**] is not directly proportional to the formation of **126b**. If the analysis is performed in this way, the C-7 regioisomer **127b** would be considered as a side product as it is not accounted for in the calculations. The original paper by Bures does not discuss how side product formation can be accounted for in the analysis, just that error in the determined order should be expected in the event of appreciable side product formation. The fact that sulfoxide **124** reacts to form more than one regioisomer complicates the analysis. However, as the purpose of visual kinetic analysis is to provide a facile means of estimating the order of reactants, it would provide a good starting point for better understanding the role of the sulfoxide.

Another thing to consider was how the concentration of sulfoxide **124** would be measured over the course of the reaction. The concentration can be calculated by deduction of the product concentration from the initial [sulfoxide **124**]. It can also be measured experimentally from the internal standard in the ^1H NMR spectra. It was discovered during these studies that there were slight discrepancies between the calculated and measured values of [sulfoxide **124**]. This is likely due to minimal side product formation, limitations in quantitative ^1H NMR analysis or a systematic error due to slight inaccuracies in the amounts of substrate added to the reaction.

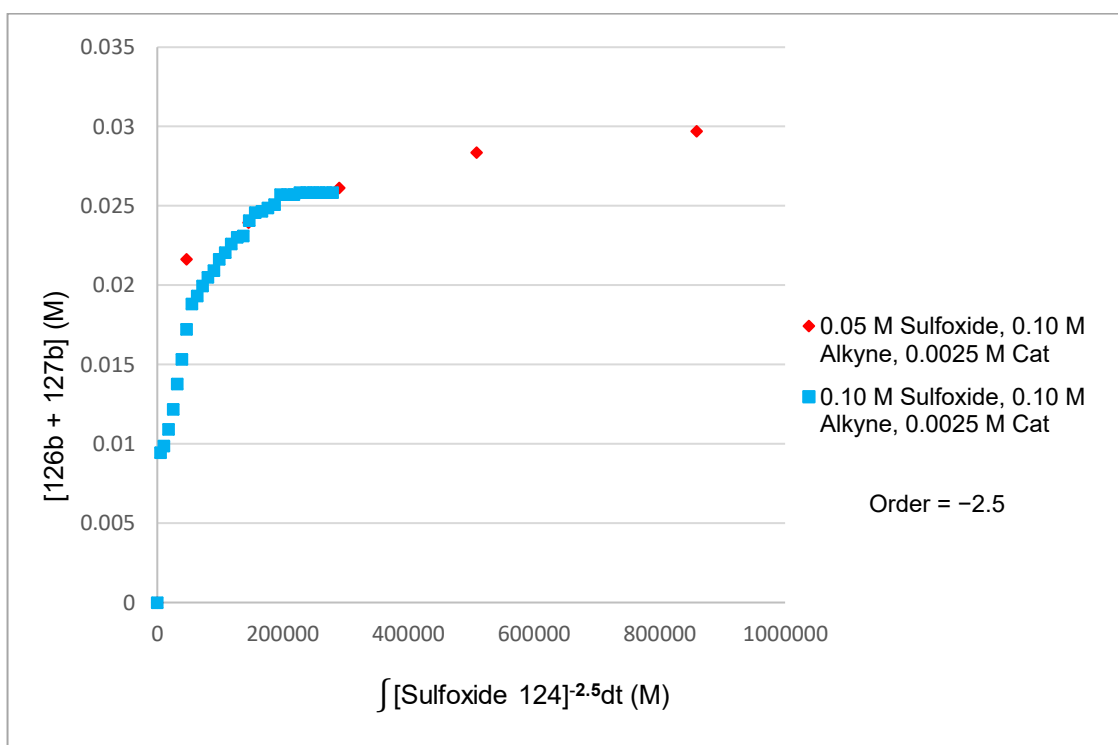
Four separate analyses were performed to account for the previously discussed limitations:

- Using measured values of [sulfoxide **124**] against [**126b** + **127b**] (Graph 1)
- Using calculated values of [sulfoxide **124**] against [**126b** + **127b**] (Graph 2)
- Using measured values of [sulfoxide **124**] against [**126b**] (Graph 3)

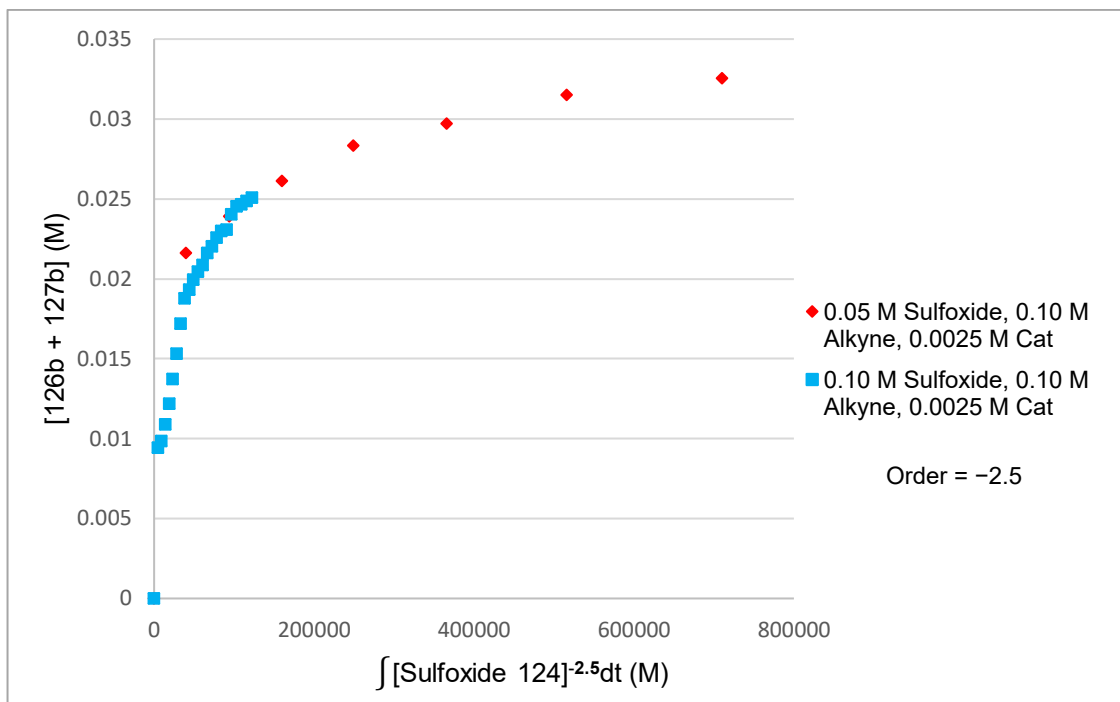
- Using calculated values of [sulfoxide **124**] against [**126b**] (Graph 4)

Fortunately, overlay of the reaction profiles for reactions 1 and 2 (Scheme 36) was possible in all four analyses. Additionally, the orders obtained across the four separate analyses were fairly consistent ranging from -2.1 to -2.7 with respect to sulfoxide **124** (Graphs 1 to 4). This shows that the complexities anticipated based on regioisomer formation and discrepancies between measured and calculated [sulfoxide **124**] did not drastically affect the results. As seen in graphs 1 to 4, there are more data points observed for reaction 2 vs reaction 1. Reaction 1 was a much faster reaction and so fewer data points were obtained over the same product concentration.

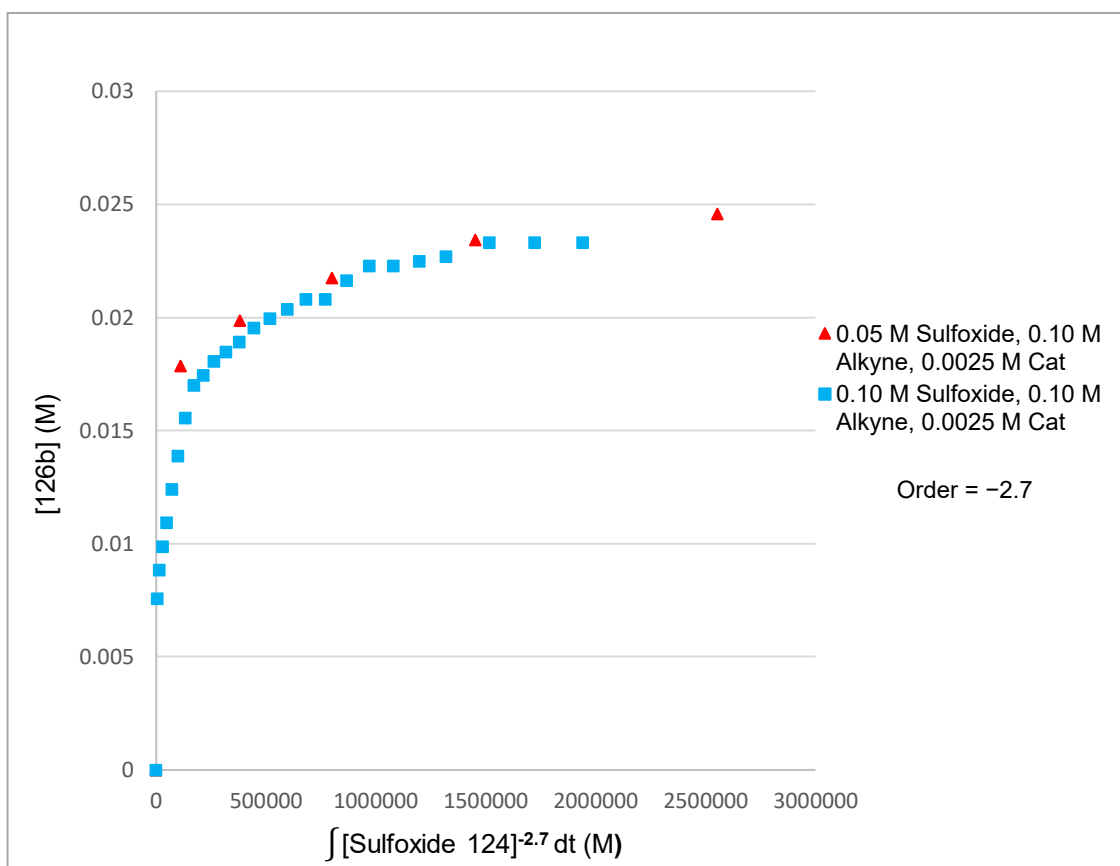
Graph 1. VTNA using [126b + 127b] and measured [Sulfoxide 124]



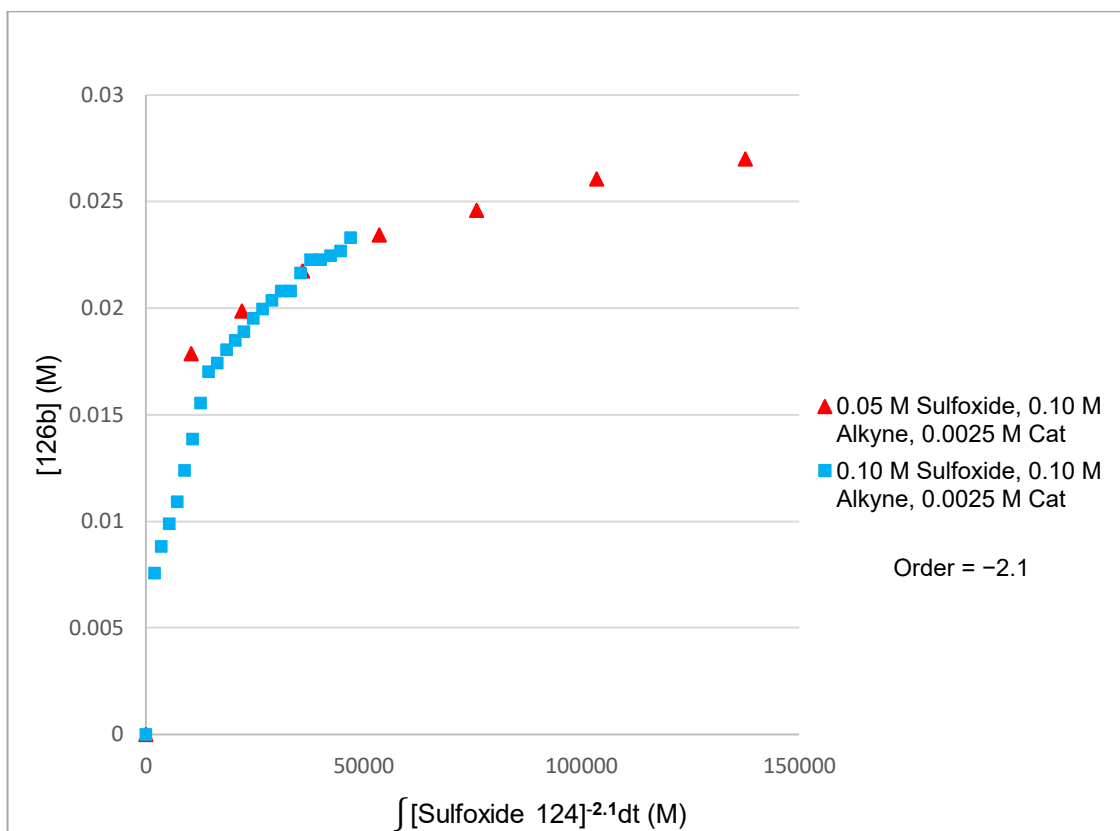
Graph 2. VTNA using [126b + 127b] and calculated [Sulfoxide 124]



Graph 3. VTNA using [126b] and measured [Sulfoxide 124]



Graph 4. VTNA using [126b] and calculated [Sulfoxide 124]

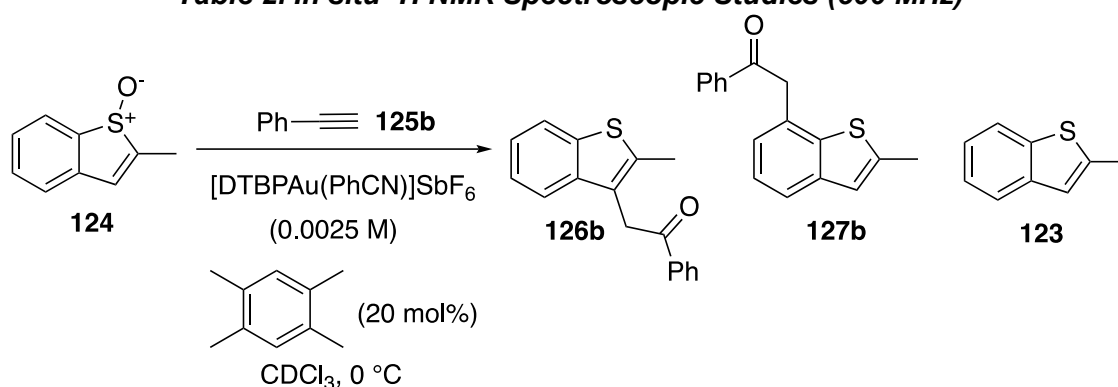


The analysis performed using calculated values of [sulfoxide **124**] against the C-3 regioisomer **126b** exclusively (graph 4) provided the least consistent order (-2.1) compared to the other three analyses (-2.5 and -2.7). A possible reason is that this analysis is subject to the most error of the four analyses; the C-7 regioisomer **127b** is not accounted for in the calculation, whilst the calculated [sulfoxide **124**] varies slightly from the measured [sulfoxide **124**] value.

Alongside the VTNA studies, which provided a negative order with respect to sulfoxide **124**, simply analysing the amount of product formed over a specific time period provided qualitative information on the effect of sulfoxide concentration. These in situ ¹H NMR spectroscopic studies show that under otherwise identical reaction conditions,

doubling the concentration of the limiting sulfoxide reagent **124** led to a substantial decrease in the product concentration over the same time period, with no significant increase in the free benzothiophene **123** (Table 2). As no other significant side-product formation was observed in these studies, it can be deduced that increasing the relative amount of sulfoxide **124** slows down the rate of oxyarylation.

Table 2. In situ ¹H NMR Spectroscopic Studies (500 MHz)



Reaction	Reaction time (mins)	Initial [124] (M)	Initial [125b] (M)	[126b+127b] (M)	[123] (M)
1	168	0.05	0.10	0.039	0.003
2	164	0.10	0.10	0.024	0.005

To further consolidate this work, a simultaneous comparison of batch- and slow-addition of sulfoxide **124** showed that slow-addition yielded more product over the same time period (Table 3). Therefore, maintaining a lower concentration of sulfoxide **124** over the course of the reaction was beneficial for product formation. As observed during optimisation, this problem is remedied in practice by increasing the equivalents of the alkyne relative to the limiting sulfoxide **124**. However, this work suggests that a

reduction of alkyne equivalents may be possible if the sulfoxide is added via syringe pump.

Table 3. Batch- vs. slow-addition of sulfoxide

Reaction	Reaction time (mins)	[126b] (M)	[127b] (M)	[126b + 127b] (M)	[123] (M)
One-pot	150	0.021	0.002	0.023	0.003
Syringe-pump addition	150	0.036	0.004	0.040	0.005

Studies were then conducted to see whether sulfoxide **124** was capable of co-ordinating to the gold-catalyst. Interestingly, an up-field shift in the ^{31}P NMR resonance of the gold catalyst $[\text{DTBPAu}(\text{PhCN})]\text{SbF}_6$ from 88 ppm to 81 ppm was observed in the presence of 2-methylbenzothiophene S-oxide **124** (Figure 9). There was no resonance for the free DTBP ligand observed in the ^{31}P NMR spectrum. In addition, the ^1H NMR and ^{13}C NMR spectra displayed resonances of the free benzonitrile. This indicates that ligand exchange at the gold centre occurs between the benzonitrile and sulfoxide **124** (Scheme 37). Together, in situ ^1H NMR spectroscopic studies, VTNA and ^{31}P NMR spectroscopic studies suggest that sulfoxide **124** is capable of co-ordinating to the gold-catalyst, temporarily removing it from the catalytic cycle.

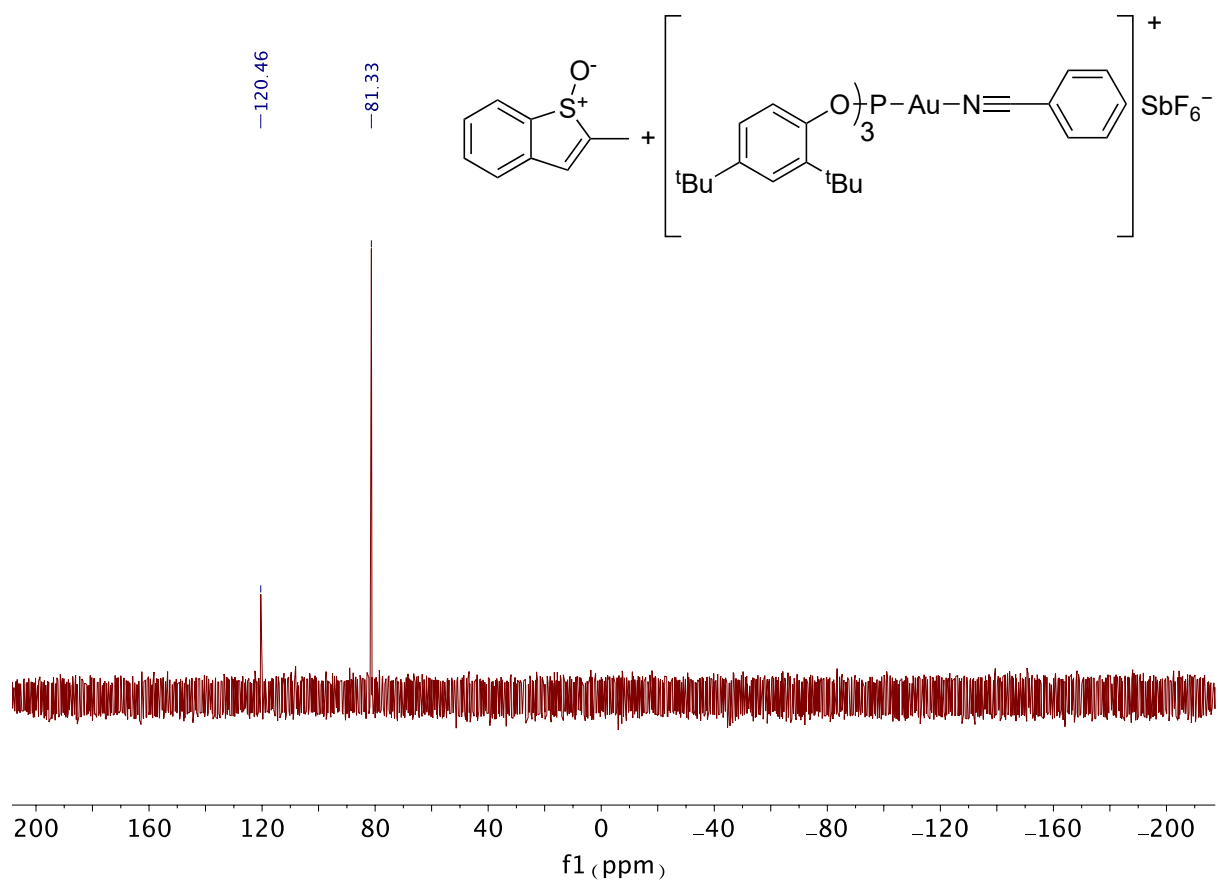
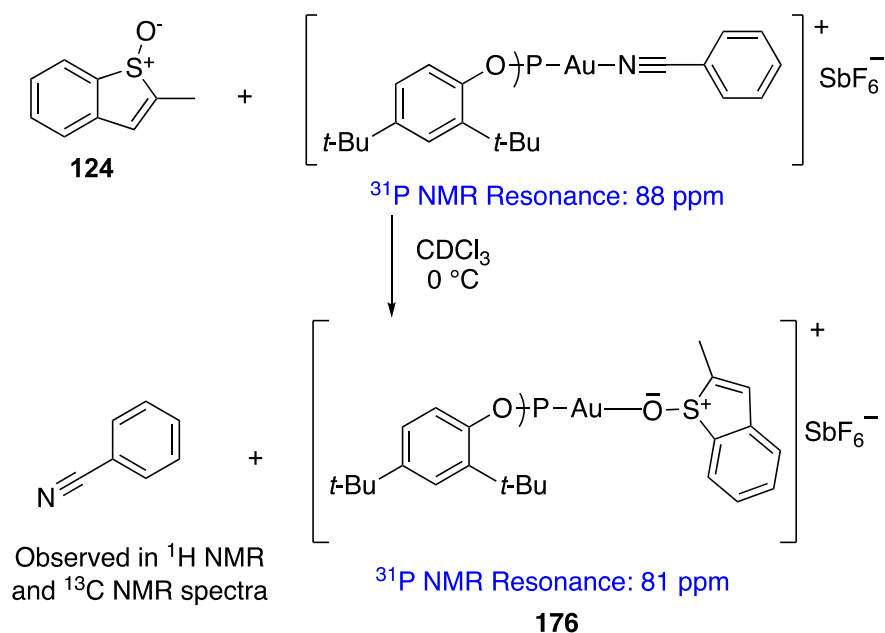
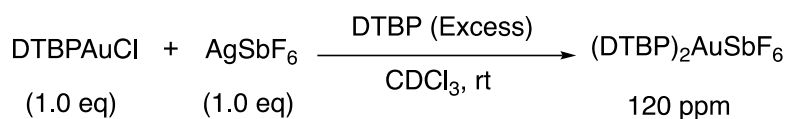


Figure 9. ^{31}P NMR spectrum of sulfoxide **124** with 5 mol% $[\text{DTBPAuNCPh}]\text{SbF}_6$ at 0 °C in CDCl_3 (202 MHz, ^1H decoupled)



Scheme 37. Sulfoxide-gold complex formed via ligand-exchange with benzonitrile

A smaller minor resonance at 120 ppm was also observed in the ^{31}P NMR spectrum when 5 mol% [DTBPAuNCPPh]SbF₆ was treated with sulfoxide **124** (Figure 9). A separate ^{31}P NMR experiment with DTBPAuCl (1.0 eq), AgSbF₆ (1.0 eq) and excess DTBP ligand in CDCl₃ also resulted in the same resonance at 120 ppm, indicating that this resonance represents the bis co-ordinated phosphite species (DTBP)₂AuSbF₆ (Scheme 38).

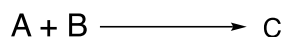


Scheme 38. ^{31}P NMR spectroscopic experiment for the formation of (DTBP)₂AuSbF₆

The resonance at 120 ppm was also observed on some occasions in the ^{31}P NMR spectrum of the untreated catalyst. As the initial catalyst tends to form this bis-phosphite gold complex in solution, a same excess experiment was performed to determine whether this species was the active catalyst or an unreactive degradation product.

2.3.3 Same Excess Experiment

Introduced by Donna Blackmond, same excess experiments are a type of visual kinetic analysis used to determine whether product inhibition or catalyst degradation are occurring during a reaction.³³ For a reaction involving two substrates A and B, the excess is described as the difference between the initial concentrations of the two substrates (Figure 10, Eq. 1). The excess is not associated with the number of equivalents; the excess remains constant even as the concentration of substrates A and B change throughout the reaction (if the reaction remains at a constant volume).



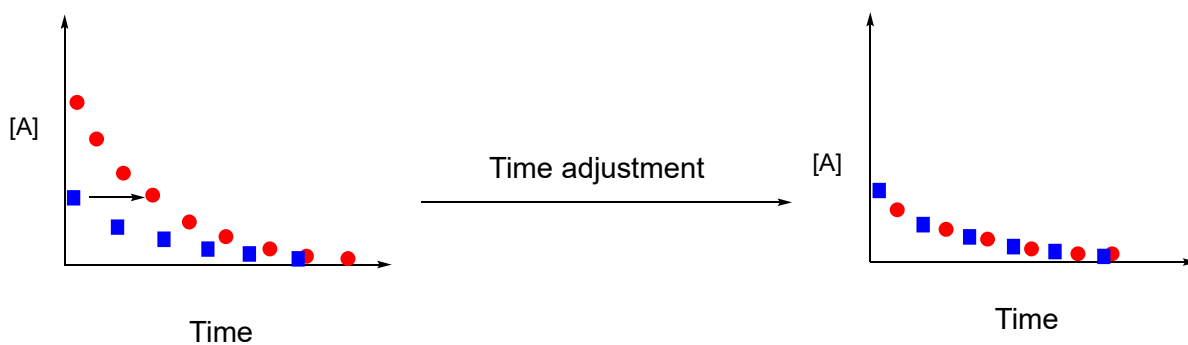
$$\text{Excess} = [A]_i - [B]_i \quad (\text{Eq. 1})$$

$$[A] = [A]_i - [B]_i + [B] = [\text{Excess}] + [B] \quad (\text{Eq. 2})$$

Figure 10. Determination of excess

In a same excess experiment, two separate reactions are performed that have different initial concentrations of both A and B, but both reactions have identical values of excess. The two experiments represent the same reaction that have both started at different places. For example, the reaction that begins with higher concentrations of A and B will eventually reach a point where both substrates are at the same concentration as the experiment that started with lower concentrations of A and B; this is possible as the [excess] remains constant over the course of the reaction. At a certain point in time the concentrations of both A and B will be identical for both reactions. However, the reactions will differ in two ways: the experiment that started with higher initial substrate concentrations will have a higher concentration of product in the reaction mixture and the catalyst turnover number will be higher. It is these differences that allow product inhibition and catalyst degradation to be probed using a same excess experiment. If there is no product inhibition or catalyst degradation, when the time adjustment is accounted for, the rates of both reactions should overlap over the period where the substrate concentrations are identical. If, however, the reaction that started with lower concentrations of substrates A and B has a higher reaction rate, then either product inhibition or catalyst degradation is taking place (Figure 11).

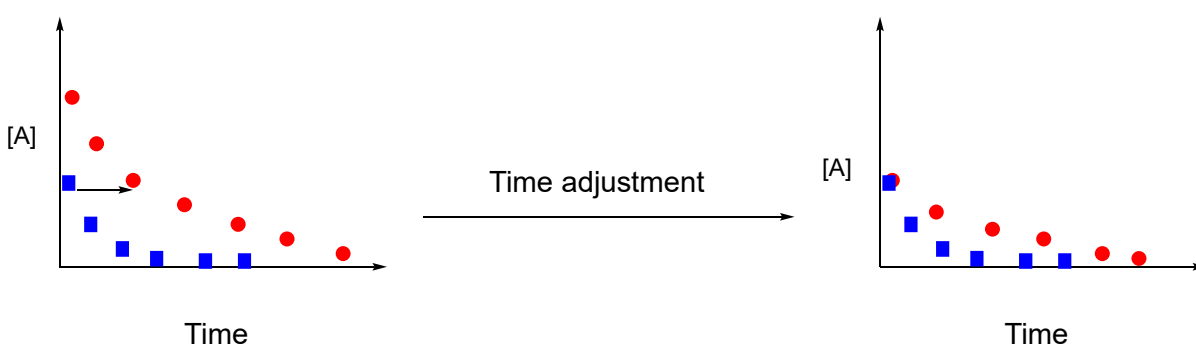
a) Example of a same excess experiment showing no catalyst degradation or product inhibition



● Exp 1: $[A]_i = 1.00 \text{ M}$ $[B]_i = 0.80 \text{ M}$, $[\text{Excess}] = 0.20 \text{ M}$

■ Exp 2: $[A]_i = 0.70 \text{ M}$ $[B]_i = 0.50 \text{ M}$, $[\text{Excess}] = 0.20 \text{ M}$

b) Example of a same excess experiment showing catalyst degradation or product inhibition



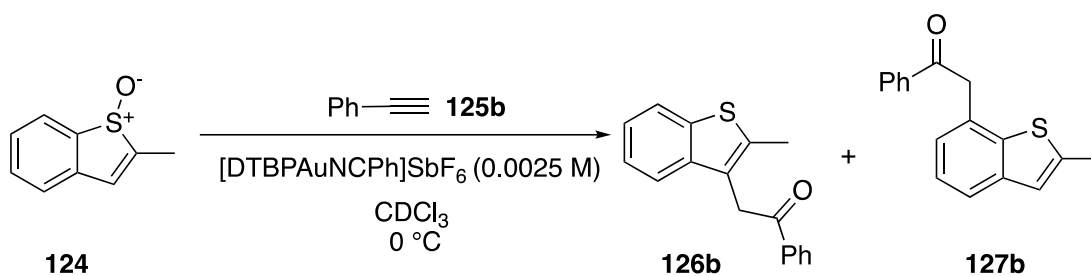
● Exp 1: $[A]_i = 1.00 \text{ M}$ $[B]_i = 0.80 \text{ M}$, $[\text{Excess}] = 0.20 \text{ M}$

■ Exp 2: $[A]_i = 0.70 \text{ M}$ $[B]_i = 0.50 \text{ M}$, $[\text{Excess}] = 0.20 \text{ M}$

Figure 11. Example of a same excess experiment a) without product inhibition or catalyst degradation and b) with product inhibition or catalyst degradation

A same excess experiment was performed for the reaction between phenylacetylene and 2-methylbenzothiophene S-oxide **124** (Scheme 39). The first experiment began with 0.15 M phenylacetylene **125b** and 0.10 M 2-methylbenzothiophene S-oxide **124**. The second experiment began with 0.10 M phenylacetylene **125b** and 0.05 M 2-methylbenzothiophene S-oxide **124**. The excess for both reactions 1 and 2 was

0.05 M (Scheme 39). The aim was to measure the rate of reaction 1 after the [sulfoxide **124**] had reached 0.05 M and compare this to the rate of reaction 2. The reactions were monitored by in situ ^1H NMR spectroscopy with a known concentration of internal standard 1,2,4,5-tetramethylbenzene.



Reaction 1: [Sulfoxide] = 0.10 M, [Alkyne] = 0.15 M, [Excess] = 0.05 M

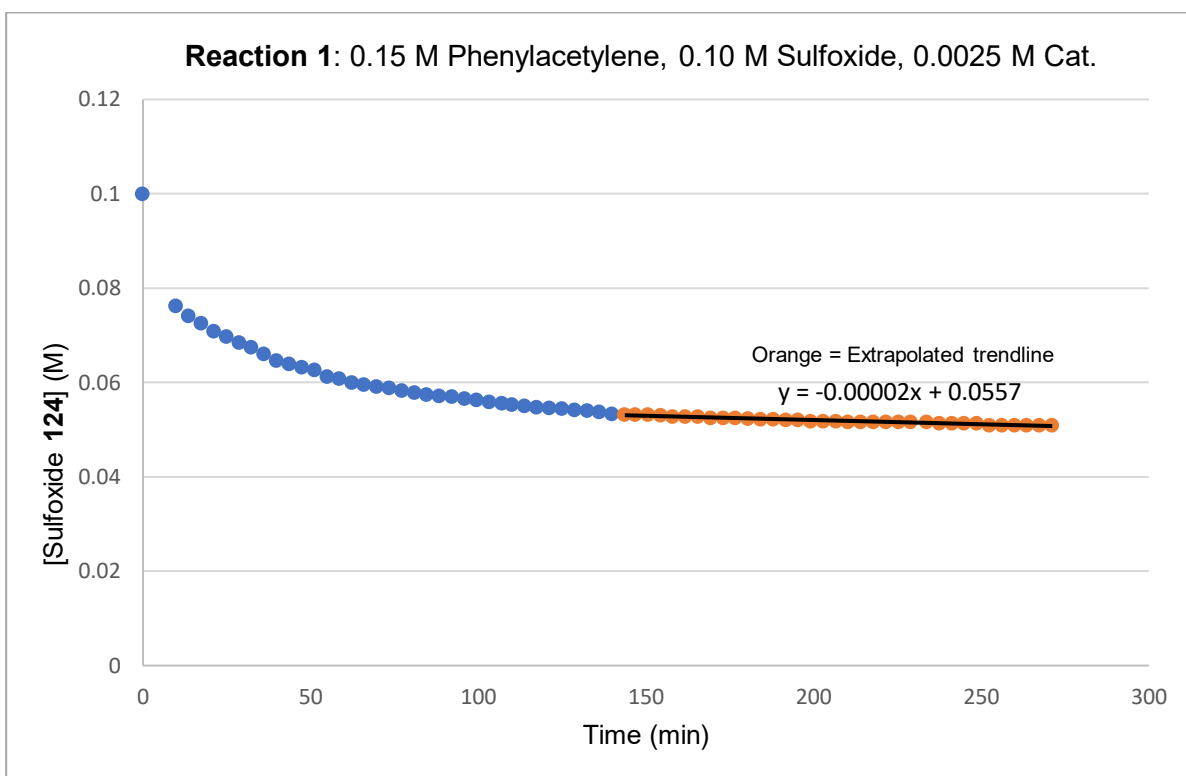
Reaction 2: [Sulfoxide] = 0.05 M, [Alkyne] = 0.10 M, [Excess] = 0.05 M

Scheme 39. Design of same excess experiment

The rate of the oxyarylation reaction was graphically represented as a change in [sulfoxide **124**] over time. Unfortunately, over the 4.5 h that reaction 1 was monitored, [sulfoxide **124**] did not reach 0.05 M and therefore did not reach the initial [sulfoxide **124**] of reaction 2 (Graph 5). After approximately 1.5 h, the rate of reaction 1 had drastically reduced and had begun to plateau. From this data, the rate of reactions 1 and 2 could not be compared over the same substrate concentrations. However, [sulfoxide **124**] had reached 0.51 M which was very close to the desired concentration for comparison with reaction 2. For this reason, a linear trendline was fitted for the last 2 h of reaction 1, where the rate had begun to plateau and resemble a straight line. Extrapolating from the trendline, to estimate the rate of reaction 1, would allow for comparison with reaction 2 and would provide an indication on whether studies into product inhibition or catalyst degradation should be pursued. Graph 5 shows the change in [sulfoxide **124**] over time for reaction 1. The trendline fitted for reaction 1 has

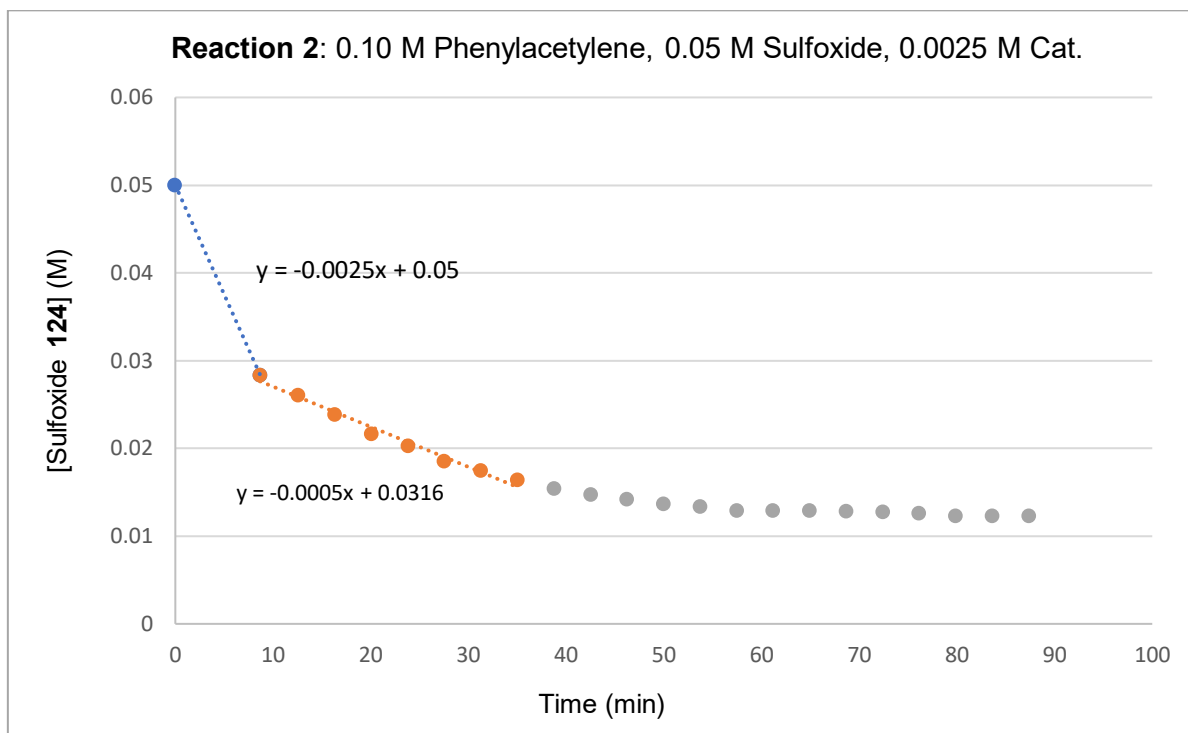
a gradient of -2×10^{-5} , estimating that 2×10^{-5} M of sulfoxide **124** was being consumed every minute over the last two hours of the reaction. After an initial decline, the rate of reaction 1 remained reasonably steady over the last 2 hours of monitoring, thus it is sensible to assume that this gradient represented a good approximation of the rate of reaction 1 if [sulfoxide **124**] were to reach 0.05 M.

Graph 5. Rate of oxyarylation for reaction 1



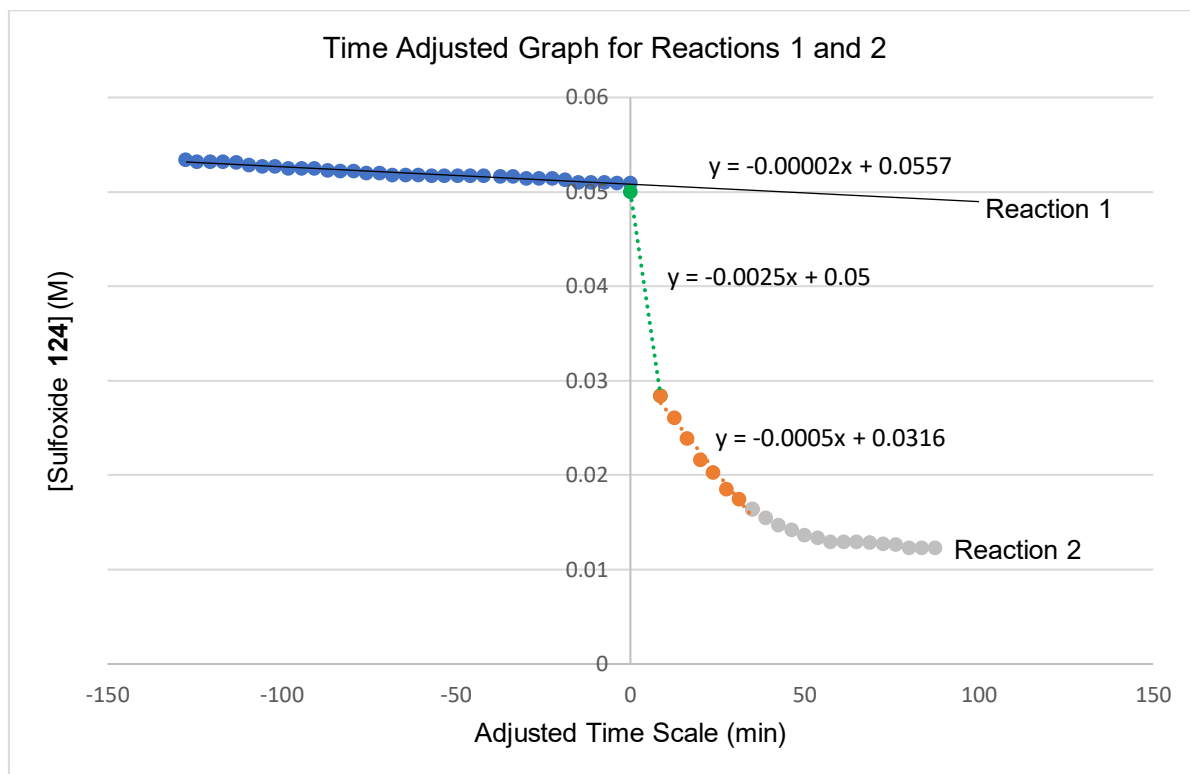
Graph 6 shows the change in [sulfoxide **124**] over time for reaction 2. The trendline for the first 10 minutes of this reaction has a gradient of -2.5×10^{-3} . This is nearly 2 orders of magnitude larger than the gradient of the trendline fitted for reaction 1 as [sulfoxide **124**] approaches 0.05 M. Even as reaction 2 begins to slow down after 10 minutes, the trendline fitted between 10 and 40 mins has a gradient of -5×10^{-4} , which is 1.4 orders of magnitude higher than the trendline fitted for reaction 1.

Graph 6. Rate of oxyarylation for reaction 2



In graph 7, a time adjustment has been performed on reaction 1 so that the extrapolated trendline can be compared to reaction 2 over the same substrate concentration. Making the reasonable assumption that the rate of reaction 1 remains steady or declines further after [sulfoxide **124**] has reached 0.05 M, it can be projected from this graph that the rate of reaction 1 was much slower than that of reaction 2 over the same substrate concentration. Due to the large discrepancy between the extrapolated rate of reaction 1 and the initial rate of reaction 2, it could be confidently determined that either product inhibition or catalyst degradation was taking place. Therefore, further studies were required into product inhibition and catalyst degradation to investigate these claims.

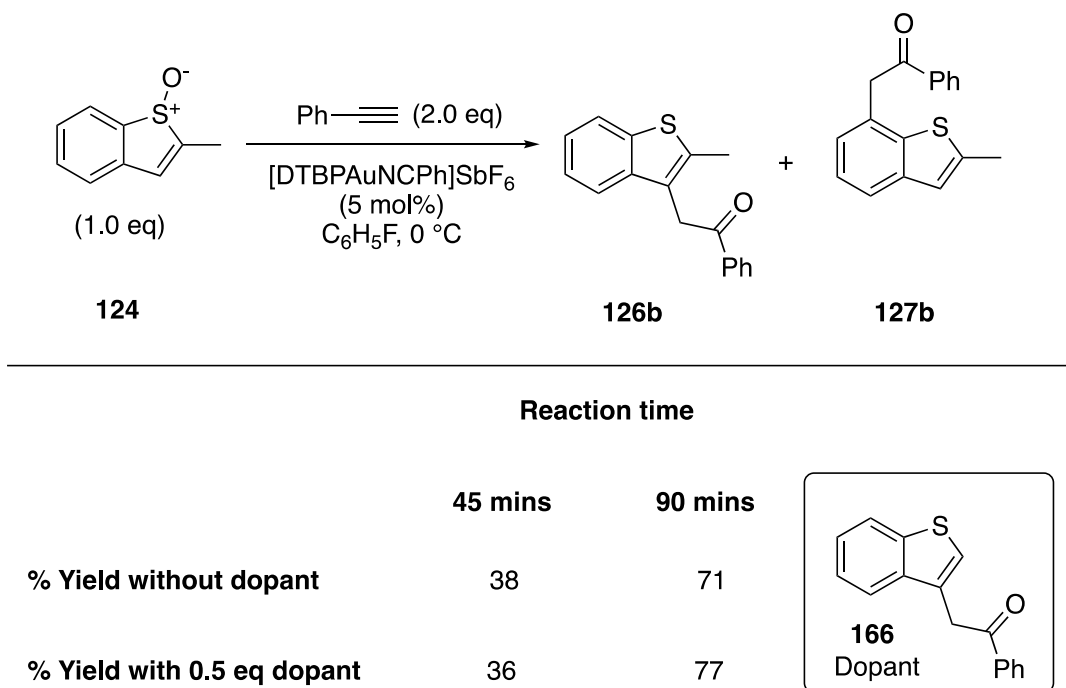
Graph 7. Time-adjusted graph for the same excess experiment with reactions 1 and 2



2.3.4 Product Inhibition Studies

Based on the results of the same excess studies, product inhibition was first explored. A doping experiment was performed to ascertain whether product inhibition occurred during the catalysis reaction. The reaction between 2-methylbenzothiophene S-oxide **124** and phenylacetylene **125b** was doped with oxyarylation product **166**. The reaction yield of the doped reaction was compared to a control reaction to see if the presence of **166** affected the product yield. To improve the reliability of these results, the study was repeated for different lengths of time, with yields taken at 45 minutes for one set of reactions and 90 minutes for the second set of reactions (Scheme 40). This study showed that the presence of the dopant had no detrimental effect on the yield of the oxyarylation products. In addition, when 5 mol% [DTBPAuNCPPh]SbF₆ was treated with

oxyarylation product **126b** in CDCl₃, there was no change in the ³¹P NMR resonance suggesting that the oxyarylation product does not undergo ligand exchange to coordinate at the gold centre.



Scheme 40. Product inhibition studies for gold-catalysed oxyarylation of alkynes with benzothiophene S-oxide

2.3.5 Catalyst Spectroscopic Studies

As product inhibition was not observed in the previous study, catalyst degradation was investigated. Previous studies had shown small amounts of (DTBP)₂AuSbF₆ were formed from [DTBPAuNCPH]SbF₆ in solution and in the presence of sulfoxide **124**. Addition of phenylacetylene **125b** to [DTBPAuNCPH]SbF₆ also saw formation of (DTBP)₂AuSbF₆. The resonance at 120 ppm was observed as one of the major resonances alongside other undetermined resonances (Figure 12).

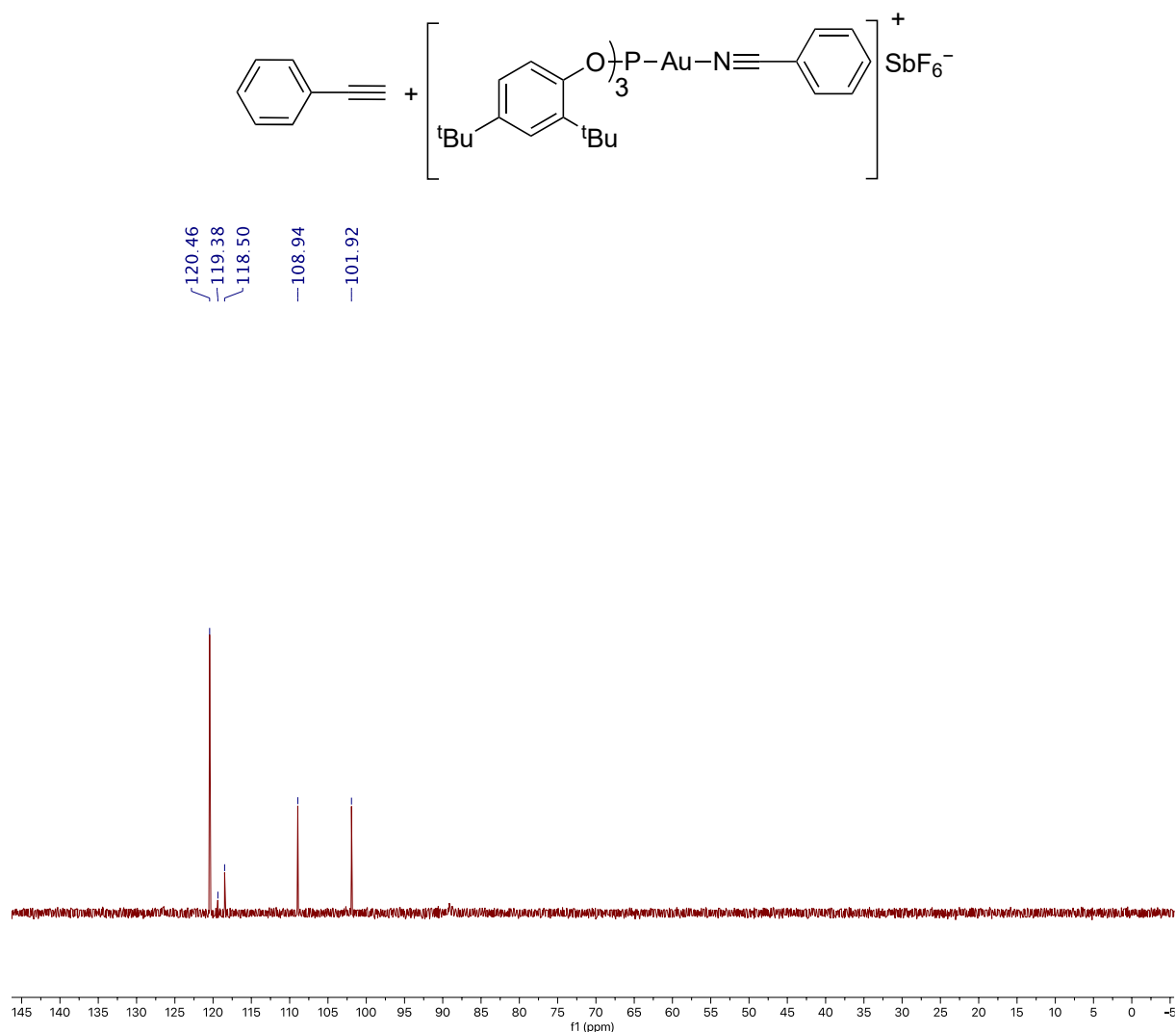
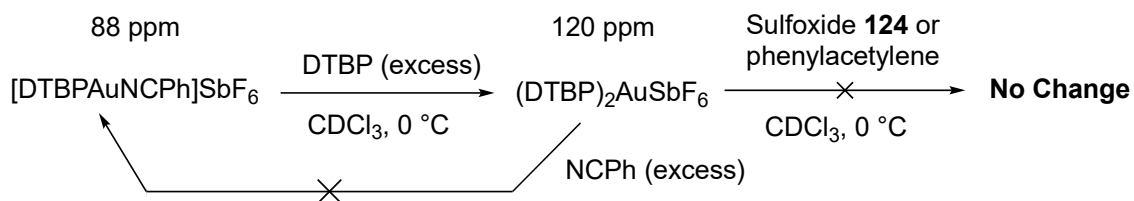


Figure 12. ^{31}P NMR spectrum of phenylacetylene with 5 mol% $[DTBPAuNCP]SbF_6$ at rt in $CDCl_3$ (162 MHz)

The bis-phosphite species $(DTBP)_2AuSbF_6$ can also be formed from the $[DTBPAuNCP]SbF_6$ catalyst in the presence of DTBP. The formation is not reversible, as addition of excess benzonitrile to $(DTBP)_2AuSbF_6$ does not reform the original catalyst. In addition, there is no change in the ^{31}P NMR resonance when 5 mol% $(DTBP)_2AuSbF_6$ was treated with sulfoxide **124** or phenylacetylene **125b** (Scheme 41). This indicates that ligand exchange at the $(DTBP)_2AuSbF_6$ catalyst is not favourable. Therefore, it is unlikely that $(DTBP)_2AuSbF_6$ can catalyse the oxyarylation reaction.



Scheme 41. ^{31}P NMR spectroscopic studies with $(\text{DTBP})_2\text{AuSbF}_6$

^{31}P NMR spectroscopic monitoring was performed on the oxyarylation reaction to study to formation of $(\text{DTBP})_2\text{AuSbF}_6$ over the course of the reaction (Figure 13). This study showed the disappearance of the $[\text{DTBPAuNCPH}]\text{SbF}_6$ resonance after addition of the substrates and an initial increase in the intensity of the $(\text{DTBP})_2\text{AuSbF}_6$ resonance at 120 ppm. Over the course of the reaction, the intensity of the $(\text{DTBP})_2\text{AuSbF}_6$ resonance gradually decreased which coincided with an increase in intensity of a resonance at 131 ppm. This resonance is only slightly downfield compared to the free DTBP ligand by 1ppm. Therefore, it is possible that this resonance represents the free DTBP ligand that is experiencing perturbation due to interactions with other species in the complex reaction solution. It was tested whether weak coordination of the free DTBP ligand with other gold species in solution at 0 °C may have caused this slight shift in the resonance. However, the ^{31}P NMR spectrum of DTBP in the presence of $(\text{DTBP})_2\text{AuSbF}_6$ and $[\text{DTBPAuNCPH}]\text{SbF}_6$ at 0 °C did not result in a shift in the resonance of the DTBP ligand, thus the identity of the resonance at 131 ppm could not be confirmed. The ^{31}P NMR spectroscopic monitoring study clearly showed that the $[\text{DTBPAuNCPH}]\text{SbF}_6$ catalyst changed over the course of the reaction and same excess studies support degradation of the catalyst to unreactive species. There were also other minor ^{31}P NMR resonances observed during this study. The resonances at 101 ppm and 108 ppm appear to represent alkyne-gold complexes as they were also

observed in the previous ^{31}P NMR spectrum of phenylacetylene **128b** with $[\text{DTBPAuNCPH}]\text{SbF}_6$ (see Figure 12).

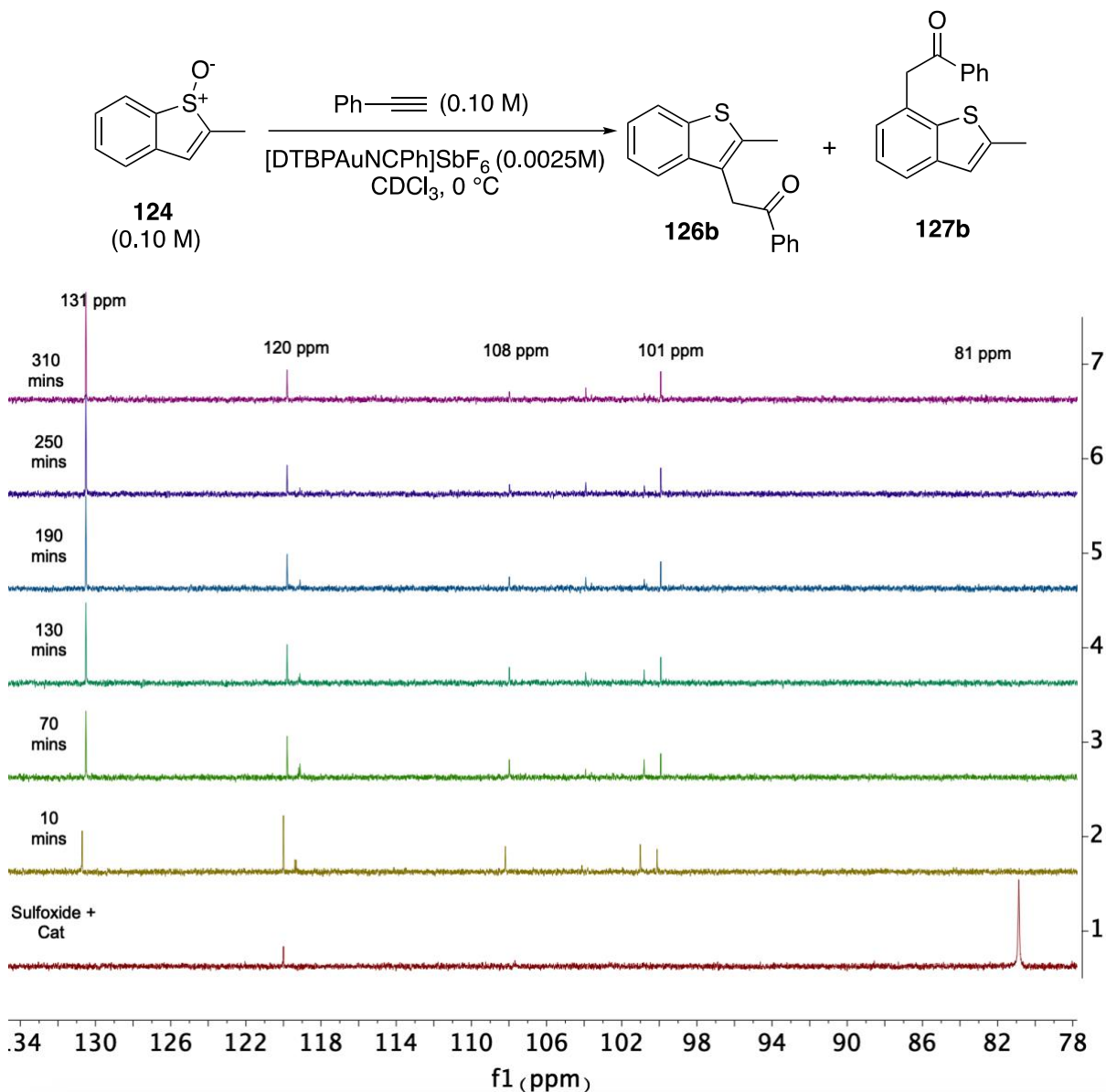
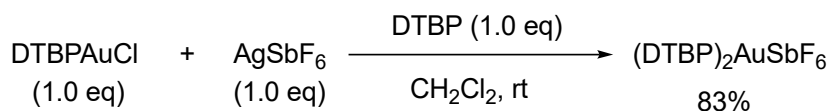


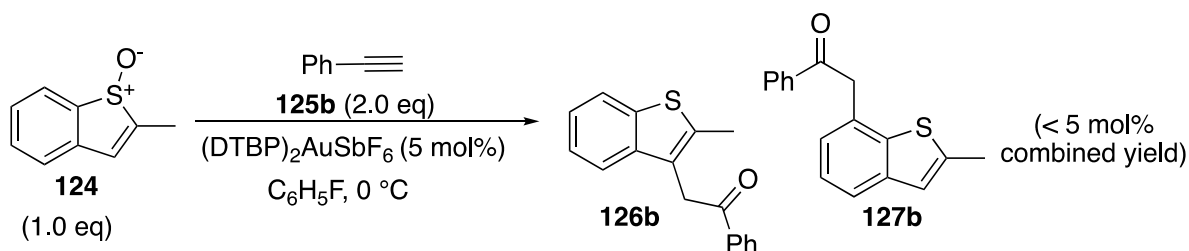
Figure 13. ^{31}P NMR spectroscopic monitoring study of oxyarylation reaction

As there was no change in the ^{31}P NMR resonance when $(\text{DTBP})_2\text{AuSbF}_6$ was treated with the sulfoxide **124**, phenylacetylene or excess benzonitrile, the complex appears to be very stable. For this reason, $(\text{DTBP})_2\text{AuSbF}_6$ was synthesised from DTBPAuCl with AgSbF_6 and the DTBP ligand, and the bis-phosphite gold complex was isolated in 83% yield (Scheme 42).



Scheme 42. Formation of the bis-phosphite gold complex (DTBP)₂AuSbF₆

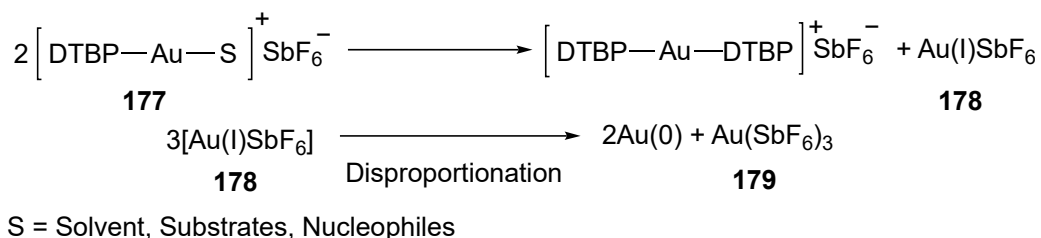
(DTBP)₂AuSbF₆ was then used in a reaction with sulfoxide **124** and phenylacetylene (Scheme 43). The reaction was performed twice and, in both cases, only a trace amount of the combined oxyarylation products **126b** and **127b** (<5%) were observed by ¹H NMR analysis of the crude reaction material after an extended reaction time (> 24h) (Scheme 43). This shows that the formation of (DTBP)₂AuSbF₆ is essentially a catalytic dead-end and therefore contributes to the reduction in rate observed in the same excess experiments. This highlights the demand for more robust phosphite gold catalysts to be developed.



Scheme 43. Attempted oxyarylation of phenylacetylene with sulfoxide **124 and (DTBP)₂AuSbF₆**

The formation of bis-coordinated gold phosphine species during catalysis has been observed by other groups.³⁴ It is reported that the formation of symmetrical bis-coordinated gold-complexes is a result of catalyst degradation that eventually leads to the disproportionation of Au(I) (Scheme 44). Ligand exchange between two gold-complexes **177** occurs to form the symmetrical bis-coordinated gold catalyst and the Au(I) salt **178**. The Au(I) salt then undergoes irreversible disproportionation to form gold nanoparticles and a gold Au(III) salt **179**. It was difficult to observe the formation of gold nanoparticles during the oxyarylation reactions as the reactions were not clear

and often coloured, however the presence of the bis-phosphite complex (DTBP)₂AuSbF₆ is indicative of gold nanoparticle formation over the course of the reaction.



Scheme 44. Proposed mechanism for the degradation of gold (I) complexes

2.4 Conclusion and Outlook

This is the first demonstration of gold-catalysed oxyarylation of alkynes to a non-benzenoid ring where the sulfoxide is integrated within the ring. The reaction was successful with a variety of electron-rich and electron-deficient aromatic and aliphatic terminal alkynes. The method can be adapted to accommodate nitrogen-containing and electron-deficient alkynes by performing the reactions at higher temperatures without detrimentally affecting product formation or regioselectivity. High C-3 regioselectivities were observed with aromatic alkynes across all benzothiophenes. Excellent yields were also obtained with aliphatic alkynes, despite the lower regioselectivities seen. The method also tolerates halogenated benzothiophenes and C-2 substituted benzothiophenes. Oxyarylation of phenylacetylene with benzothiophene S-oxide was successful using a telescoped oxidation-catalysis protocol. Overall, a robust method has been developed for the synthesis of a diverse range of C-3 alkylated benzothiophenes under mild conditions. Most alkyne and benzothiophene S-oxide starting materials can be synthesised in one step, providing an efficient means to access a range of alkylated benzothiophenes. The novel

substitution pattern contains a carbonyl moiety, providing a synthetic handle for further elaboration.

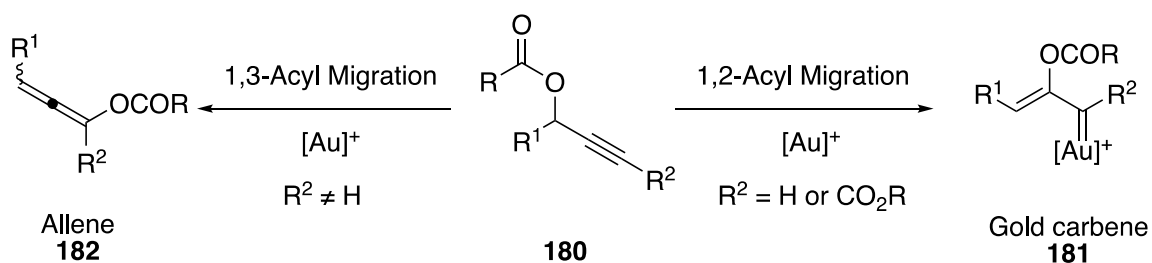
The mechanistic studies support a pathway consistent with what was described by Ujaque and Asensio, where addition of the sulfoxide to the alkyne generates a vinyl gold carbenoid intermediate which proceeds via [3,3]-sigmatropic rearrangement.¹¹ Intermolecular nucleophilic capture of an intermediate gold carbene was ruled out by cross-over experiments. In addition, VTNA and in situ ¹H NMR spectroscopic studies show that increasing the concentration of the benzothiophene S-oxide inhibits catalytic activity. One proposed reason for the observed reduction in reactivity is that the sulfoxide coordinates to the gold catalyst, temporarily removing it from the catalytic cycle. This is supported by an up-field shift in the ³¹P NMR resonance of the [DTBPAuNCPPh]SbF₆ catalyst in the presence of 2-methylbenzothiophene S-oxide. Slow addition of sulfoxide or increasing the relative concentration of the alkyne can remedy sulfoxide inhibition, allowing oxyarylation to proceed excellently. Decomposition of the [DTBPAuNCPPh]SbF₆ catalyst was supported by a same excess experiment and ³¹P NMR spectroscopic monitoring saw the formation of (DTBP)₂AuSbF₆, which is essentially a catalytic dead end for the desired process. Product inhibition from the functionalised benzothiophene was ruled out by a doping experiment. This study provides a greater understanding of the role of sulfoxides in gold-catalysed reactions and may aid the development of more efficient sulfoxide-based reactions in the future. In addition, these studies highlight to need for more robust electron deficient, cationic Au(I) catalysts that have a higher catalytic turn-over.

**Chapter 3: Gold-Catalysed
Rearrangements of Sulfenylated
Propargyl Carboxylates**

3.1 Introduction

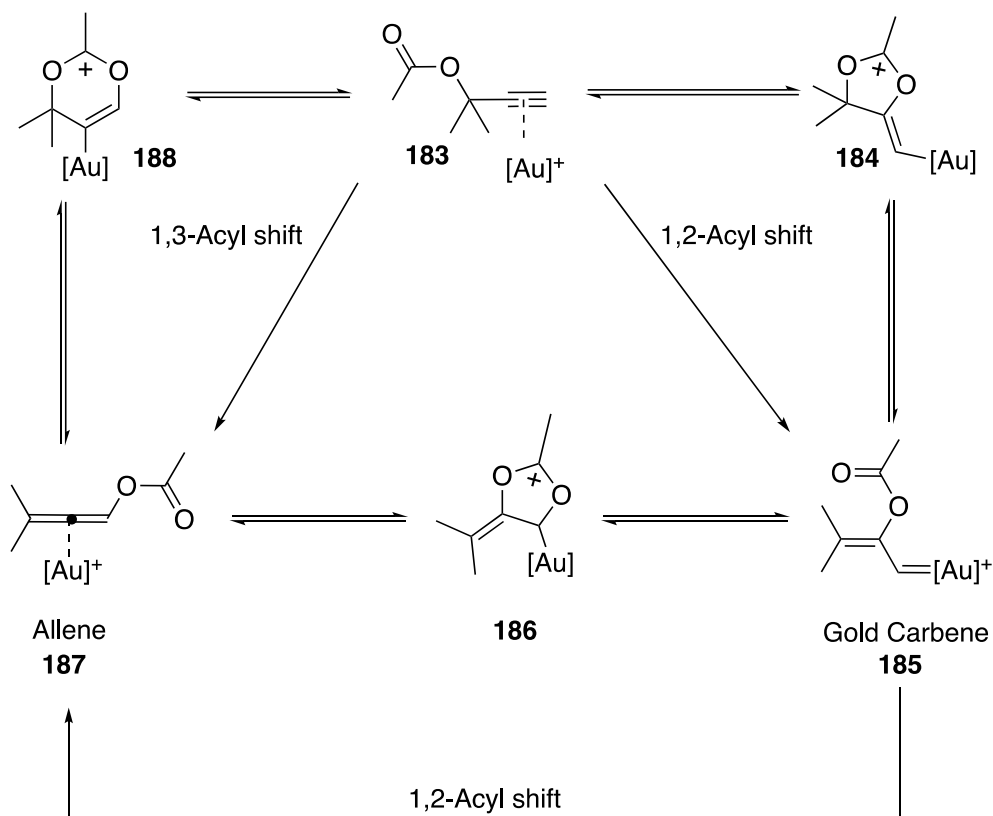
3.1.1 Gold-Catalysed Rearrangements of Propargyl Carboxylates

Propargyl carboxylates **180** are highly versatile substrates when subject to gold catalysis. Their readiness to undergo either 1,2- or 1,3-acyl migration leads to the formation of reactive gold carbene **181** or allene **182** intermediates respectively (Scheme 45)³⁵. Following 1,3-acyl migration, the generated allene can be further activated by the gold catalyst, rendering it electrophilic. Both intermediates can undergo a variety of transformations leading to products with great structural complexity, some of which will be discussed in this section. The reactivity of these substrates can usually be anticipated; terminal and electron deficient propargyl carboxylates generally favour 1,2-acyl migration whilst internal and electronically unbiased propargyl carboxylates generally favour 1,3-acyl migration.³⁵⁻³⁶



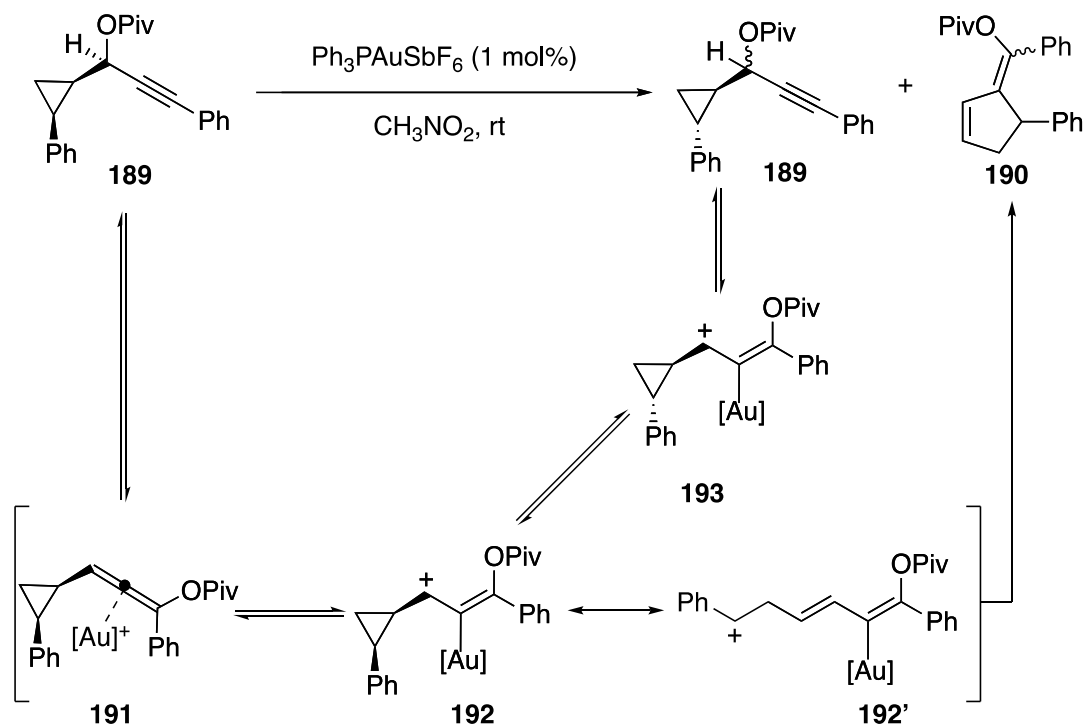
Scheme 45. Gold-catalysed rearrangement pathways of propargyl carboxylates

It is proposed that the gold carbene and gold-activated allene intermediates are interconvertible. Nolan reports a reversible process supported by DFT calculations based on both $IMe-$ and PMe_3 -ligated gold catalysts. This equilibrium was coined the “Golden Carousel in Catalysis” (Scheme 46).³⁷ These DFT calculations show that formation of the allene **187** by a double 1,2-acyl shift is favoured over direct 1,3-acyl migration. However, the preference is minimal and experimentally the pathways would be influenced by the nature of the substrate and reaction conditions.



Scheme 46. The “golden carousel” of propargyl carboxylates according to Nolan

Toste provided experimental evidence for the reversibility of these rearrangements, consolidating the computational work reported by Nolan.³⁸ Propargylic carboxylate **189**, that is stereodefined at the propargylic position, undergoes 1,3-acyl migration followed by cyclopropane ring opening to provide cyclopentene **190**. In situ ¹H NMR reaction monitoring saw scrambling of the stereochemistry at the propargylic position after 2 minutes, providing evidence for a rapidly reversible 1,3-pivalate migration process (Scheme 47). *Cis* to *trans* isomerisation of the cyclopropane also took place but was slower, taking over 1 hour, providing the thermodynamically favourable *trans* cyclopropane as a mixture of 1:1 diastereoisomers with respect to the pivalate (Scheme 47). This highlights the cationic nature of the gold-bound intermediates, with the positive charge being stabilised by the phenyl-substituted cyclopropane.

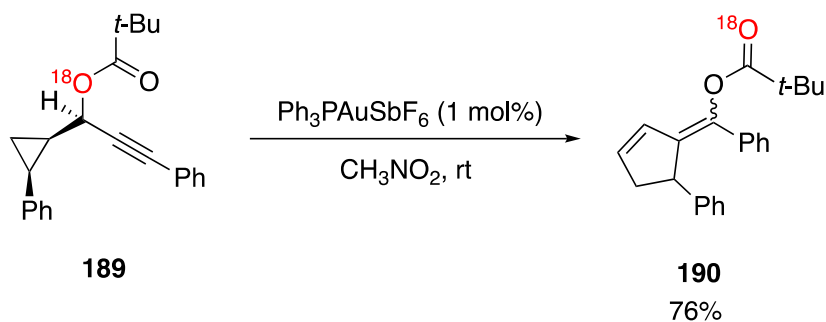


¹H NMR reaction monitoring results:

Time	Yield 189	189 <i>Trans:Cis</i>	189 d.r.	Yield 190
t = 2min	59%	40:60	1:1	41%
t = 10 min	33%	75:25	1:1	54%
t = 1 h	12%	>97:3	1:1	66%
t = 8 h	0%			75%

Scheme 47. Rearrangement and scrambling of substrate 189 stereochemistry by Toste

In this same study by Toste and co-workers, an ¹⁸O-labelling study provided evidence that the allene **191** is generated via direct 1,3-acyl migration rather than double 1,2-acyl migration (Scheme 48). If a double migration process was in effect, then the ¹⁸O-label would be directly bonded to the alkene in the product **190**. This contrasts with the computational studies reported by Nolan. However, Nolan's studies involved terminal alkyne **183** whilst Toste explored the reactivity of internal alkyne **189**, and so it is expected for these substrates to favour different rearrangement pathways. The result of the ¹⁸O-labelling study is also consistent with a mechanism that does not involve ionisation of the pivalate.

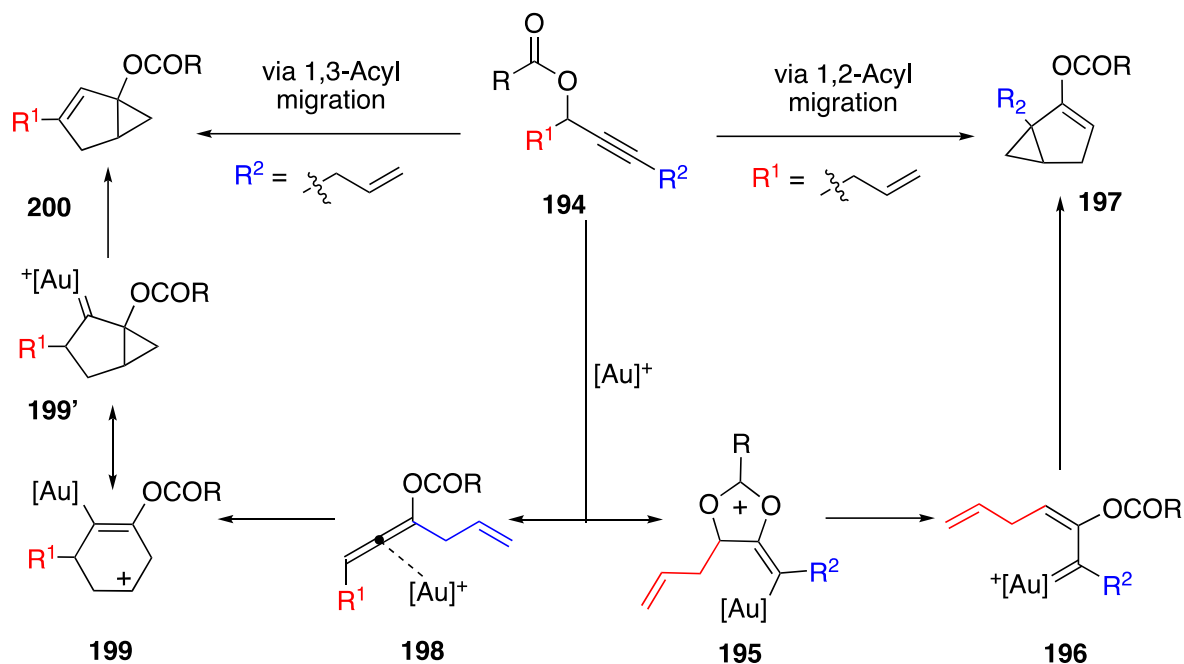


Scheme 48. ¹⁸O-labelling study supporting direct 1,3-pivalate migration by Toste

3.1.2 Intramolecular Cyclisation Reactions of Propargyl Carboxylates

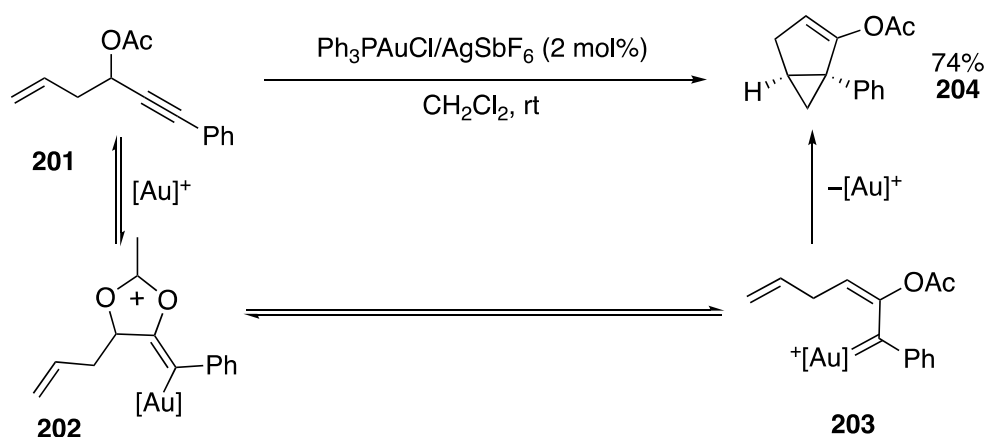
3.1.2.1 Cycloisomerisation of Enyne Carboxylates

Propargyl carboxylates with an allyl substituent at either the propargylic position or the alkyne terminus undergo cycloisomerisation under gold catalysis (Scheme 49). With the allyl substituent at the propargylic position, 1,2-acyl migration occurs to generate a gold-carbene intermediate **196** via **195**. Cyclopropanation of the tethered alkene at the gold carbene results in the final bicyclo[3,1,0]hexene product **197**. In comparison to what is known about the rearrangements of propargyl carboxylates, substrates of this type undergo 1,2-acyl migration even when the alkyne is internal. This is likely due to the fact that there is no productive downstream pathway available for these substrates after 1,3-acyl migration.³⁹ On the other hand, when the allyl substituent is positioned at the alkyne terminus, 1,3-acyl migration occurs to generate an allene intermediate **198**. A 6-*endo*-trig cyclisation at the gold-activated allene is proposed for the formation of intermediate **199**, followed by gold carbene formation. Finally, 1,2-C-H migration at the gold carbene leads to the final bicyclo[3,1,0]hexene product **200**.



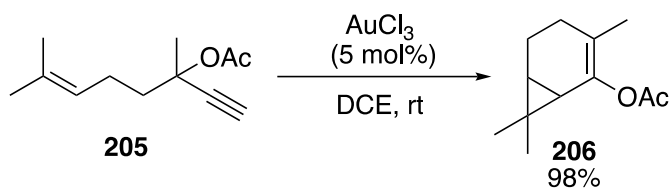
Scheme 49. Gold-catalysed cycloisomerisation of enyne carboxylates

The potential of gold-catalysed rearrangements of propargyl carboxylates was not realised until the early 2000s when Fürstner demonstrated the cycloisomerisation of 1,5-enyne acetate **201** (Scheme 50).⁴⁰ As the allyl substituent is positioned at the propargylic position, the transformation proceeds via 1,2-acyl migration followed by cyclopropanation at the gold carbene **203**.



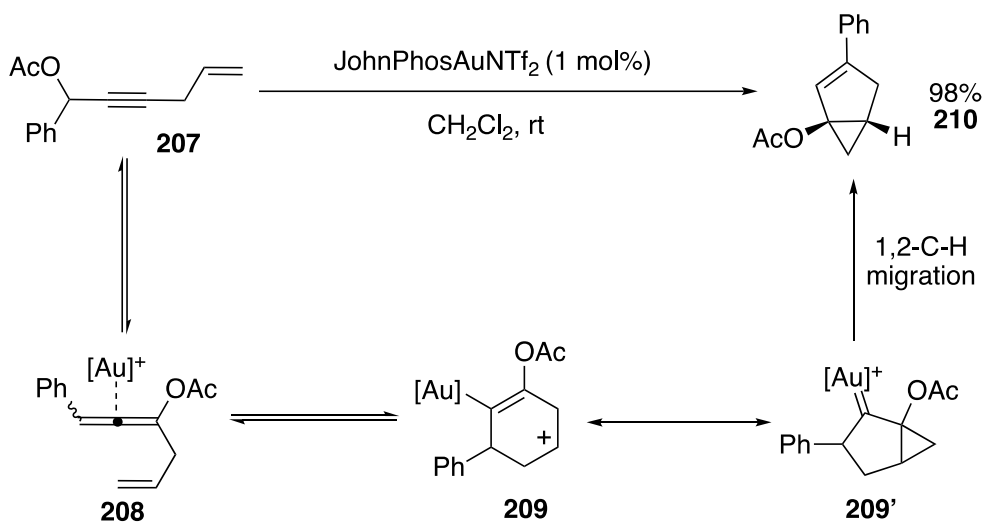
Scheme 50. Gold-catalysed cycloisomerisation of 1,5-enyne acetate by Fürstner

Fürstner also demonstrated that 1,6-enyne acetate **205** could undergo gold-catalysed cycloisomerisation to provide the bicyclo[1,4,0]heptene product **206** (Scheme 51).⁴¹



Scheme 51. Cycloisomerisation of 1,6-enyne carboxylate by Fürstner

Gagosz demonstrated the gold-catalysed cycloisomerisation of 1,4-enyne acetate **207** (Scheme 52).⁴² As the allyl substituent is positioned at the alkyne terminus, 1,3-acyl migration takes place. Gagosz and co-workers used this methodology to synthesise the bicyclo[3,1,0]hexene product **210**, which is an isomer of product **204** previously reported by Fürstner.

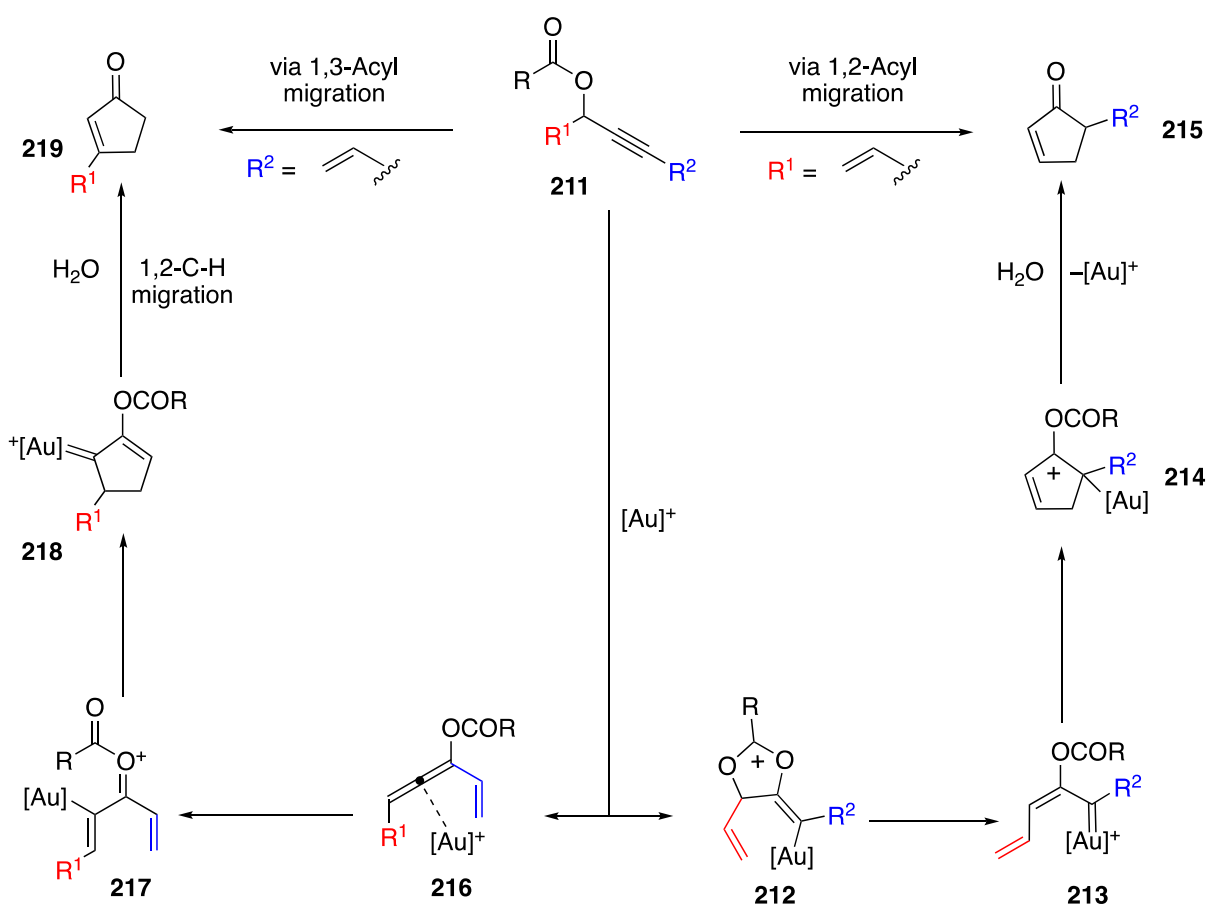


Scheme 52. Proposed mechanistic pathway for the gold-catalysed rearrangement and cyclopropanation of 1,4-enyne acetate by Gagosz

3.1.2.2 Nazarov Cyclisation Reactions of Enyne Carboxylates

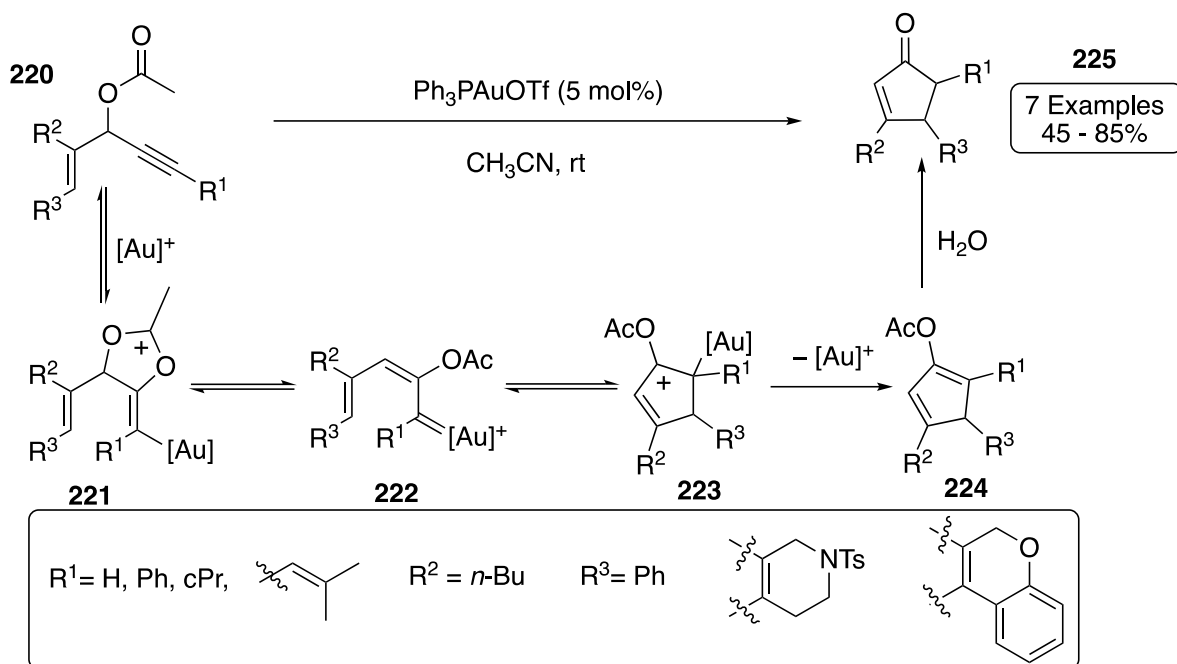
Propargyl carboxylates with a vinyl substituent at either the propargylic position or the alkyne terminus undergo gold-catalysed Nazarov rearrangements to yield cyclopentenone products after hydrolysis of the carboxylate (Scheme 53). The position of the vinyl substituent on the propargyl carboxylate skeleton determines the type of product formed and the mechanistic pathway taken. With the vinyl substituent at the

propargylic position, the substrate **211** undergoes 1,2-acyl migration to generate the gold-carbene intermediate **213** via **212**. Nazarov cyclisation, loss of the cationic gold catalyst and carboxylate hydrolysis forms the cyclopentenone **215**. When the vinyl substituent is at the alkyne terminus, 1,3-acyl migration takes place followed by Nazarov cyclisation of intermediate **217**. 1,2-C-H migration at the gold carbene **218** yields a cyclopentadiene product which is hydrolysed to the cyclopentenone **219** under the reaction conditions.



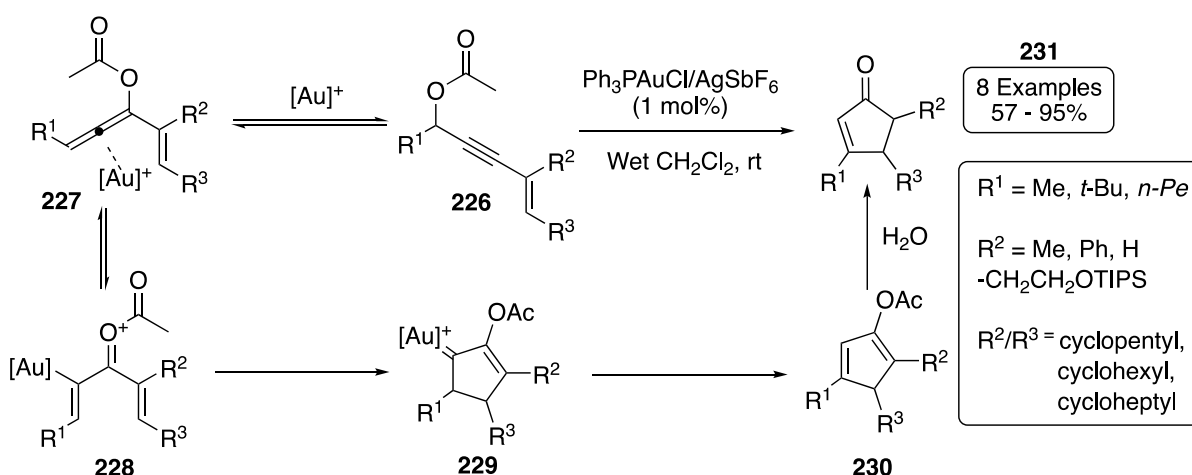
Scheme 53. Gold-catalysed rearrangements of enyne carboxylates with the vinyl substituent at either the propargylic position or the alkyne terminus

In 2005 Toste discovered that gold-catalysed Nazarov rearrangements of 1,4-enyne acetates **220** lead to cyclopentenones **225**.⁴³ With the vinyl substituent at the propargylic position, **223** undergoes a 1,2-acyl migration mechanism (Scheme 54).



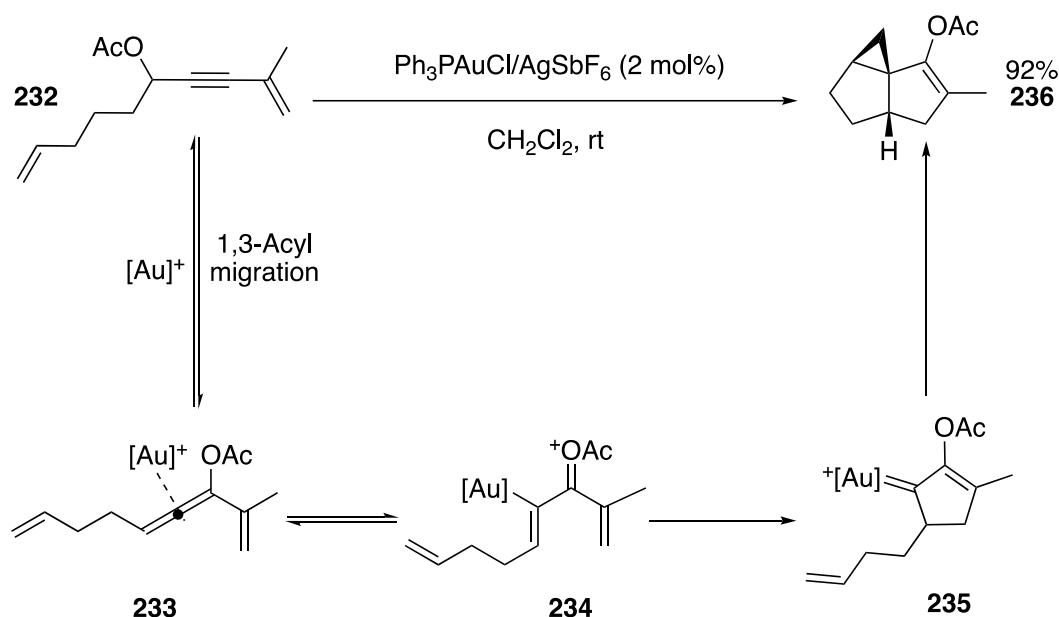
Scheme 54. Gold-catalysed Nazarov cyclisation of 1,4-enyne acetates with the vinyl substituent at the propargylic position by Toste

Zhang demonstrated the formation of cyclopentenones via gold-catalysed Nazarov cyclisation of 1,3-enyne acetates **226** with vinyl substituents at the alkyne terminus.⁴⁴ As previously described, substrates of this type undergo a 1,3-acyl migration pathway via the allene intermediate **227** (Scheme 55).



Scheme 55. Gold-catalysed Nazarov cyclisation of 1,3-enyne acetates with the vinyl substituent at the alkyne terminus by Zhang

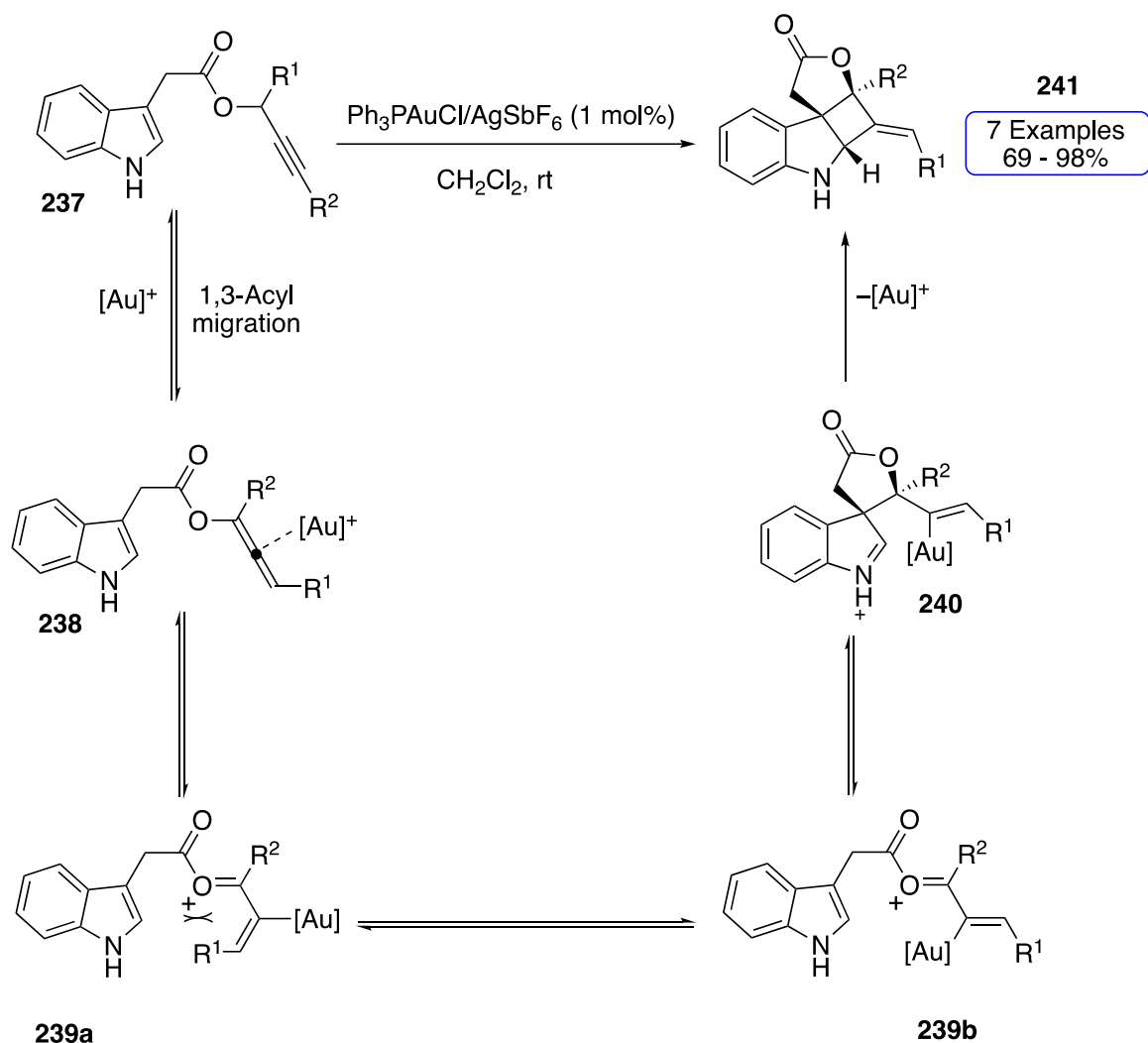
In 2007, Malacria demonstrated tandem Nazarov-cyclization followed by cyclopropanation with propargyl carboxylate **232**.⁴⁵ After Nazarov cyclization of **234** provides intermediate **235**, instead of 1,2-C-H migration, cyclopropanation of the alkene at the gold carbene forms the final tricyclic product **236** (Scheme 56). This tandem reaction demonstrates an alternative way of quenching the gold carbene intermediate following migration of the carboxylate.



Scheme 56. Tandem Nazarov cyclisation and cyclopropanation reaction by Malacria

3.1.2.3 Intramolecular Cyclisation Reactions: The Use of Nucleophilic Substituents

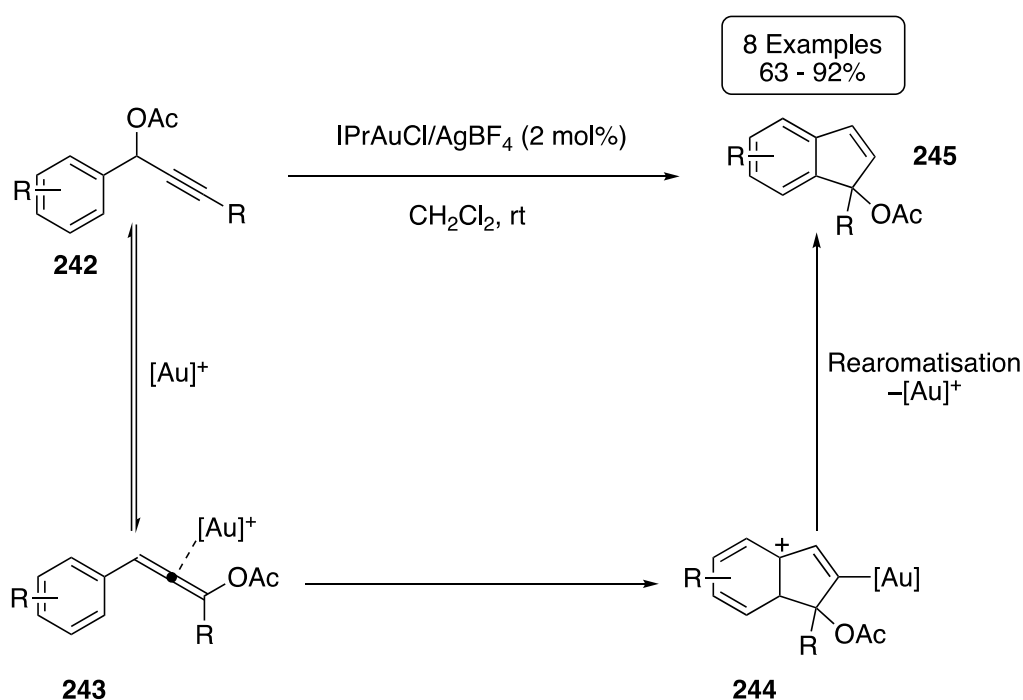
In addition to the previously described cyclopropanation and Nazarov cyclisation reactions, other tethered nucleophiles have been used in gold-catalysed rearrangements of propargyl carboxylates. With an indoyl substituent tethered to the propargyl carboxylate, Zhang reported the synthesis of 2,3-indoline fused cyclobutanes **241** through a gold-catalysed formal [2+2] cycloaddition reaction (Scheme 57).⁴⁶



Scheme 57. Tandem gold-catalysed rearrangement and formal [2+2] cycloaddition to synthesise cyclobutane-fused indolines by Zhang

During catalysis, the allene intermediate **238** is formed via 1,3-acyl migration. Zhang then proposes the formation of two oxocarbenium intermediates that are in equilibrium (Scheme 57, **239a** and **239b**). It is proposed that **239b** is the favoured intermediate as it suffers from less 1,3-allylic strain due to the extended [Au]-C bond. At this point, the oxocarbenium is attacked by the indole at the C-3 position, forming intermediate **240**. This is followed by intramolecular trapping of the iminium by the [Au]-C bond to form the cyclobutane-fused indoline **241** as a single stereoisomer.

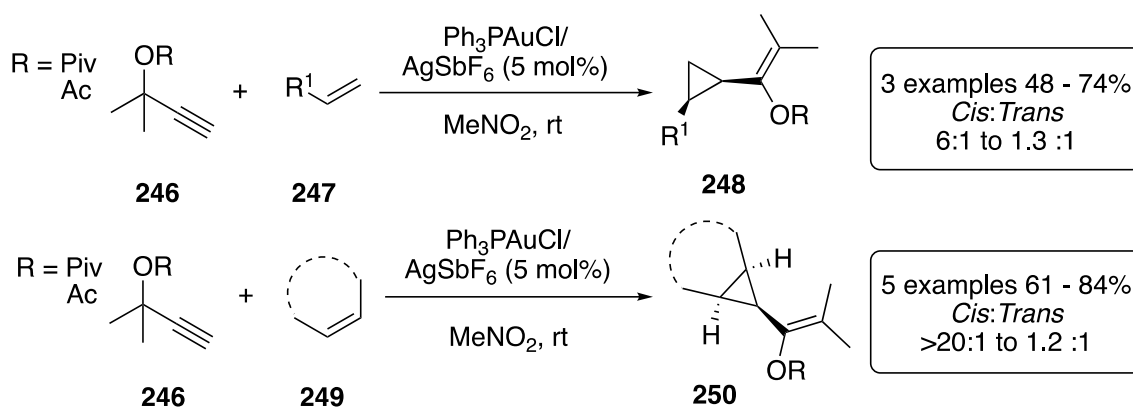
Nolan reported the gold-catalysed formation of indenenes from propargyl carboxylates with aryl substituents at the propargylic position.⁴⁷ Propargyl acetate **242** undergoes 1,3-acyl migration followed by nucleophilic attack of the phenyl ring to the activated allene **243** to provide intermediate **244**. Rearomatisation of the phenyl ring and protodeauration yields the desired indene **245** (Scheme 58).



Scheme 58. Gold-catalysed formation of indenenes from propargyl carboxylates by Nolan

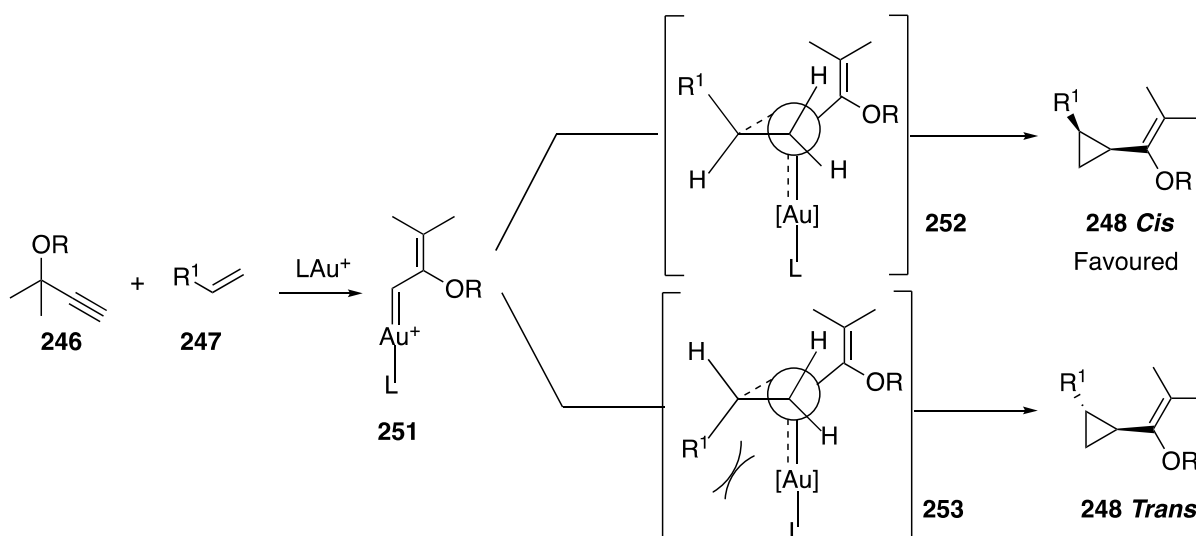
3.1.3 Intermolecular Gold-Catalysed Reactions of Propargyl Carboxylates with Nucleophiles

In addition to gold-catalysed intramolecular cyclisation reactions of propargyl carboxylates, a catalogue of intermolecular transformations has also been reported with a range of nucleophiles. A notable publication by Toste demonstrates stereoselective cyclopropanation with alkene substrates (Scheme 59).⁴⁸



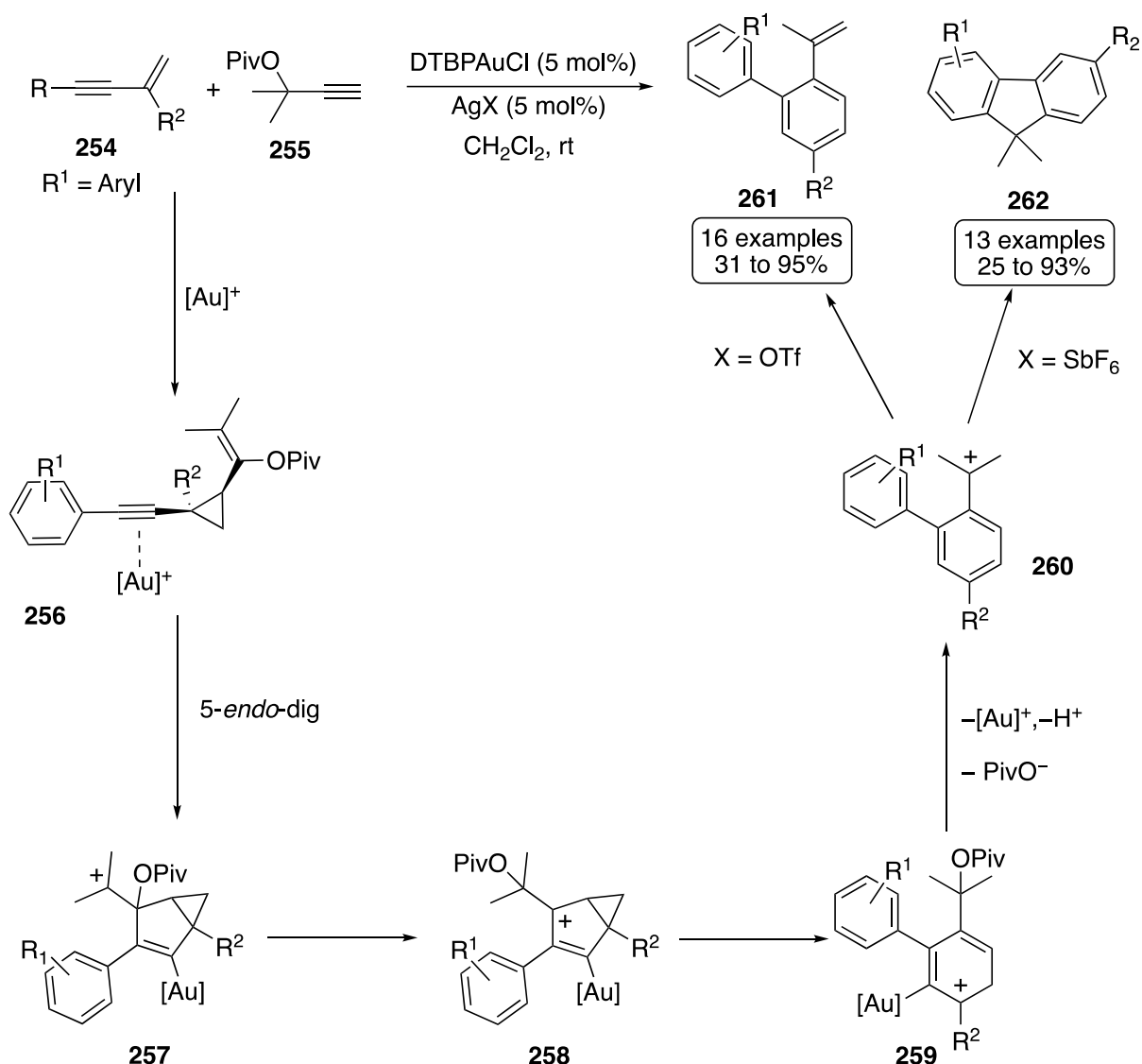
Scheme 59. Gold-catalysed stereoselective cyclopropanation by Toste

1,2-acyl migration of the terminal propargyl carboxylate **246** generates an intermediate gold carbene **251** (Scheme 60). The *cis* selectivity is rationalised using Newman projections for the approach of the alkene **247** to the gold-carbene intermediate (Scheme 60). The Newman projection **253** shows that as the alkene approaches the gold carbene for *trans* **248** cyclopropane formation, there is steric interference between the alkene substituent and the gold catalyst. There is less steric interference during *cis* **248** cyclopropane formation, as shown by the Newman projection **252**, and therefore the *cis* cyclopropane is formed predominantly.



Scheme 60. Newman projections for the gold-catalysed cyclopropanation of alkenes with propargyl carboxylates described by Toste

Toste built upon the stereoselective cyclopropanation of propargyl carboxylates and developed a method for the preparation of fluorenes and styrenes (Scheme 61).⁴⁹

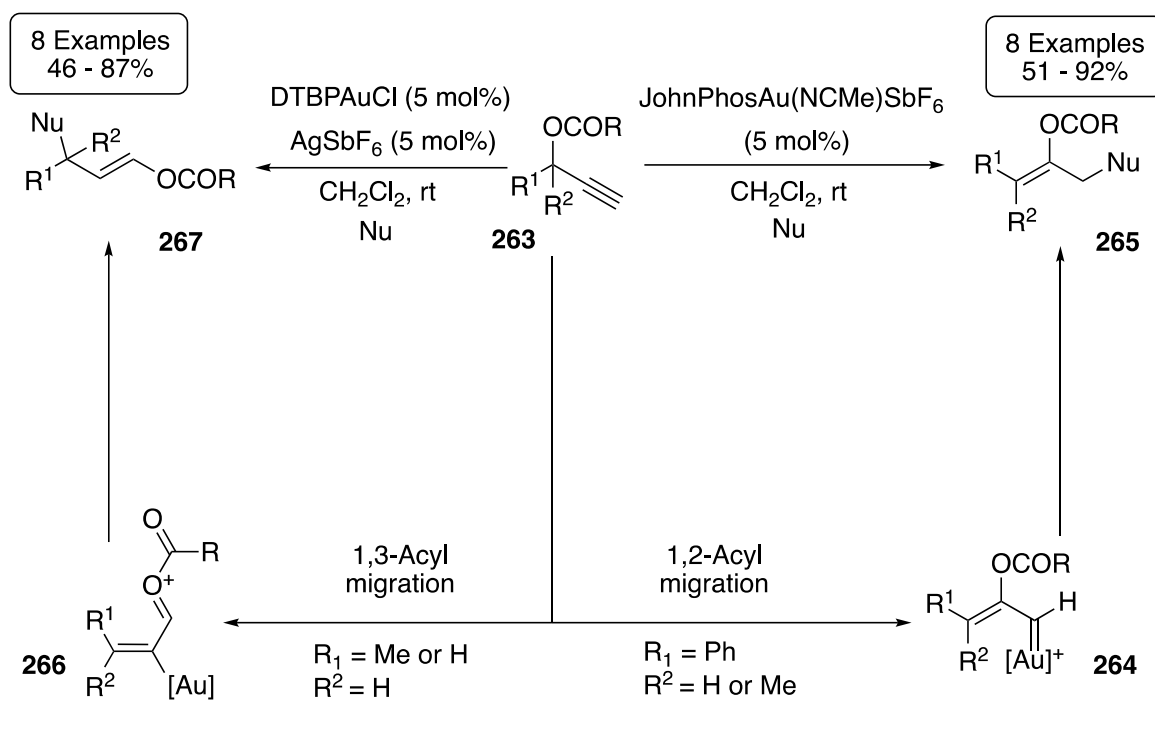


Scheme 61. Proposed mechanistic pathways for the formation of fluorenes and styrenes from gold catalysis of propargyl carboxylates with 1,3-enynes by Toste

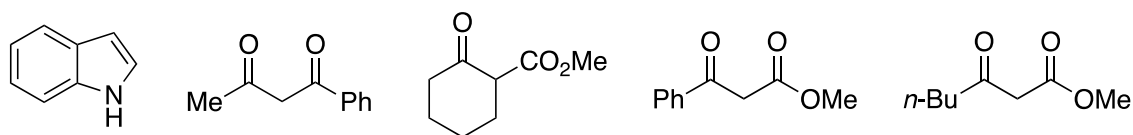
1,2-Acyl migration of propargyl carboxylate **255** followed by cyclopropanation with **254** generates the *cis* cyclopropane **256**. The cyclopropane **256** undergoes 5-*endo*-dig cyclisation to provide intermediate **257**. It was later discovered that only the *cis* cyclopropane can undergo cyclisation. Migration of the pivalate leads to intermediate **258**. Cyclopropane ring opening forms the 6-membered ring **259**. Rearomatization and

protodeauration occur, along with elimination of the pivalic acid, to yield styrene products **261**. Another pathway involves loss of the pivalate from **259** followed by nucleophilic trapping of the tertiary cation by the aromatic substituent to generate fluorenes **262**. The divergent pathways are controlled by changing the silver salt used in the gold-catalysed reaction. This tandem reaction highlights the range of pathways available to propargyl carboxylates under gold catalysis, and the ability for these simple substrates to yield complex and useful products (Scheme 61).

Echavarren reported the intermolecular nucleophilic addition of various carbon nucleophiles, including dicarbonyls and electron rich arenes, to propargyl carboxylates under gold catalysis (Scheme 62).⁵⁰ This study shows the synthesis of a wide range of products by varying the nucleophile and by manipulating the rearrangement pathway taken by the propargyl carboxylate. Dimethyl-substituted and phenyl-substituted terminal propargyl carboxylates underwent 1,2-acyl migration, providing alkene products **265** after addition of the nucleophile. All of the products **265** were formed as the *Z* isomers exclusively. Terminal propargyl carboxylates that exhibit a single methyl substituent or those that were unsubstituted at the propargylic position underwent 1,3-acyl migration affording products **267** as the *trans* alkene in all cases (Scheme 62). The favoured 1,3-acyl migration pathway of the terminal propargyl carboxylates used to prepare compounds **267** is unprecedented based on what is known about the rearrangements of propargyl carboxylates; terminal propargyl carboxylates typically favour 1,2-acyl migration. For this reason, this work has been referred to as an example in which the rearrangement of the propargyl carboxylate contradicts what is anticipated.³⁹



Nucleophiles include:

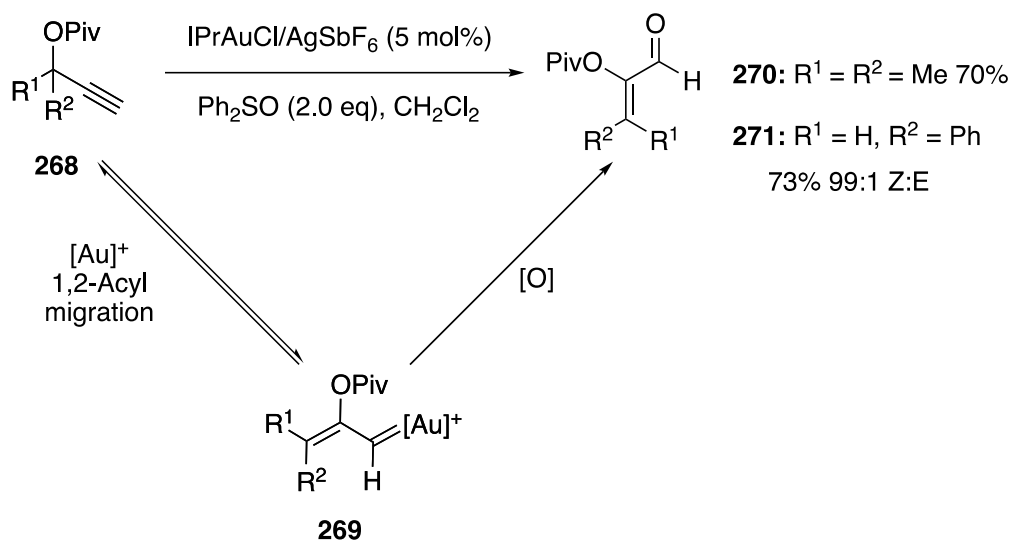


Scheme 62. Gold-catalysed addition of carbon nucleophiles to propargyl carboxylates by Echavarren

3.1.4 Gold-Catalysed Oxidation of Propargyl Carboxylates

The propensity of propargyl carboxylates to favour certain rearrangement pathways means that they are perfect candidates for regioselective oxidation. In addition, the carboxylate group polarises the alkyne bond and should also allow for regioselective oxidation, if oxidation were to occur prior to carboxylate migration. However, from what is known of the literature, there are very few reports of tandem gold-catalysed rearrangement and oxidation reactions of propargyl carboxylates.⁵¹ The first example was demonstrated by Toste with the formation of captodative olefins **270** and **271** with diphenyl sulfoxide (Scheme 63).^{51b} Captodative olefin **271** was formed with a very high

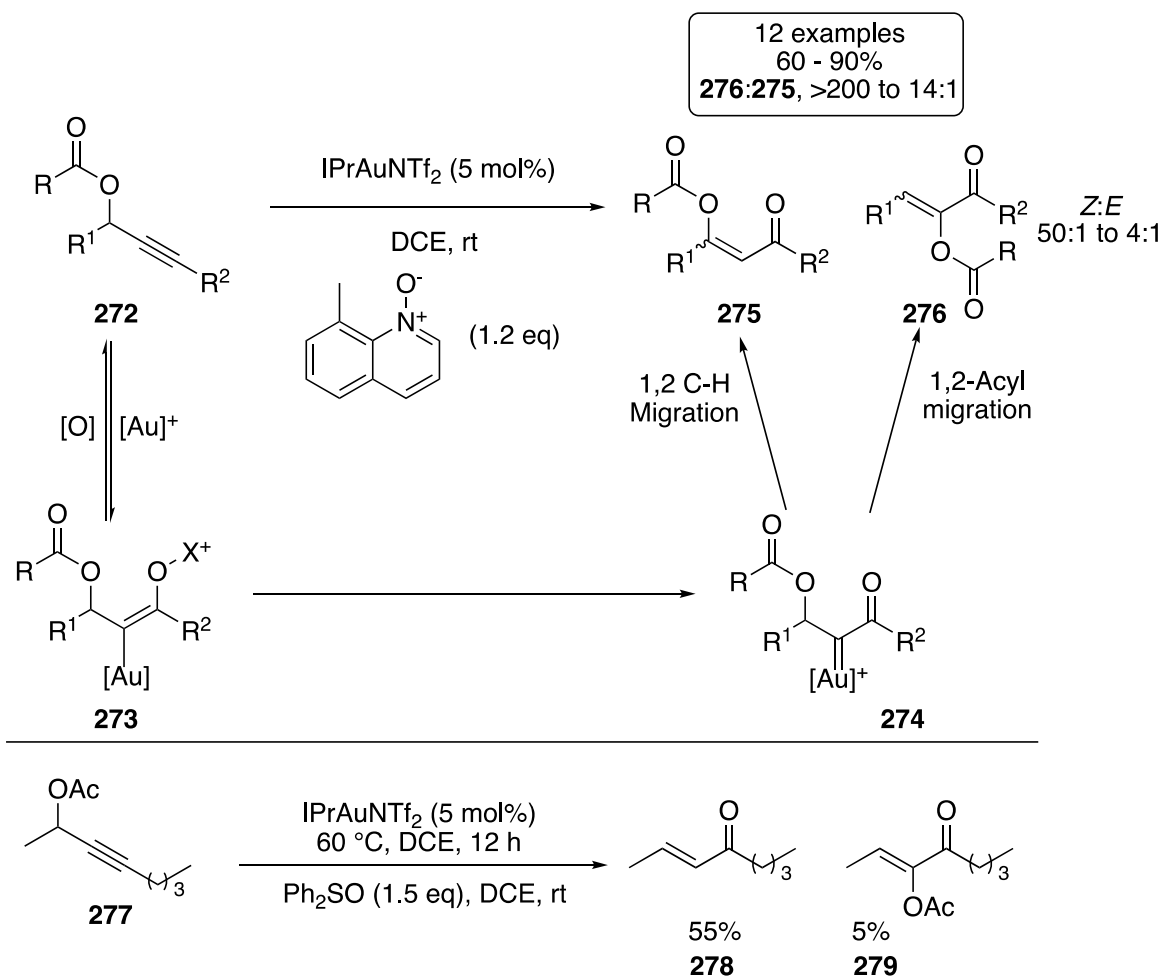
Zselectivity. The formation of **270** and **271** are proposed to occur via 1,2-acyl migration of propargyl carboxylate **268**, followed by direct oxidation of the gold carbene intermediate **269**.



Scheme 63. Gold-catalysed tandem rearrangement and regioselective oxidation of propargyl carboxylates by Toste

In 2013 Zhang's group synthesised a library of compounds from tandem oxidation and rearrangement of propargyl carboxylates (Scheme 64).^{51c} Zhang proposes that, in contrast to the work described by Toste, captodative olefins **276** are formed via initial regioselective oxidation of the propargyl carboxylate **272** and subsequent migration of the carboxylate. This mechanistic pathway is supported by an experiment that shows only 5% of product **279** was formed when diphenyl sulfoxide was used as the oxidant for the gold-catalysed oxidation of **277**. Diphenyl sulfoxide is not an efficient oxidant for the direct oxidation of alkynes, but is capable of oxidising gold carbenes, thus the low yield supports a mechanism via direct alkyne oxidation.^{11, 52} Alternatively, product **278** from acetate hydrolysis was observed with diphenyl sulfoxide. Whilst captodative olefins **276** are formed as the major products under the optimised conditions, they are

isolated as a mixture with products **275**, formed via 1,2-C-H migration at the gold carbene intermediate **274**.

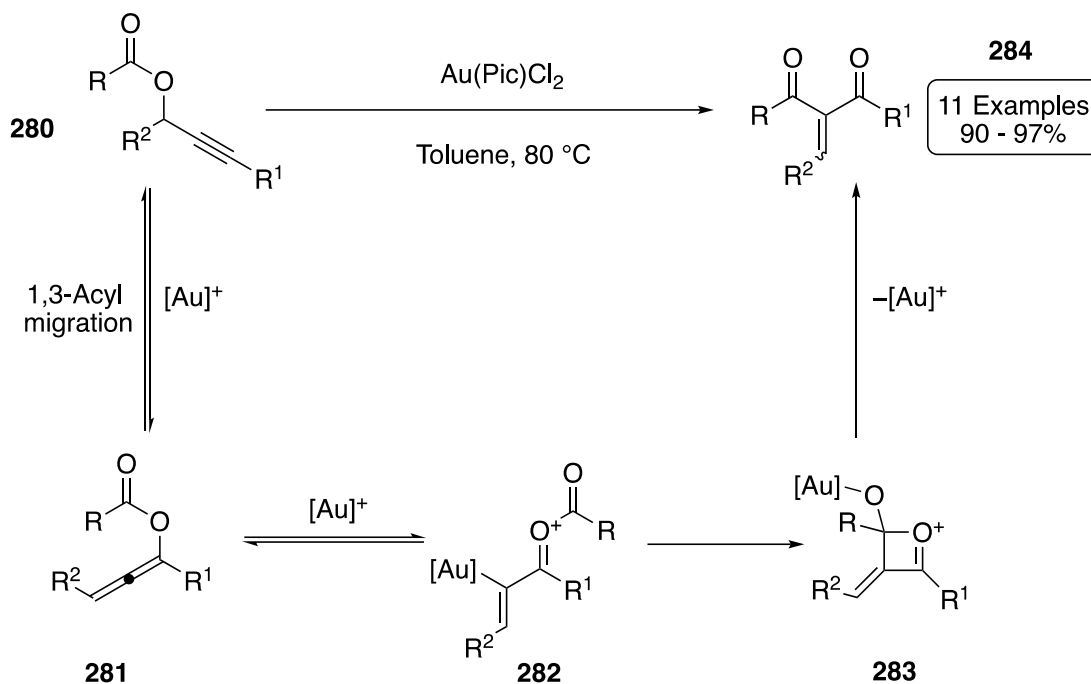


Scheme 64. Gold-catalysed tandem rearrangement and regioselective oxidation of propargyl carboxylates by Zhang

3.1.5 Gold-Catalysed Rearrangements of Propargyl Carboxylates in the Absence of Nucleophiles

All of the previously discussed work has involved the inter- or intramolecular addition of nucleophiles or oxidants to propargyl carboxylates. Interestingly, a range of pathways are available to propargyl carboxylates in the absence of nucleophiles. In

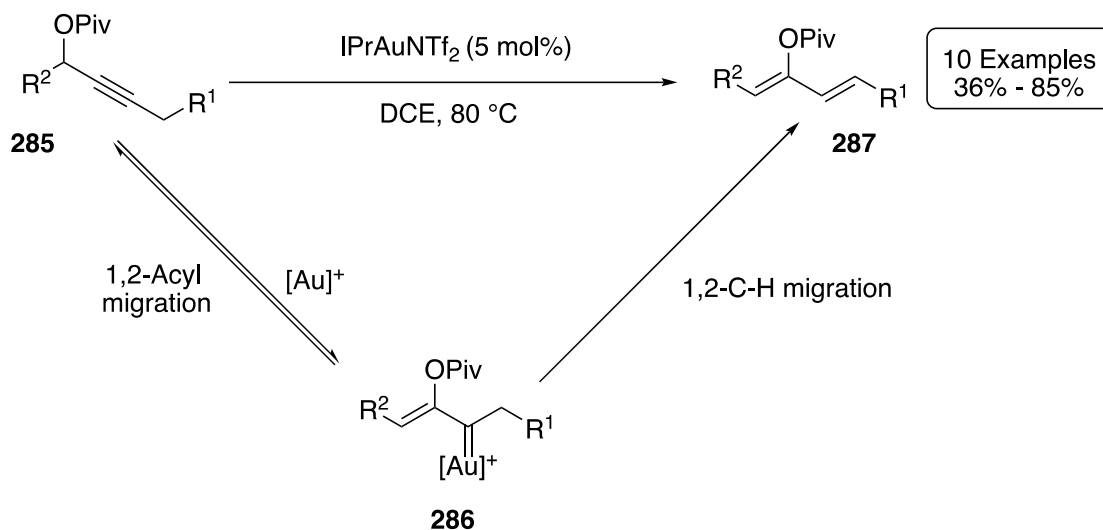
2006, Zhang reported the formation of a range of diketones **284** from the gold-catalysed rearrangement of internal propargyl carboxylates **280** (Scheme 65).⁵³



Scheme 65. Gold-catalysed formation of diketones via intramolecular rearrangement of propargyl carboxylates by Zhang

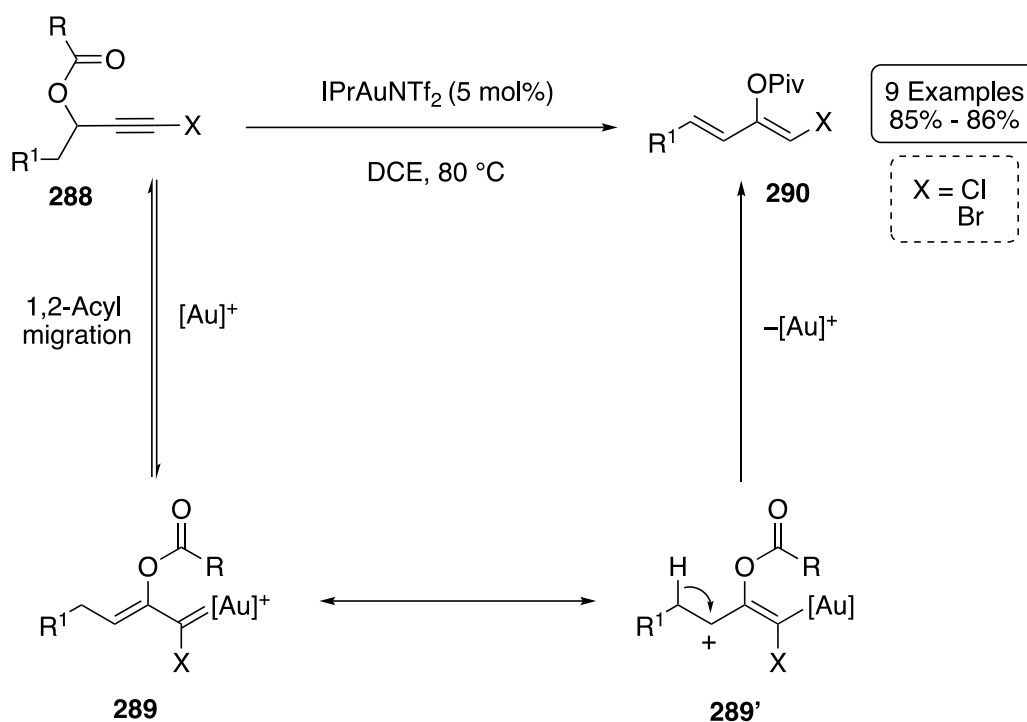
This work was particularly interesting as it exploited the nucleophilic nature of the [Au]-C bond. The mechanistic pathway towards diketones **284** follows 1,3-acyl migration to form allene **281**, which is further activated by gold to provide the oxocarbenium intermediate **282**. The [Au]-C bond then attacks the C=O bond, attached to the oxocarbenium, generating intermediate **283**. Collapse of intermediate **283** results in the desired diketone product (Scheme 65). Crossover experiments support the formation of **283** rather than an intermolecular reaction with an acylium ion. The products were formed with high *E* stereoselectivity. A separate experiment supports a 1,3-acyl migration pathway; an intermediate carboxyallene was synthesised and treated under the optimised conditions to yield the diketone product in high yield.

Zhang also reports the formation of pivaloxy dienes **287** from propargyl pivalates **285**.³⁹ This work shows how the nature of the substrate can be manipulated to encourage otherwise unfavourable reaction pathways (Scheme 66).



Scheme 66. Gold-catalysed formation of pivaloxy dienes via intramolecular rearrangement of propargyl carboxylates by Zhang

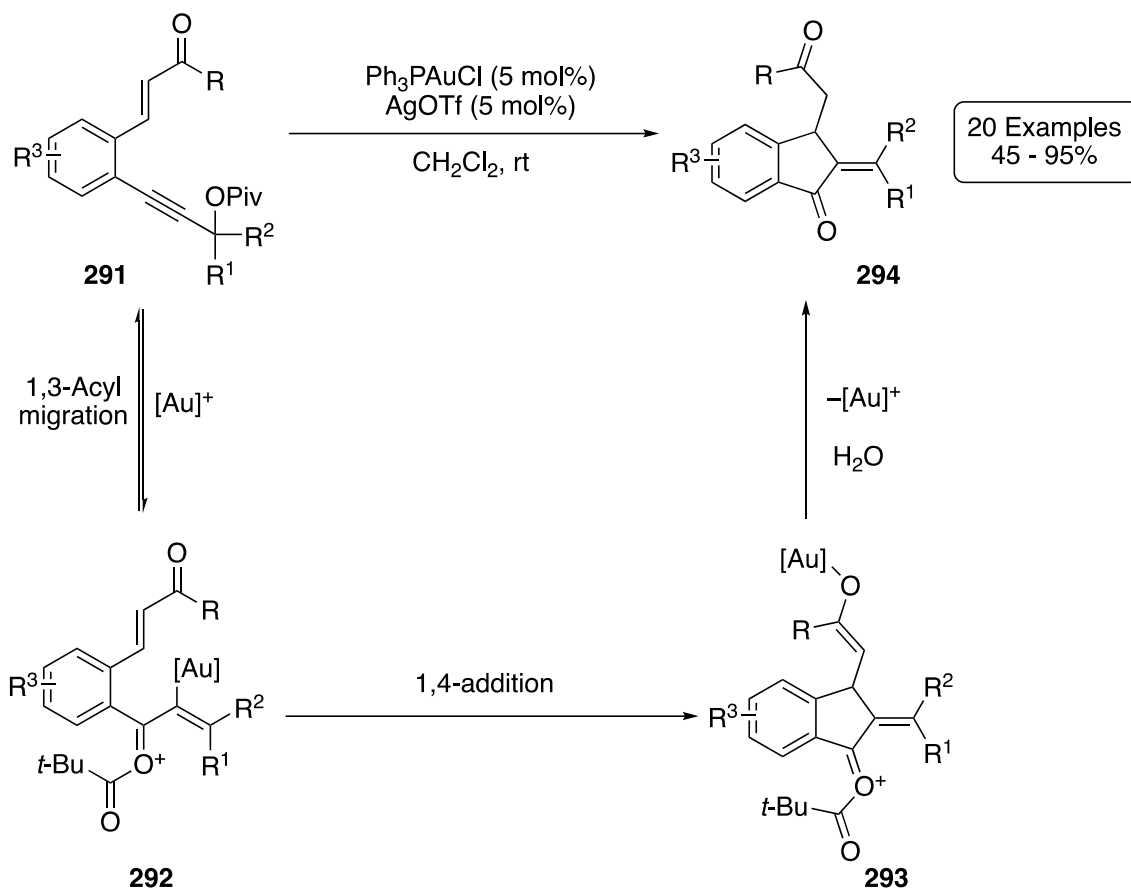
Internal propargyl carboxylates **285** typically favour 1,3-acyl migration. However, as the migration process is reversible, Zhang proposed that if the available pathways after 1,2-acyl migration were more energetically favourable than the pathways following 1,3-acyl migration, then products from 1,2-acyl migration should be observed. After 1,2-acyl migration, a H-substituent α to the gold carbene **286** would provide a facile downstream pathway for the formation of pivaloxy dienes **287** via 1,2 C-H migration (Scheme 66). Indeed, diketone products **284** (see Scheme 65) from 1,3-acyl migration were also observed, but optimised conditions allowed the formation of the pivaloxy dienes **287** in high yield. In relation to this work, Zhang also showed that the rearrangement of internal propargyl carboxylates could be tuned by the presence of an electron withdrawing halogen at the alkyne terminus (Scheme 67).^{36c}



Scheme 67. Regioselective gold-catalysed rearrangements of propargyl carboxylates using halogen substituents by Zhang

The presence of an electron-withdrawing halogen substituent at the alkyne terminus destabilises positive charge build-up at the vicinal alkyne carbon and disfavours 1,3-acyl migration. These substrates underwent facile 1,2-acyl migration to form dienes **290** (Scheme 67).

After Zhang reported the synthesis of diketones **284** (see Scheme 65), other reactions were reported where the nucleophilicity of the [Au]-C bond was exploited in the rearrangement of propargyl carboxylates. In 2014, Liang and co-workers reported the synthesis of inden-1-ones **294** (Scheme 68).⁵⁴ Propargyl carboxylate **291** undergoes 1,3-acyl migration to provide the intermediate oxocarbenium **292**. Michael addition of the [Au]-C bond at the enone provides intermediate **293**. Hydrolysis of the pivalate and loss of the gold catalyst generates the final product **294** with high *E* stereoselectivity.



Scheme 68. Gold-catalysed formation of inden-1-ones via rearrangement of propargyl carboxylates by Liang

3.1.6 Conclusion

The ability for propargyl carboxylates to undergo both 1,2- and 1,3-acyl migration under gold catalysis has enabled a plethora of novel transformations to be explored. Typically, internal and electronically unbiased propargyl carboxylates favour 1,3-acyl migration to generate electrophilic allene intermediates. Terminal and electron deficient propargyl carboxylates usually undergo 1,2-acyl migration to generate gold carbene intermediates. However, due to the reversibility of the migration process, substrates that are predisposed to favour a certain migration pathway can be encouraged to react through the less favoured migration pathway. This is possible when a facile downstream route is available following the less favoured migration step.

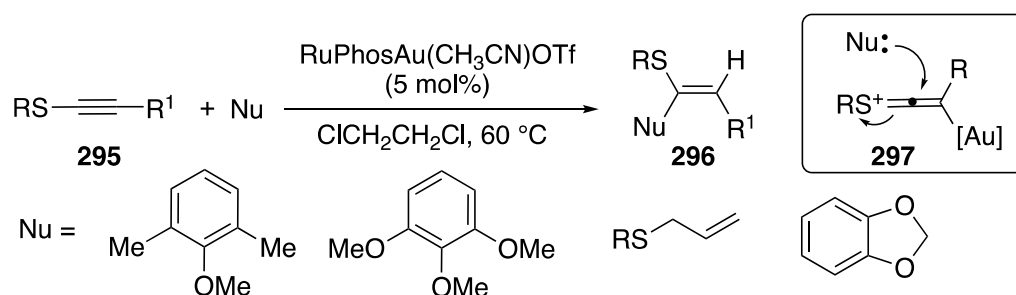
This is observed during cycloisomerisation reactions of internal 1,4-enyne carboxylates, and the formation of pivaloxy dienes described by Zhang. Both intra and intermolecular nucleophilic addition and cyclisation reactions have been described, alongside regioselective oxidation of propargyl carboxylates. Various nucleophiles have been explored including arenes, alkenes, and diketones. In the absence of nucleophiles, other pathways are available such as C-H migration and nucleophilic addition of [Au]-C bonds to electrophilic species. Whilst the exceptional versatility of these substrates has been demonstrated in many studies, there is still much to be explored. Other than the use of halogens at the alkyne terminus and the few examples of gold catalysis with ynamide propargyl esters, the use of other heteroatoms has mostly been neglected.^{36a, c, 55} This chapter will discuss the reactivity of sulfenylated propargyl carboxylates under gold-catalysis.

3.2 Aims and Objectives

The aim of this project was to understand the influence of sulfur substituents in gold-catalysed transformations of alkynes. Propargyl carboxylates were deemed appropriate systems for this investigation as they can react via 1,2- and 1,3-acyl migration pathways. Therefore, these substrates may allow the role of sulfur to be probed by comparing the migratory pathways of sulfenylated and non-sulfenylated systems.

The use of alkynyl thioethers in gold catalysis is still fairly scarce, possibly linked to concern that the sulfur atom may coordinate to, and temporarily poison, the catalyst. However, preliminary studies have shown that sulfur substitution can enhance, and in some cases alter, the reactivity of alkynes. The Davies group has shown that the reactivity of sulfenylated ynamides with nitrenoids that have diminished nucleophilicity

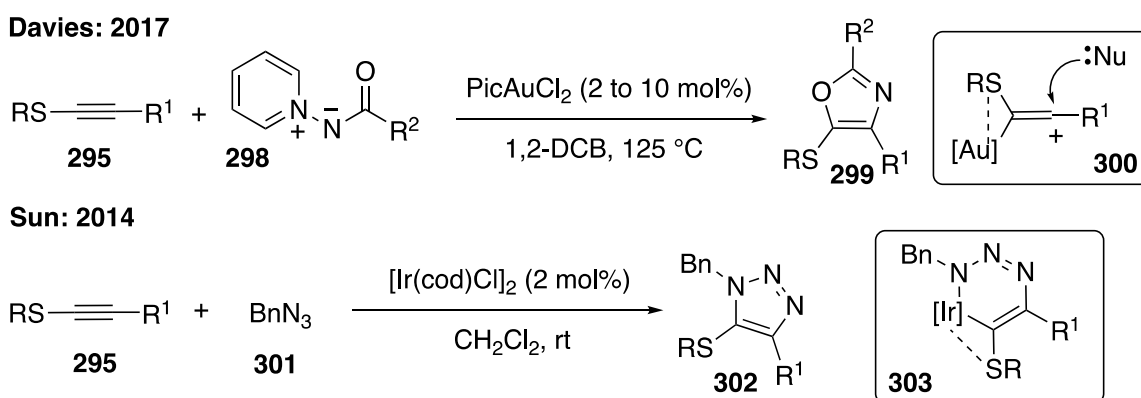
was superior than that of simple aryl-substituted ynamides.⁵⁶ The presence of sulfur has also been shown to influence the regioselectivity of nucleophilic attack to alkynyl thioethers in gold- and acid-catalysed processes.⁵⁷ A ketenthionium intermediate **297** is often invoked for regioselective nucleophilic attack at the α position of alkynyl thioethers, as seen in the gold-catalysed addition of carbon and sulfur nucleophiles to alkynyl thioethers by Shi (Scheme 69).^{57b} In this work, only alkynyl thioethers with alkyl and phenyl substituents at R^1 were tested, whilst electron-rich and electron-deficient alkyne substituents were not explored. Therefore, the electronic influence of alkyne substituents on the regioselectivity of nucleophilic addition is unknown. In addition, alkyl sulfur substituents saw reduced yields in the transformation. It is possible that varying the sulfur substituent effects the ability of the sulfur atom to conjugate with the alkyne bond.



Scheme 69. Gold-catalysed nucleophilic addition to the α -carbon of alkynyl thioethers by Shi

In contrast, the Davies group reported the formation of thioether-substituted oxazoles from alkynyl thioethers via Au(III)-mediated reactions with *N*-acyl pyridinium *N*-aminides; this transformation favoured nucleophilic attack at the alkynyl thioether β -position (Scheme 70).⁵⁸ A favourable sulfur-gold interaction is invoked to explain the unexpected regioselectivity, either through dative sulfur lone-pair donation at the gold centre or hyperconjugative $\sigma_{\text{C-Au}}$ to $\sigma^*_{\text{C-S}}$ interactions (Scheme 70, **300**). Electron-rich

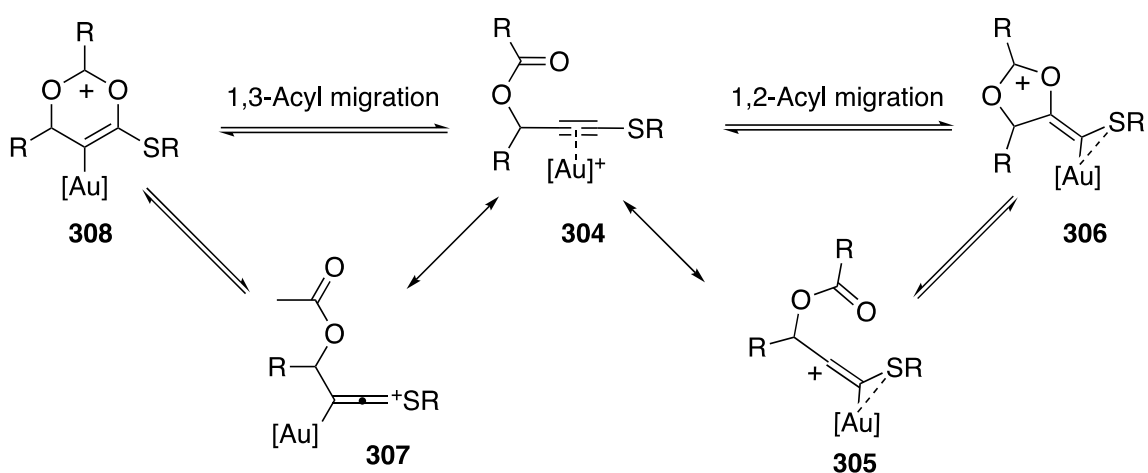
aryl-substituted alkynes saw higher β -regioselectivity, whilst a *para*-ester aryl substituent shut down reactivity. This is consistent with a sulfur-gold interaction rather than a ketenthionium intermediate. Phenyl, benzyl and isopropyl sulfur substituents saw lower β -regioselectivity compared to methyl and ethyl sulfur substituents. The sulfur substituent therefore influences sulfur-gold coordination vs ketenthionium activation modes. A sulfur-metal interaction has also been described by Sun for the iridium-catalysed cycloaddition reaction of alkynyl thioethers with azides (Scheme 70, **303**).⁵⁹



Scheme 70. Metal-catalysed nucleophilic addition at the β -carbon of alkynyl thioethers

Alkynyl thioethers can provide different reaction outcomes depending on the sulfur interactions at play. With limited studies on gold-catalysed nucleophilic addition to alkynyl thioethers, the factors influencing the alternative modes of sulfur activation require further investigation. Sulfenylated propargyl carboxylates are set up to directly probe the regioselectivity of carboxylate nucleophilic addition and migration at the alkyne bond. Their reactivity may provide insight into the role of sulfur substituents in gold-catalysed processes, whilst also improving pathway control (Scheme 71). If sulfenylated propargyl carboxylates **304** react via a 1,3-acyl migration pathway, the sulfur substituent may confer enhanced reactivity via a gold ketenthionium

intermediate **307**. On the other hand, a sulfur-gold interaction (Scheme 71, **305**) resulting in 1,2-acyl migration would allow new reactivity to be explored for internal propargyl carboxylates that typically favour 1,3-acyl migration. Sulfur substituents would also enable further functionalisation of products. This chapter discusses preliminary studies into the gold-catalysed rearrangements of novel sulfenylated propargyl carboxylates through the study of nucleophilic addition and oxidation reactions.



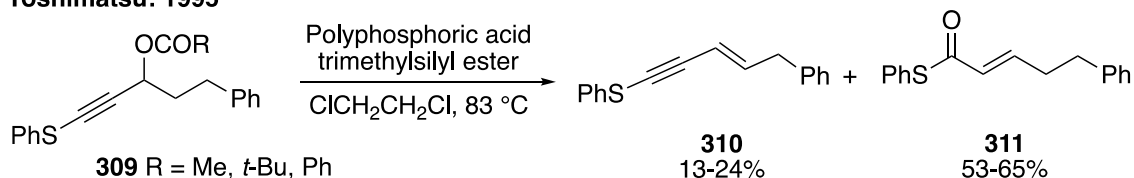
Scheme 71. Possible gold-catalysed pathways of sulfenylated propargyl carboxylates

3.3 Synthesis of Sulfenylated Propargyl Carboxylates

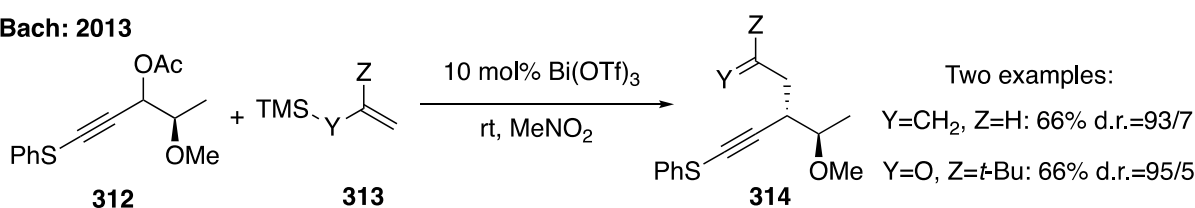
Investigations into the gold-catalysed rearrangements of sulfenylated propargyl carboxylates required the synthesis of a range of novel substrates. Due to the fluidity of the project, the methodology for substrate synthesis was developed throughout the course of the whole investigation. For continuity, all starting material preparation is discussed in this section. The challenges faced during the synthesis of sulfenylated propargyl carboxylates will be highlighted in this section. The rationale for the use of specific substrates will become clear during later discussion into gold-catalysed rearrangements and thus will not be discussed in this section.

There was no previous research into gold-catalysed reactions of sulfenylated propargyl carboxylates. Research into the chemistry of these species was all-together scarce, with only a handful of reactions reported (Scheme 72).⁶⁰

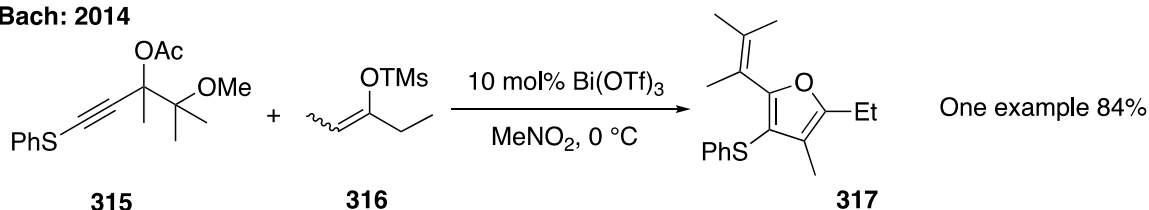
Yoshimatsu: 1995



Bach: 2013



Bach: 2014

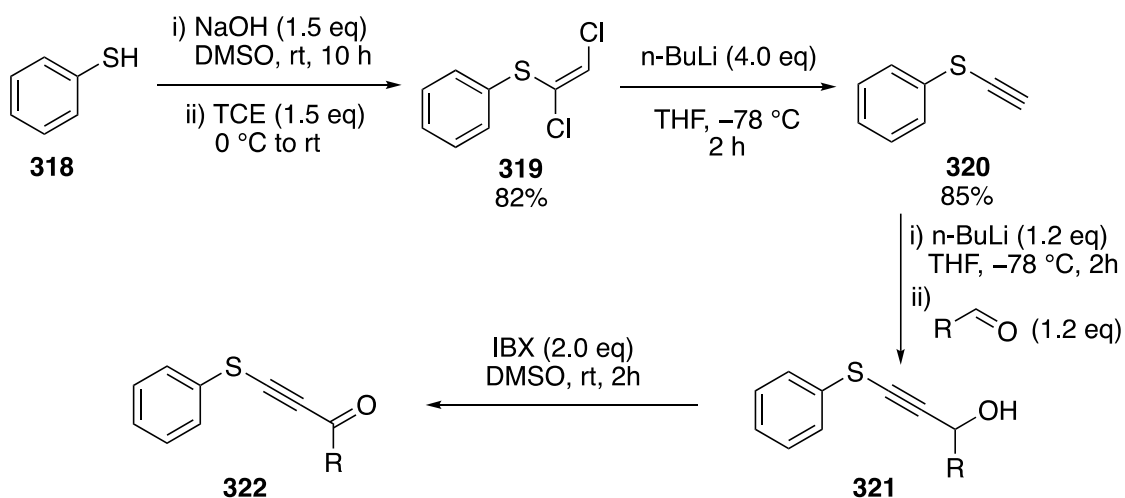


Scheme 72. Reported reactions of sulfenylated propargyl carboxylates

The reported transformations do not involve carboxylate migration. Instead, Bach's work involves carboxylate substitution, whilst Yoshimatsu suggests that thioester **311** is formed via Meyer-Schuster rearrangement of the corresponding propargyl alcohol after hydrolysis of **309** (Scheme 72).

With limited groundwork to build upon, the first challenge was deciding upon a synthetic route towards sulfenylated propargyl carboxylates. In 2019 Liu and co-workers published their work on the gold-catalysed oxidation of thioalkynyl ketones **322** that were prepared via oxidation of sulfenylated propargyl alcohols **321** (Scheme

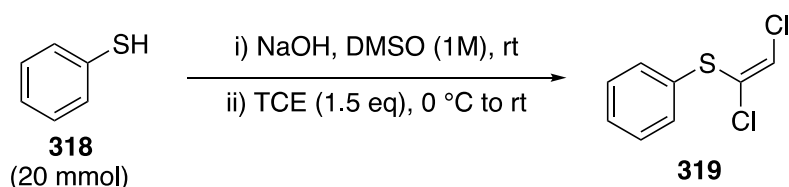
73).⁶¹ It was decided to prepare the desired substrates from the corresponding propargyl alcohols utilising this methodology.



Scheme 73. Preparation of thioalkynyl ketones by Liu and co-workers

The synthesis of the dichloroalkene **319** required optimisation, as applying the stated conditions did not produce yields comparable to those reported by Liu (Table 4).

Table 4. Optimisation for the preparation of 319



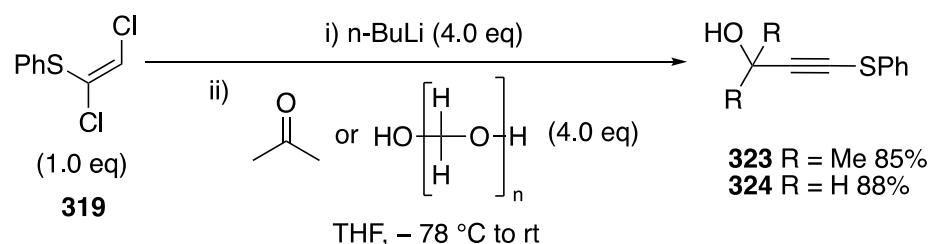
Entry	NaOH eq.	DMSO:H ₂ O	Yield/% ^a
1	1.5	-	55
2	2.0	-	54
3	2.5	-	66
4	2.5	2:1	78

^aIsolated yields after column chromatography

It was observed that the NaOH was not fully solvated by DMSO during the reaction, even after sonication of the reaction solution, and so increasing the equivalents of

NaOH and adding H₂O as a co-solvent increased the yield from 55% to 78% (Table 1, entries 1 and 4). Using 1.5 eq. of NaOH alongside H₂O was not attempted, although this may have been sufficient to improve the yield of **319** due to better solvation of NaOH. This reaction could be performed on a 20 mmol scale, however the large-scale synthesis of **319** had to be performed with caution. The reaction is highly exothermic and involves the formation of dichloroethylene which is explosive in high concentrations in the gas phase. Therefore, slow addition of TCE over 1 hour via syringe pump at 0 °C was required.

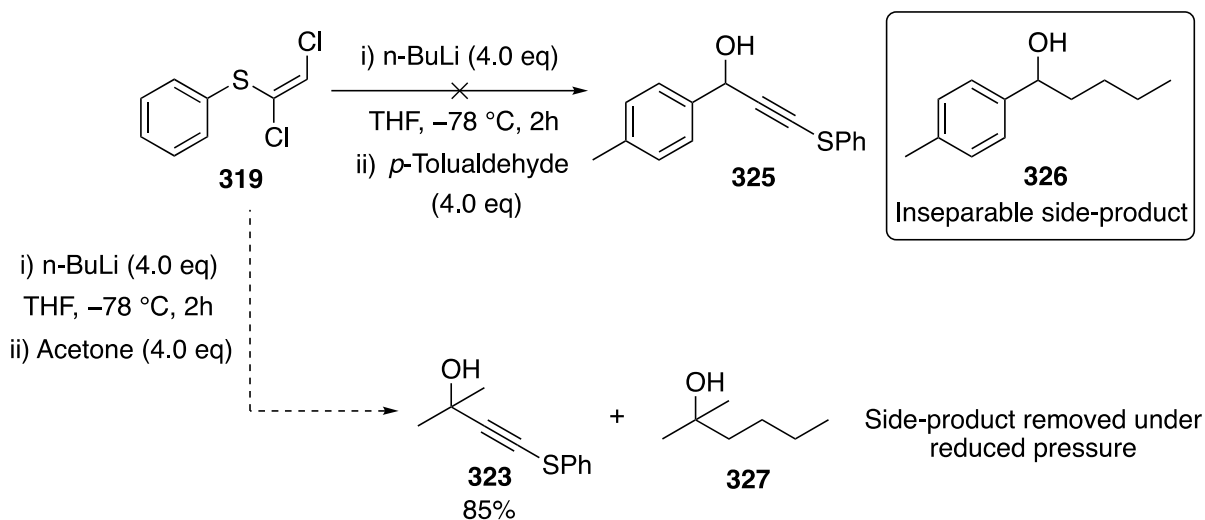
Propargyl alcohols **323** and **324** could both be successfully synthesised in one step from a reaction between dichloroalkene **319** and n-BuLi, followed by direct trapping of the lithiated intermediate with acetone and paraformaldehyde respectively (Scheme 74). This was beneficial as the isolation of alkynyl thioether **320** was avoided, reducing the number of lithiation reactions required. Analogous transformations for the synthesis of ynamides from dichloroenamides require only 2.5 eq of n-BuLi.⁶² However, using less than 4.0 eq of n-BuLi in this reaction led to the formation of substantial amounts of an undetermined side product.



Scheme 74. Direct formation of sulfenylated propargyl alcohols from dichloroalkene **319**

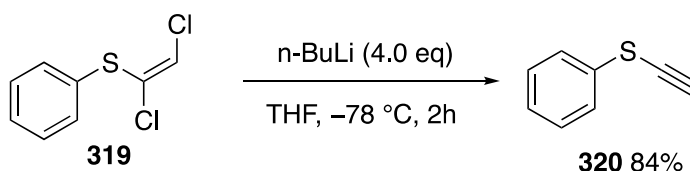
In contrast, aromatic substituted propargyl alcohol **325** could not be synthesised directly from dichloroalkene **319** and *p*-tolualdehyde (Scheme 75). Due to the excess

amounts of n-BuLi required for the transformation, an appreciable amount of the alkylated product **326** was also formed during the reaction from the direct addition of n-BuLi to *p*-tolualdehyde. Alcohol **326** was inseparable from the desired product **325** by column chromatography. It is likely that the analogous alkylated side product **327** was formed during the synthesis of **323** but not observed due to its low boiling point (64 – 67 °C at 35 Torr).⁶³



Scheme 75. Attempted direct synthesis of propargyl alcohol **325 from dichloroalkene**

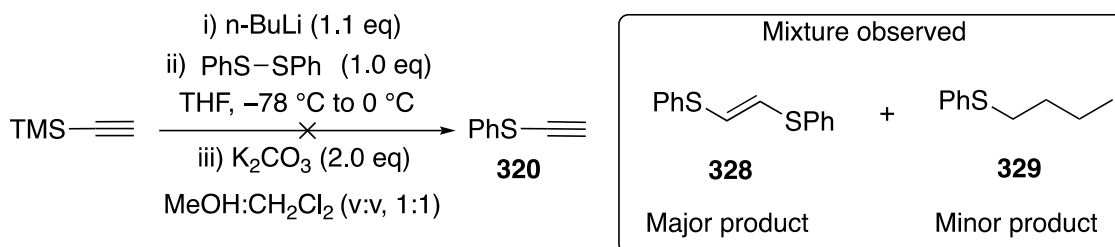
The use of n-BuLi in large excess for the synthesis of propargyl alcohols from dichloroalkene **319** was likely to pose purification issues in future cases, and so alkynyl thioether **320** was synthesised in 84% yield using the method described by Liu (Scheme 76).



Scheme 76. Synthesis of alkynyl thioether **320**

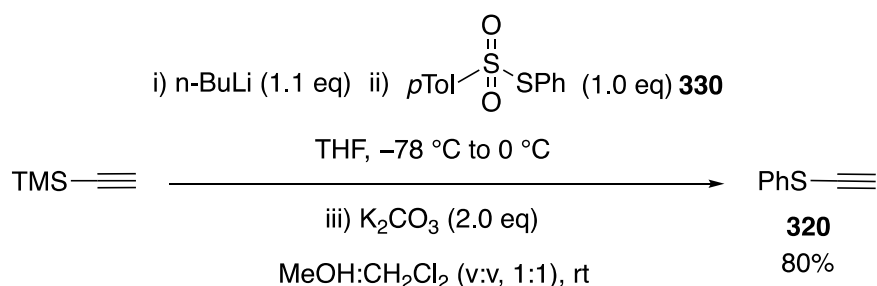
In practice, the use of n-BuLi in large excess was not favourable and the preparation of dichloroalkene **319** involved high risk, hence more efficient methods for the

synthesis of alkynyl thioether **320** were explored. The literature described a method involving the lithiation of ethynyltrimethylacetylene followed by addition of diphenyl disulfide.⁶⁴ Unexpectedly, bis(phenylthiol)ethene **328** was observed as the major product, alongside butyl(phenyl)sulfane **329** obtained from the direct reaction between n-BuLi and diphenyldisulfide (Scheme 77).



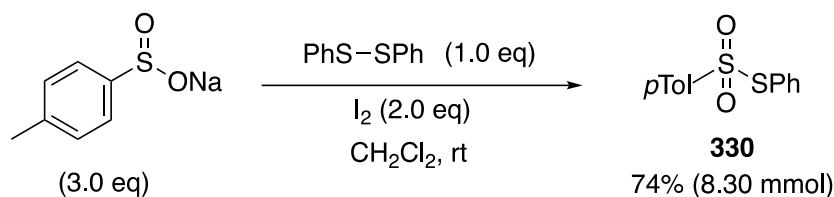
Scheme 77. Attempted synthesis of alkynyl thioether 320

For this reason, thiosulfonate **330** was used instead of diphenyl disulfide and alkynyl thioether **320** was afforded in 80% yield (Scheme 78).



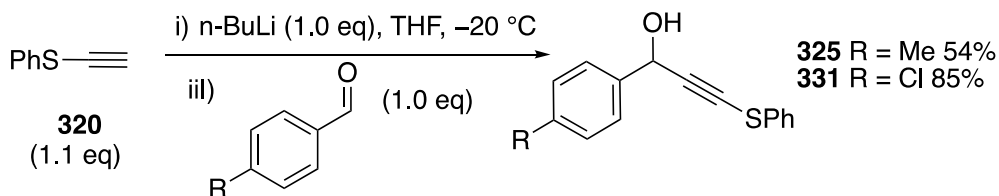
Scheme 78. Synthesis of alkynyl thioether 320 from ethynyltrimethylsilane

Whilst both methods for the synthesis of alkynyl thioether **320** provided excellent yields, the method from ethynyltrimethylsilane was more efficient and the synthesis of the thiosulfonate electrophile **330** was simple and scalable (Scheme 79). However, direct formation of propargyl alcohols from dichloroalkene **319** should be considered if the side product from n-BuLi addition to the aldehyde has a low boiling point and is easily separated from the desired product.



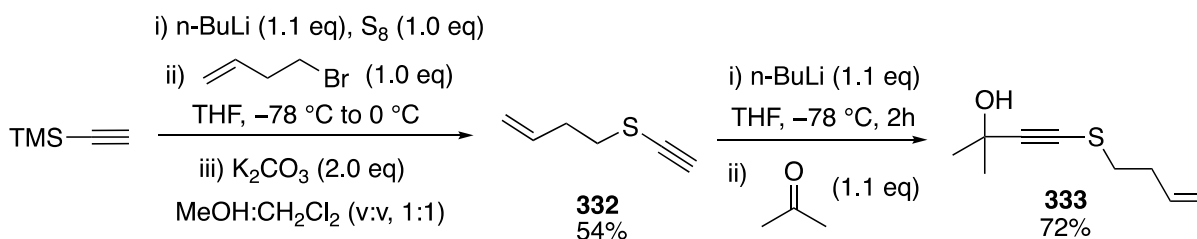
Scheme 79. Large scale synthesis of thiosulfonate

Propargyl alcohols **325** and **331** were synthesised from alkynyl thioether **320** (Scheme 80). The lithiation of **320** was performed at $-20\text{ }^\circ\text{C}$ according to a literature procedure that described the synthesis of analogous substrates.⁶⁵ When the lithiation was performed at $-78\text{ }^\circ\text{C}$, direct n-BuLi addition to the aldehydes was also observed, hence there was not efficient deprotonation of **320** at this temperature.



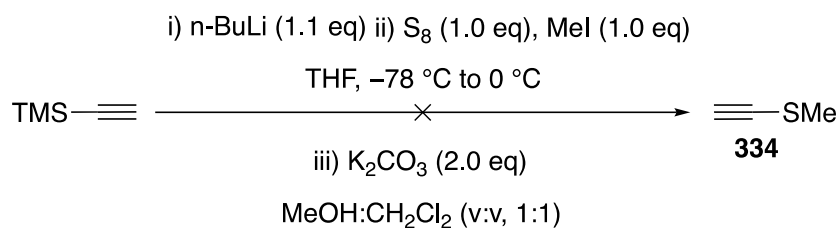
Scheme 80. Synthesis of propargyl alcohols from alkynyl thioether 320

Substrate **333** with a homoallyl sulfur substituent was also synthesised (Scheme 81). Alkynyl thioether **332** was prepared according to a literature procedure, reported by the Davies group, for the preparation of analogous substrates.⁶⁶ Lithiation of ethynyltrimethylsilane and subsequent trapping with sulfur generated an intermediate thiolate which was then alkylated with 4-bromo-1-butene. Following deprotection, alkynyl thioether **333** was reacted with n-BuLi and acetone to yield the desired product **333** in 72% yield.



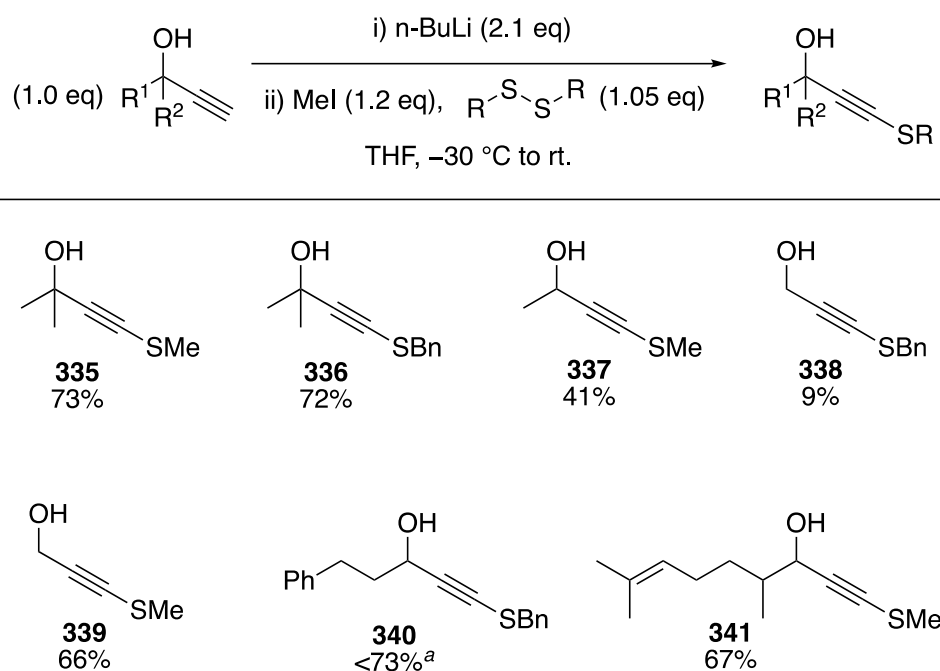
Scheme 81. Synthesis of propargyl alcohol 333

For *S*-methyl substituted propargyl alcohols, an analogous approach was attempted but the corresponding alkynyl thioether **334** could not be isolated due to its low boiling point (70 °C at 1 atm)⁶⁷ (Scheme 82).



Scheme 82. Attempted synthesis of alkynyl thioether 334

A new synthetic route, adapted from the literature, was used involving the deprotonation of propargyl alcohols and subsequent reaction with dimethyl disulfide and methyl iodide (Scheme 83).⁶⁸



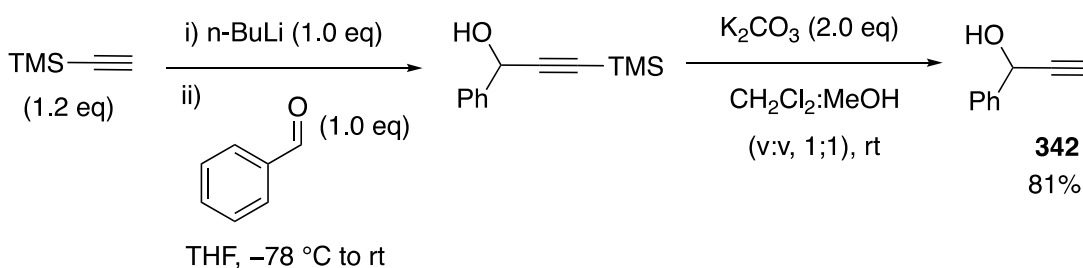
^aIsolated product contains minor impurities.

Scheme 83. Preparation of *S*-methyl and *S*-benzyl substituted propargyl alcohols

Propargyl alcohol substrates have two acidic protons (the alcohol and the alkyne protons), and so 2.1 eq. of *n*-BuLi were used. This route was also successful for the preparation of *S*-benzyl derivatives. It is unclear why **338** was obtained in low yield; as

the starting material appeared to be consumed by ^1H NMR spectroscopic analysis of the crude reaction mixture, it is likely that the loss of yield occurred during the purification process. Since performing this work, a new protocol has been developed using a similar preparative method from lithiation of propargyl alcohols at $0\text{ }^\circ\text{C}$ with elemental sulfur and alkyl halides.^{57c}

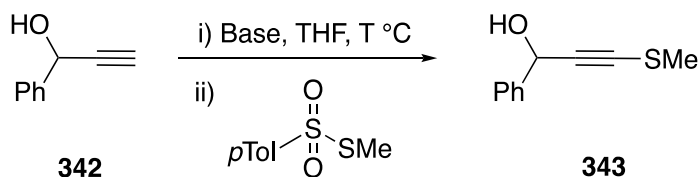
Sulfenylation of propargyl alcohols was an ideal route into the desired substrates due to the facile preparation of propargyl alcohols from aldehydes. However, methyl iodide is highly toxic and carcinogenic and the equimolar generation of volatile and potentially toxic sulfide side products was not ideal. These reactions had to be always handled within a fume-hood during work up and purification, whilst all glassware and equipment had to be soaked in bleach after use. New methods were therefore tested for the sulfenylation of propargyl alcohols with innocuous thiosulfonate electrophiles. 1-Phenyl-2-propyn-1-ol **342** was used for optimisation studies, which was synthesised in 81% yield over two steps from ethynyltrimethylsilane and benzaldehyde (Scheme 84).



Scheme 84. Preparation of propargyl alcohol 342 from benzaldehyde

The preparation of sulfenylated propargyl alcohol **342** was explored using a variety of bases and conditions (Table 5).

Table 5. Reaction screening for the sulfenylation of 342 with thiosulfonate



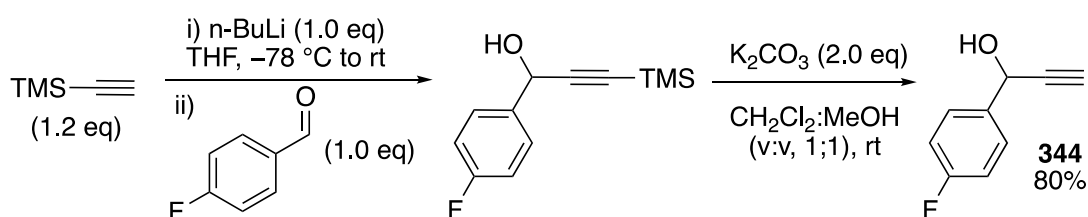
Entry	Base (eq.)	Thiosulfonate eq.	T/°C	Result
1	n-BuLi (2.5)	2.5	- 78 to rt	Mainly starting material
2	n-BuLi (2.5)	2.5	- 20 to rt	Intractable mixture
3	KHMDS (3.0)	1.2	- 78 to - 20	Intractable mixture
4	LiHMDS (3.0 eq)	1.2	0 to rt	49% ^a

^aIsolated yield after column chromatography. ^bReactions were performed under dry conditions: heat-gun dried flask under argon with anhydrous solvent.

Stoichiometric equivalents of the thiosulfonate were used with n-BuLi as it is a nucleophilic base. With n-BuLi at -78 °C, only a trace amount of **343** was observed in the crude reaction mixture alongside starting material, indicating there was not efficient deprotonation to generate the di-anionic acetylide (Table 5, entry 1). Unfortunately, the reaction with n-BuLi at -20 °C was intractable (Table 5, entry 2). Weaker, non-nucleophilic bases KHMDS and LiHMDS were then tested, at which point the equivalents of the thiosulfonate could be reduced. With KHMDS, the reaction provided a complex mixture and no starting material or product were observed at the end of the reaction (Table 5, entry 3). Fortunately, formation of the desired compound was successful with LiHMDS (Table 5, entry 4). At -20 °C, unreacted starting material was observed in the ¹H NMR spectrum of the crude reaction material which was problematic as it was completely inseparable from the product by column chromatography. For the reaction at 0 °C, aliquots were taken for ¹H NMR analysis every 2-3 h and a higher consumption of starting material was observed. If starting

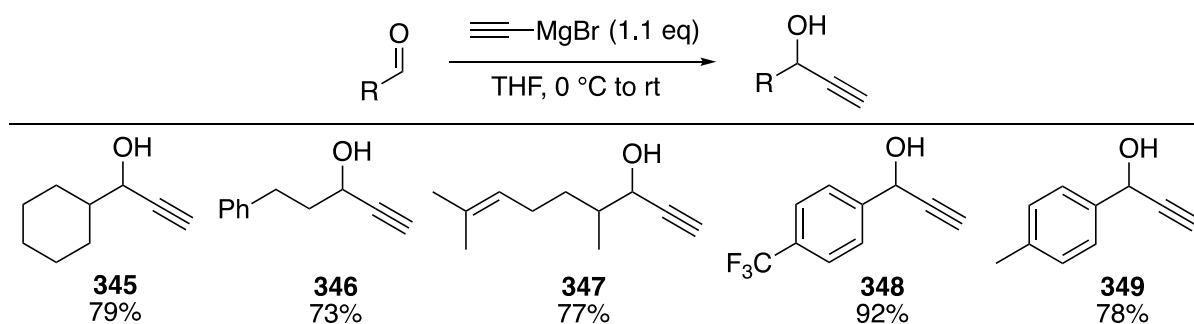
material was still present, the reaction solution was cooled to 0 °C and more LiHMDS was added. Overall, 3.0 equivalents of LiHMDS were required for complete consumption of the starting material. This method led to a slightly messier crude material compared to the reaction at –20 °C, however the other undetermined side products did not affect purification and **343** was isolated in 49% yield (Table 5, entry 4). Direct sulfenylation of terminal propargyl carboxylates was attempted, however the reactions were intractable, thus carboxylate preparation had to be performed after lithiation.

A range of propargyl alcohols were then synthesised from the corresponding aldehydes. Propargyl alcohol **344** was synthesised in 80% yield from ethynyltrimethylsilane and 4-fluorobenzaldehyde (Scheme 85).



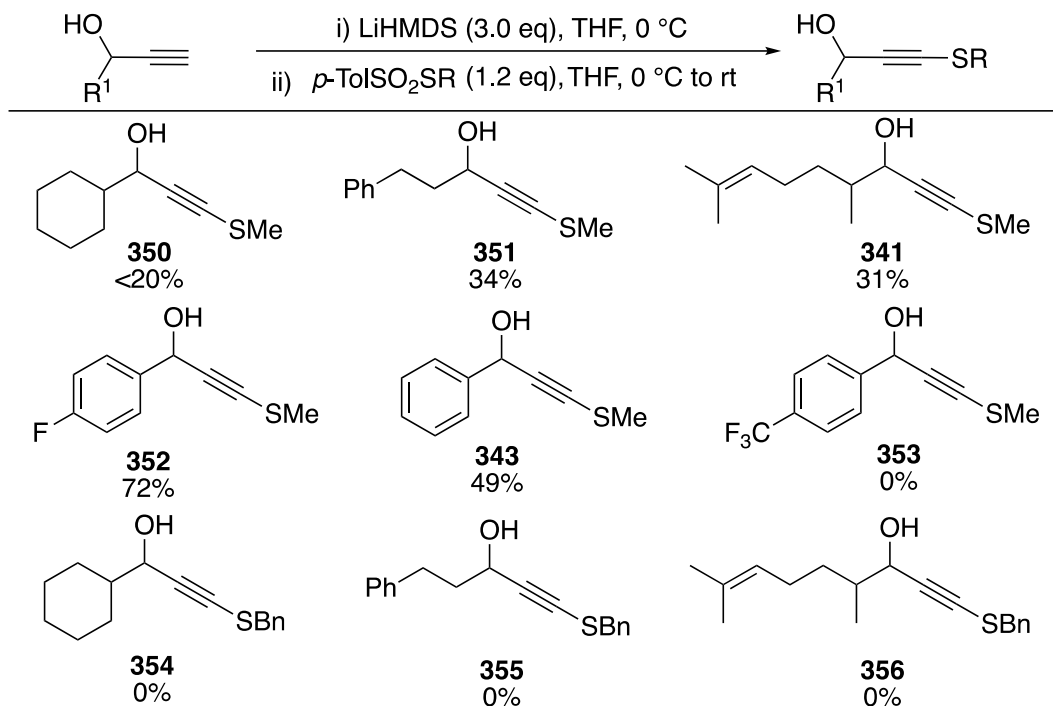
Scheme 85. Preparation of propargyl alcohol 344

Propargyl alcohols **344** to **349** were prepared in good yield from ethynylmagnesium bromide and the corresponding aldehyde in one step (Scheme 86).



Scheme 86. Preparation of propargyl alcohols with ethynylmagnesium bromide

The newly developed method for propargyl alcohol sulfenylation with thiosulfonates was then tested (Scheme 87).

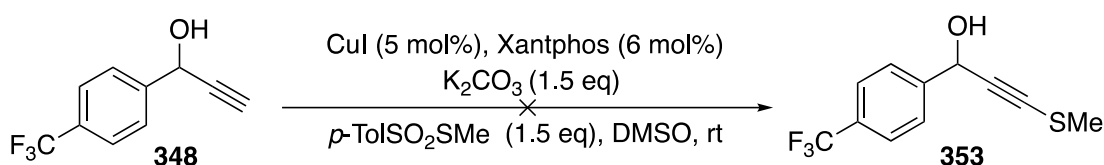


^aIsolated product contains minor impurities

Scheme 87. Preparation of sulfenylated propargyl alcohols with thiosulfonates

Sulfenylated propargyl alcohols **350**, **351** and **341** were only obtained in low yield, with lots of starting material left over. The same protocol was applied involving ¹H NMR analysis of reaction aliquots followed by addition of excess LiHMDS, but the starting material was still not consumed. This implies that generation or subsequent electrophilic trapping of the di-anionic acetylide was not efficient for these substrates. Difficult separation between the starting material and product meant that several chromatographic purifications were performed, contributing to the low yields obtained. On the other hand, **352** and **343** were isolated in moderate to good yield. The synthesis of **353** was unsuccessful, with no desired product observed in the ¹H NMR spectrum of the crude reaction material. Unfortunately, all reactions with the S-benzyl thiosulfonate were unsuccessful (Scheme 88, **354** to **356**). Whilst this method was able

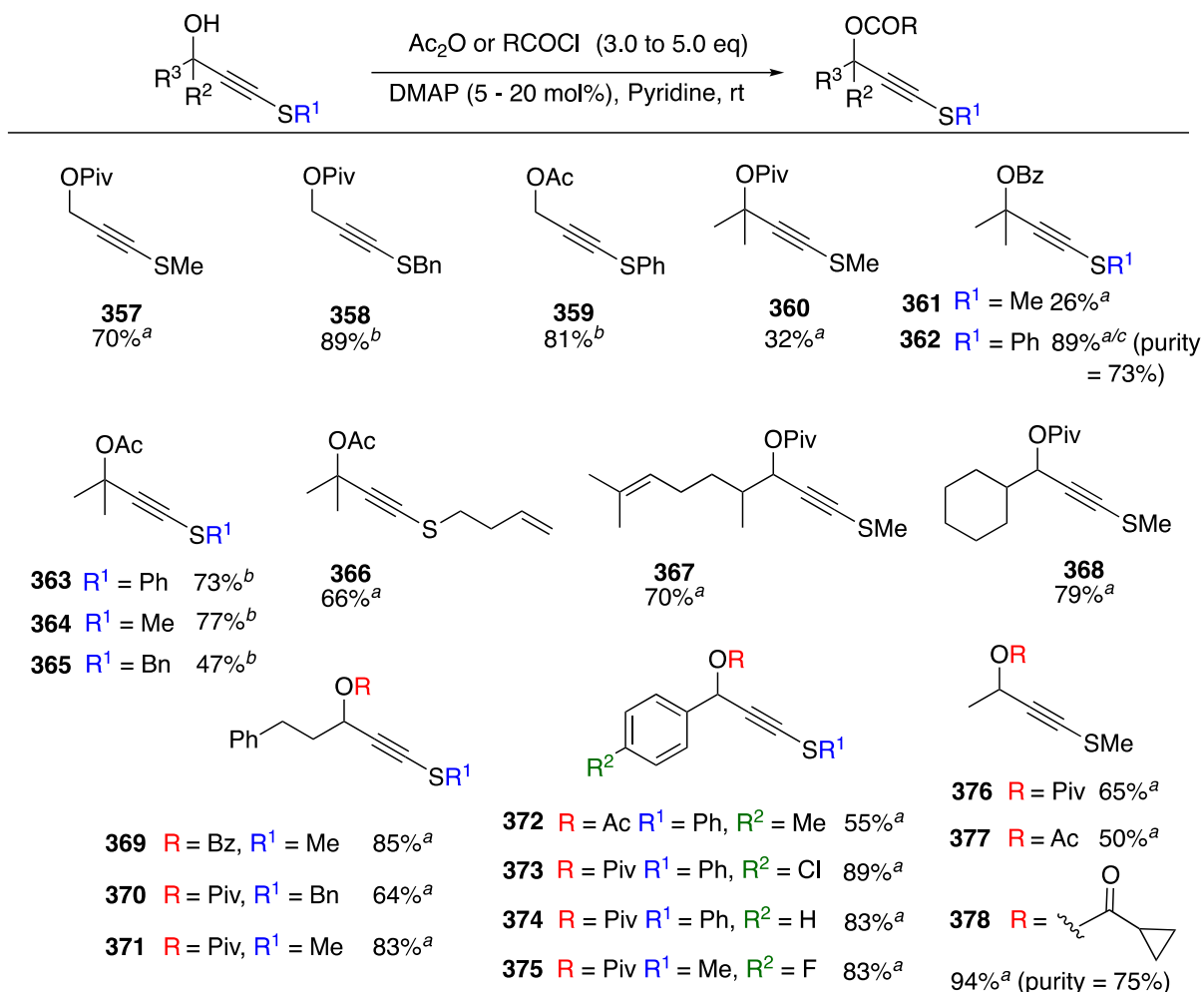
to provide some sulfenylated propargyl alcohols in good yield, further optimisation is required to improve substrate scope. A copper-catalysed method, adapted from the literature, was also attempted for the preparation of **353** however this was unsuccessful (Scheme 88).⁶⁹



Scheme 88. Alternative method to prepare 353

With a range of sulfenylated propargyl alcohols successfully synthesised, the corresponding carboxylates were prepared using anhydrides or acid chlorides with DMAP in pyridine (Scheme 89). Acetates were synthesised in good to excellent yields (Scheme 89, **359** and **363 – 366**). In some cases, the pivalates suffered from lower yields due to the numerous NaHCO_3 extractions required to remove excess pivalic acid (Scheme 89, **360**, **370** and **376**). This problem was later remedied by gently heating the samples under reduced pressure ($\sim 2\text{-}3 \times 10^{-2}$ mbar) to remove the pivalic acid. Whilst this method of purification was time-consuming, loss of product was prevented. Propargyl benzoate **362** was isolated at 73% purity alongside 27% benzoyl chloride starting material (purity was determined by ^1H NMR spectroscopy). In this case, not all of the benzoyl chloride could be removed, even after several basic work-ups or gentle heating under reduced pressure. Cyclopropane carboxylate **378** was also isolated at 75% purity, alongside the terminal propargyl carboxylate without the sulfenyl group. The yields of **362** and **378** takes this into account, with the yield referring to the products in the absence of the impurity. The difficulties encountered during the synthesis of propargyl carboxylates was due to the large excess of acid chloride required for their synthesis. Propargyl alcohol starting material consumption could not

be monitored by TLC as it was masked by the pyridine on the TLC plate. Therefore, to ensure high conversion, a large excess of acid chloride was used.



^a3.0 eq of RCOCl or Ac₂O was used. ^b5.0 eq of Ac₂O was used. ^cProduct isolated alongside BzCl impurity.

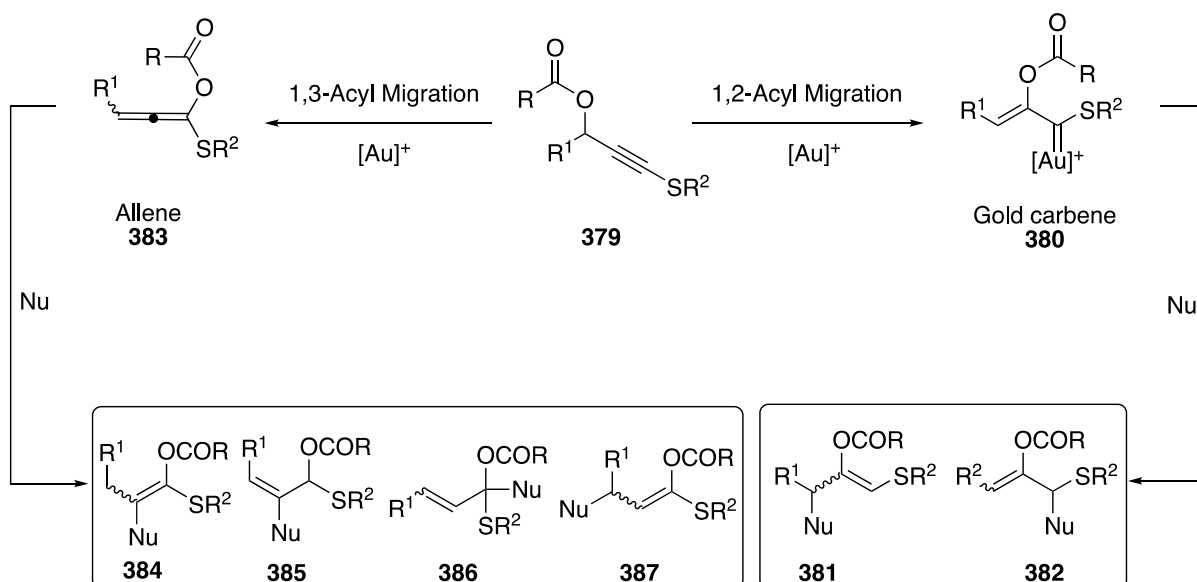
Scheme 89. Synthesis of sulfenylated propargyl carboxylates

The method for the synthesis of sulfenylated propargyl carboxylates was developed alongside investigation into gold-catalysed transformations. Therefore, not all of the substrates shown in Scheme 89 were used for each catalysis investigation. The rationale for the use of specific substrates will be explained throughout the following sections.

3.4 Gold-Catalysed Nucleophilic Addition Reactions with Sulfenylated Propargyl Carboxylates

3.4.1 Initial Studies into the Gold Catalysis of Propargyl Carboxylates

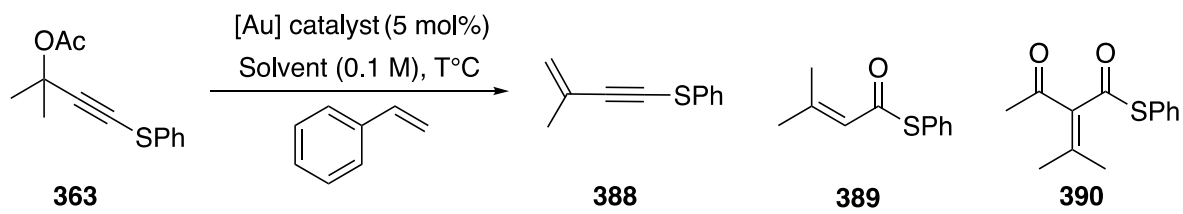
Initial investigations began by studying gold-catalysed intermolecular nucleophilic addition and cyclopropanation reactions with sulfenylated propargyl carboxylates. Identification of the products formed from nucleophilic addition should provide insight into the favoured mechanistic pathway/pathways of the propargyl carboxylates (Scheme 90). Owing to the many reactive pathways available to propargyl carboxylates under gold catalysis (as discussed in the introduction) a relatively simple substrate was required for initial reaction discovery. Whilst a sulfur substituent may enhance pathway control, stereo- and regio-isomeric alkene products were anticipated during these investigations (Scheme 90).



Scheme 90. Possible pathways for the rearrangement of sulfenylated propargyl carboxylates and subsequent nucleophilic addition

Dimethyl substituted propargyl carboxylate **363** was selected as it would reduce the number of isomers obtained and result in less complex reaction mixtures during the early exploration stages of the project (Table 6).

Table 6. Reaction screening for gold-catalysed addition of styrene to compound 363

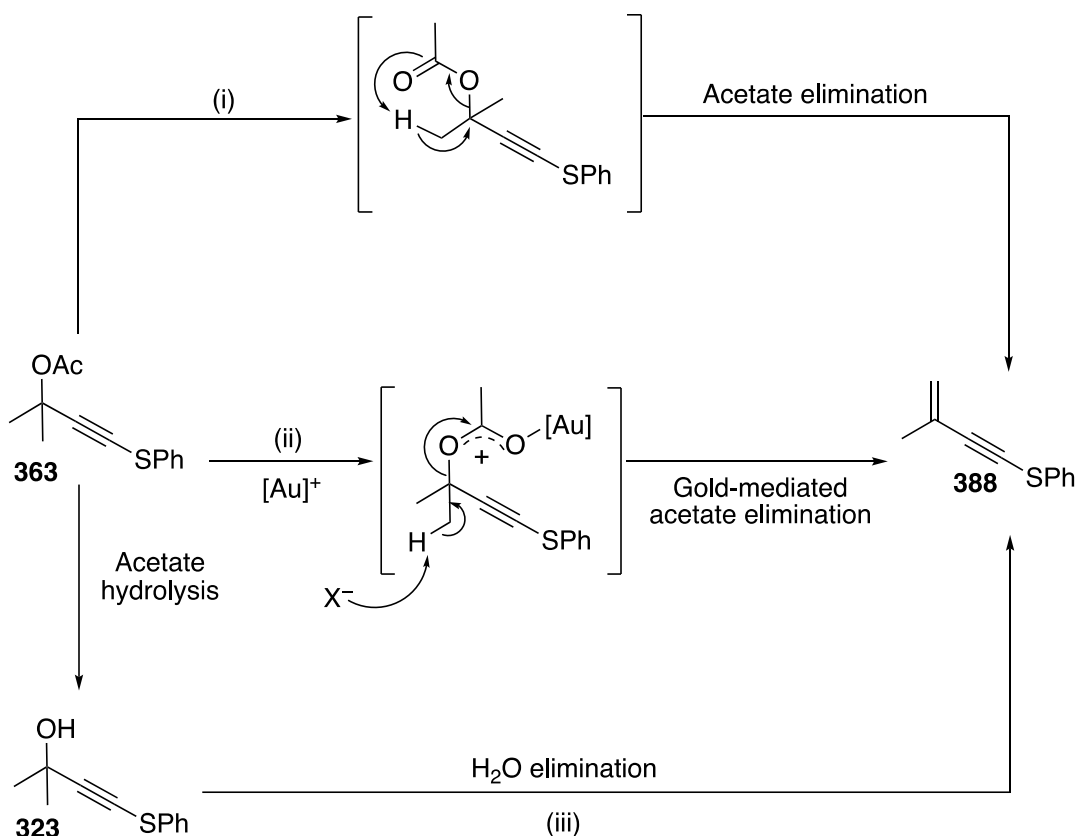


Entry	[Au] catalyst	Solvent	Time /h	Dry Cond. ^a	T/ ^o C	Styrene eq.	Yields/% ^b		
							388	389	390
1	SPhosAuNTf ₂	PhMe	24	N	rt	1.1	11	3	-
2	SPhosAuNTf ₂	PhMe	24	Y	rt	1.1	34	6	-
3	SPhosAuNTf ₂	PhMe	24	Y	50	1.1	46	- ^c	-
4	SPhosAuNTf ₂	PhMe	24	Y	0	2.0	37 ^d	-	-
5	SPhosAuNTf ₂	CH ₂ Cl ₂	24	Y	rt	1.1	- ^c	- ^c	-
6	[DTBPAuNCPPh]SbF ₆	PhMe	21	Y	rt	1.1	-	4	-
7	[DTBPAuNCPPh]SbF ₆	CH ₂ Cl ₂	18	Y	rt	1.1	-	- ^c	-
8	KAuCl ₄	PhMe	18	N	rt	2.0	-	<9 ^e	50 ^d
9	KAuCl ₄	CH ₂ Cl ₂	18	N	rt	2.0	-	-	99 ^d

^aDry conditions: Heat-gun dried flask under argon with anhydrous solvent. ^bYields and ratios were determined by ¹H NMR spectroscopy using a known concentration of 1,2,4,5-tetramethylbenzene as internal standard. ^cCompound was observed in ¹H NMR spectrum of crude reaction material but the yield could not be determined due to overlapping resonances. ^dIsolated yield after column chromatography. ^eProduct was observed in isolated fractions, but the yield is an overestimation as the product was not pure. ^fIf a yield is not stated then the compound was not observed in the ¹H NMR spectrum of the crude reaction material or after column chromatography.

Styrene was chosen for initial screening studies as alkenes are often used in both intra- and intermolecular gold-catalysed cyclopropanation of propargyl carboxylates.^{48, 70} Toluene was chosen as a non-coordinating solvent that would allow for heating if necessary. For initial studies, Au(I) catalysts SPhosAuNTf₂ and [DTBPAuNCPPh]SbF₆ were tested to explore electron-rich and electron-deficient ligands, alongside the Au(III) catalyst KAuCl₄. Unfortunately, cyclopropanation was not observed in any of the reactions. Enyne **388** was observed only in reactions with the SPhosAuNTf₂ catalyst and is formed as a result of acetic acid elimination from substrate **363** (Table 6, entries 1-5). The structure assignment of **388** was based on the observed coupling of the geminal alkene protons with the alkene methyl group in the ¹H NMR spectra of the crude reaction material. The α,β-unsaturated thioester **389** was observed in low yields across the majority of reactions with all three catalysts. The structure of **389** was determined from the ¹H NMR spectra of the crude reaction material from long-range coupling between the alkene methyl groups and the alkene proton. Both products **388** and **389** were also separately isolated and characterised. The starting material was fully consumed in all reactions that used SPhosAuNTf₂ and [DTBPAuNCPPh]SbF₆ (Table 6, entries 1-7). Other than the identified products **388** and **389**, the reaction mixtures were largely intractable, particularly with [DTBPAuNCPPh]SbF₆, and changing the solvent to CH₂Cl₂ did not provide cleaner outcomes. Catalysis of **363** with KAuCl₄ produced interesting results, affording enone **390**. In toluene at rt, **390** was formed in 50% yield alongside unreacted starting material, whilst the reaction in CH₂Cl₂ at rt saw quantitative conversion to **390** (Table 6, entries 8 and 9). This transformation is analogous to that discovered by Zhang for the formation of diketones (see section 3.1.5, Scheme 65).⁵³

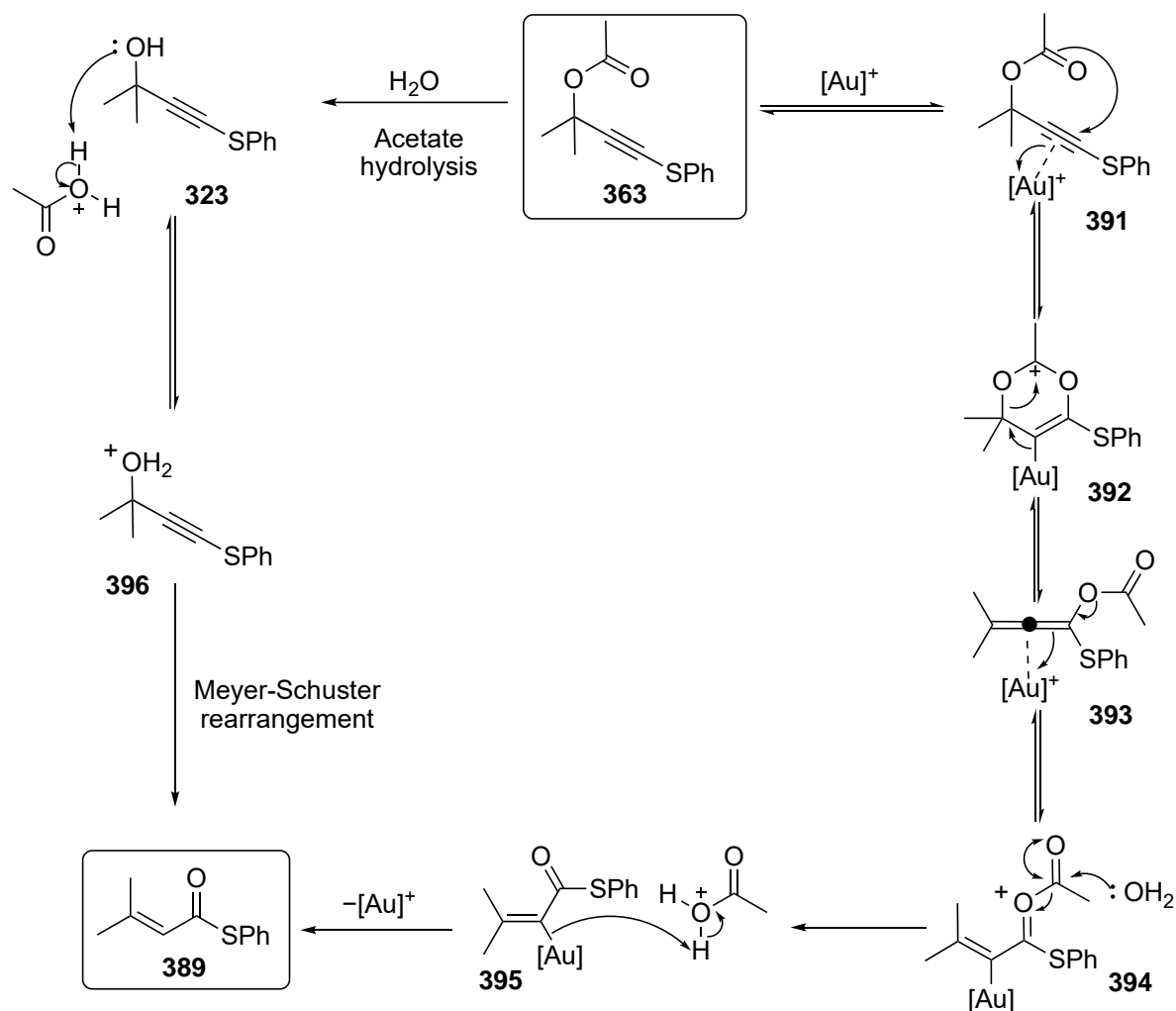
There are several plausible pathways for the formation of enyne **388** (Scheme 91). Direct formation of **388** from acetate elimination appears to be more likely than acetate hydrolysis and subsequent H₂O elimination of **323** (Scheme 91, (iii)); product **388** was observed in higher yield under dry conditions (Table 6, entry 1 vs. 2). As the formation of **388** was not observed with the other two catalysts, elimination of acetic acid may be mediated by SPhosAuNTf₂, or any generated triflimide, rather than an intramolecular elimination mechanism (Scheme 91, (i) vs (ii)). The formation of **388** is likely to be facilitated by the methyl groups stabilising positive charge built up at the propargylic position.



Scheme 91. Proposed mechanistic pathways for the formation of 388

Thioester **389** may be formed via initial hydrolysis of **363** to generate alcohol **323**, followed by a Meyer-Schuster rearrangement (Scheme 92).⁷¹ Gold catalysts have been shown to facilitate the Meyer-Schuster rearrangement of propargyl alcohols.⁷²

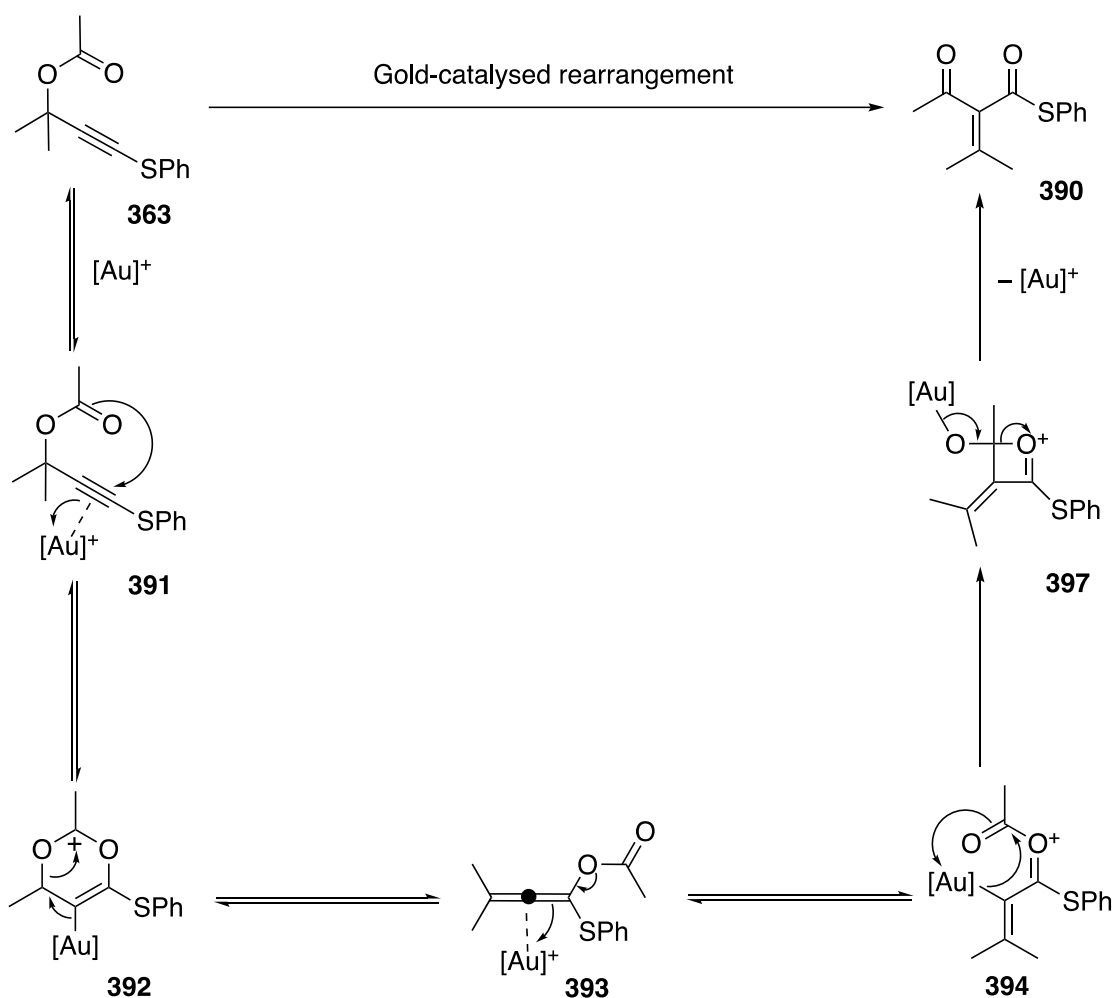
This product could also be formed via gold-mediated 1,3-migration of the acetate, at which point water intercepts the electrophilic intermediate **394** to form thioester **389** after protodeauration of **395** (Scheme 92). Zhang and co-workers describe an analogous reaction for the preparation of α,β -unsaturated ketones from the gold catalysis of propargyl acetates.⁷³



Scheme 92. Proposed mechanistic pathways for the formation of product 389

The proposed mechanism towards enone **390** follows a 1,3-acetate migration pathway towards carboxyallene **393**, which is further activated by the gold catalyst giving rise to oxocarbenium intermediate **394** (Scheme 93). Nucleophilic attack of the $[\text{Au}]$ -C bond at the acetyl $\text{C}=\text{O}$ forms intermediate **397**, which then collapses to afford the enone

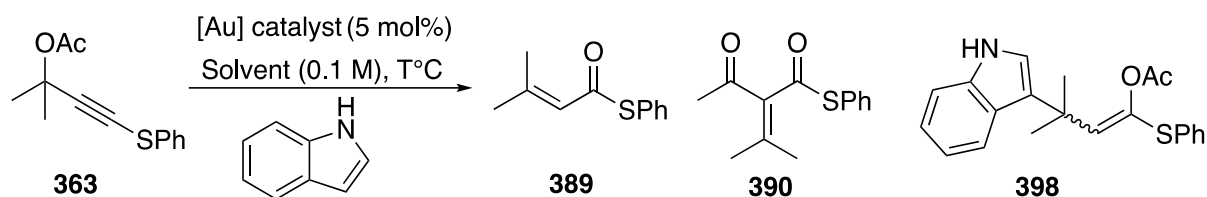
product **390** (Scheme 93). These preliminary studies demonstrate that substrate **363** favours 1,3-acetate migration under gold catalysis, rather than a 1,2-acetate migration pathway facilitated by a sulfur-gold interaction (see section 3.2, Scheme 71). Although internal alkynes have a propensity to undergo 1,3-acyl migration, the quantitative yield obtained for **390** (Table 2, entry 9) could be a result of the sulfur facilitating 1,3-acyl migration through a gold ketenthionium intermediate.



Scheme 93. Proposed mechanism for the gold-catalysed rearrangement **363 to provide enone **390****

As styrene was not sufficient to trap the carboxyallene intermediate **393** or oxocarbenium **394** before rearrangement to enone **390**, indole was explored as a nucleophile (Table 7).

Table 7. Reaction screening for gold-catalysed addition of indole to substrate 363

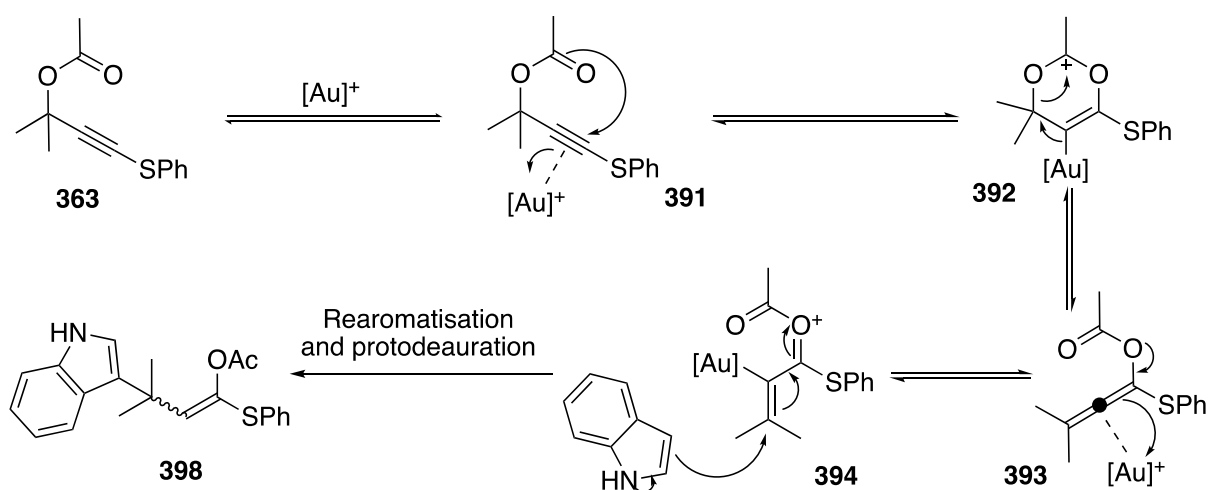


Entry	[Au] catalyst	Solvent	Time /h	T/°C	Indole eq.	Yields/% ^a			
						389	390	398	363
1	SPhosAuNTf ₂	PhMe	21	rt	1.1	3	-	7	43
2	[DTBPAuNCPPh]SbF ₆	PhMe	21	rt	1.1	6	-	-	54
3	KAuCl ₄	PhMe	22	rt	2.0	18	14	8	24
4	KAuCl ₄	CH ₂ Cl ₂	22	rt	2.0	46 ^b	29 ^b	-	-
5	AuBr ₃	PhMe	18	rt	2.0	-	86	-	-
6	Me ₂ SAuCl	PhMe	3	60	1.1	-	82 ^b	-	-
7	KAuCl ₄	PhMe ^d	24	rt	2.0	Trace ^c	Trace ^c	23 ^b	-

^aYields and ratios were determined by ¹H NMR spectroscopy using a known concentration of 1,2,4,5-tetramethylbenzene as internal standard. ^bIsolated yield after column chromatography. ^cTrace amount of product was observed in impure isolated fractions. ^dReaction was performed at 0.2 M. ^eAll reactions were performed under dry conditions: heat-gun dried flask under argon with anhydrous solvents. ^fIf no yield is reported the product was not observed by ¹H NMR spectroscopy of the crude reaction or after column chromatography.

The study between indole and **363** provided more fruitful results. All reactions were performed under dry conditions in an attempt to avoid the formation of enyne **388** and thioester **389**. With both SPhosAuNTf₂ and KAuCl₄, nucleophilic addition of indole was observed affording product **398**. With SPhosAuNTf₂ at rt in toluene (Table 3, entry 1), 43% of starting material remained after 21 h and a trace amount of **389** was also observed. As seen in the study with styrene, no rearrangement product **390** was observed with SPhosAuNTf₂. Electron deficient Au(I) catalyst [DTBPAuNCPPh]SbF₆ did

not afford the nucleophilic addition product **398**; 54% of the starting material remained after 21 h and the reaction was particularly messy (Table 3, entry 2). With KAuCl_4 , the amount of indole was increased to 2.0 eq to promote nucleophilic addition, however the reaction gave a similar result to that with SPhosAuNTf_2 , and 8% of **398** was observed after 22 h (Table 3, entry 4). With KAuCl_4 , increasing the concentration from 0.1 M to 0.2 M saw an increase in the formation of **398**, producing a 23% isolated yield. With AuBr_3 , the rearrangement product **390** was the sole product observed after stirring for 18 h at rt (Table 3, entry 5). The Au(I) catalyst Me_2SAuCl was tested as it was suspected that a smaller ligand may lead to a more reactive catalyst towards the highly substituted substrate, however only starting material was seen by TLC after stirring overnight at rt. Therefore, a separate reaction was performed at 60 °C and rearrangement product **390** was the only product observed after 3 h (Table 3, entry 6). Formation of the nucleophilic addition product **398** should follow a similar initial trajectory to the formation of enone **390**, with nucleophilic addition of indole occurring at oxocarbenium **394** (Scheme 94).



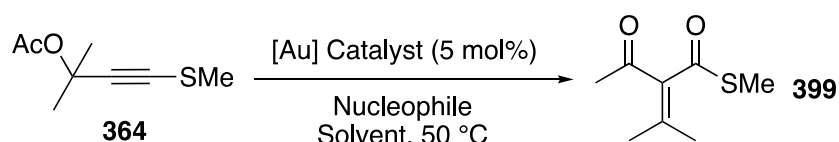
Scheme 94. Proposed mechanism for gold-catalysed addition of indole to 363

Whilst **398** was observed as a single stereoisomer, the stereochemistry of the alkene could not be determined as no key interactions were observed in the NOESY spectrum and a crystal could not be obtained for X-ray crystallography.

3.4.2 Variation of Sulfur Substituents

It was suspected that steric bulk around the alkyne in **363** may hinder nucleophilic addition and so substrate **364** with a smaller S-methyl group was explored. A different sulfur substituent may also allow nucleophilic addition at different positions of the electrophilic intermediates or see a different rearrangement pathway entirely. Gold-catalysed nucleophilic addition reactions with **364** were tested (Table 8).

Table 8. Reaction screening for gold-catalysed addition of indole to substrate 364

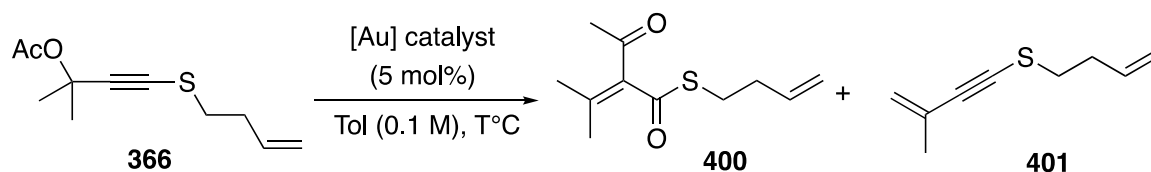


Entry	[Au] catalyst	Nucleophile (eq.)	Solvent	Time /h	Result
1	KAuCl ₄	Indole (1.1)	PhMe	21	Quantitative ^a
2	KAuCl ₄	Indole (2.0)	1,4-Dioxane	21	Quantitative ^a
3	Me ₂ SAuCl	Indole (1.1)	PhMe	22	Quantitative ^a
4	[DTBPAuNCPH]SbF ₆	Indole (2.0)	PhMe	22	Intractable
5	KAuCl ₄	Benzoylacetone (2.0)	PhMe	21	Quantitative ^a
6	KAuCl ₄	Anisole (2.0)	PhMe	21	Quantitative ^a

^aQuantitative yields were determined by ¹H NMR analysis of the crude reaction material. Only **399** was observed and no other species were present. The entire crude reaction material dissolved in CDCl₃ and an aliquot was taken for ¹H NMR spectroscopic analysis. ^bAll reactions performed under dry conditions: heat-gun dried flask under argon with anhydrous solvents.

No nucleophilic addition products were observed during gold-catalysis of **364** with indole. The reactions were very slow at rt, with mainly starting material observed by TLC, and so the reactions were heated to 50 °C. Reactions with KAuCl₄ and Me₂SAuCl were very clean providing quantitative yields of the rearrangement product **399**. As observed during the previous studies with propargyl acetate **363**, use of catalyst [DTBPAuNCPH]SbF₆ resulted in a complex mixture and neither rearrangement nor nucleophilic addition was observed. Benzoylacetone and anisole were also tested as nucleophiles and, once again, quantitative conversion to the rearrangement product **399** was observed. An intramolecular quench was next explored with substrate **366** to explore whether intramolecular cyclopropanation of the tethered alkene would out-compete the rearrangement pathway (Table 9).

Table 9. Reaction screening for the intramolecular gold-catalysed reaction of 369



Entry	[Au] catalyst	T/°C	Yield/%	
			400 ^a	401 ^a
1	KAuCl ₄	rt	-	-
2	KAuCl ₄	50	82	-
3	KAuCl ₄	70	72	-
4	SPhosAuCl/AgNTf ₂ ^c	50		31

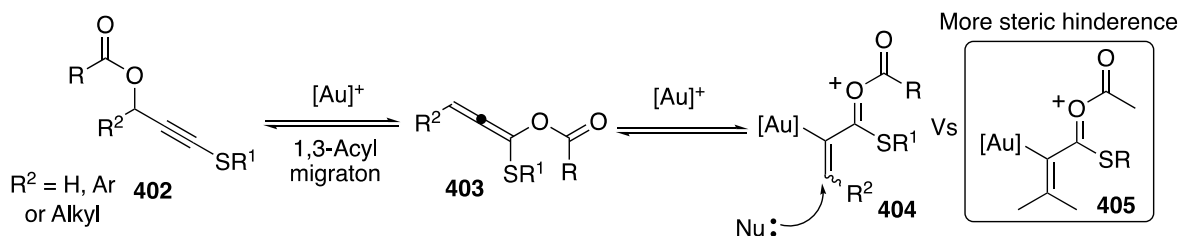
^aIsolated yield after column chromatography. ^b[Au] = 5 mol%, AgX = 7.5 mol%. ^cWhere yield is not given the product was not observed.

Cyclopropanation of the tethered alkene was not observed. Instead, the rearrangement product **400** was observed in very high yields with KAuCl₄, as seen with substrates **363** and **364**. No reactivity was observed at rt with either catalyst tested.

The reactions had to be heated to 50 °C before any reactivity was observed and the yield of enone product **400** was higher at 50 °C than at 70 °C with KAuCl₄. With SPhosAuNTf₂, no rearrangement product **400** was observed but enyne **401**, from acetic acid elimination, was isolated in 31% yield. The rearrangement pathway to form the enone products appeared to be the reaction sink for the dimethyl-substituted sulfenylated propargyl acetate derivatives.

3.4.3 Variation of Substituents at the Propargylic Position

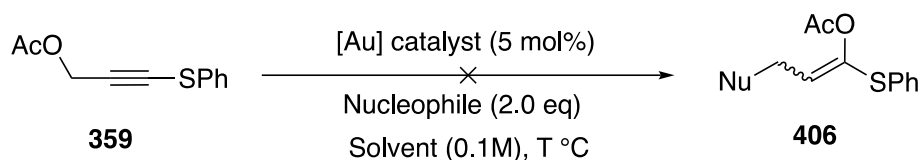
Having explored different sulfur substituents, variation of the propargylic substituents was investigated to reduce the steric hindrance at that position. It was suspected that dimethyl-substituted systems could be blocking nucleophilic addition at the electrophilic intermediates generated after carboxylate rearrangement. The gold-catalysed studies with sulfenylated propargyl carboxylates thus far had formed products via 1,3-acyl migration followed by nucleophilic addition or rearrangement of a carboxyallene intermediate. Therefore, if substrates that are unsubstituted or monosubstituted at the propargylic position proceed through a 1,3-migration pathway, a less sterically-hindered carboxyallene intermediate will be formed, and should allow for facile nucleophilic addition (Scheme 95, **404** vs **405**). It has been shown that dimethyl substituents slow down the addition of nucleophiles to enones compared to those with only one substituent.⁷⁴



Scheme 95. Proposed nucleophilic addition to less sterically-hindered propargyl carboxylates

Substrate **359** was first explored which is unsubstituted at the propargylic position. Several gold-catalysed reactions were performed with styrene and indole (Table 10).

Table 10. Reaction screening for gold-catalysed nucleophilic addition to 359

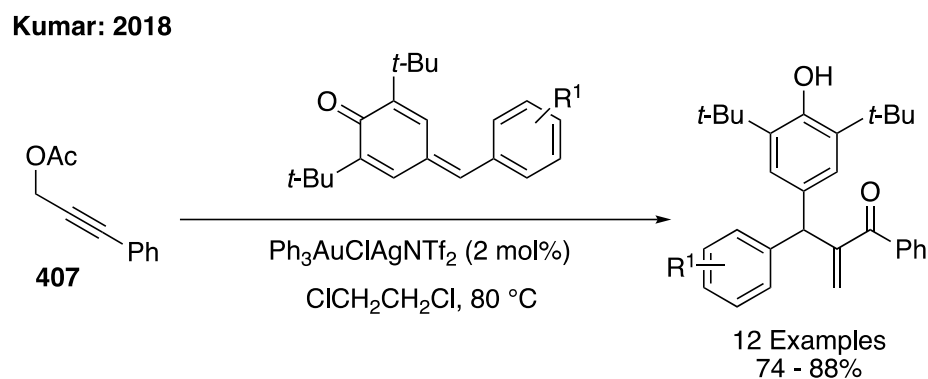


Entry	[Au] catalyst	Solvent	T/°C	Nucleophile	Result ^b
1	SPhosAuNTf ₂	PhMe	70	Styrene	No reaction
2	KAuCl ₄	PhMe	85	Styrene	No reaction
3	KAuCl ₄	PhMe	90	Indole	No reaction
4	SPhosAuNTf ₂	PhMe	90	Indole	No reaction
5	[DTBPAAuNCPH]SbF ₆	PhMe	90	Indole	No reaction
6	KAuCl ₄	CH ₂ Cl	rt	Indole	No reaction
7	SPhosAuNTf ₂	CH ₂ Cl	rt	Indole	No reaction

^aReactions were not performed under dry or inert conditions. ^bOnly the starting material **359** was observed in the ¹H NMR spectrum of the crude reaction material.

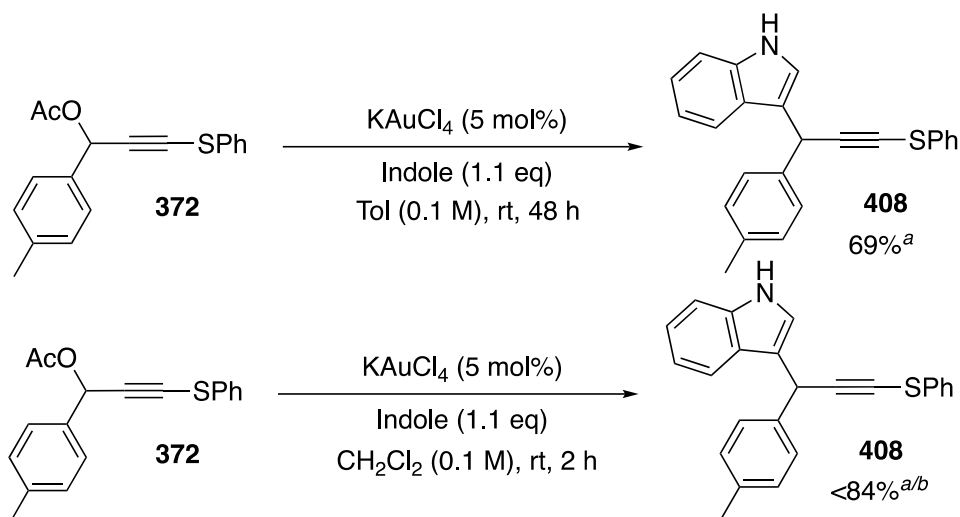
Nucleophilic addition to **359** was unsuccessful under gold-catalysis. Intriguingly, only starting material was observed at the end of all of the reactions screened, even when the reactions were performed at 90 °C (Table 10, entries 3 – 5). The absence of substituents at the propargylic position may prevent migration due to the lack of stabilisation of positive charge build up at this position. In 2018, Kumar demonstrated electrophilic trapping of the carboxyallene intermediate after 1,3-acyl migration of the propargyl acetate **407** (Scheme 96).⁷⁵ This suggests that the presence of the sulfur atom impedes the rearrangement process for this substrate, or that nucleophilic addition to electrophilic intermediates generated after migration of **359** is not favoured.

It is possible that the absence of substituents at the propargylic position changes the energy of the triple bond LUMO, hindering sulfur conjugation and stabilisation through a ketenthionium.



Scheme 96. Gold-catalysed rearrangement of propargyl acetate 407 and subsequent electrophilic trapping by Kumar

As **359** displayed no reactivity, substrates that were monosubstituted at the propargylic position were explored. The presence of one propargylic substituent should stabilise cationic character allowing carboxylate migration without sterically hindering nucleophilic addition. An aromatic substituent vicinal to the carboxylate would provide more scope to tune the reactivity by varying the substituents around the aromatic ring. In addition, the use of an aromatic propargylic substituent may result in a different migration pathway. As an aromatic substituent can stabilise cationic character at the propargylic position through resonance, the need for sulfur stabilisation through a ketenthionium intermediate may be reduced. This could allow for sulfur-gold interactions and encourage a 1,2-acyl migration pathway of the internal sulfenylated propargyl carboxylate. Substrate **372** was chosen as it exhibits a slightly electron-rich *p*-methylbenzene substituent to allow the hypothesis to be explored (Scheme 97). A para-substituent would also simplify the aromatic region in the ^1H NMR spectra of the crude/isolated products, aiding product determination.



^aIsolated yield after column chromatography. ^bIsolated product contained minor impurities.

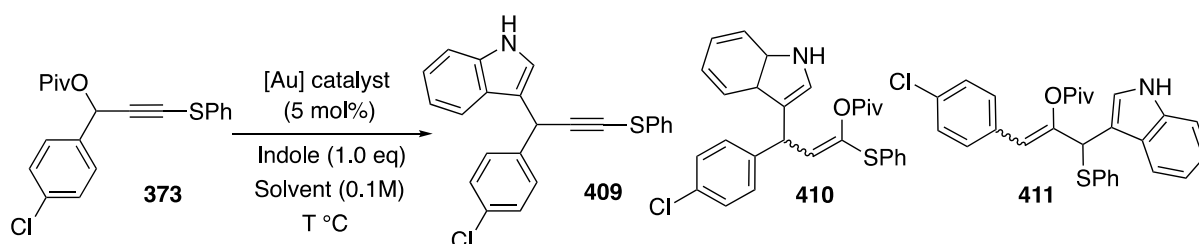
Scheme 97. Gold catalysis of propargyl carboxylate **372** with indole

KAuCl₄ was used as it had already shown high reactivity towards sulfenylated propargyl carboxylates and would provide a direct comparison to the dimethyl-substituted systems. When propargyl acetate **372** was used in gold catalysed reactions with indole, no rearrangement was observed. Instead, nucleophilic substitution at the propargylic position occurred, yielding the propargylated indole **408** as the major product in both toluene and CH₂Cl₂ (Scheme 97). The reaction in toluene was much slower than the reaction performed in CH₂Cl₂ and starting material was still present after 48 h. It is uncertain whether substitution occurred at the acetate **372** or the corresponding alcohol after acetate hydrolysis. Gold-catalysed nucleophilic substitution of propargyl alcohols has been previously demonstrated.⁷⁶ In addition, Brønsted acid-catalysed propargylation of indole with *p*-toluenesulfonic acid and propargyl alcohols has also been shown.⁷⁷ On the other hand, similar nucleophilic substitution reactions have also been observed with propargyl carboxylates under gold catalysis.⁵⁰ C-3 substituted indoles are highly prevalent in biologically active molecules and C-3 propargylation allows for further functionalisation of these scaffolds at the triple

bond. Aluminium- and cerium-catalysed protocols for indole propargylation have both been previously demonstrated.⁷⁸

To discourage direct substitution of the carboxylate, the *p*-chlorobenzene substituted propargyl carboxylate **373** was subjected to the same conditions (Table 11). An electron-withdrawing chlorine substituent was expected to reduce the possibility for direct substitution by preventing the potential ionization of the carboxylate if the reaction occurs via an S_N1 mechanism. A pivalate group was also used as they are less susceptible to hydrolysis than acetates and thus less nucleophilic substitution should be observed if it occurs via the propargyl alcohol.

Table 11. Reaction screening for gold-catalysed nucleophilic addition of indole to 373



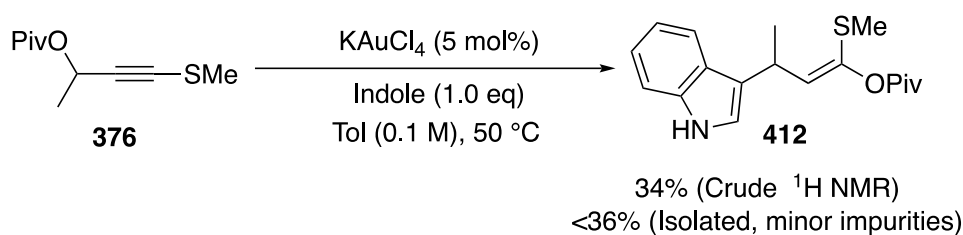
Entry	[Au] catalyst	Solvent	T/°C	Yield/%		
				409	410	411
1	KAuCl ₄	PhMe	rt	No reaction		
2	KAuCl ₄	PhMe	90	Intractable mixture		
3	KAuCl ₄	CH ₂ Cl ₂	rt	13% ^a	-	-
4	[IPrAuNCMe]SbF ₆	PhMe	90	No reaction		
5	[DTBPAuNCPh]SbF ₆	PhMe	50	Intractable mixture		

^aIsolated yield after column chromatography. ^bAll reactions were performed under dry conditions: heat-gun dried flask under argon with anhydrous solvent. ^cWhen no yield is reported the product was not observed.

As expected, these modifications to the substrate reduced the amount of direct nucleophilic substitution of the carboxylate. However, the changes also rendered the substrate less reactive (Table 11). Unlike the *p*-tolyl substituted substrate **372**, the *p*-chlorobenzene-substituted propargyl carboxylate **373** did not show any reactivity in KAuCl₄ in toluene at rt (Table 11, entry 1). With KAuCl₄ in CH₂Cl₂, the nucleophilic substitution product **409** was isolated in 13% yield, alongside unreacted starting material (Table 11, entry 3). With [IPrAuNCMe]SbF₆, KAuCl₄ and [DTBPAuNCPh]SbF₆ as catalysts the reaction temperature was raised by 10 °C every 3 – 4 hours. There was no reaction observed with [IPrAuNCMe]SbF₆ at 90 °C. When reaction was seen at 90 °C and 50 °C with KAuCl₄ and [DTBPAuNCPh]SbF₆ respectively, the reaction material was intractable (Table 11, entry 2 and 5). The products **410** and **411** from nucleophilic addition of indole after 1,2- or 1,3-acyl migration were not observed in any of the reactions.

Aromatic substrates **372** and **373** either showed little to no reactivity under gold-catalysis with indole or formed undesired products from direct nucleophilic substitution at the carboxylate. Substrate **376** with a single methyl substituent at the propargylic position was then explored. This substrate would provide a direct comparison to the dimethyl substituted systems to explore whether steric bulk was a contributing factor in obstructing nucleophilic addition. A pivalate was also used in attempt to avoid hydrolysis pathways. When this substrate was subjected to gold catalysis, 34% of the nucleophilic addition product **412** was obtained, which is higher than the yields obtained for any of the dimethyl-substituted propargyl carboxylates explored (Scheme 98). It was suspected, from the ¹H NMR spectrum of the crude reaction material, that

other nucleophilic addition products had also been formed as other vinylic protons were observed with complex splitting patterns. However, these resonances were very small in comparison to the resonances observed for **412**, and these side products could not be isolated or characterised. These results imply that substrate **376** with a single methyl substituent generates a carboxyallene intermediate that is more reactive towards nucleophilic addition compared to the dimethyl-substituted analogues previously discussed.



Scheme 98. Gold catalysed nucleophilic addition of indole to 376

Product **412** was isolated as a single stereoisomer. The stereochemistry could not be identified from the NOESY spectrum, therefore, X-ray crystallography was used and the stereochemistry of **412** was ascertained as the *Z* alkene (Figure 14).

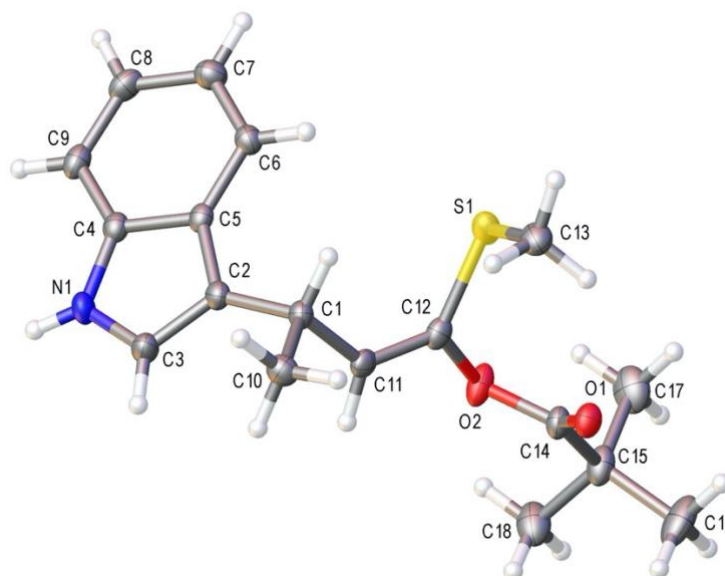
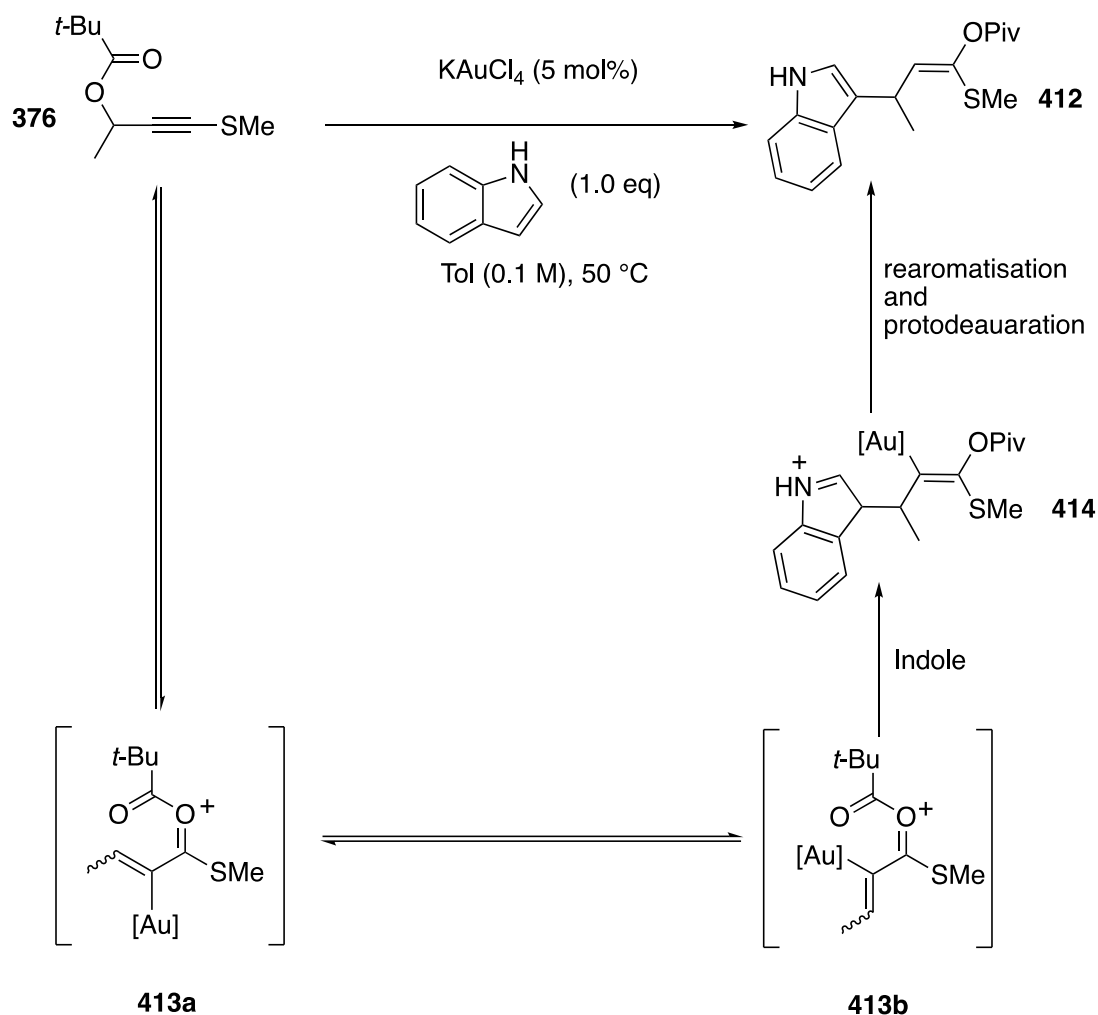


Figure 14. Crystal Structure of 412 with ellipsoids drawn at the 50% probability level.

X-ray Crystallography was carried out and data solved by Dr. Louise Male (UoB)

The observed stereochemistry of the major product **412** can be rationalised by considering the electrophilic intermediates that react with the indole nucleophile (Scheme 99).



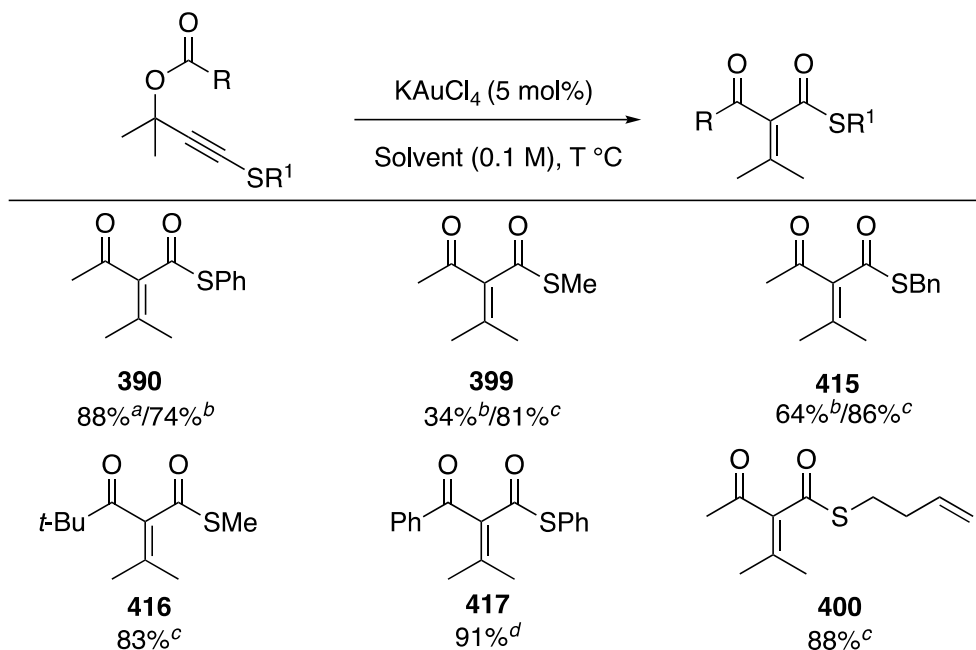
Scheme 99. Proposed mechanism for gold-catalysed addition of indole to sulfenylated propargyl carboxylate 376

During the transformation, the oxocarbenium intermediate **413** is proposed to interconvert between rotamers **413a** and **413b**. Addition of indole to oxocarbenium **413a** should result in the *E* isomer of **412**. However, as only the *Z* isomer was observed, it is proposed that indole undergoes 1,4-addition at oxocarbenium **413b**. The equilibrium between oxocarbeniums **413a/b** may be favoured towards **413b** due

to oxygen-gold interactions stabilising this intermediate through a 6-membered chelate ring. On the other hand, it could be that the formation of *Z*-**412** is due to a lower energy barrier for nucleophilic addition of indole to oxocarbenium **413b** compared to **413a**. It is also possible that **412** can be isomerised under gold-catalysis to form the more thermodynamically stable *Z* alkene.

3.5 Gold-Catalysed Rearrangements of Sulfenylated Propargyl carboxylates

Whilst the reactivity of sulfenylated propargyl carboxylates towards nucleophilic addition proved to be complex and difficult to optimise, the rearrangement to generate enones provided excellent yields. Knoevenagel condensation reactions, typically used for the preparation of such unsaturated dicarbonyls, often succumb to self-condensation and controlling side product formation can be difficult.⁷⁹ From what is known in the literature, there are only two reports of β -ketothioesters being used as Knoevenagel donors.⁸⁰ However, the scope is limited and therefore a complimentary gold-catalysed method would be useful as the presence of a thioester should allow for further elaboration of these scaffolds. In addition, a gold-catalysed process may provide more control of the alkene stereochemistry compared to Knoevenagel condensation reactions, in which the stereochemistry is highly dependent on the substituents of both reactants. High yields of enones **390** and **399** had already been obtained for the gold-catalysed rearrangement during the previous studies into nucleophilic addition. The gold-catalysed rearrangement was therefore tested on a range of dimethyl-substituted substrates in the absence of nucleophiles (Scheme 100).



Reaction performed in: ^aCH₂Cl₂ at rt. ^bToluene at rt. ^cToluene at 50 °C. ^dToluene at 60 °C. ^eAll yields represent the isolated yield after column chromatography.

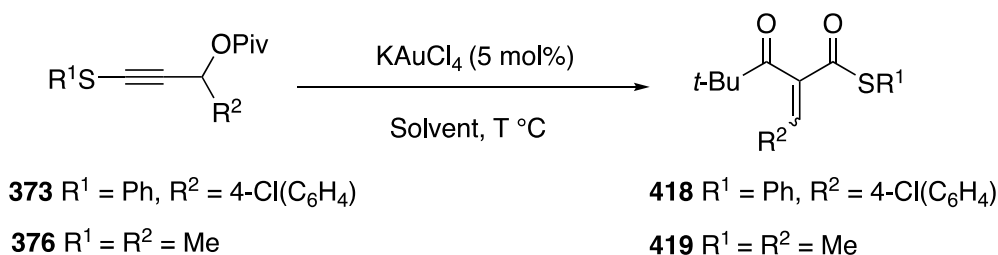
Scheme 100. Gold-catalysed rearrangement of sulfenylated propargyl carboxylates

All of the substrates provided the enone products in excellent yields. Enone **390** was obtained in high yields in both CH₂Cl₂ and toluene at rt over 18 h. Large scale catalysis was also demonstrated with 2.5 mol% KAuCl₄; the reaction in toluene was performed on a 0.89 mmol scale providing **390** in 74% yield. For the formation of S-methyl and S-benzyl derivatives **399** and **415**, the reactions proceeded at rt but an appreciable amount of starting material remained after 16 h. Excellent yields were obtained by simply heating to 50 °C. As previously shown, enone **400** with a tethered alkene was formed in 88% yield. The reaction was extremely clean with no evidence of intramolecular nucleophilic addition from the alkene, showing that the gold-catalysed transformation is a highly favoured pathway. This was an interesting result as there were no examples for the transformation of substrates with tethered alkenes in the analogous work by Zhang (see section 3.2, Scheme 65). Formation of **416** and **417**

show that benzoates and pivalates are also capable of undergoing the transformation superbly when heated. The reaction is very robust; it did not require an inert atmosphere and used undried commercial solvents. The conditions are mild, and the catalyst is commercially available.

The rearrangement of substrates **373** and **376**, with one propargylic substituent, were then tested. This would also allow the stereoselectivity of the transformation to be investigated (Table 12).

Table 12. Attempting gold-catalysed rearrangement of propargyl pivalates 373 and 376

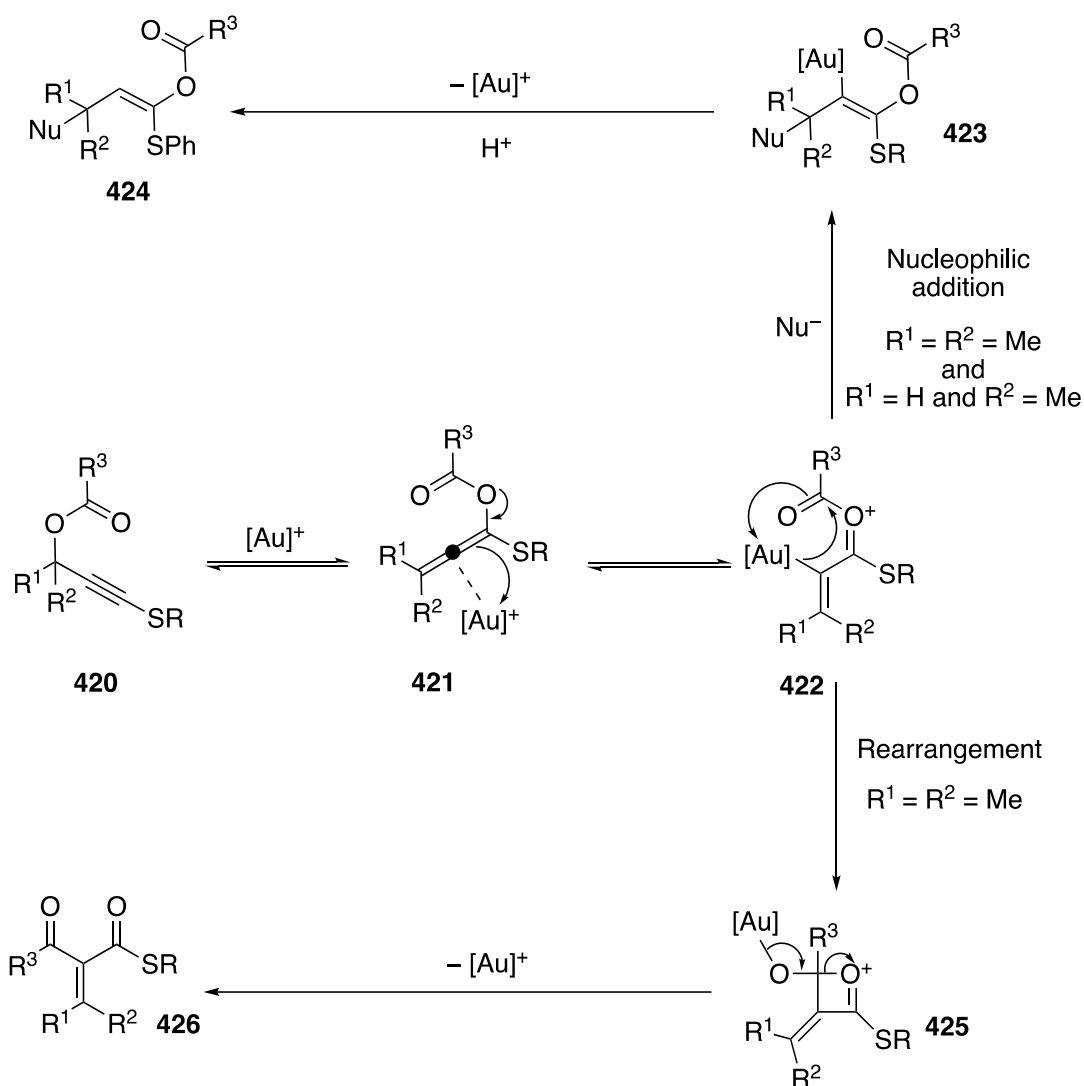


Entry	R ¹	R ²	Solvent	T/°C	Observations
1	Ph	4-Cl(C ₆ H ₄)	Toluene	rt to 110	Intractable
2	Me	Me	Toluene	rt	Mainly starting material
3	Me	Me	Toluene	50	Intractable
4	Me	Me	CH ₂ Cl ₂	rt	Mainly starting material

Under the tested conditions, rearrangement of substrates **373** or **376** did not occur to form the enones **418** and **419** respectively (Table 12). With substrate **373**, no change in the reaction by TLC was observed until the reaction was heated to 110 °C at which point the ¹H NMR spectrum of the crude reaction material was messy and the results

were inconclusive (Table 12, entry 1). As seen when studying nucleophilic addition reactions with **373**, the presence of the electron deficient *p*-chlorobenzene substituent greatly reduced the reactivity of the substrate. This is likely due to the lack of stabilisation of positive charge build up at the propargylic position, thus migration of the carboxylate is discouraged. As for substrate **376**, there was slight evidence of a new product on the baseline of the ¹H NMR spectra of the crude reaction material when both CH₂Cl₂ and toluene were used at rt (Table 12, entries 2 and 4). However, the new resonances were of very low intensity and mainly starting material was recovered. Heating the reaction with **376** at 50 °C in toluene resulted in a very messy crude reaction material, as observed by ¹H NMR spectroscopy, and the results were inconclusive (Table 12, entry 3).

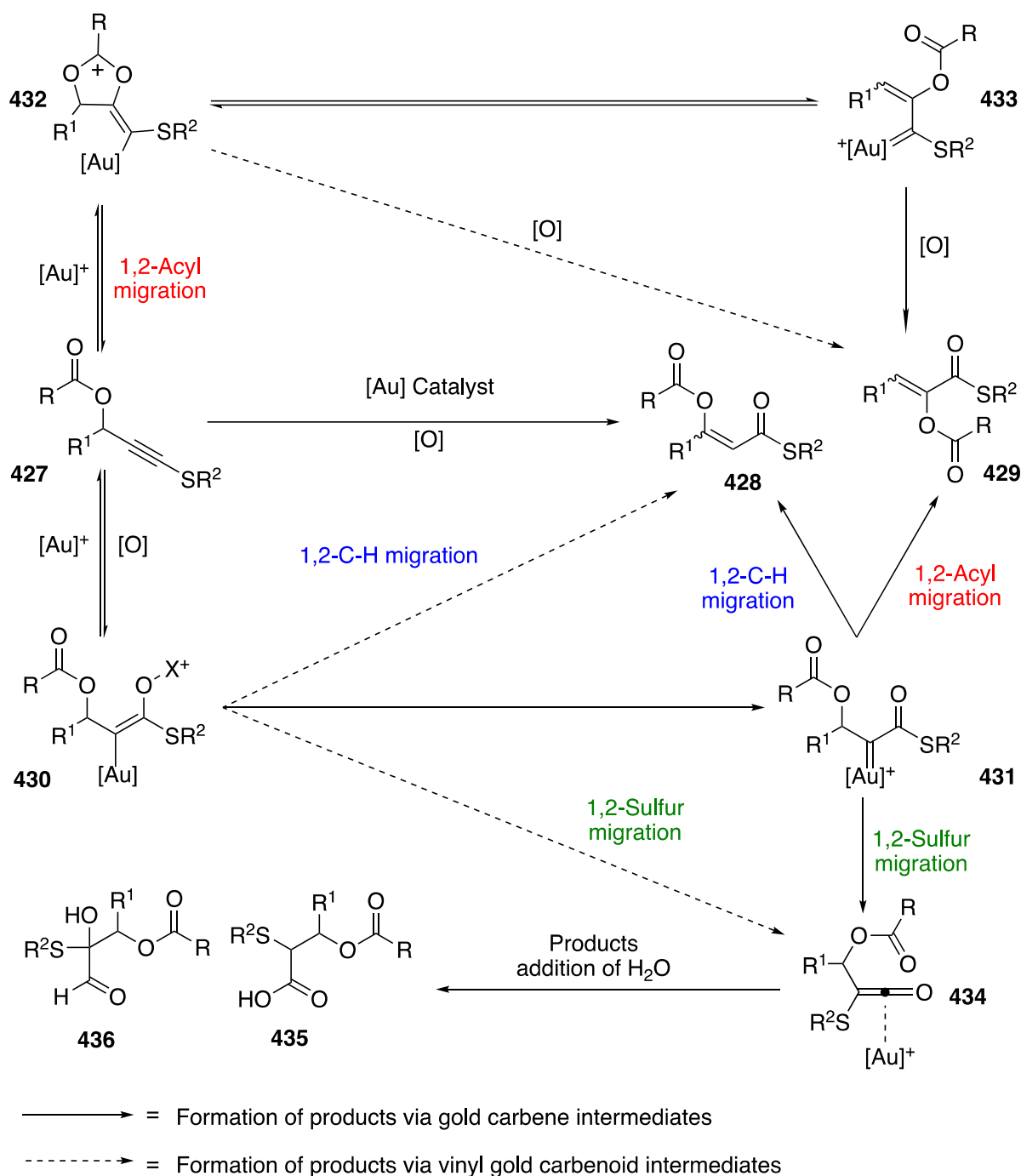
From previous studies it was known that **376** reacts with indole to form **412** via a carboxyallene intermediate (see Scheme 99). The rearrangement to form enones **426** should also occur via the carboxyallene intermediate (Scheme 101, **422 – 426** vs **422 – 424**) but the rearrangement is not observed in the case of **376**. As the transformation exploits the nucleophilicity of the [Au]-C bond, it is postulated that the propargylic methyl and *p*-chlorobenzene substituents do not provide sufficient electron donation to allow nucleophilic attack of the organoaurate to the C=O attached to the oxocarbenium (Scheme 101, **422 – 425**), whilst the dimethyl substituted substrates can undergo this transformation. Further studies for the formation of enones **426** should involve substrates that are able to enhance the nucleophilicity of the [Au]-C bond (Scheme 101). In addition, different catalysts should be explored, particularly those with electron-rich ligands.



Scheme 101. Substituent effects at the propargylic position on rearrangement vs nucleophilic addition

3.6 Gold-Catalysed Oxidation Reactions

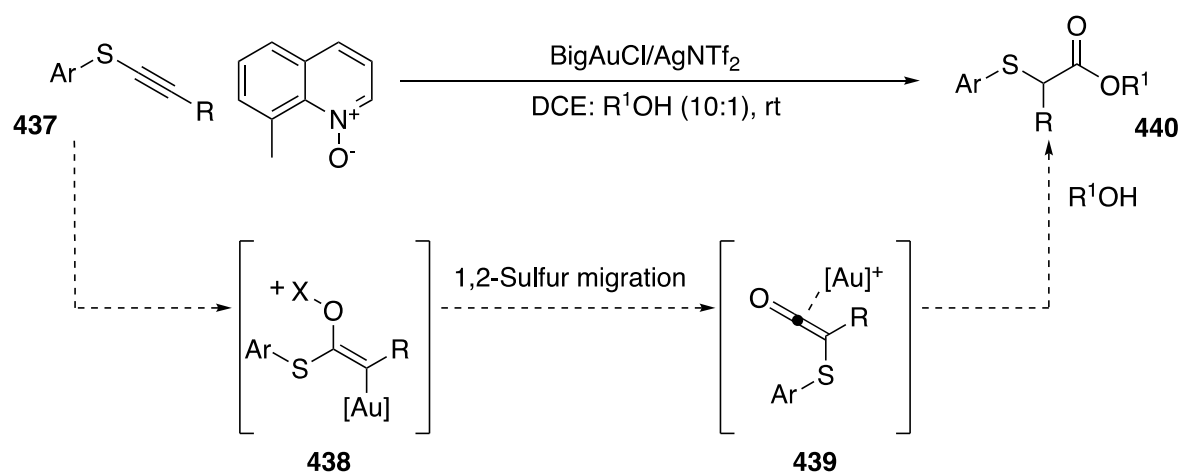
Oxidation was explored to investigate whether another alkyne activation mode could provide insight into the reactivity of sulfenylated propargyl carboxylates. Captodative olefin products **429** were anticipated from the oxidation reactions, and such products are very useful scaffolds for the synthetic chemist. There are two potential pathways for the formation of captodative olefin products **429** (Scheme 102).



Scheme 102. Possible mechanistic pathways for gold-catalysed oxidative rearrangement of propargyl carboxylates

The reaction could occur via initial oxidation of the alkyne **427** to generate vinyl gold-carbenoid **430** or gold carbene intermediate **431**. From here, 1,2-acyl migration followed by loss of the gold catalyst would provide the desired product **429**. On the

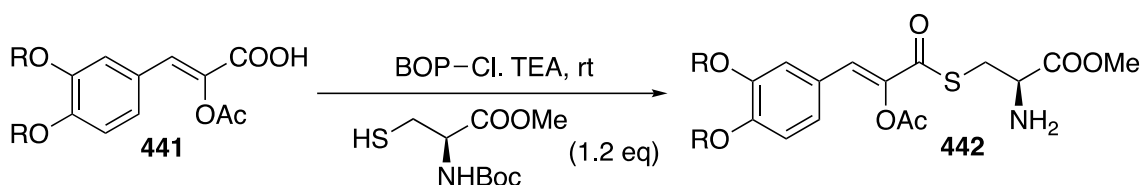
other hand, gold-catalysed 1,2-acyl migration could occur first to generate gold-carbene intermediate **433**. Direct oxidation of the gold carbene would also provide the captodative olefin product **429**. There is also the potential for the formation of the regioisomer **428** via 1,2-C-H migration at the gold carbene of intermediate **431**. This was observed in the analogous work by Zhang (see section 3.1.4, Scheme 64).^{51c} Furthermore, Liu previously developed a method for regioselective oxidation of alkynyl thioethers where 1,2-sulfur migration takes place at the vinyl gold carbenoid **438** to form ketene **439** (Scheme 103).^{61a} This reaction manifold may also be possible for sulfenylated propargyl carboxylates to generate ketene **434**, which can be further trapped by nucleophiles in the reaction solution (Scheme 102).



Scheme 103. Gold-catalysed oxidation of alkynyl thioethers by Liu

Captodative olefins are extremely useful scaffolds for further exploitation by synthetic chemists, with several transformations being reported; a large range of cycloadditions⁸¹ have been described alongside Friedel-Crafts addition⁸² and cross-coupling reactions⁸³. Captodative olefins are interesting due to the synergistic electron-deficient and electron-rich nature of the alkene because of the electron-withdrawing thioester group and the electron-donating carboxylate. The captodative olefins generated from sulfenylated propargyl carboxylates would harbour a thioester moiety

that could also be further exploited, expanding the range of transformations available to these useful substrates. The only method found for the synthesis of such compounds involves a multistep synthesis to form the corresponding carboxylic acid **441**, followed by a substitution reaction to generate the thioester **442** (Scheme 104).

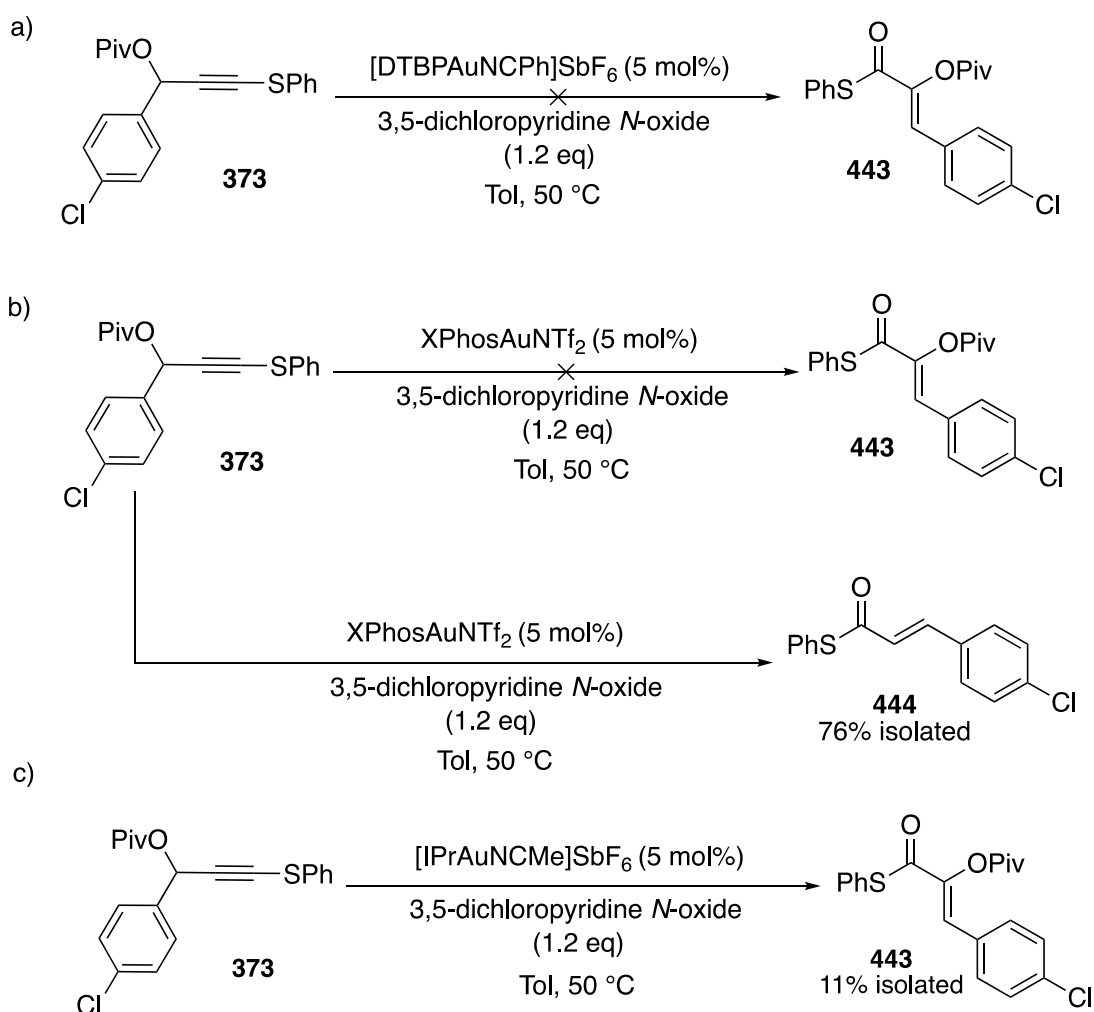


Scheme 104. Synthesis of captodative olefin 442

3.6.1 Initial Studies into Oxidative Gold Catalysis

Substrate **373** was subjected to preliminary studies to see if oxidative gold catalysis was successful at synthesising captodative olefin **443** (Scheme 105). Substrate **373** would provide useful information on the oxidation mechanism. As seen during previous work into nucleophilic addition and gold-catalysed rearrangement, **373** does not tend to undergo pivalate migration in the presence of a gold catalyst. Therefore, formation of the oxidised product would suggest that alkyne oxidation occurs prior to migration of the pivalate (see Scheme 102). [DTBPAuNCPPh]SbF₆ or XPhosAuNTf₂ catalysts did not produce the desired transformation, with XPhosAuNTf₂ catalysing the formation of the α,β -unsaturated thioester **444** in 76% yield (Scheme 105). This is consistent with the work of Zhang who saw optimal yields with IPr-derived catalysts in the analogous reaction (see section 3.1.4, Scheme 64).^{51c} Upon reaction with an IPr-ligated Au(I) catalyst, **443** was isolated in 11% yield. However, the yield could not be determined by ¹H NMR spectroscopic analysis of the crude reaction material as the alkene proton had a high chemical shift in the aromatic region and was therefore overlapping with the other aromatic protons. The formation of **443** indicates a mechanism via initial

oxidation followed by migration, as **373** does not tend to undergo initial carboxylate migration, though further investigation into the mechanism is discussed later. These preliminary studies also show that IPr-ligated gold catalysts are suitable for the desired transformation.

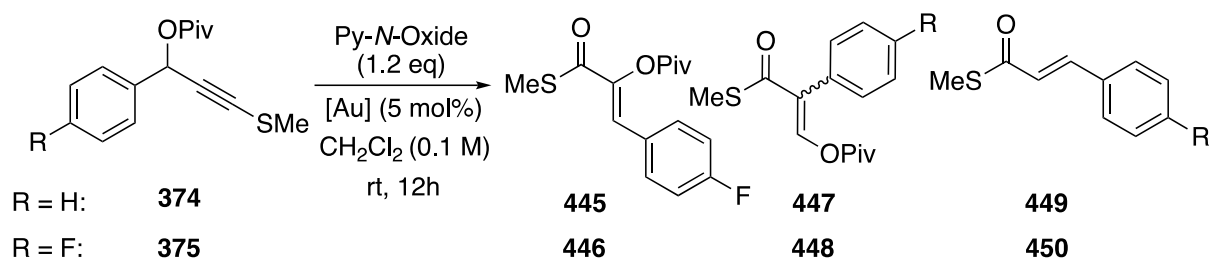


Scheme 105. Preliminary experiments for the gold-catalysed oxidation of **373**

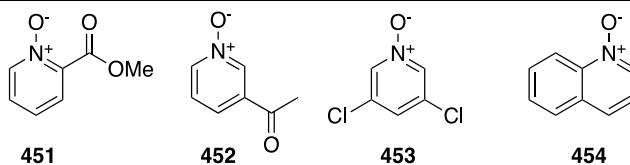
3.6.2 Optimisation Studies

Optimisation studies were performed with substrates **374** and **375** with range of pyridine *N*-oxides and IPr-ligated gold catalysts (Table 13). An *S*-methyl substituent simplified the aromatic region allowing the ¹H NMR yields of the captodative olefin products to be obtained from the crude reaction mixtures.

Table 13. Reaction screening for the gold-catalysed oxidation of 374 and 375

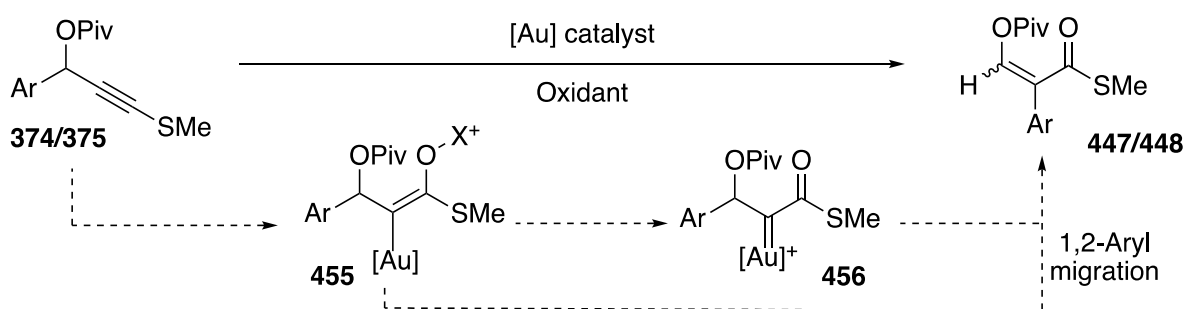


Entry	R	[Au] Catalyst	Solvent	Py N-Oxide	Yield/% ^b			
					445/446	447/448	449/450	SM
1	H	[IPrAuNCMe]SbF ₆	CH ₂ Cl ₂	451	15	11	13	34
2	H	[IPrAuNCMe]SbF ₆	CH ₂ Cl ₂	452	32	15	20	0
3	H	[IPrAuNCMe]SbF ₆	CH ₂ Cl ₂	453	9	2	16	- ^c
4	H	[IPrAuNCMe]SbF ₆	CH ₂ Cl ₂	454	12	9	9	49
5	F	[IPrAuNCMe]SbF ₆	CH ₂ Cl ₂	451	23	18	15	6 ^d
6	F	[IPrAuNCMe]SbF ₆	CH ₂ Cl ₂	452	39	18	12	5 ^d
7	F	[IPrAuNCMe]SbF ₆	CH ₂ Cl ₂	453	19	8	28	0
8	F	[IPrAuNCMe]SbF ₆	PhCF ₃	451	25	17	6	7 ^d
9	F	IPrAuCl/AgNTf ₂ ^e	CH ₂ Cl ₂	451	19	14	13	20 ^d
10	F	IPrAuCl/AgOTf ^e	CH ₂ Cl ₂	451	13 ^d	11 ^d	10 ^d	23 ^d
11	F	IPrAuCl/AgNTf ₂ ^e	CH ₂ Cl ₂	454	19	6	34	0



^aAll reactions were performed under dry conditions: heat-gun dried flask under argon with anhydrous solvent. ^bYields were determined by ¹H NMR spectroscopy using a known concentration of 1,2,4,5-tetramethylbenzene as internal standard. ^cProduct yield could not be obtained due to overlapping resonances. ^dProduct yield is an estimation due to overlapping resonances. ^eCatalyst was generated in situ with LAuCl (5 mol%) and AgX (7.5 mol%).

It was discovered that a range of products were formed during the oxidative gold catalysis of **374** and the highest yield obtained for the captodative olefin **445** was 32% (Table 13, entry 2). Interestingly, **447** was also formed in appreciable amounts in most reactions from 1,2-aryl migration at the gold carbene intermediate (Scheme 106), alongside the side product **449** from pivalate hydrolysis. Substrate **375** was explored to determine whether a more electron-deficient substrate would be less susceptible to 1,2-aryl migration. Use of substrate **375**, however, still saw formation of the regioisomer **448** from 1,2-aryl migration under all of the conditions tested. For both substrates, the captodative olefin products **445** and **446** were formed in higher yields than the regioisomers from 1,2-aryl migration, however controlling unfavourable pathways was difficult and the yields of the desired products were often low. Overall, the best yields were obtained using [IPrAuNCMe]SbF₆ alongside 3-acetylpyridine *N*-oxide (Table 23, entries 2 and 6). These conditions provided **445** and **447** in 32% and 39% yield respectively as the *Z* isomers exclusively (determination of stereochemistry is discussed in section 3.6.6.1).



Scheme 106. 1,2-Aryl migration pathway for the formation of **447 and **448****

Whilst the isomers from 1,2-aryl migration were not isolated exclusively, the structure of **448** was predicted from the isolated mixture with the captodative olefin **446**, as the ¹³C NMR resonances were distinct for each product. Captodative olefin **446** was also isolated pure thus, by deduction, the proton and carbon resonances could be

determined for isomer **448**. HMBC and HSQC experiments were used to identify the key ^{13}C NMR resonances (Figure 15).

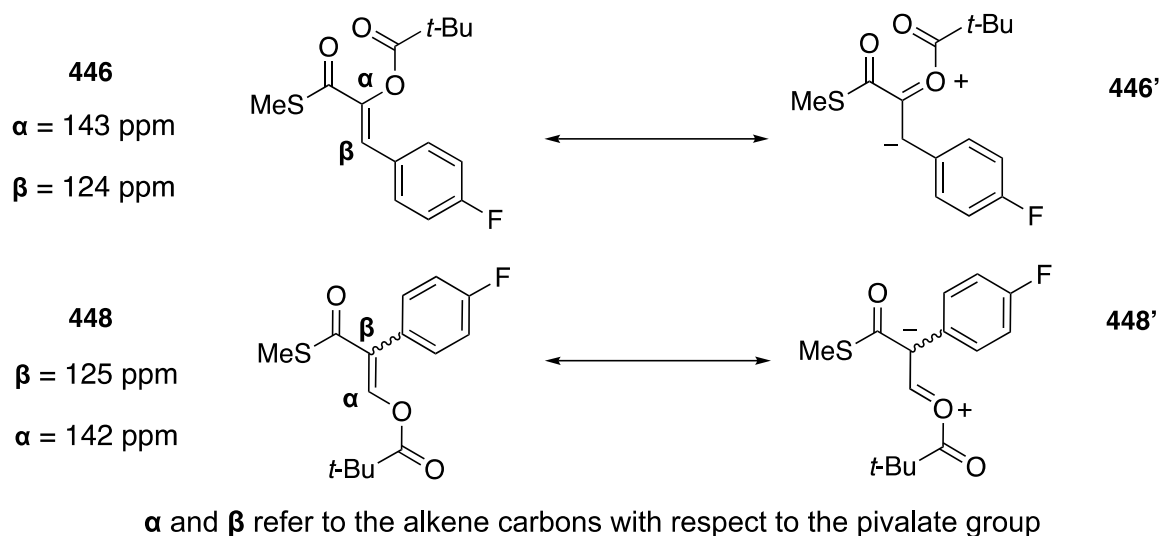


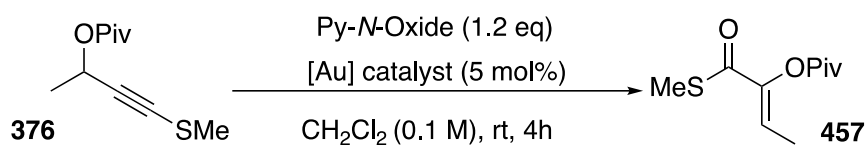
Figure 15. Important ^{13}C NMR resonances for compounds **446 and **448****

Product **446** has alkene ^{13}C NMR resonances consistent with a captodative olefin; the alkene carbon α to the pivalate and thioester has a high δ of 143 ppm, whilst the β alkene carbon has a lower δ at 124 ppm.^{51c, 84} The low α -carbon δ is due increased electron density from pivalate donation as seen in the resonance form **446'**. Isomer **448** was consistent with a regioisomer of **446**, with the ^1H NMR and ^{13}C NMR resonances representing a tetrasubstituted alkene bearing a thioester and a pivalate. In contrast to captodative olefin **446**, the vinylic proton of **448** was attached to a carbon with a δ of 142 ppm. The other alkene carbon had a lower δ of 125 ppm, indicating this carbon is β to the pivalate group. Therefore, the vinylic proton and the pivalate group are both attached to the alkene carbon at 142 ppm. Thus, the aryl group and the thioester are directly attached to the carbon at 125 ppm (Figure 15, **448**). An interaction between the aromatic protons and the thioester C=O is seen in the HMBC spectrum of **448**, which is not observed for captodative olefin **446**. Interestingly, the vinylic proton of both 1,2-aryl migration products **447** and **448** have a high δ at 8.39 ppm due to

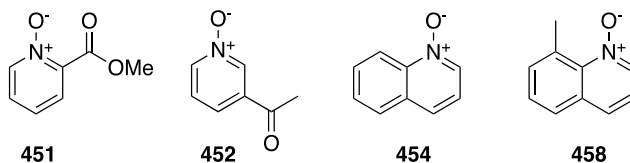
deshielding by the geminal oxygen. Since performing this analysis, product **448** has been isolated and characterised by another member of the group, confirming the structure. The stereochemistry of **448** has not yet been determined, however further studies are being performed within the group.

The initial optimisation studies for the aromatic systems provided a good starting point for the optimisation of aliphatic propargyl carboxylate **376** (Table 14).

Table 14. Reaction screening for the gold-catalysed oxidation of 376



Exp	[Au] Catalyst	Pyridine <i>N</i> -Oxide	Yield/% ^d	
			457	376
1	[IPrAuNCMe]SbF ₆ ^b	451	58	0
2	[IPrAuNCMe]SbF ₆	451	67	0
3	IPrAuCl/AgSbF ₆	451	49	0
4	[IPrAuNCMe]SbF ₆	454	26	20
5	[IPrAuNCMe]SbF ₆	458	37	4
6	[IPrAuNCMe]SbF ₆	452	75	0



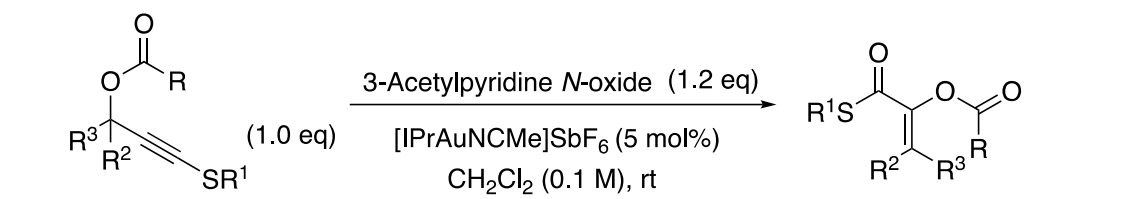
^aAll reactions were stirred for 4 h under dry conditions: heat-gun dried flask under argon with anhydrous solvent unless stated otherwise. ^bReaction was performed with undried commercial solvent under air for 4h. ^cCatalyst generated in situ with LAuCl (5 mol%) and AgSbF₆ (7.5 mol%). ^dYields were determined by ¹H NMR spectroscopy using a known concentration of 1,2,4,5-tetramethylbenzene as internal standard.

The reaction under an inert atmosphere with anhydrous solvent provided a higher yield of the desired product **457** with 2-(methoxycarbonyl)pyridine *N*-oxide, therefore the rest of the reactions were performed under dry conditions (Table 14, entry 1 vs 2). With 2-(methoxycarbonyl)pyridine *N*-oxide, the preformed catalyst yielded the desired product **457** with a higher yield compared to when the catalyst was formed in situ (Table 14, entry 1 vs 3). Use of quinoline *N*-oxides saw only moderate yields of the captodative olefin **457** and there were several undetermined side products observed in the ¹H NMR spectra of the crude reaction material (Table 14, entries 4 and 5). As with the aromatic substrates, 3-acetylpyridine *N*-oxide was the best oxidant, affording the captodative olefin **457** in 75% yield in only 4 h at rt (Table 14, entry 6). The aliphatic system underwent the transformation superbly, yielding captodative olefin **457** as the single *Z* isomer (see determination of stereochemistry in section 3.6.6.1). This process was also regioselective with no products from 1,2-C-H or 1,2-alkyl migration observed.

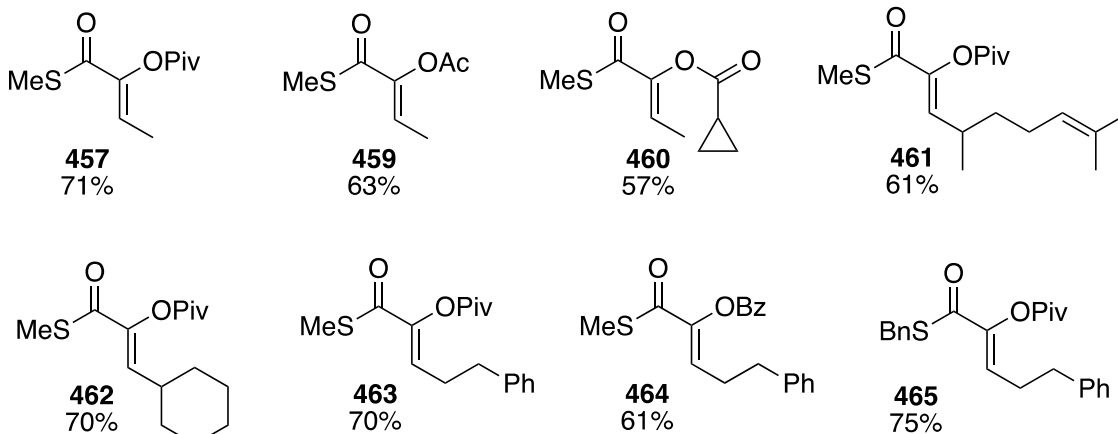
During the optimisation of both aromatic substrates **374** and **375** and aliphatic substrate **376**, no products were observed from the 1,2-sulfur migration pathway (see Scheme 102). It is likely that the migration of the carboxylate groups is more favourable than sulfur migration at the vinyl gold carbenoid/gold carbene intermediates. In the gold-catalysed oxidation of alkynyl thioethers described by Liu, the absence of another group that can readily migrate may allow for a more accessible 1,2-sulfur migration pathway.

3.6.3 Scope of the Gold-Catalysed Oxidation Reaction

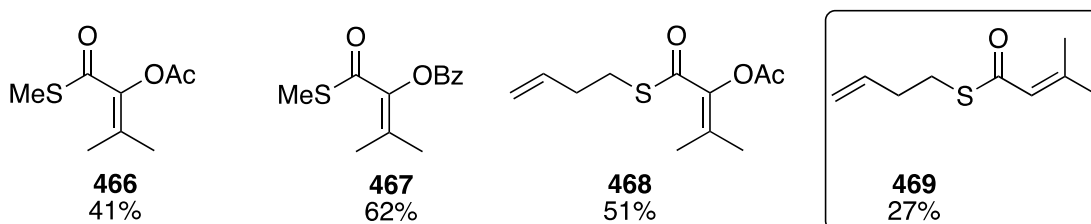
A range of aliphatic sulfenylated propargyl carboxylates were then subjected to the optimised conditions for oxidative gold catalysis (Scheme 107).



Aliphatic tri-substituted captodative olefins



Aliphatic tetra-substituted captodative olefins

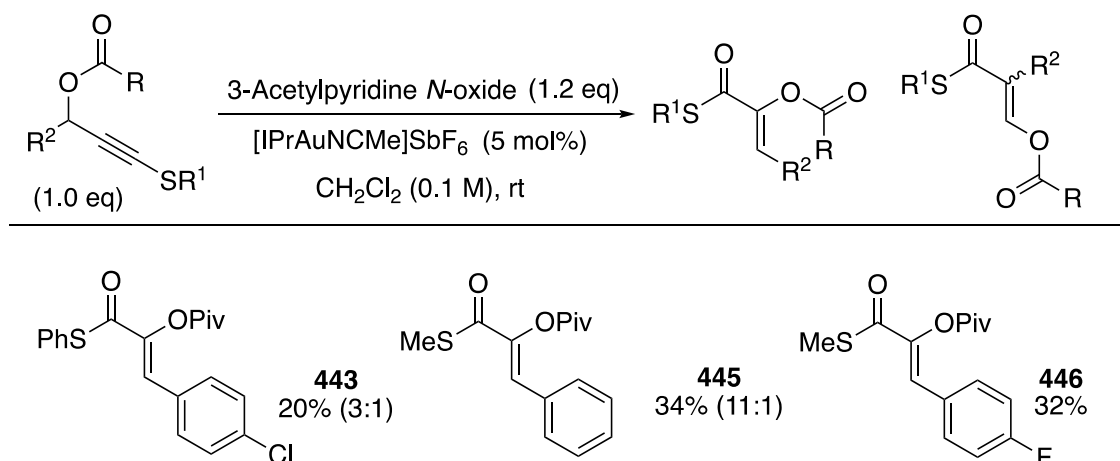


Scheme 107. Gold-catalysed oxidation of sulfenylated propargyl carboxylates with aliphatic substituents

Catalysis of all substrates with one aliphatic propargylic substituent were completely stereoselective, producing the *Z* isomers exclusively (determination of stereochemistry is discussed in section 3.6.6.1). Long chain aliphatic and cyclohexyl substituents were well tolerated and did not sterically hinder nucleophilic addition of the oxidant (Scheme 107, **461** – **465**). Dimethyl-substituted propargyl carboxylates were also successful in the transformation, providing good to acceptable yields of the tetra-substituted captodative olefin products (Scheme 107, **466** and **468**). Tethered alkenes were not problematic, and the desired captodative olefins were afforded in good yields (Scheme

107, **461** and **468**). The substrate used to generate **461** bearing an electron-rich alkene saw side product formation, however the side products were minor and could not be isolated or characterised. As expected, higher yields were obtained with pivalates and benzoates than with acetates (Scheme 107, **457** vs **459**, and **467** vs **466**). This is likely due to the acetates being more susceptible to hydrolysis. For example, the α,β -unsaturated thioester product **469** was isolated in 27% yield from the same reaction that provided **468** in 53% yield. Interestingly, the cyclopropane carboxylate underwent the oxidative gold-catalysed rearrangement successfully, and the product **460** was afforded in 59% yield with respect to the reactive carboxylate. No products from 1,2-C-H or 1,2-alkyl migration were observed.

The use of aromatic substrates resulted in the formation of the captodative olefin as the major product, alongside the regioisomers from 1,2-aryl migration (Scheme 108).

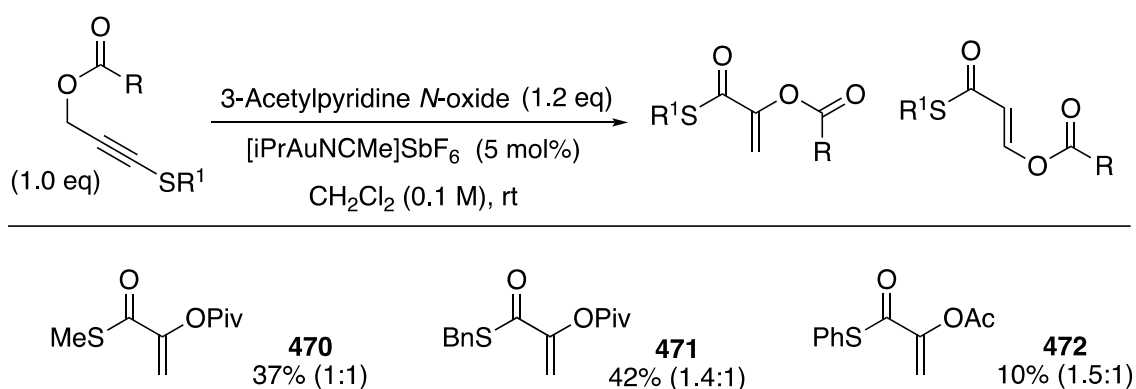


Scheme 108. Gold-catalysed oxidation of sulfenylated propargyl carboxylates with aromatic substituents

Captodative olefins **443** and **445** were isolated as a mixture of regioisomers (Scheme 108). Captodative olefin **446** could be separated from the 1,2-aryl migration product and was isolated as the single regioisomer. The yields for these aryl-substituted

captodative olefins were much lower than the aliphatic analogues. Therefore, the catalysis should be further optimised for the aromatic substrates to find conditions that reduce undesirable migration pathways. Alternative substrates should also be explored to investigate the factors that influence 1,2-aryl migration.

Systems that were unsubstituted at the propargylic position were then tested under the optimised reaction conditions (Scheme 109).



Scheme 109. Gold-catalysed oxidation of sulfenylated propargyl carboxylates with no propargylic substituents

Intriguingly, these substrates saw the formation of regioisomers from 1,2-C-H migration at the gold carbene intermediate alongside the desired captodative olefin products and were isolated as a mixture (Scheme 109). The 1,2-C-H migration pathway formed the *trans* isomers exclusively, determined by the large coupling constants of $J = 12.4$ Hz for the vinylic protons in the ^1H NMR spectra. Products **470** and **471** were difficult to separate from the starting sulfenylated propargyl carboxylates and there was still some starting material present in the isolated compounds; the yield therefore takes this into account. The formation of **472** required a higher temperature therefore it was stirred at 50 °C in chloroform. The product **472** was only obtained in 10% yield and a substantial amount of starting material was still present by TLC at the end of the reaction. The

lower yields obtained for these substrates is consistent with what was observed during the studies into nucleophilic addition, where substrates that were unsubstituted at the propargylic position displayed no reactivity even at high temperatures. This is likely due to the lack of stabilisation of positive charge build up at the propargylic position during the migration step.

3.6.3.1 Mechanism and Stereoselectivity

The stereochemistry of the tri-substituted captodative olefins was determined by NOESY experiments. Several of the captodative olefins failed to provide the necessary interactions in the NOESY spectra to enable the stereochemistry to be determined. The products shown in Figure 16 provided useful interactions in the NOESY spectra and the *Z* alkene stereochemistry was determined (Figure 16).

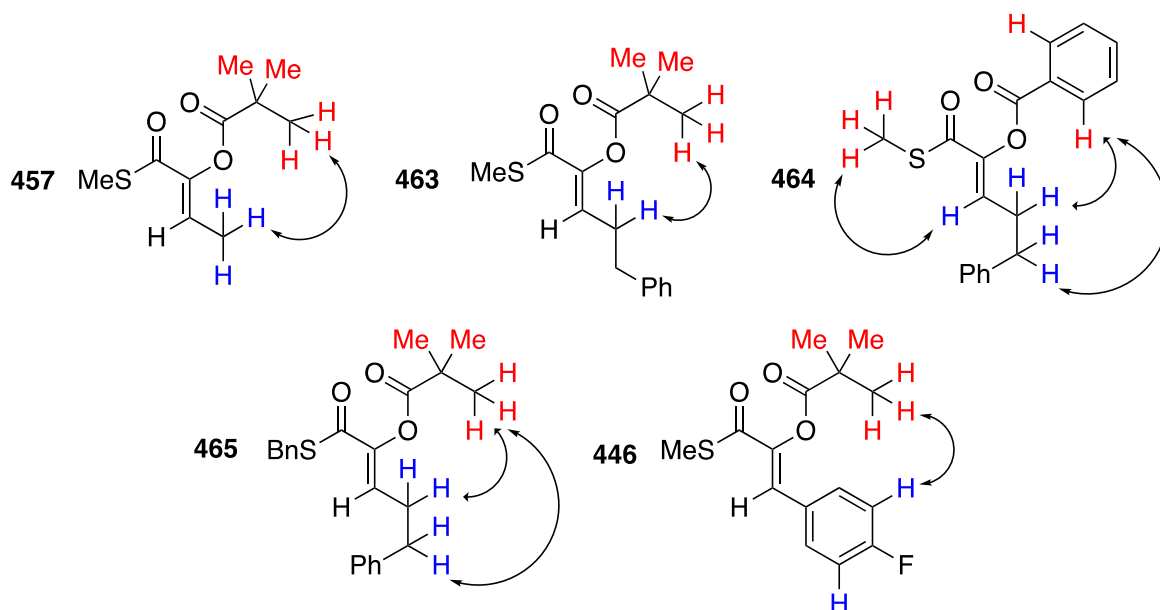


Figure 16. Observed NOESY interactions to determine alkene stereochemistry

Product **457** displayed an interaction between the methyl substituent and the *t*-butyl group. Products **463** and **465** displayed interactions between the CH₂ of the aliphatic chain and the *t*-butyl groups. Compound **464** displayed an interaction between the CH₂

of the aliphatic chain and the benzoate aromatic protons, alongside an interaction between the alkene proton and the methyl of the thioester. Aromatic substituted captodative olefin **446** displayed an interaction between the aromatic protons of the *p*-fluorobenzene substituent and the *t*-butyl group. Based on these results, the rest of the tri-substituted captodative olefins were also assigned as *Z* isomers. The chemical shifts of the alkene proton and alkene carbons of the captodative olefins were also consistent across similarly substituted products (Figure 17).

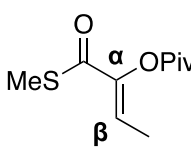
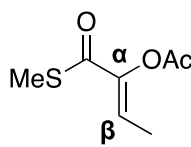
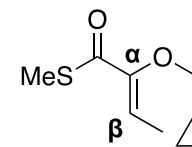
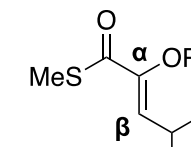
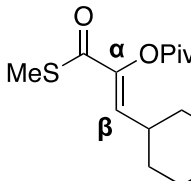
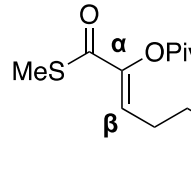
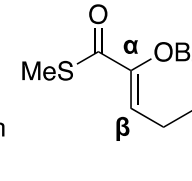
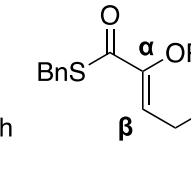
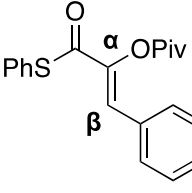
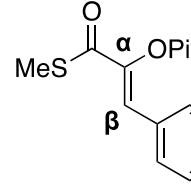
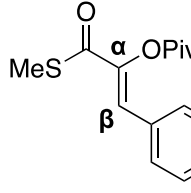
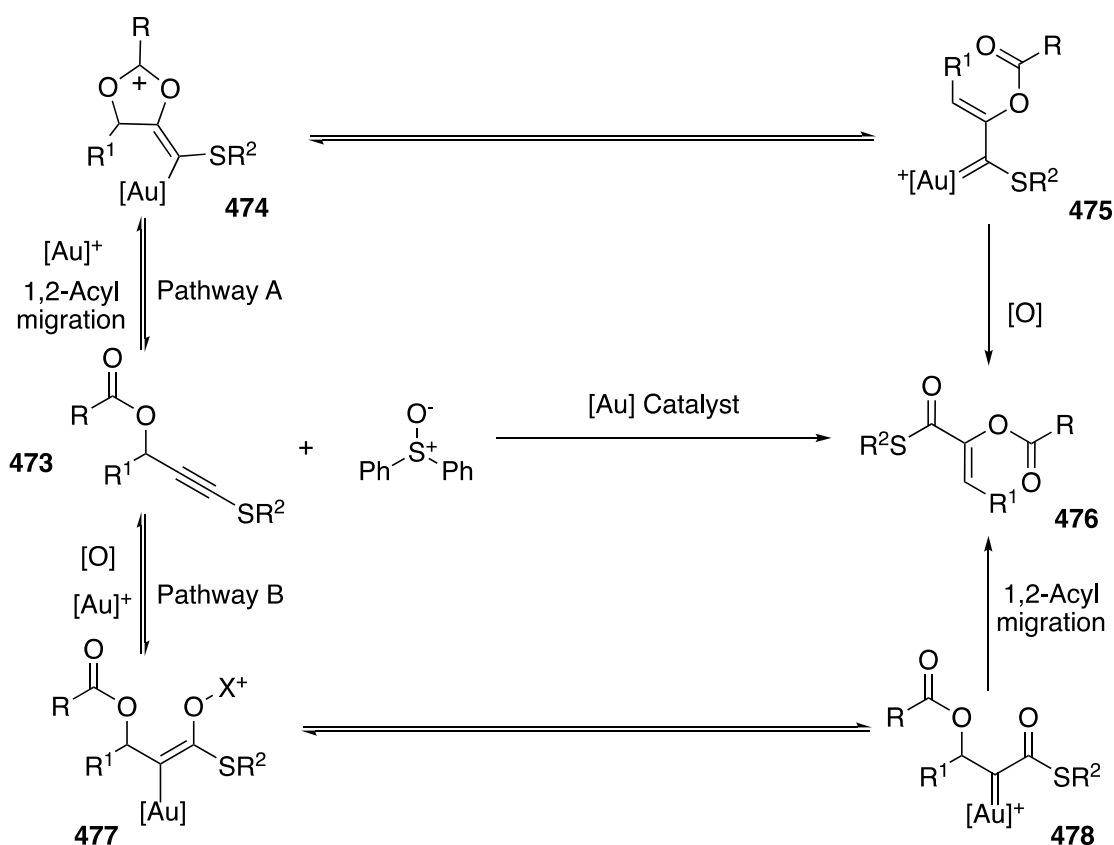
	457	459	460	461
				
¹³ C NMR δ: α	144.9	144.8	144.6	143.3
¹³ C NMR δ: β	124.1	124.7	124.5	124.0
¹ H NMR δ: β	6.61	6.63	6.61	6.33
	462	463	464	465
				
¹³ C NMR δ: α	142.6	144.2	144.0	144.0
¹³ C NMR δ: β	133.6	126.4	126.4	128.4
¹ H NMR δ: β	6.39	6.56	6.69	6.55
	443	445	446	
				
¹³ C NMR δ: α	143.1	143.0	142.8	
¹³ C NMR δ: β	124.9	125.1	123.9	
¹ H NMR δ: β	7.35	7.33	7.29	

Figure 17. Alkene ¹H NMR and ¹³C NMR resonances of captodative olefin products

There ^{13}C NMR resonance of the β -carbon of product **462** is higher than the other captodative olefin products. Therefore, the stereochemistry of this product should be further explored. However, in analogous work by Zhang, the aliphatic-substituted *Z* captodative olefins have alkene β -carbon resonances ranging from 126.6 to 131.9. Thus, product **462** may still exist as the *Z* isomer despite having a higher ^{13}C NMR resonance at the β -carbon compared to the other *Z* captodative olefins.

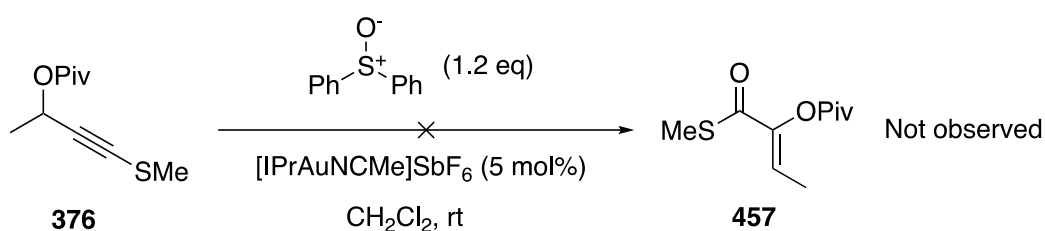
The stereochemistry of the captodative olefins is consistent with the work performed by Zhang, thus suggesting that the transformation follows a similar mechanism. Zhang proposes initial oxidation followed by 1,2-acyl migration, and the products are formed as the *Z* isomers predominantly (Scheme 110, pathway B).



Scheme 110. Possible mechanistic pathways for the formation of captodative olefins

As mentioned in the introduction, diphenyl sulfoxide is not efficient at oxidising alkynes under gold-catalysis but is capable of oxidising gold carbenes. Therefore, if the formation of captodative olefins **476** proceeds via pathway A (Scheme 110), the product should be observed with diphenyl sulfoxide. However, if **476** is formed via initial oxidation as seen in pathway B, then the use of diphenyl sulfoxide should see very low or no product formation (Scheme 110).

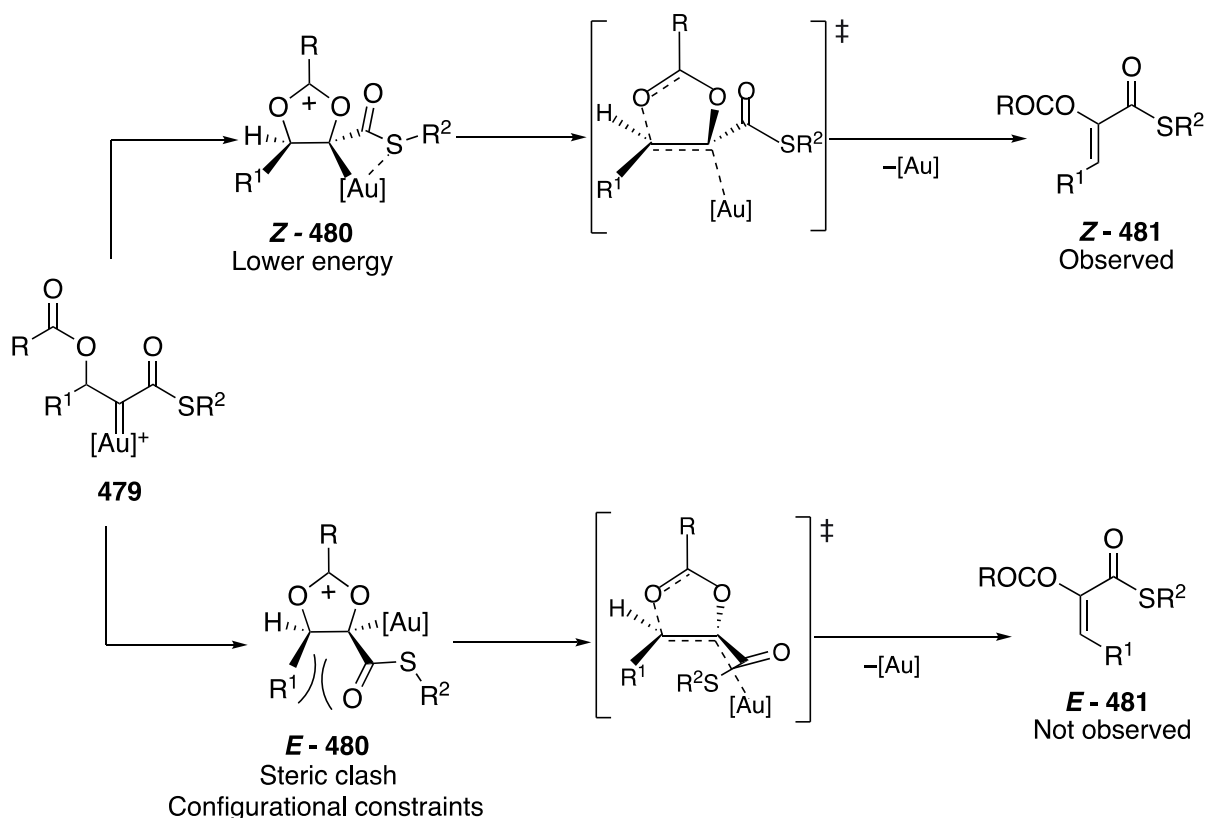
A reaction was therefore performed with substrate **376** and diphenyl sulfoxide (Scheme 111) and saw no formation of the product **457** by ^1H NMR spectroscopy of the crude reaction material. This indicated that the mechanism occurs via initial alkyne oxidation followed by 1,2-acyl migration, thus diphenyl sulfoxide is not capable of undergoing this transformation.



Scheme 111. Reaction between 376 and diphenyl sulfoxide

The gold-catalysed oxidation of sulfenylated propargyl carboxylates was completely stereoselective to form *Z* tri-substituted alkenes. With the mechanism determined, a rationale for the observed stereoselectivity was postulated from the gold carbene **479** (Scheme 112). It is proposed that the *E* captodative olefin, **E-481**, would be formed via intermediate **E-480**, and steric clash between the propargylic substituent and the thioester group may result in a higher energy intermediate. The intermediate **Z-480** towards the *Z* captodative olefin, **Z-481**, should exhibit less steric interference. Zhang saw a mixture of *E/Z* isomers, favouring the *Z* isomer for the oxidation of propargyl

carboxylates without sulfur substituents.^{51c} In this work, no *E* isomer was observed, indicating that sulfur plays a role in enhancing stereoselectivity. In the intermediate **Z-480**, and the transition state towards the *Z* alkene, a favourable Au-S interaction is proposed to exist. Such Au-S interactions may not be possible in intermediate **E-480** or the transition state towards the *E* alkene due to configurational constraints as a result of steric clash between the thioester and the propargylic substituent. Such configurational constraints could mean that thioester cannot arrange into a suitable position to allow for a successful Au-S interaction. Therefore, both unfavourable steric interactions towards the *E* alkene and favourable Au-S interactions towards the *Z* alkene may contribute to the stereoselective process.



Scheme 112. Proposed intermediates for stereoselective captodative olefin formation

In addition, no products from 1,2-C-H migration were observed with the aliphatic substituted propargyl carboxylates. This again contrasts with the work of Zhang where

1,2-C-H migration was observed during gold-catalysed oxidation of propargyl carboxylates without sulfur substituents.^{51c} It is postulated that a sulfur-gold interaction in the gold carbene **479**, or in the preceding vinyl gold-carbenoid intermediate, stabilises the intermediate leading to a more selective reaction manifold. Liu has described such Au-S interactions exist in vinyl gold carbenoid intermediates during the gold-catalysed oxidative rearrangements of alkynyl thioethers (see Scheme 103).^{61a}

3.7 Conclusion and Outlook

The preliminary studies discussed in this chapter provide a foundation for further investigation into the role of sulfur in gold-catalysed transformations. Gaining further insight into how sulfur substituents can influence reactivity may enable pathways to be predicted and also enhance pathway control. Knowledge of how the surrounding organic framework of substrates can affect sulfur interaction modes, through either sulfur-gold coordination or ketenthionium intermediates, is also of interest. As seen in the gold-catalysed oxidation studies, sulfur substitution can allow for stereoselective processes and also result in synthetically useful moieties to be incorporated in catalysis products. Further understanding may allow different sulfur substituents to be exploited for the purpose of reaction control and improved stereoselectivity and also for the potential discovery of novel reaction manifolds as demonstrated by Liu with the discovery of 1,2-sulfur migration pathways at gold carbene intermediates.

During nucleophilic addition studies, sulfenylated propargyl carboxylates were seen to favour a 1,3-acyl migration pathway to generate carboxyallene intermediates. This regioselective pathway may be enhanced by the sulfur substituent via the generation of a gold ketenthionium intermediate. However, as internal propargyl carboxylates

have a propensity towards 1,3-acyl migration it is difficult to conclude whether this pathway is augmented by the sulfur substituent. Following 1,3-acyl migration, dimethyl-substituted systems undergo intramolecular rearrangement superbly to form enones. The presence of two methyl substituents is believed to sterically hinder nucleophilic addition at the carboxyallene intermediate. Furthermore, the presence of the two methyl substituents may aid gold-catalysed rearrangement towards enones by increasing the nucleophilicity of the Au-C bond. A single methyl substituent at the propargylic position saw increased nucleophilic addition of indole to the carboxyallene intermediate, however rearrangement to the enone did not occur.

Gold-catalysed migration occurred more readily for propargyl carboxylates with aliphatic propargylic substituents than those with aromatic propargylic substituents. The electron rich *p*-tolyl substituent of substrate **372** encouraged direct nucleophilic substitution of the acetate with indole, whilst the electron deficient *p*-chlorobenzene substituent of **373** drastically reduced the reactivity of the substrate. Sulfenylated propargyl carboxylate **359** that is unsubstituted at the propargylic position did not undergo gold-catalysed nucleophilic addition under any of the conditions tested. It is possible that different sulfur substituents, or a different migrating group, may improve the reactivity of these systems.

Novel oxidative rearrangements of sulfenylated propargyl carboxylates were also described, with studies supporting a mechanism via initial oxidation followed by acyl migration. Oxidative gold-catalysis was completely stereoselective for sulfenylated propargyl carboxylates with one propargylic substituent and no side-product formation

from 1,2-C-H or 1,2-alkyl migration was observed for the alkyl-substituted systems. The stereoselective transformation is attributed to favourable sulfur-gold interactions stabilising reaction intermediates, alongside unfavourable steric interactions towards to *E* alkene facilitating a stereoselective process. Sulfenylated propargyl carboxylates with no propargylic substituents suffered from low yields and saw the regioisomeric products from the competing 1,2-C-H migration pathway, whilst aromatic-substituted propargyl carboxylates saw products from 1,2-aryl migration. The presence of a thioester moiety should allow for further manipulation of the captodative olefin products. Thioesters have been shown to undergo a range of nucleophilic substitution reactions alongside cross-coupling.⁸⁵ A range of transformations are also available to captodative olefins, thus these substrates are expected to be very useful for further exploitation.

Chapter 4: Experimental Section

4.1 General Experimental

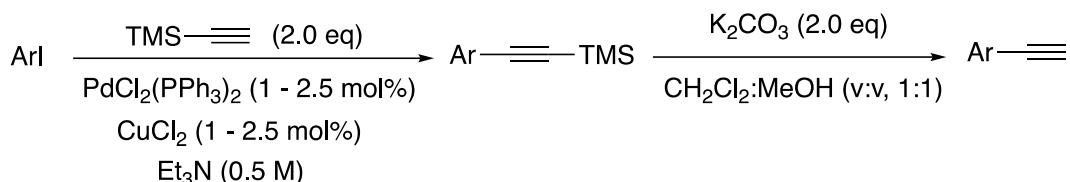
Commercially available chemicals/reagents were purchased from major suppliers (Sigma-Aldrich, Fisher, Acros, Alfa Aesar, Strem, Fluorochem or VWR) and used without further purification. Anhydrous THF, CH₂Cl₂ and Toluene was purified using Pure Solv-MD solvent purification system and were dispensed under nitrogen. Glassware used for reactions under dry conditions was heat-gun dried under reduced pressure, then cycles of argon backfill and evacuation were performed three times. All solid reagents were measured on a balance that can allow for accuracies up to and including 0.01mg. All reactions were stirred using Teflon-coated magnetic stirrer bars. Dry ice/acetone baths were used to obtain -78 °C. For catalysis reactions performed at 0 °C, the temperature was maintained using the JULABO FT902 immersion cooler with an external temperature probe placed in an ethylene glycol/water (v:v, 1:1) solution. For all other reactions performed at 0 °C, the temperature was maintained using an NaCl/ice bath. The JULABO FT902 immersion cooler was also used for reactions performed at -20 °C and -30 °C. For reactions that were run above rt, the reactions were heated by placing the flask in an oil bath and the temperature was maintained with an external temperature probe placed in the oil bath. Reactions were monitored using Merck silica gel 60 F₂₅₄ TLC plates which were developed using UV fluorescence (254 nm) and KMnO₄/Δ and vanillin/Δ visualising agents. Manual flash column chromatography was carried out on Sigma-Aldrich silica gel (pore size 60 Å, 230 – 400 mesh particle size); automated flash column chromatography was carried using a Teledyne Isco Combiflash NextGen 100 instrument, using either Teledyne Isco Redisep RediSep® Normal-phase, RediSep Rf Gold® Normal-Phase, or InterChim Puriflash IR Silica flash columns. Melting points were measured in open capillary tubes

using a Stuart Scientific melting point apparatus and are uncorrected. Infrared spectra were recorded using a Perkin-Elmer Spectrum 100 FTIR spectrometer using an ATR attachment; selected absorbencies (ν_{\max}) are reported. Mass spectra were obtained using Waters GCT Premier (EI), Waters LCT (ES), Waters Synapt (ES) or Bruker MicroTOF spectrometers. All spectra were recorded using a TOF mass analyser. Both the calculated and measured values are reported as neutral species with Waters MassLynx (V4.1 used). The HRMS for all compounds therefore reports the mass of neutral species. High resolution spectra used a lock-mass to adjust the calibrated mass scale. NMR spectra were recorded using Bruker AVIII300 (^1H = 300 MHz, ^{31}P = 121 MHz), Bruker AVIII400 (^1H = 400 MHz, ^{13}C = 101 MHz) and Bruker Avance NEO console (^1H = 500 MHz, ^{31}P = 202 MHz) spectrometers at ambient temperatures. In situ NMR studies were recorded using Bruker Avance Neo (^1H = 500 MHz, ^{31}P = 121 MHz). Chemical shifts (δ) are given in ppm relative to TMS and are calibrated using residual solvent peaks (CDCl_3 : $\delta_{\text{C}} \equiv 77.16$ ppm; residual CHCl_3 in CDCl_3 : $\delta_{\text{H}} \equiv 7.26$ ppm). NMR spectra were run in both TMS-free CDCl_3 and TMS-containing CDCl_3 . Multiplicity of resonances in ^1H NMR spectra were denoted as follows: s (singlet), d (doublet), t (triplet), m (multiplet), *app.* (apparent). Coupling constants (J) are quoted to one decimal place. Proton decoupled ^{13}C NMR spectra were recorded using the UDEFT or PENDANT pulse sequences from the Bruker standard pulse program library. ^{13}C DEPT spectra and 2D COSY, HSQC and HMBC spectra were recorded to assist with NMR assignment when necessary. NMR spectra were processed using MestreNova software.

4.2 Alkynes

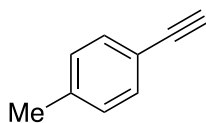
General Procedure 1 (GP1):

Based on an existing literature protocol.⁸⁶



The aryl halide was dissolved in Et₃N in a two-neck round-bottom flask and a positive pressure of argon was bubbled through the solution using a needle for ~10 min. PdCl₂(PPh₃)₂ (2 – 5 mol%) and CuCl₂ (1 – 2 mol%) were added to the solution under a positive pressure of argon and the solution was stirred under argon at rt. Ethynyltrimethylsilane (2.0 eq) was added dropwise to the solution over 10 min and the solution was stirred for 4 h. The solution was filtered under gravity, and the organic phase was washed with aqueous NH₄Cl (sat.), extracted with CH₂Cl₂ (~3 × 2 mL/mmol), dried (Na₂SO₄), concentrated under reduced pressure and purified by column chromatography.

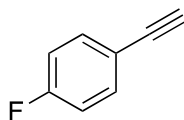
128: 1-Ethynyl-4-methylbenzene



The title compound was prepared according to **GP1** using iodotoluene (545 mg, 2.50 mmol), ethynyltrimethylsilane (0.71 mL, 5.00 mmol), PdCl₂(PPh₃)₂ (17.5 mg, 2.5 mol%) and CuI (4.80 mg, 2.5 mol%) in Et₃N (5 mL). Column chromatography (hexane) afforded the product as a pale orange oil (715 mg, 77%); **IR** (**Neat**): $\nu_{\text{max}}/\text{cm}^{-1}$ 3291, 2955, 2108, 1738, 1507, 815, 653; **¹H NMR** (300 MHz, CDCl₃)

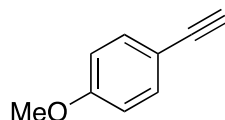
δ 7.39 (d, J = 8.1 Hz, 2H), 7.13 (d, J = 8.1 Hz, 2H), 3.03 (s, 1H), 2.36 (s, 3H). Data matches that reported in the literature.⁸⁷

129: 1-Ethynyl-4-fluorobenzene



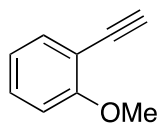
The title compound was prepared according to **GP1** using 1-fluoro-4-iodobenzene (2.40 mL, 12.0 mmol), ethynyltrimethylsilane (3.40 mL, 24.0 mmol), PdCl₂(PPh₃)₂ (84.0 mg, 1 mol%) and CuI (22.8 mg, 1 mol%) in Et₃N (24 mL). Column chromatography (hexane) afforded the product as yellow oil (1.10 g, 77%); **¹H NMR** (300 MHz, CDCl₃) δ 7.48 (dd, J = 8.9, 5.4 Hz, 2H), 7.02 (*app. t*, J = 8.8 Hz, 2H), 3.04 (s, 1H); **LR-MS** (EI-TOF) m/z : [M]⁺ calcd for C₉H₅F 120.04 found 120.03. Data matches that reported in the literature.⁸⁸

130: 1-Ethynyl-4-methoxybenzene



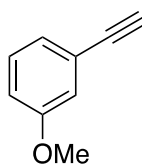
The title compound was prepared according to **GP1** using 1-iodo-4-methoxybenzene (889 mg, 3.80 mmol), ethynyltrimethylsilane (1.10 mL, 7.60 mmol), PdCl₂(PPh₃)₂ (53.6 mg, 2 mol%) and CuI (7.20 mg, 1 mol%) in Et₃N (7.6 mL). Column chromatography (10% EtOAc in hexane) afforded the product as a pale orange oil (336 mg, 73%); **IR (Neat)**: $\nu_{\max}/\text{cm}^{-1}$ 3287, 2106, 1606, 1507, 1291, 1248, 1170, 1031, 832; **¹H NMR** (300 MHz, CDCl₃) δ 7.43 (d, J = 8.8 Hz, 2H), 6.84 (d, J = 8.8 Hz, 2H), 3.81 (s, 3H), 3.00 (s, 1H). Data matches that reported in the literature.⁸⁷

131: 1-Ethynyl-2-methoxybenzene



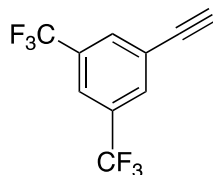
The title compound was prepared according to **GP1** using 1-iodo-2-methoxybenzene (697 mg, 2.98 mmol), ethynyltrimethylsilane (0.86 mL, 5.96 mmol), PdCl₂(PPh₃)₂ (53.6 mg, 2 mol%) and CuI (7.20 mg, 1 mol%) in Et₃N (6 mL). Column chromatography (10% EtOAc in hexane) afforded the product as a yellow oil (300 mg, 76%); **¹H NMR** (300 MHz, CDCl₃) δ 7.47 (dd, *J* = 7.5 and 1.8 Hz, 1H), 7.33 (ddd, *J* = 8.4, 7.5 and 1.8 Hz, 1H), 6.95 – 6.86 (m, 2H), 3.91 (s, 3H), 3.31 (s, 1H). Data matches that reported in the literature.⁸⁹

132: 1-Ethynyl-3-methoxybenzene



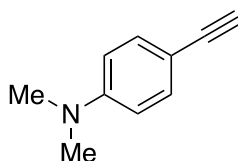
The title compound was prepared according to **GP1** using 1-iodo-3-methoxybenzene (697 mg, 2.98 mmol), ethynyltrimethylsilane (0.84 mL, 5.96 mmol), PdCl₂(PPh₃)₂ (42.0 mg, 2 mol%) and CuI (5.60 mg, 1 mol%) in Et₃N (6 mL). Column chromatography (10% EtOAc in hexane) afforded the product as a pale orange oil (268 mg, 68%); **¹H NMR** (300 MHz, CDCl₃) δ 7.23 (dd, *J* = 8.3 and 7.6 Hz, 1H), 7.09 (*app.* dt, *J* = 7.6 and 1.2 Hz, 1H), 7.02 (dd, *J* = 2.4 and 1.4 Hz, 1H), 6.91 (ddd, *J* = 8.3, 2.4 and 1.0 Hz, 1H), 3.80 (s, 3H), 3.06 (s, 1H). Data matches that reported in the literature.⁹⁰

133: 1-Ethynyl-3,5-bis(trifluoromethyl)benzene



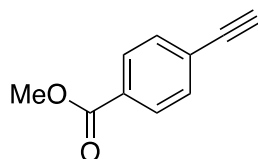
The title compound was prepared according to **GP1** using 1-bromo-3,5-(trifluoromethyl)benzene (1.70 mL, 10.0 mmol), ethynyltrimethylsilane (2.80 mL, 20.0 mmol), PdCl₂(PPh₃)₂ (175 mg, 2.5 mol%) and CuI (47.0 mg, 2.5 mol%) in Et₃N (20 mL). Column chromatography (10% EtOAc in hexane) afforded the product as an orange oil (1.38 g, 58%); **IR (Neat):** $\nu_{\text{max}}/\text{cm}^{-1}$ 3307, 1375, 1276, 1173, 1132, 899, 733 **¹H NMR** (300 MHz, CDCl₃) δ 7.92 (s, 2H), 7.84 (s, 1H), 3.27 (s, 1H). Data matches that reported in the literature.⁹¹

134: 4-Ethynyl-*N,N*-dimethylaniline



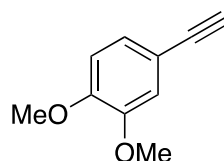
The title compound was prepared according to **GP1** using 4-iodo-*N,N*-dimethylaniline (605 mg, 2.45 mmol), ethynyltrimethylsilane (0.70 mL, 4.90 mmol), PdCl₂(PPh₃)₂ (17.2 mg, 1 mol%) and CuI (4.60 mg, 1 mol%) in Et₃N (5 mL). Column chromatography (10% EtOAc in hexane) afforded the product as an amorphous yellow solid (313 mg, 88%); **IR (Neat):** $\nu_{\text{max}}/\text{cm}^{-1}$ 3291, 2108, 1507, 814, 608, 528; **¹H NMR** (400 MHz, CDCl₃) δ 7.36 (d, *J* = 9.0 Hz, 2H), 6.62 (d, *J* = 9.0 Hz, 2H), 2.98 (s, 6H), 2.97 (s, 1H); Data matches that reported in the literature.⁹²

135: Methyl-4-ethynylbenzoate



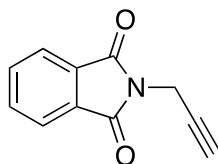
The title compound was prepared according to **GP1** using methyl-4-iodobenzoate (131 mg, 5.00 mmol), ethynyltrimethylsilane (1.40 mL, 10.0 mmol), PdCl₂(PPh₃)₂ (35.0 mg, 1 mol%) and CuI (19.0 mg, 2 mol%) in Et₃N (10 mL). Column chromatography (10% EtOAc in hexane) afforded the product as a beige amorphous solid (530 mg, 66%); **IR (Neat)**: $\nu_{\text{max}}/\text{cm}^{-1}$ 3242, 1700, 1606, 1434, 1276, 1107, 859, 770; **¹H NMR** (300 MHz, CDCl₃) δ 7.98 (d, J = 8.4 Hz, 2H), 7.54 (d, J = 8.4 Hz, 2H), 3.91 (s, 3H), 3.23 (s, 1H). Data matches that reported in the literature.⁹³

138: 4-Ethynyl-1,2-dimethoxybenzene



The title product was prepared according to a literature procedure.⁹⁴ 4-(2,2-dibromovinyl)-1,2-dimethoxybenzene (771 mg, 2.38 mmol) was added to a solution of PPh₃ (2.49 g, 9.52 mmol) and CBr₄ (1.58 g, 4.76 mmol) in CH₂Cl₂ (24 mL) in a round-bottom flask. The reaction was stirred for 1 h at rt. The reaction was then quenched with H₂O (50 mL), filtered under gravity, extracted with CH₂Cl₂ (3 × 25 mL), dried (Na₂SO₄) and purified by column chromatography (20% EtOAc in hexane) to yield the product as an amorphous white solid (315 mg, 81%); **¹H NMR** (300 MHz, CDCl₃) δ 7.10 (dd, J = 8.3 and 1.9 Hz, 1H), 6.99 (d, J = 1.9 Hz, 1H), 6.80 (d, J = 8.3 Hz, 1H), 3.88 (s, 3H), 3.87 (s, 3H), 3.00 (s, 1H). Data matches that reported in the literature.⁹⁴

140: *N*-Propargylphthalimide



The title compound was prepared according to a literature procedure.⁹⁵ Phthalimide (735 mg, 5.00 mmol), propargyl bromide (1.10 mL, 10.0 mmol) and K_2CO_3 (1.73 g, 12.5 mmol) were dissolved in acetone (40 mL) in a round-bottom flask. The reaction was stirred at 55 °C for 16 h. The reaction was cooled to rt and poured into aqueous HCl (1M, 20 mL) extracted with EtOAc, dried (Na_2SO_4) and purified by column chromatography (40% EtOAc in hexane) to afford to product as an amorphous beige solid (752 mg, 81%); **IR (Neat):** ν_{max}/cm^{-1} 3293, 1770, 1709, 1428, 1396, 1326, 1119, 725, 691; **1H NMR** (400 MHz, $CDCl_3$) δ 7.88 (dd, $J = 5.5$ and 3.0 Hz, 2H), 7.74 (dd, $J = 5.5$ and 3.0 Hz, 2H), 4.46 (d, $J = 2.5$ Hz, 2H), 2.22 (t, $J = 2.5$ Hz, 1H). Data matches that reported in the literature.⁹⁶

4.3 Gold Complexes

DTBPAuCl

Prepared as a white amorphous solid (375 mg, 87%) according to a literature procedure.⁹⁷ **1H NMR** (300 MHz, $CDCl_3$) δ 7.45 – 7.38 (m, 6H), 7.13 (dd, $J = 8.7, 2.4$ Hz, 3H), 1.45 (s, 27H), 1.29 (s, 27H). Data matches that reported in the literature.⁹⁷

[DTBPAuNCPPh] SbF_6

DTBPAuCl (242 mg, 0.28 mmol) was dissolved in CH_2Cl_2 (1.4 mL) in a heat-gun dried round-bottom flask under argon and the flask was covered in aluminium foil. Benzonitrile (31.8 μ L, 0.31 mmol) was added to the solution, followed by $AgSbF_6$ (96.2 mg, 0.28 mmol). The solution was stirred for 1 h at rt. The solution was filtered

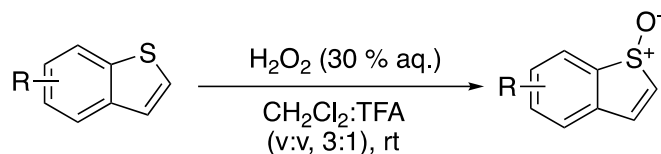
through a short pad of celite and the celite was further washed with CH₂Cl₂ (approx. 3 mL). CH₂Cl₂ was removed under reduced pressure to afford the product as a white amorphous solid (262 mg, 80%); **IR (Neat)**: $\nu_{\text{max}}/\text{cm}^{-1}$ 2958, 2870, 1489, 1174, 1073, 946, 890, 656; **³¹P NMR** (121 MHz, CDCl₃): δ 87.8 (s); **¹H NMR** (300 MHz, CDCl₃): δ 7.91 (d, $J = 7.3$ Hz, 2H), 7.75 (*app. t*, $J = 7.7$ Hz, 1H), 7.56 (*app. t*, $J = 7.8$ Hz, 2H), 7.47 (s, 3H), 7.42 (dd, $J = 8.6$ and 1.4 Hz, 3H), 7.27 (dd, $J = 8.6$ and 2.4 Hz, 3H), 1.46 (s, 27H), 1.31 (s, 27H); **¹³C NMR** (101 MHz, CDCl₃): δ 149.1, 147.2 (C-P, $^3J_{\text{C-P}} = 6.6$ Hz), 139.3 (C-P, $^3J_{\text{C-P}} = 7.0$ Hz), 136.3, 134.4, 129.9, 125.9, 124.9, 119.2 (C-P, $^2J_{\text{C-P}} = 9.0$ Hz), 107.0, 35.3, 34.9, 31.5, 30.7, The resonance for CN was not observed. Data matches that reported in the literature.⁹⁷

[(DTBP)₂Au]SbF₆

DTBPAuCl (83.7 mg, 0.11 mmol) was dissolved in CH₂Cl₂ (1 mL) in a heat-gun dried round-bottom flask under argon and the flask was covered in aluminium foil. DTBP (68.5 mg, 0.11 mmol) was added to the solution, followed by AgSbF₆ (40.3 mg, 0.12 mmol). The solution was stirred for 1 h at rt. The solution was filtered through a short pad of celite and the celite was further washed with CH₂Cl₂ (~ 2 mL). CH₂Cl₂ was removed under reduced pressure to afford the product as a white solid (152 mg, 83%); **IR (Neat)**: $\nu_{\text{max}}/\text{cm}^{-1}$ 2960, 2870, 1484, 1363, 1175, 1072, 947, 891, 818, 714, 655; **³¹P NMR** (121 MHz, CDCl₃): δ 120 (s) **¹H NMR** (300 MHz, CDCl₃): δ 7.48 (s, 6H), 7.90 – 7.00 (m, 12H), 1.30 (s, 54H), 1.28 (s, 54H); **¹³C NMR** (101 MHz, CDCl₃): δ 149.8, 146.7, 139.5, 126.3, 124.5, 119.1, 31.2, 34.9, 31.5, 30.5, **HR-MS** (ESI+) m/z : [M] Calcd for C₈₄H₁₂₆O₆AuP₂ 1489.8695; found: 1489.8730; **HRMS** (ESI-) m/z : [M] Calcd for SbF₆ 234.8942; Found 234.8948.

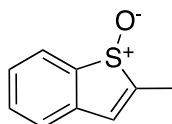
4.4 Benzothiophene S-oxides

General Procedure GP2:



The benzothiophene was stirred in CH_2Cl_2 (0.5 M) and TFA (1.5 M) in a round-bottom flask at rt. H_2O_2 (1.00 eq, 30% aq. in soln.) was added and the reaction was left to stir for 30 min before checking consumption of the benzothiophene by TLC. If the benzothiophene was still present, H_2O_2 was added in small amounts (approx. 0.25 eq each time) until it was consumed (after addition of each portion of H_2O_2 , the reaction was left to stir for 30 min before checking the progress of the reaction by TLC. This prevented over-oxidation of the benzothiophene to the sulfone). When the reaction was complete, the solution was cooled to 0 °C and quenched with aq. NaHCO_3 (sat.) until there was no further effervescence upon addition of aq. NaHCO_3 . H_2O was added (10 mL/mmol) and the aqueous layer was extracted with CH_2Cl_2 (3 × 15 mL/mmol), dried (Na_2SO_4) and filtered. The solvent was removed under reduced pressure and purified by flash column chromatography to afford the benzothiophene S-oxide.

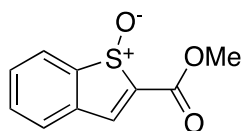
124: 2-Methylbenzothiophene S-oxide



The title compound was prepared according to **GP2** using 2-methylbenzothiophene (2.74 g, 18.5 mmol) and H_2O_2 (30% in aq. soln.). Column chromatography (40% hexane in EtOAc) afforded the product as a pale yellow solid (2.20 mg, 73%); R_f

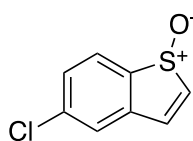
0.30 (40% hexane in EtOAc, Visualisation UV and KMNO₄); **IR (Neat):** $\nu_{\max}/\text{cm}^{-1}$ 3036, 1612, 1588, 1574, 1457, 1440, 1202, 1056, 1019, 906, 877, 766; **mp:** 67 – 71 °C; **¹H NMR** (300 MHz, CDCl₃): δ 7.85 (d, $J = 7.1$ Hz, 1H), 7.46 (*app. t*, $J = 7.5$ Hz, 1H), 7.41 – 7.32 (m, 2H), 6.78 (q, $J = 1.4$ Hz, 1H), 2.39 (d, $J = 1.4$ Hz, 3H); **¹³C NMR** (101 MHz, CDCl₃) δ 150.6, 144.7, 138.3, 132.2, 128.8, 127.78, 126.4, 123.8, 13.2.; **LRMS** (ESI) m/z : [M + H]⁺ Calcd for C₉H₉OS 165.03; Found 165.03. Data matches that reported in the literature. ¹⁸

141: Methylbenzothiophene-2-carboxylate S-oxide



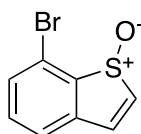
The title compound was prepared according to **GP2** using methylbenzothiophene-2-carboxylate (115 mg, 0.60 mmol) and H₂O₂ (30% in aq. soln.). Column chromatography (40% hexane in EtOAc) afforded the product as an amorphous white solid (90.2 mg, 73%); **R_f:** 0.25 (40% hexane in EtOAc, visualisation UV and KMnO₄); **mp:** 125 – 128 °C; **IR (Neat):** $\nu_{\max}/\text{cm}^{-1}$ 1717 (C=O stretch), 1561, 1236, 1175, 1068, 1033, 757, 727; **¹H NMR** (400 MHz, CDCl₃): δ 7.98 – 7.94 (m, 2H), 7.66 – 7.56 (m, 3H), 3.98 (s, 3H); **¹³C NMR** (101 MHz, CDCl₃): δ 161.7, 146.9, 143.3, 142.7, 135.3, 132.6, 131.7, 127.12, 127.05, 53.2; **HRMS** (ASAP) m/z : [M + H] Calcd for C₁₀H₉O₃S 209.0272; Found 209.0272.

142: 5-Chlorobenzothiophene-S-oxide



The title compound was prepared according to **GP2** using 5-chlorobenzothiophene (252 mg, 1.50 mmol) and H₂O₂ (30% in aq. soln.). Column chromatography (40% Hexane in EtOAc) afforded the product as an amorphous pale yellow solid (225 mg, 81%); **R_f**: 0.25 (40% hexane in EtOAc, visualisation UV and KMnO₄); **mp**: 125 – 128 °C; **IR (Neat)**: $\nu_{\text{max}}/\text{cm}^{-1}$ 3055, 2924, 1581, 1498, 1446, 1340, 1313, 1194, 1077 1026, 887, 812, 729, 706; **¹H NMR** (400 MHz, CDCl₃): δ 7.85 (d, *J* = 8.1 Hz, 1H), 7.51 – 7.43 (m, 2H), 7.19 – 7.13 (m, 2H); **¹³C NMR** (101 MHz, CDCl₃): δ 143.5, 139.6, 139.0, 138.6, 133.9, 129.0, 127.4, 125.3; **HRMS** (ASAP) *m/z*: [M + H] Calcd for C₈H₆OSCl 184.9828; Found 184.9830.

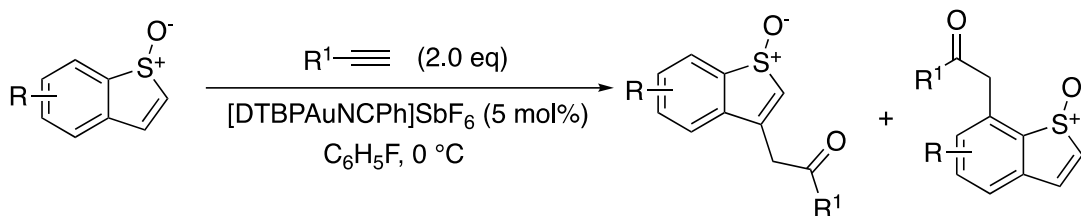
143: 7-Bromobenzothiophene-S-oxide



The title compound was prepared according to **GP2** using 7-bromobenzothiophene (127 mg, 0.60 mmol) and H₂O₂ (30% in aq. soln.). Column chromatography (40% Hexane in EtOAc) afforded the product as an amorphous pale yellow solid (89.3 mg, 65%); **R_f**: 0.30 (40% hexane in EtOAc, visualisation UV and KMnO₄); **mp**: 64 – 66 °C; **IR (Neat)**: $\nu_{\text{max}}/\text{cm}^{-1}$ 3047, 1442, 1180, 1034, 1019, 794, 723, 700; **¹H NMR** (400 MHz, CDCl₃): δ 7.54 (d, *J* = 7.9 Hz, 1H), 7.44 (dd, *J* = 7.5 and 1.1 Hz, 1H), 7.41 – 7.34 (m, 1H), 7.21 (d, *J* = 6.1 Hz, 1H), 7.13 (d, *J* = 6.1 Hz, 1H); **¹³C NMR** (101 MHz, CDCl₃): δ 144.4, 139.6, 138.3, 134.3, 133.8, 132.8, 124.0, 122.1; **HRMS** (ASAP) *m/z*: [M + H] Calcd for C₈H₆OSBr 228.9323; Found 228.9325.

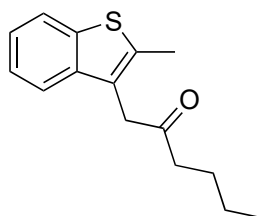
4.5 C-3 Substituted Benzothiophenes

General Procedure 3 (GP3):



The benzothiophene S-oxide (1.0 eq.) was added to a Radley carousel tube and dissolved in fluorobenzene (0.1 M). The alkyne (2.0 eq.) was then added and the solution was cooled (using the JULABO FT902 immersion cooler with an external temperature probe placed in an ethylene glycol:water bath (v:v, 1:1)) or heated (using an oil bath with an external temperature probe) to the appropriate temperature (dependant on the particular substrates used). [DTBPAuNCPH]SbF₆ (5 mol%) was added and the reaction was stirred until consumption of the benzothiophene S-oxide was observed by TLC. CH₂Cl₂ (5 mL/mmol) was added to the reaction mixture and the solution was filtered through a short pad of celite. The silica was then washed with EtOAc (3 × 5 mL/mmol). The solution was concentrated under reduced pressure and purified by flash column chromatography, affording the product as the C-3 functionalized benzothiophene or as a mixture of C-3/C-7 functionalised regioisomers.

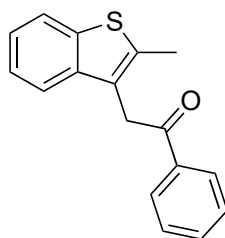
126a: 1-(2-Methylbenzo[b]thiophen-3-yl)hexan-2-one



The title compound was prepared according to **GP3** using 2-methylbenzothiophene S-oxide (21.3 mg, 0.13 mmol) and 1-hexyne (30.0 μl, 0.26 mmol) at 0 °C.

2-Methylbenzothiophene S-oxide was consumed after 5 h. Column chromatography (0 – 20% EtOAc in hexane) afforded the product as a clear oil (26.4 mg, 82%) as mixture of regioisomers (2.6:1, C-3:C-7); **R_f**: 0.30 (10% EtOAc in hexane, visualisation UV and KMnO₄). **IR (Neat)**: $\nu_{\text{max}}/\text{cm}^{-1}$ 2957, 2930, 2871, 1710, 1461, 1436, 1408, 1175, 1154, 827, 758, 729; **¹H NMR** (400 MHz, CDCl₃): δ 7.76 (d, *J* = 7.8 Hz, 1H), 7.61 – 7.55 (m, 1H), 7.37 – 7.32 (m, 1H), 7.31 – 7.27 (m, 1H), 3.82 (s, 2H), 2.53 (s, 3H), 2.39 (t, *J* = 7.4 Hz, 2H) 1.60 – 1.41 (m, 2H), 1.32 – 1.17 (m, 2H), 0.83 (t, *J* = 7.5 Hz, 3H); **¹³C NMR** (101 MHz, CDCl₃): δ 207.9 (C=O), 140.1 (C), 138.3 (C), 137.3 (C), 124.5 (C), 124.4 (CH), 123.9 (CH), 122.3 (CH), 121.2 (CH), 41.4 (CH₂), 41.3 (CH₂), 25.9 (CH₂), 22.3 (CH₂), 14.2 (CH₃), 13.9 (CH₃); **HRMS** (ESI) *m/z*: [M + NH₄] Calcd for C₁₅H₂₂NOS 264.1422; Found 264.1429.

126b – 2-(2-Methylbenzo[b]thiophen-3-yl)-1-phenylethan-1-one



The title compound was prepared according to **GP3** using 2-methylbenzothiophene S-oxide (82.3 mg, 0.50 mmol) and phenylacetylene (110 μl , 1.00 mmol) at 0 °C. The solution was stirred for 4 h. Column chromatography (0 – 40% CH₂Cl₂ in hexane) afforded the product as a white solid (113 mg, 85%) as mixture of regioisomers (7.6:1, C-3:C-7). Recrystallisation with MeOH afforded the C-3 regioisomer as white needles (89.3 mg, 67%, first crop); **R_f**: 0.40 (40% CH₂Cl₂ in hexane, visualisation UV and KMnO₄); **mp**: 153 – 155 °C (MeOH); **IR (Neat)**: $\nu_{\text{max}}/\text{cm}^{-1}$ 2925, 1742, 1677 (C=O stretch), 1433, 1328, 1213, 1000, 757, 747, 728, 687; **¹H NMR** (400 MHz,

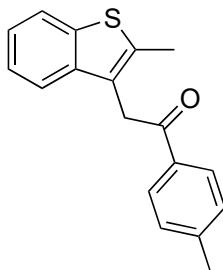
CDCl₃): δ 8.07 (d, J = 8.5 Hz, 2H), 7.76 (d, J = 7.0 Hz, 1H), 7.60 (tt, J = 7.4 and 1.4 Hz, 1H), 7.53 – 7.45 (m, 3H), 7.33 – 7.22 (m, 2H), 4.44 (s, 2H), 2.51 (s, 3H); ¹³C NMR (101 MHz, CDCl₃): δ 196.5 (C=O), 140.3 (C), 138.3 (C), 137.4 (C), 136.9 (C), 133.4 (CH), 128.9 (CH), 128.4 (CH), 124.5 (C), 124.2 (CH), 123.8 (CH), 122.3 (CH), 121.2 (CH), 36.6 (CH₂), 14.3 (CH₃); HRMS (ESI) m/z : [M + Na] Calcd for C₁₇H₁₄OSNa 289.0663; Found 289.0668.

1.00 mmol scale reaction protocol

2-Methylbenzothiophene S-oxide (165 mg, 1.00 mmol) was dissolved in fluorobenzene (10 mL) and the mixture was sonicated until all of the material was in solution. Phenylacetylene (219 μ l, 2.00 mmol) was added to the solution via microsyringe, and the solution was cooled to 0 °C. [DTBPAuNCPPh]SbF₆ (56.0 mg, 5 mol%) was added to the solution and the solution was stirred at 0 °C. 2-Methylbenzothiophene S-oxide was consumed after 5 h. The solution was filtered through a short pad of celite which was subsequently washed with EtOAc (3 \times 5 ml). The solvent was removed under reduced pressure before being dry-loaded onto a minimum amount of silica with CH₂Cl₂. The product was purified by flash column chromatography (0 – 30% CH₂Cl₂ in hexane) affording the pure C-3 regioisomer (**126b**) as a white amorphous solid (154 mg, 58%) alongside a mixture of regioisomers (2:1, C-3:C-7) as a white amorphous solid (68.5 mg, 26%). The mixture of regioisomers was suspended in MeOH (approx. 5 mL) and stirred at 64 °C until all of the material had dissolved. The flask was then wrapped in cotton wool and aluminium foil and left to cool slowly, whereupon **126b** crystallized. The crystals were collected and dried by vacuum filtration, attaining the pure C-3 regioisomer (**126b**) as white needles (27.8 mg, 10%).

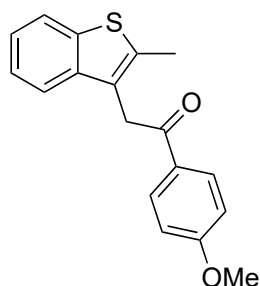
From this procedure the total amount of the pure C-3 regioisomer (**126b**) was 68% (182 mg).

144: 2-(2-Methylbenzo[*b*]thiophen-3-yl)-1-(*p*-tolyl)ethan-1-one



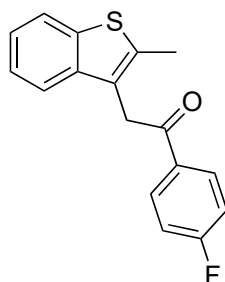
The title compound was prepared according to **GP3** using 2-methylbenzothiophene *S*-oxide (32.5 mg, 0.20 mmol) and 1-ethyny-4-methylbenzene (46.5 mg, 0.40 mmol) at 0 °C. 2-Methylbenzothiophene *S*-oxide was consumed after 6 h. Column chromatography (0–30% CH₂Cl₂ in hexane) afforded the product as a pale yellow amorphous solid (36.5 mg, 65 %) as a mixture of regioisomers (7.5:1, C-3:C-7); **R_f**: 0.35 (30% CH₂Cl₂ in hexane, visualisation UV and KMnO₄); **mp**: 76 – 78 °C; **IR (Neat)**: $\nu_{\text{max}}/\text{cm}^{-1}$ 2934, 1677 (C=O stretch), 1600, 1547, 1434, 1323, 1259, 1218, 1170, 980, 816, 759, 746, 724; **¹H NMR** (400 MHz, CDCl₃): δ 7.96 (d, *J* = 8.2 Hz, 2H), 7.75 (d, *J* = 7.3 Hz, 1H), 7.51 (d, *J* = 7.0 Hz, 1H), 7.33 – 7.22 (m, 4H), 4.41 (s, 2H), 2.50 (s, 3H), 2.43 (s, 3H), **¹³C NMR** (101 MHz, CDCl₃): δ 196.2 (C=O), 144.3 (C), 140.4 (C), 138.3 (C), 137.3 (C), 134.4 (C), 129.5 (CH), 128.6 (CH), 124.8 (C), 124.2 (CH), 123.7 (CH), 122.3 (CH), 121.2 (CH), 36.5 (CH₂), 21.8 (CH₃), 14.4 (CH₃); **HRMS** (ESI) *m/z*: [M + Na] Calcd for C₁₈H₁₆OSNa 303.0820; Found 303.0819.

145: 1-(4-Methoxyphenyl)-2-(2-methylbenzo[b]thiophen-3-yl)ethan-1-one



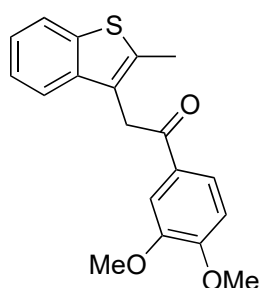
The title compound was prepared according to **GP3** using 2-methylbenzothiophene S-oxide (82.1 mg, 0.50 mmol) and 1-ethynyl-4-methoxybenzene (132 mg, 1.00 mmol) at 0 °C. The reaction was left for 8 h. Column chromatography (0–30 % CH₂Cl₂ in hexane) afforded the product as beige amorphous solid (103 mg, 70%) as a mixture of regioisomers (5.3:1, C-3:C-7); **R_f**: 0.31 (30% CH₂Cl₂ in hexane, visualisation UV and KMnO₄); **mp**: 118 – 120 °C; **IR (Neat)**: $\nu_{\text{max}}/\text{cm}^{-1}$ 2912, 1673 (C=O stretch), 1598, 1318, 1253, 1217, 1176, 1032, 984, 832, 748; **¹H NMR** (400 MHz, CDCl₃): δ 8.05 (d, *J* = 8.8 Hz, 2H), 7.75 (d, *J* = 7.2 Hz, 1H), 7.52 (d, *J* = 7.5 Hz, 1H), 7.33 – 7.22 (m, 2H), 6.96 (d, *J* = 8.8 Hz, 2H), 4.38 (s, 2H), 3.88 (s, 3H), 2.51 (s, 3H); **¹³C NMR** (101 MHz, CDCl₃): δ 195.0 (C=O), 163.8 (C), 140.4 (C), 138.3 (C), 137.2 (C), 130.7 (CH), 130.0 (C), 124.9 (C), 124.2 (CH), 123.7 (CH), 122.2 (CH), 121.2 (CH), 114.0 (CH), 55.7 (CH₃), 36.4 (CH₂), 14.3 (CH₃); **HRMS** (ESI) *m/z*: [M + Na] Calcd for C₁₈H₁₆O₂SNa 319.0769; Found 319.0770.

146: 1-(4-Fluorophenyl)-2-(2-methylbenzo[b]thiophen-3-yl)ethan-1-one



The title compound was prepared according to **GP3** using 2-methylbenzothiophene S-oxide (82.4 mg, 0.50 mmol) and 1-ethynyl-4-fluorobenzene (121 mg, 1.00 mmol) at 0 °C. The reaction was left for 16 h. Column chromatography (0–30% CH₂Cl₂ in hexane) afforded the product as a yellow amorphous solid (127 mg, 89%) as a mixture of regioisomers (8.8:1, C-3:C-7). This solid was recrystallized from CH₂Cl₂ with hexane to afford the pure C-3 regioisomer (**146**) as pale yellow crystalline needles (98.2 mg, 69%); **R_f**: 0.25 (30% CH₂Cl₂ in hexane, visualisation UV and KMnO₄); **mp**: 110 – 113 °C (recrystallised from CH₂Cl with hexane); **IR (Neat)**: $\nu_{\text{max}}/\text{cm}^{-1}$ 3068, 2915, 1686 (C=O stretch), 1596, 1505, 1435, 1410, 1223, 1208, 1159, 981, 839, 812, 755, 730; **¹H NMR** (400 MHz, CDCl₃): δ 8.08 (dd, *J* = 8.9 and 5.4 Hz, 2H), 7.76 (dd, *J* = 6.7 and 1.7 Hz, 1H), 7.50 (dd, *J* = 6.9 and 1.9 Hz, 1H), 7.34 – 7.23 (m, 2H), 7.15 (*app. t*, *J* = 8.7 Hz, 2H), 4.41 (s, 2H), 2.51 (s, 3H); **¹³C NMR** (101 MHz, CDCl₃): δ 194.9 (C=O), 166.0 (C-F, ¹*J*_{C-F} = 255.2 Hz, C), 140.2 (C), 138.3 (C), 137.5 (C), 133.3 (C-F, ⁴*J*_{C-F} = 3.0 Hz, C), 131.1 (C-F, ³*J*_{C-F} = 9.3 Hz, CH), 124.32 (C), 124.27 (CH), 123.8 (CH), 122.3 (CH), 121.1 (CH), 116.0 (C-F, ²*J*_{C-F} = 21.8 Hz, CH), 36.6 (CH₂), 14.3 (CH₃); **¹⁹F NMR** (376 MHz, CDCl₃): δ –104.7; **HRMS** (EI) *m/z*: [M] Calcd for C₁₇H₁₃OFS 284.0671; Found 284.0672.

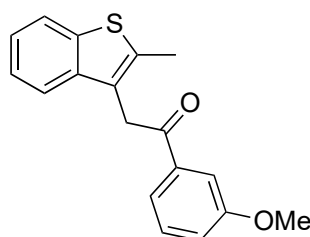
147: 1-(3,4-Dimethoxyphenyl)-2-(2-methylbenzo[b]thiophen-3-yl)ethan-1-one



The title compound was prepared according to **GP3** using 2-methylbenzothiophene S-oxide (82.2 mg, 0.50 mmol) and 4-ethynyl-1,2-dimethoxybenzene (162 mg, 1.00 mmol)

at 0 °C. The reaction was left for 16 h. Column chromatography (40–80% CH₂Cl₂ in hexane) afforded the product as a pale yellow amorphous solid (101 mg, 62%), as a mixture of regioisomers (5.8:1, C-3:C-7); **R_f**: 0.39 (80% CH₂Cl₂ in hexane, visualisation UV and KMnO₄); **mp**: 152 – 154 °C; **IR (Neat)**: $\nu_{\text{max}}/\text{cm}^{-1}$ 3005, 2964, 2833, 1678 (C=O stretch), 1586, 1514, 1417, 1260, 1160, 1148, 874, 801, 765, 747, 728, 612; **¹H NMR** (400 MHz, CDCl₃): δ 7.78 – 7.72 (m, 2H), 7.60 – 7.52 (m, 2H), 7.34 – 7.22 (m, 2H), 6.91 (d, *J* = 8.4 Hz, 1H), 4.40 (s, 2H), 3.96 (s, 3H), 3.87 (s, 3H), 2.51 (s, 3H); **¹³C NMR** (101 MHz, CDCl₃): δ 195.2 (C=O), 153.5 (C), 149.2 (C), 140.4 (C), 138.3 (C), 137.3 (C), 130.0 (C), 125.0 (C), 124.2 (CH), 123.8 (CH), 123.0 (CH), 122.3 (CH), 121.2 (CH), 110.6 (CH), 110.2 (CH), 56.2 (CH₃), 56.1 (CH₃), 36.4 (CH₂), 14.4 (CH₃); **HRMS** (EI) *m/z*: [M] Calcd for C₁₉H₁₈O₃S 326.0977; Found 326.0973.

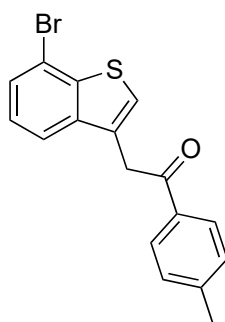
148: 1-(3-Methoxyphenyl)-2-(2-methylbenzo[b]thiophen-3-yl)ethan-1-one



The title compound was prepared according to **GP3** using 2-methylbenzothiophene S-oxide (82.6 mg, 0.50 mmol) and 1-ethynyl-3-methoxybenzene (134 mg, 1.00 mmol) at 0 °C. The reaction was left for 4.5 h. Column chromatography (0–40% CH₂Cl₂ in hexane) afforded the product as a pale yellow solid (127 mg, 86%) as a mixture of regioisomers (8.3:1, C-3:C-7); **R_f**: 0.29 (40% CH₂Cl₂ in hexane, visualisation UV and KMnO₄); **mp**: 115 – 118 °C; **IR (Neat)**: $\nu_{\text{max}}/\text{cm}^{-1}$ 2922, 1679 (C=O stretch), 1596, 1462, 1427, 1258, 1164, 1017, 870, 787, 760, 683; **¹H NMR** (400 MHz, CDCl₃): δ 7.76 (d, *J* = 8.0 Hz, 1H), 7.67 (ddd, *J* = 7.7, 1.6 and 1.0 Hz, 1H), 7.54 (dd, *J* = 2.7 and 1.6

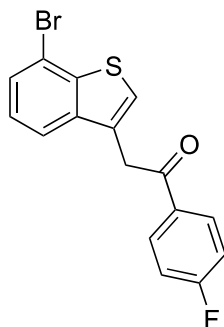
Hz, 1 H), 7.52 (d, $J = 8.0$ Hz, 1H), 7.40 (app. t, $J = 8.0$ Hz, 1H), 7.33–7.23 (m, 2H), 7.14 (ddd, $J = 8.3, 2.7$ and 1.0 Hz, 1H), 4.42 (s, 2H), 3.83 (s, 3H), 2.51 (s, 3H); ^{13}C NMR (101 MHz, CDCl_3): δ 196.4 (C=O), 160.0 (C), 140.3 (C), 138.3 (C), 138.2 (C), 137.4 (C), 129.8 (CH), 124.5 (C), 124.2 (CH), 123.8 (CH), 122.3 (CH), 121.2 (CH), 121.0 (CH), 120.0 (CH), 112.7 (CH), 55.6 (CH_3), 36.8 (CH_2), 14.3 (CH_3); **HRMS** (ESI) m/z : [M+H] calcd for $\text{C}_{18}\text{H}_{17}\text{O}_2\text{S}$ 297.0949; Found 297.0950.

149: 2-(7-Bromobenzo[*b*]thiophen-3-yl)-1-(*p*Tolyl)ethan-1-one



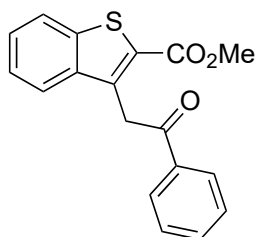
The title compound was prepared according to **GP3** using 7-bromobenzo[*b*]thiophene *S*-oxide (45.5 mg, 0.20 mmol) and 1-ethynyl-4-methylbenzene (46.0 mg, 0.40 mmol) at 0 °C. The reaction was left for 18 h. Column chromatography (10 – 30% CH_2Cl_2 in hexane) afforded the product as a yellow amorphous solid (35.3 mg, 52%); **R_f**: 0.27 (30% CH_2Cl_2 in hexane, visualisation UV and KMnO_4); **mp**: 128 – 133 °C; **IR (Neat)**: $\nu_{\text{max}}/\text{cm}^{-1}$ 2918, 1679 (C=O stretch), 1605, 1392, 1322, 1217, 1180, 804, 784, 716; ^1H NMR (400 MHz, CDCl_3): 7.94 (d, $J = 8.2$ Hz, 2H), 7.69 (d, $J = 8.2$ Hz, 1H), 7.52 (d, $J = 7.6$ Hz, 1H), 7.35 (s, 1H), 7.31 – 7.24 (m, 3H), 4.46 (d, $J = 1.0$ Hz, 2H), 2.42 (s, 3H); ^{13}C NMR (101 MHz, CDCl_3): δ 196.0 (C=O), 144.5 (C), 142.1 (C), 140.1 (C), 134.0 (C), 130.5 (C), 129.6 (CH), 128.8 (CH), 127.4 (CH), 125.8 (CH), 125.6 (CH), 121.0 (CH), 116.5 (C), 39.0 (CH_2), 21.8 (CH_3); **HRMS** (EI) m/z : [M] Calcd for $\text{C}_{17}\text{H}_{13}\text{OS}^{79}\text{Br}$ 343.9870; Found 343.9872.

150: 2-(7-Bromobenzo[b]thiophen-3-yl)-1-(4-fluorophenyl)ethan-1-one



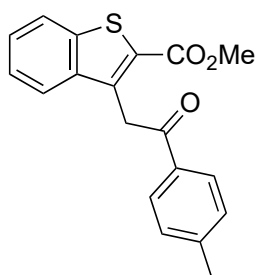
The title compound was prepared according to **GP3** using 7-bromobenzothiophene S-oxide (45.6 mg, 0.20 mmol) and 1-ethynyl-4-fluorobenzene (47.0 mg, 0.40 mmol) at 0 °C. The reaction was left for 18 h. Column chromatography (10 – 40% CH₂Cl₂ in hexane) afforded the product as a yellow amorphous solid (37.5 mg, 54%); **R_f**: 0.30 (40% CH₂Cl₂ in hexane, visualisation UV and KMnO₄); **mp**: 125 – 129 °C; **IR (Neat)**: $\nu_{\text{max}}/\text{cm}^{-1}$ 2905, 1683 (C=O stretch), 1595, 1504, 1409, 1321, 1206, 1154, 988, 737, 785, 717, 637; **¹H NMR** (400 MHz, CDCl₃): δ 8.07 (dd, *J* = 8.5 and 5.3 Hz, 2H), 7.68 (dd, *J* = 8.1 and 1.0 Hz, 1H), 7.53 (d, *J* = 7.7 Hz, 1H), 7.36 (s, 1H), 7.29 (*app. t*, *J* = 7.7 Hz, 1H), 7.15 (*app. t*, *J* = 8.5 Hz, 2H), 4.46 (d, *J* = 1.0 Hz, 2H); **¹³C NMR** (101 MHz, CDCl₃): δ 194.8 (C=O), 166.1 (C-F, ¹*J*_{C-F} = 255.5 Hz, C), 142.1 (C), 139.9 (C), 132.8 (C-F, ⁴*J*_{C-F} = 3.1 Hz, C), 131.3 (C-F, ³*J*_{C-F} = 9.4 Hz, CH), 130.0 (C), 127.5 (CH), 125.8 (2 × overlapping CH), 120.9 (CH), 116.6 (C), 116.1 (C-F, ²*J*_{C-F} = 22.1 Hz, CH), 39.1 (CH₃); **¹⁹F NMR** (376 MHz, CDCl₃): δ -104.3; **HRMS** (ASAP) *m/z*: [M + H] Calcd for C₁₆H₁₁⁷⁹BrFOS 348.9698; Found 348.9703.

151: Methyl 3-(2-oxo-2-phenylethyl)benzo[b]thiophene-2-carboxylate



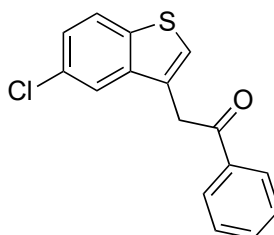
The title compound was prepared according to **GP3** using methylbenzothiophene-2-carboxylate *S*-oxide (35.2 mg, 0.17 mmol) and phenylacetylene (37.0 μ L, 0.34 mmol) at 0 °C. The reaction was left for 24 h. Column chromatography (10% EtOAc in hexane) afforded the product as a cream amorphous solid (30.9 mg, 59%) as a mixture of regioisomers (2.7:1, C-3:C-7); **R_f**: 0.30 (10% EtOAc in hexane, visualisation UV and KMnO₄); **mp**: 135 – 138 °C; **IR (Neat)**: $\nu_{\text{max}}/\text{cm}^{-1}$ 2922, 1708 (C=O stretch), 1680 (C=O stretch), 1532, 1448, 1323, 1272, 1248, 1210, 1108, 979, 755, 682; **¹H NMR** (300 MHz, CDCl₃) δ 8.13 (d, *J* = 7.0 Hz, 2H), 7.87 (d, *J* = 8.1 Hz, 1H), 7.73 (d, *J* = 8.1 Hz, 1H), 7.62 (t, *J* = 7.3 Hz, 1H), 7.56 – 7.31 (m, 4H) 5.08 (s, 2H), 3.87 (s, 3H); **¹³C NMR** (101 MHz, CDCl₃) δ 196.0 (C=O), 163.7 (C=O), 140.7 (C), 139.8 (C), 138.0 (C), 137.0 (C), 133.5 (CH), 128.9 (CH), 128.5 (CH), 127.5 (CH), 125.0 (CH), 123.7 (CH), 123.0 (CH), 52.4 (CH₃), 37.5 (CH₂), a quaternary carbon was not observed (C-CO₂Me); **HRMS** (ASAP) *m/z*: [M + H] Calcd for C₁₈H₁₅O₃S 311.0742; Found 311.0744.

152: Methyl 3-(2-oxo-2-(p-tolyl)ethyl)benzo[b]thiophene-2-carboxylate



The title compound was prepared according to **GP3** using methylbenzothiophene-2-carboxylate S-oxide (29.6 mg, 0.14 mmol) and 1-ethynyl-4-methylbenzene (33.0 mg, 0.28 mmol) at 0 °C. Methylbenzothiophene-2-carboxylate S-oxide was consumed after 4h. Column chromatography (10% EtOAc in hexane) afforded the product as a white amorphous solid (30.3 mg, 67%) as a mixture of regioisomers (3.8:1, C-3:C-7); **R_f**: 0.31 (10% EtOAc in hexane, visualisation UV and KMnO₄); **mp**: 167 – 170 °C; **IR (Neat)**: $\nu_{\text{max}}/\text{cm}^{-1}$ 2920, 1706 (C=O stretch), 1686, 1606, 1529, 1269, 1246, 1217, 975, 759; **¹H NMR** (400 MHz, CDCl₃) δ 8.02 (d, *J* = 8.2 Hz, 2H), 7.86 (d, *J* = 8.2 Hz, 1H), 7.73 (d, *J* = 8.2 Hz, 1H), 7.47 (ddd, *J* = 8.2, 7.1 and 1.2 Hz, 1H), 7.39 (ddd, *J* = 8.2, 7.1 and 1.1 Hz, 1H), 7.31 (d, *J* = 8.1 Hz, 2H), 5.05 (s, 2H), 3.86 (s, 3H), 2.44 (s, 3H,); **¹³C NMR** (101 MHz, CDCl₃) δ 195.6 (C=O), 163.7 (C=O), 144.3 (C), 140.7 (C), 139.9 (C), 138.2 (C), 134.5 (C), 129.5 (CH), 128.6 (CH), 127.4 (CH), 124.9 (CH), 123.8 (CH), 122.9 (CH), 52.4 (CH₃), 37.4 (CH₂), 21.9 (CH₃), a quaternary carbon was not observed (C-CO₂Me); **HRMS** (ASAP) *m/z*: [M + H] Calcd for C₁₉H₁₇O₃S 325.0898; Found 325.0908.

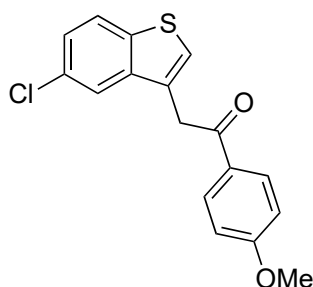
153: 2-(5-Chlorobenzo[*b*]thiophen-3-yl)-1-phenylethan-1-one



The title compound was prepared according to **GP3** using 5-chlorobenzothiophene S-oxide (27.9 mg, 0.15 mmol) and phenylacetylene (33.0 μ l, 0.30 mmol) at 0 °C. The reaction was left for 18 h. Column chromatography (0 – 30% CH₂Cl₂ in hexane) afforded the product as a pale yellow amorphous solid (27.1 mg, 63%) as a mixture of

regioisomers (25:1, C-3:C-7); **R_f**: 0.31 (30% DCM in hexane, visualisation UV and KMnO₄); **mp**: 74 – 77 °C; **IR (Neat)**: $\nu_{\text{max}}/\text{cm}^{-1}$ 3096, 2924, 1684 (C=O stretch), 1422, 1211, 1076, 983, 824, 749, 685; **¹H NMR** (400 MHz, CDCl₃): δ 8.05 (d, *J* = 7.8 Hz, 2H), 7.77 (d, *J* = 7.6 Hz, 1H), 7.69 (d, *J* = 1.8 Hz, 1H), 7.61 (*app. t*, *J* = 8.0 Hz, 1H), 7.50 (*app. t*, *J* = 8.0 Hz, 2H), 7.37 – 7.30 (m, 2H), 4.48 (s, 2H); **¹³C NMR** (101 MHz, CDCl₃): δ 196.3 (C=O), 140.2 (C), 138.5 (C), 136.5 (C), 133.7 (CH), 130.8 (C), 129.0 (CH), 128.7 (CH), 126.7 (CH), 125.1 (CH), 124.0 (CH), 121.7 (CH), 38.4 (CH₃), a quaternary carbon was not observed; **HRMS** (EI) *m/z*: [M] Calcd for C₁₆H₁₁OS³⁵Cl 286.0219; Found 286.0216.

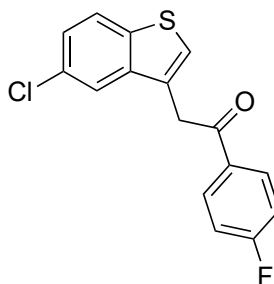
154: 2-(5-Chlorobenzo[b]thiophen-3-yl)-1-(4-methoxyphenyl)ethan-1-one



The title compound was prepared according to **GP3** using 5-chlorobenzothiophen S-oxide (55.5 mg, 0.30 mmol) and 1-ethynyl-4-methoxybenzene (80.5 mg, 0.60 mmol) at 0 °C. The reaction was left for 15 h. Column chromatography (0 – 30% CH₂Cl₂ in hexane) followed by trituration with cold methanol (approx. 1 mL/mmol) afforded the product as a white amorphous solid (49.5 mg, 52%) as the single C-3 regioisomer; **R_f**: 0.30 (10% EtOAc in hexane, visualisation UV and KMnO₄); **mp**: 155 – 160 °C; **IR (Neat)**: $\nu_{\text{max}}/\text{cm}^{-1}$ 3108, 3008, 2965, 2932, 1670 (C=O stretch), 1595, 1508, 1416, 1258, 1216, 1169, 988, 824, 796, 722; **¹H NMR** (400 MHz, CDCl₃) δ 8.03 (d, *J* = 8.9 Hz, 2H), 7.77 (dd, *J* = 8.6 and 0.6 Hz, 1H), 7.71 (dd, *J* = 2.0 and 0.6 Hz, 1H), 7.35 – 7.29 (m, 2H), 6.96 (d, *J* = 8.9 Hz, 2H), 4.42 (d, *J* = 1.0 Hz, 2H), 3.88

(s, 3H); ^{13}C NMR (101 MHz, CDCl_3) δ 194.8 (C=O), 164.0 (C), 140.3 (C), 138.5 (C), 131.0 (CH), 130.8 (C), 129.5 (C), 129.1 (C), 126.5 (CH), 125.0 (CH), 124.0 (CH), 121.7 (CH), 114.1 (CH), 55.7 (CH_3), 38.2 (CH_3); **HRMS** (ASAP) m/z : $[\text{M} + \text{H}]$ Calcd for $\text{C}_{17}\text{H}_{14}\text{O}_2\text{S}$ 317.0403; Found 317.0398.

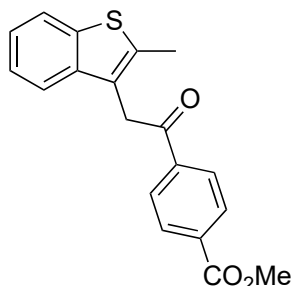
155: 2-(5-Chlorobenzo[*b*]thiophen-3-yl)-1-(4-fluorophenyl)ethan-1-one



The title compound was prepared according to **GP3** using 5-chlorobenzothiophene *S*-oxide (35.0 mg, 0.19 mmol) and 1-ethynyl-4-fluorobenzene (48.2 mg, 0.40 mmol) at 0 °C. The reaction was left for 18 h. Column chromatography (0 – 30% CH_2Cl_2 in hexane) afforded the product as a yellow amorphous solid (34.8 mg, 60%) as a mixture of regioisomers (20:1, C-3:C-7). Trituration with cold methanol (approx. 1 mL/mmol) affords the pure C-3 regioisomer as a pale yellow amorphous solid (32.0 mg, 55%); **R_f**: 0.33 (30% CH_2Cl_2 in hexane, visualisation UV and KMnO_4); **mp**: 93 – 97 °C; **IR (Neat)**: $\nu_{\text{max}}/\text{cm}^{-1}$ 2906, 1682 (C=O stretch), 1595, 1504, 1409, 1323, 1207, 1155, 1075, 989, 868, 826, 780, 636; ^1H NMR (400 MHz, CDCl_3): δ 8.08 (dd, $J = 9.0$ and 5.4 Hz, 2H), 7.78 (dd, $J = 8.6$ and 0.5 Hz, 1H), 7.68 (d, $J = 1.5$ Hz, 1H), 7.36 – 7.31 (m, 2H), 7.16 (app. t, $J = 8.0$ Hz, 2H), 4.44 (d, $J = 1.0$ Hz, 2H); ^{13}C NMR (101 MHz, CDCl_3): δ 194.7 (C=O), 166.1 (C-F, $^1J_{\text{C-F}} = 255.7$ Hz, C), 140.1 (C), 138.5 (C), 132.8 (C-F, $^4J_{\text{C-F}} = 3.0$ Hz, C), 131.3 (C-F, $^3J_{\text{C-F}} = 9.4$ Hz, CH), 130.9 (C), 128.4 (C), 126.7 (CH), 125.1 (CH), 124.0 (CH), 121.6 (CH), 116.1 (C-F, $^2J_{\text{C-F}} =$

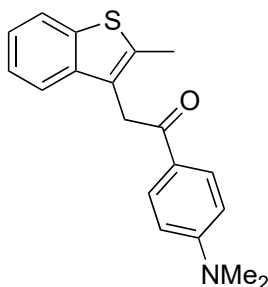
21.9 Hz, CH), 38.4 (CH₃); **¹⁹F NMR** (376 MHz, CDCl₃): δ -104.3; **HRMS** (ASAP) m/z: [M + H] Calcd for C₁₆H₁₁³⁵ClFOS 305.0203; Found 305.0201.

156: Methyl 4-(2-(2-methylbenzo[b]thiophen-3-yl)acetyl)benzoate



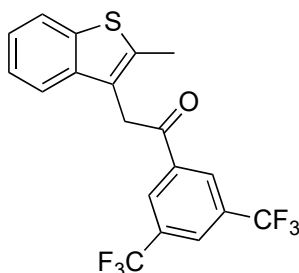
The title compound was prepared according to **GP3** using 2-methylbenzothiophen S-oxide (32.8 mg, 0.20 mmol) and methyl-4-ethylbenzoate (32.3 mg, 0.20 mmol) at 50 °C. The reaction was left for 24 h. Column chromatography (0 – 100 % Et₂O in hexane) afforded the product as a beige amorphous solid (54.4 mg, 84%) as mixture of regioisomers (8.0:1, C-3:C-7); **R_f**: 0.28 (20% Et₂O in hexane, visualisation UV and KMnO₄); **mp**: 108 – 110 °C; **IR (Neat)**: $\nu_{\text{max}}/\text{cm}^{-1}$ 2955, 2917, 2850, 1708 (C=O stretch), 1680 (C=O stretch), 1433, 1277, 1202, 1109, 984, 960, 868, 826, 766, 723, 695; **¹H NMR** (400 MHz, CDCl₃) δ 8.14 (d, *J* = 8.8 Hz, 2H), 8.08 (d, *J* = 8.8 Hz, 2H), 7.76 (d, *J* = 6.8 Hz, 1H), 7.50 (d, *J* = 7.4 Hz, 1H), 7.34 – 7.25 (m, 2H), 4.45 (s, 2H), 3.95 (s, 3H), 2.51 (s, 3H); **¹³C NMR** (101 MHz, CDCl₃) δ 196.1 (C=O), 166.3 (C=O), 140.2 (C), 140.1 (C), 138.3 (C), 137.7 (C), 134.2 (C), 130.1 (CH), 128.3 (CH), 124.3 (CH), 124.0 (C), 123.9 (CH), 122.3 (CH), 121.0 (CH), 52.7 (CH₃), 37.1 (CH₂), 14.4 (CH₃); **HRMS** (ESI) m/z: [M + H] Calcd for C₁₉H₁₇O₃S 325.0898; Found: 325.0894.

157: 1-(4-(Dimethylamino)phenyl)-2-(2-methylbenzo[b]thiophen-3-yl)ethan-1-one



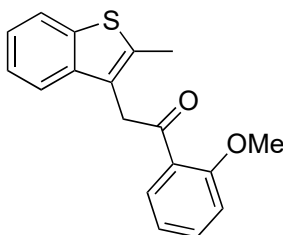
The title compound was prepared according to **GP3** using 2-methylbenzothiophene S-oxide (42.1 mg, 0.25 mmol) and 4-ethynyl-*N,N*-dimethylaniline (72.8 mg, 0.50 mmol) at 70 °C. 2-Methylbenzothiophene S-oxide was consumed after 1.5 h. Column chromatography (0 – 50% CH₂Cl₂ in hexane) afforded the product as a pale yellow amorphous solid (44.3 mg, 57%) as a mixture of regioisomers (3.9:1, C-3:C-7); **R_f**: 0.29 (50% CH₂Cl₂ in hexane, visualisation UV and KMnO₄); **mp**: 174 – 176 °C; **IR (Neat)**: $\nu_{\text{max}}/\text{cm}^{-1}$ 2901, 2819, 1661 (C=O stretch), 1592, 1547, 1434, 1369, 1325, 1235, 1176, 1007, 813, 766; **¹H NMR** (400 MHz, CDCl₃): δ 7.98 (d, *J* = 9.1 Hz, 2H) 7.74 (d, *J* = 7.2 Hz, 1H), 7.56 (d, *J* = 7.2 Hz, 1H), 7.32 – 7.20 (m, 2H), 6.67 (d, *J* = 9.1 Hz, 2H), 4.35 (s, 2H), 3.07 (s, 6H), 2.51 (s, 3H); **¹³C NMR** (101 MHz, CDCl₃): δ 194.5 (C=O), 153.6 (C), 140.6 (C), 138.3 (C), 136.8 (C), 130.7 (CH), 125.7 (C), 124.9 (C), 124.1 (CH), 123.6 (CH), 122.2 (CH), 121.4 (CH), 110.9 (CH), 40.2 (CH₃), 36.0 (CH₂), 14.4 (CH₃); **HRMS** (ESI) *m/z*: [M + Na] Calcd for C₁₉H₁₉NOSNa 332.1085; Found 332.1086.

158: 1-(3,5-Bis(trifluoromethyl)phenyl)-2-(2-methylbenzo[b]thiophen-3-yl)ethan-1-one



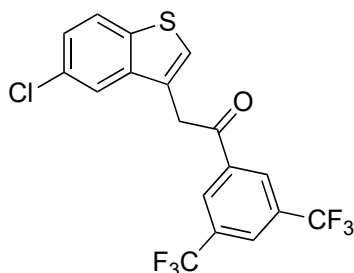
The title compound was prepared according to **GP3** using 2-methylbenzothiophene S-oxide (82.3 mg, 0.50 mmol) and 1-ethynyl-3,5-bis(trifluoromethyl)benzene (240 mg, 1.00 mmol) at 70 °C. 2-Methylbenzothiophene S-oxide was consumed after 5 h. Column chromatography (0–20 % CH₂Cl₂ in hexane) afforded the product as a pale yellow amorphous solid (150 mg, 75%), as a mixture of regioisomers (11.5:1, C-3:C-7); **R_f**: 0.32 (20% CH₂Cl₂ in hexane, visualisation UV and KMnO₄); **mp**: 123 – 125 °C; **IR (Neat)**: $\nu_{\text{max}}/\text{cm}^{-1}$ 2909, 1694 (C=O stretch), 1615, 1381, 1277, 1170, 1131, 919, 889, 840, 775, 761, 697, 681; **¹H NMR** (400 MHz, CDCl₃): δ 8.45 (s, 2H), 8.06 (s, 1H), 7.77 (d, $J = 7.2$, 1H), 7.52 (d, $J = 7.3$, 1H), 7.36 – 7.25 (m, 2H), 4.47 (s, 2H), 2.55 (s, 3H); **¹³C NMR** (101 MHz, CDCl₃): δ 193.8 (C=O), 139.8 (C), 138.4 (C), 138.10 (C), 138.04 (C), 132.6 (C-F, $^2J_{\text{C-F}} = 34.1$ Hz, C), 128.5 (C-F, $^3J_{\text{C-F}} = 4.3$ Hz, CH), 126.6 (C-F, $^3J_{\text{C-F}} = 3.5$ Hz, CH), 124.5 (CH), 124.1 (CH), 123.0 (C-F, $^1J_{\text{C-F}} = 273.7$ Hz, C), 122.9 (C), 122.4 (CH), 121.0 (CH), 37.4 (CH₂), 14.3 (CH₃); **¹⁹F NMR** (376 MHz, CDCl₃): δ -62.9; **HR-MS** (ESI) m/z : [M + Na] Calcd for C₁₉H₁₂F₆OSNa 425.0405; Found: 425.0402.

159: 1-(2-Methoxyphenyl)-2-(2-methylbenzo[b]thiophen-3-yl)ethan-1-one



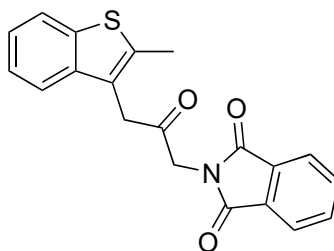
The title compound was prepared according to **GP3** using 2-methylbenzothiophene S-oxide (41.1 mg, 0.20 mmol) and 1-ethynyl-2-methoxybenzene (52.9 mg, 40 mmol) at 75 °C. The reaction was left for 8 h. Column chromatography (0–40% CH₂Cl₂ in hexane) afforded the product as a pale yellow oil (11.7 mg, <20%) as a mixture of regioisomers (1.4:1, C-3:C-7); **R_f**: 0.20 (40% CH₂Cl₂ in hexane, visualisation UV and KMnO₄); **IR (Neat)**: $\nu_{\text{max}}/\text{cm}^{-1}$ 2917, 1676, 1597, 1484, 1463, 1436, 1283, 1244, 1180, 1162, 1021, 982, 754, 727; **¹H NMR** (400 MHz, CDCl₃): δ (Major isomer) 7.75 – 7.68 (m, 1H), 7.56 – 7.49 (m, 1H), 7.48 – 7.41 (m, 1H), 7.32 – 7.19 (m, 2H), 7.03 – 6.93 (m, 3H), 4.45 (s, 2H), 3.96 (s, 3H), 2.56 (s, 3H); (Minor isomer) 7.75 – 7.68 (m, 1H), 7.59 (dd, J = 7.7, 1.8 Hz, 1H), 7.57 – 7.49 (m, 1H), 7.48 – 7.41 (m, 1H), 7.32 – 7.19 (m, 2H), 7.08 (dd, J = 7.3, 1.1 Hz, 1H), 7.03 – 6.93 (m, 1H), 4.52 (s, 2H), 3.91 (s, 3H), 2.57 (d, J = 1.2 Hz, 3H); **¹³C NMR** (101 MHz, CDCl₃): δ (all distinct resonances) 199.3 (C=O), 198.8 (C=O), 158.6 (C), 158.3 (C), 140.8 (C), 140.6 (C), 140.5 (C), 138.3 (C), 137.5 (C), 133.8 (CH), 133.5 (CH), 130.9 (CH), 130.4 (CH), 129.5 (C), 128.7 (C), 125.4 (C), 124.6 (CH), 124.1 (CH), 123.6 (CH), 122.4 (CH), 122.4 (CH), 121.4 (CH), 121.0 (CH), 120.9 (CH), 111.6 (CH), 111.5 (CH), 55.71 (CH₃), 55.67 (CH₃), 49.5 (CH₂), 41.5 (CH₂), 16.3 (CH₃), 14.2 (CH₃); **HRMS** (ESI) m/z: [M + H] Calcd for C₁₈H₁₇O₂S 297.0949; Found 297.0956.

160: 1-(3,5-Bis(trifluoromethyl)phenyl)-2-(5-chlorobenzo[b]thiophen-3-yl)ethan-1-one



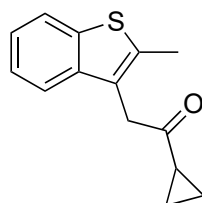
The title compound was prepared according to **GP3** using 5-chlorobenzothiophen S-oxide (55.4 mg, 0.30 mmol) and 1-ethynyl-3,5-bis-(trifluoromethyl)benzene (142 mg, 0.60 mmol) at 70 °C. The reaction was left for 15 h. Column chromatography (30% CH₂Cl₂ in hexane) followed by trituration with cold methanol (approx. 1 mL/mmol) afforded the product as a yellow amorphous solid (55.4 mg, 44%) as the single C-3 regioisomer; **R_f**: 0.30 (10% EtOAc in hexane, visualisation UV and KMnO₄); **mp**: 120 – 124 °C; **IR (Neat)**: $\nu_{\text{max}}/\text{cm}^{-1}$ 2924, 1698 (C=O stretch), 1320, 1278, 1129, 1077, 892, 697, 681; **¹H NMR** (400 MHz, CDCl₃) δ 8.48 (s, 2H), 8.10 (s, 1H), 7.79 (dd, *J* = 8.6 Hz, 1H), 7.68 (dd, *J* = 2.1 Hz, 1H), 7.40 (s, 1H), 7.36 (dd, *J* = 8.6 and 2.0 Hz, 1H), 4.55 (d, *J* = 0.8 Hz, 2H); **¹³C NMR** (101 MHz, CDCl₃) δ 193.4 (C=O), 139.8 (C), 138.6 (C), 137.8 (C), 132.9 (C-F, ²*J*_{C-F} = 34.0 Hz, C), 131.1 (C), 128.6 (CH), 127.4 (CH), 127.0 (C), 126.8 (C-F, ³*J*_{C-F} = 3.5 Hz, CH), 125.4 (CH), 124.2 (CH), 122.9 (C-F, ¹*J*_{C-F} = 273.2 Hz, C), 121.5 (CH), 38.8 (CH₂); **¹⁹F NMR** (376 MHz, CDCl₃): δ -62.9; **HRMS** (ASAP) *m/z*: [M] Calcd for C₁₈H₉ClF₆OS 412.9967; Found 421.9958.

161: 2-(3-(2-Methylbenzo[b]thiophen-3-yl)-2-oxopropyl)isoindoline-1,3-dione



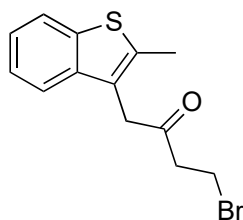
The title compound was prepared according to **GP3** using 2-methylbenzothiophen S-oxide (32.8 mg, 0.20 mmol) and 2-(prop-2-yn-1-yl)isoindoline-1,3-dione (37.1 mg, 0.20 mmol) at 50 °C. 2-Methylbenzothiophene S-oxide was consumed after 2h. Column chromatography (30% CH₂Cl₂ in hexane) followed by trituration with cold methanol (approx. 1 mL/mmol) afforded the product as a pale yellow amorphous solid (49.9 mg, 71%) as mixture of regioisomers (2.3:1, C-3:C-7); **R_f**: 0.30 (10% EtOAc in hexane, visualisation UV and KMnO₄); **mp**: 198 – 200 °C; **IR (Neat)**: $\nu_{\text{max}}/\text{cm}^{-1}$ 2934, 1772, 1715, 1411, 1311, 1195, 1068, 759, 715; **¹H NMR** (400 MHz, CDCl₃) δ 7.83 (dd, *J* = 5.6 and 3.0 Hz, 2H), 7.77 (d, *J* = 8.1, 1H), 7.72 (dd, *J* = 5.6 and 3.0 Hz, 2H), 7.60 (d, *J* = 7.9 Hz, 1H), 7.38 (ddd, *J* = 8.1, 7.2 and 1.2 Hz, 1H), 7.30 (ddd, *J* = 8.2, 7.2 and 1.2 Hz, 1H) 4.43 (s, 2H), 3.98 (s, 2H), 2.56 (s, 3H, Me); **¹³C NMR** (101 MHz, CDCl₃) δ 199.5 (C=O), 167.7 (C=O), 139.8 (C), 138.50 (C), 138.46 (C), 134.3 (CH), 132.2 (C), 124.7 (CH), 124.2 (CH), 123.6 (CH), 122.8 (C), 122.4 (CH), 121.0 (CH), 45.8, (CH₂) 38.9 (CH₂), 14.2 (CH₃); **HRMS** (ASAP) *m/z*: [M + H] Calcd for C₂₀H₁₆NO₃S 350.0851; Found: 350.0851.

162: 1-Cyclopropyl-2-(2-methylbenzo[b]thiophen-3-yl)ethan-1-one



The title compound was prepared according to **GP3** using 2-methylbenzothiophene S-oxide (65.8 mg, 0.40 mmol) and cyclopropylacetylene (68.0 μ l, 0.80 mmol) at 0 °C. The reaction was left for 10 h. Column chromatography (5% Et₂O in hexane) afforded the product as a yellow oil (79.8 mg, 87%) as a mixture of regioisomers (3.8:1, C-3:C-7); **R_f**: 0.31 (5% Et₂O in hexane, visualisation UV and KMnO₄); **IR (Neat)**: $\nu_{\text{max}}/\text{cm}^{-1}$ 3007, 2917, 1692 (C=O stretch), 1460, 1435, 1378, 1195, 1062, 899, 753, 728, 611; **¹H NMR** (400 MHz, CDCl₃): δ (Major isomer) 7.76 (ddd, $J = 7.7, 1.4$ and 0.7 Hz, 1H), 7.59 (d, $J = 7.5$ Hz, 1H), 7.40 – 7.24 (m, 2H), 3.94 (s, 2H), 2.54 (s, 3H), 1.90 (tt, $J = 7.8, 4.5$ Hz, 1H), 1.14 – 0.96 (m, 2H), 0.88 – 0.72 (m, 2H); (Minor isomer) 7.40 – 7.24 (m, 2H), 7.13 (d, $J = 7.8$ Hz, 1H), 7.01 (q, $J = 1.2$ Hz, 1H), 4.00 (s, 2H), 2.59 (d, $J = 1.3$ Hz, 3H), 2.06 – 1.94 (m, 1H), 1.14 – 0.96 (m, 2H), 0.88 – 0.72 (m, 2H); **¹³C NMR** (101 MHz, CDCl₃): δ (all distinct resonances for both regioisomers) 207.8 (C=O), 207.5 (C=O), 141.0 (C), 140.8 (C), 140.3 (C), 138.3 (C), 137.4 (C), 128.4 (C), 124.8 (CH), 124.7 (CH), 124.6 (C), 124.3 (CH), 123.9 (CH), 122.5 (CH), 122.3 (CH), 121.7 (CH), 121.2 (CH), 50.0 (CH₂), 41.8 (CH₂), 20.1 (CH₃), 19.6 (CH₃), 16.3 (CH) 14.2 (CH), 11.7 (CH₂), 11.5 (CH₂); **HRMS** (EI) m/z : [M] Calcd for C₁₄H₁₄OS 230.0765; Found 230.0766.

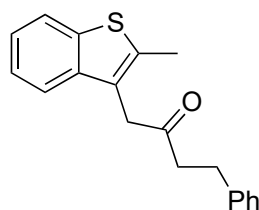
163: 4-Bromo-1-(2-methylbenzo[*b*]thiophen-3-yl)butan-2-one



The title compound was prepared according to **GP3** using 2-methylbenzothiophene S-oxide (82.1 mg, 0.50 mmol) and 4-bromobut-1-yne (94.0 μ l, 1.00 mmol) 0 °C. The reaction was left for 14 h. Column chromatography (0 – 30 % CH₂Cl₂ in hexane)

afforded the product as a pale yellow oil (123 mg, 83%) as a mixture of regioisomers (2.8:1, C-3:C-7); **R_f**: 0.35 (30% CH₂Cl₂) in hexane, visualisation UV and KMnO₄); **IR (Neat)**: $\nu_{\text{max}}/\text{cm}^{-1}$ 3058, 2916, 1712 (C=O stretch), 1434, 1408, 1070, 754, 728; **¹H NMR** (400 MHz, CDCl₃): δ (Major isomer) 7.77 (d, J = 7.3 Hz, 1H), 7.55 (d, J = 7.4 Hz, 1H), 7.39 – 7.23 (m, 2H), 3.87 (s, 2H), 3.55 – 3.44 (m, 2H), 2.96 (t, J = 6.7 Hz, 2H), 2.54 (s, 3H); (Minor isomer) 7.60 (d, J = 9.2 Hz, 1H), 7.39 – 7.23 (m, 1H), 7.11 (d, J = 7.9 Hz, 1H), 7.02 (q, J = 1.2 Hz, 1H), 3.90 (s, 2H), 3.51 (t, J = 6.8 Hz, 2H), 3.04 (t, J = 6.8 Hz, 2H), 2.60 (d, J = 1.2 Hz, 3H); **¹³C NMR** (101 MHz, CDCl₃): δ (all distinct resonances for both regioisomers) 204.5 (C=O), 204.4 (C=O), 141.2 (C), 141.0 (C), 140.1 (C), 139.9 (C), 138.4 (C), 138.0 (C), 127.4 (C), 125.0 (CH), 124.8 (CH), 124.6 (CH), 124.1 (CH), 123.4 (C), 122.5 (CH), 122.4 (CH), 122.1 (CH), 121.0 (CH), 49.7 (CH₂), 44.4 (CH₂), 44.0 (CH₂), 41.7 (CH₂), 25.4 (CH₂), 25.3 (CH₂), 16.3 (CH₃) 14.2 (CH₃); **HRMS** (ESI) m/z : [M + Na]⁺ Calcd for C₁₃H₁₃⁷⁹BrNaOS 318.9763; Found 318.9763.

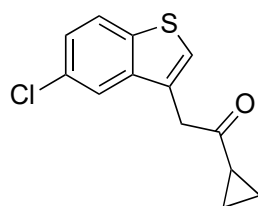
164: 1-(2-Methylbenzo[*b*]thiophen-3-yl)-4-phenylbutan-2-one



The title compound was prepared according to **GP3** using 2-methylbenzothiophene S-oxide (82.1 mg, 0.50 mmol) and 4-phenylbut-1-yne (141 μ l, 1.00 mmol) at 0 °C. 2-Methylbenzothiophene S-oxide was consumed after 6 h. Column chromatography (0 – 30% CH₂Cl₂ in hexane) afforded the product as a pale yellow oil (129 mg, 88%) as a mixture of regioisomers (2.5:1, C-3:C-7); **R_f**: 0.34 (30% CH₂Cl₂ in hexane, visualisation UV and KMnO₄); **IR (Neat)**: $\nu_{\text{max}}/\text{cm}^{-1}$ 3061, 2917, 1709 (C=O stretch),

1435, 1085, 751, 729, 698; **¹H NMR** (400 MHz, CDCl₃): δ (Major isomer) 7.75 (d, *J* = 7.2 Hz, 1H), 7.50 (d, *J* = 7.5, 1H), 7.36 – 7.20 (m, 4H), 7.19 – 7.03 (m, 3H), 3.80 (s, 2H), 2.93 – 2.65 (m, 4H), 2.47 (s, 3H); (Minor isomer) δ 7.57 (d, *J* = 8.9 Hz, 1H), 7.36 – 7.03 (m, 7H), 7.00 (q, *J* = 1.3 Hz, 1H), 3.86 (s, 2H), 2.90 – 2.68 (m, 4H), 2.59 (d, *J* = 1.2 Hz, 3H); **¹³C NMR** (101 MHz, CDCl₃): δ (all distinct resonances for both regioisomers) 206.8 (C=O), 206.7 (C=O), 140.9 (C), 140.1 (C), 138.3 (C), 137.5 (C), 128.59 (CH), 128.56 (CH), 128.5 (CH), 128.4 (CH), 128.1 (C), 126.3 (CH), 126.1 (CH), 124.9 (CH), 124.7 (CH), 124.4 (CH), 124.1 (C), 124.0 (CH), 122.5 (CH), 122.3 (CH), 121.8 (CH), 121.2 (CH), 50.0 (CH₂), 43.5 (CH₂), 43.0 (CH₂), 41.6 (CH₂), 29.9 (CH₂), 16.3 (CH₃), 14.2 (CH₃); **HRMS** (EI) *m/z*: [M] Calcd for C₁₉H₁₈OS 294.1078; Found 294.1080.

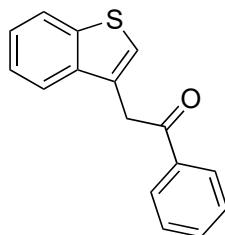
165: 2-(5-Chlorobenzo[*b*]thiophen-3-yl)-1-cyclopropylethan-1-one



The title compound was prepared according to **GP3** using 5-chlorobenzothiophene S-oxide (36.5 mg, 0.20 mmol) and cyclopropylacetylene (34.0 μl, 0.40 mmol) at 0 °C. The reaction was left for 15 h. Column chromatography (10% EtOAc in hexane) afforded the product as a low melting point pale yellow amorphous solid (25.0 mg, 50%) as a mixture of regioisomers (7.8:1, C-3:C-7); **R_f**: 0.30 (10% EtOAc in hexane, visualisation UV and KMnO₄); **mp**: 45 – 50°C; **IR (Neat)**: $\nu_{\text{max}}/\text{cm}^{-1}$ 3007, 2923, 1692 (C=O stretch), 1585, 1420, 1378, 1068, 1009, 898, 829, 772, 753, 728; **¹H NMR** (400 MHz, CDCl₃): δ 7.77 (dd, *J* = 8.5 and 0.5 Hz, 1H), 7.66 (*J* = 2.0 Hz, 1H), 7.38 (q, *J* = 0.8 Hz, 1H), 7.32 (ddd, *J* = 8.6, 2.0 and 0.5 Hz, 1H), 4.02

(d, $J = 0.8$ Hz, 2H), 2.02 (tt, $J = 7.8$ and 4.5 Hz, 1H), 1.13 – 1.04 (m, 2H), 0.95 – 0.83 (m, 2H); ^{13}C NMR (101 MHz, CDCl_3): δ 207.1 (C=O), 140.2 (C), 138.5 (C), 130.9 (C), 128.6 (C), 126.6 (CH), 125.1 (CH), 124.0 (CH), 121.6 (CH), 43.5 (CH_2), 20.2 (CH_2), 11.8 (CH_3); HRMS (EI) m/z : [M] Calcd for $\text{C}_{13}\text{H}_{11}\text{OSCl}$ 250.0219; Found 250.0220.

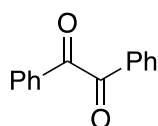
166: 2-(Benzo[b]thiophen-3-yl)-1-phenylethan-1-one



Benzothiophene (67.4 mg, 0.50 mmol) was stirred in CH_2Cl_2 (1 mL) and TFA (1 mL) in a round-bottom flask at rt. H_2O_2 (30% aq, 52.0 μl) was added and the reaction was left to stir for 30 min, before checking consumption of benzothiophene by TLC. If benzothiophene was not consumed, H_2O_2 was added in small amounts (~5 – 10 μl each time) until benzothiophene was consumed (after addition of each portion of H_2O_2 , the reaction was left to stir for 30 min before checking the reaction progress by TLC to prevent over-oxidation to sulfone). When the reaction was complete, the solution was cooled to 0 °C and quenched with NaHCO_3 until there was no further effervescence. H_2O (10 mL) was added and the aqueous layer was extracted with CH_2Cl_2 (3 \times 10 mL), dried (Na_2SO_4) and filtered. The solvent was removed under reduced pressure in a 25 °C water bath to a minimum amount of CH_2Cl_2 (approx. 2 mL/mmol). At this point fluorobenzene was added to the solution (5 mL), and the remaining CH_2Cl_2 was removed under reduced pressure in a 25 °C water bath. Phenylacetylene was added to the solution (110 μl , 1.00 mmol) followed by $[\text{DTBPAuNCPH}]\text{SbF}_6$ (28.0 mg, 5 mol%) and the reaction was stirred for 16 h at 0 °C.

Column chromatography (0 – 40 % CH₂Cl₂ in hexane) afforded the product as a yellow viscous oil that solidified upon standing. Trituration with methanol afforded the product as a white crystalline solid (98.4 mg, 79%) as a mixture of regioisomers (9.4:1, C-3:C-7); **R_f**: 0.34 (10% EtOAc in hexane, visualisation UV and KMnO₄); **mp**: 103 – 105 °C; **IR (Neat)**: $\nu_{\text{max}}/\text{cm}^{-1}$; 2892, 1684 (C=O stretch), 1594, 1331, 1208, 979, 753, 688; **¹H NMR** (400 MHz, CDCl₃) δ 8.08 – 8.03 (m, 2H), 7.88 – 7.83 (m, 1H), 7.77 – 7.73 (m, 1H), 7.58 (tt, $J = 8.1$ and 1.3 Hz, 1H), 7.48 (*app. t*, $J = 7.8$ Hz, 2H), 7.44 – 7.32 (m, 2H), 7.28 (q, $J = 1.0$ Hz, 1H), 4.51 (d, $J = 1.0$ Hz, 2H); **¹³C NMR** (101 MHz, CDCl₃) δ 196.8 (C=O), 140.4 (C), 138.9 (C), 136.6 (C), 133.5 (CH), 129.1 (C), 128.9 (CH), 128.7 (CH), 124.7 (CH), 124.6 (CH), 124.4 (CH), 123.0 (CH), 121.9 (CH), 38.7 (CH₂); **HRMS** (ASAP) m/z : [M + H] Calcd for C₁₆H₁₃OS 253.0687; Found 253.0695.

170: Benzil



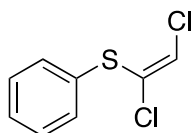
2-Methylbenzothiophene S-oxide (82.1 mg, 0.50 mmol) was added to a round-bottom flask and dissolved in fluorobenzene (5 ml). Diphenylacetylene (178 μl , 1.00 mmol) was added to the solution and the solution was cooled to 0 °C. [DTBPAuNCPPh]SbF₆ (29.5 mg, 5 mol%) was added to the solution and the reaction was stirred at 0 °C for 24 h. The solution was allowed to reach rt. before CH₂Cl₂ (2.5 mL) was added to the reaction mixture and the solution was filtered through a short pad of celite. The celite was then washed with EtOAc (3 \times 2.5 mL). The solution was concentrated under reduced pressure and purified by flash column chromatography (hexane), affording the product as an amorphous white solid (51.7 mg, 98%); **¹H NMR** (300 MHz, CDCl₃): δ

7.98 (dd, $J = 8.4, 1.4$ Hz, 4H), 7.66 (tt, $J = 7.4$ and 1.3 Hz, 2H), 7.52 (t, $J = 7.6$ Hz, 4H).

Data matched that reported in the literature.¹⁹

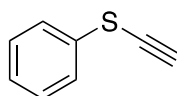
4.6 Alkynyl Thioethers and Thiosulfonates

319: (*E*) –(1,2-Dichlorovinyl)(phenyl)sulfane



Compound **319** was prepared according to a literature procedure.^{61a} Thiophenol (2.03 mL, 20.0 mmol) was dissolved in DMSO (20 mL) in a round-bottom flask. NaOH (2.00 g, 50.0 mmol) was added to the solution, followed by H₂O (10 mL), and the resulting solution was stirred for 16 h at rt. The solution was cooled to 0 °C and stirred vigorously while trichloroethylene (2.70 mL, 30.0 mmol) was added via syringe pump over 1 h. Following the addition of trichloroethylene, the solution was warmed to rt and stirred vigorously for a further 2h. The resulting mixture was diluted with H₂O (10 mL), extracted with Et₂O (2 × 15 mL), washed with H₂O (3 × 10 mL), dried (Na₂SO₄), filtered and concentrated under reduced pressure. The product was purified by flash column chromatography (hexane) to afford the product as a yellow oil (3.20 g, 78%); **IR (Neat)**: $\nu_{\text{max}}/\text{cm}^{-1}$ 3062, 1582, 1476, 1440, 1249, 1024, 912, 813, 739, 687; **¹H NMR** (300 MHz, CDCl₃) δ 7.50 – 7.40 (m, 2H), 7.41 – 7.33 (m, 3H), 6.58 (s, 1H); **HRMS** (ASAP+) m/z : [M + H] Calcd for C₈H₇Cl₂S 204.9646; Found 204.9640. Data matches that reported in the literature.^{61b}

320: Ethynyl(phenyl)sulfane



Method One:

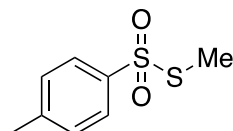
The title compound was prepared according to a literature procedure.^{61a} (*E*)-(1,2-Dichlorovinyl)(phenyl)sulfane (1.51 g, 7.35 mmol) was dissolved in THF (37 mL) in a heat-gun dried round-bottom flask under argon and the solution was stirred at $-78\text{ }^{\circ}\text{C}$. *n*-BuLi (18.4 mL, 29.4 mmol) was added to the solution over 15 min. The solution was stirred at $-78\text{ }^{\circ}\text{C}$ for 2 h and then quenched with aqueous NH_4Cl (sat.) (20 mL), extracted with Et_2O ($3 \times 20\text{ mL}$), dried (Na_2SO_4), filtered and concentrated under reduced pressure. The product was purified by flash column chromatography (hexane) to afford the product as a yellow oil (830 mg, 84%).

Method Two:

The title compound was prepared according to a literature procedure.⁹⁸ Ethynyltrimethylsilane (1.12 mL, 8.00 mmol) was dissolved in THF (32 mL) in a heat-gun dried round-bottom flask under argon and the solution was stirred to $-78\text{ }^{\circ}\text{C}$. *n*-BuLi (5.50 mL, 8.80 mmol) was added to the solution over 10 min and the solution was stirred at $-78\text{ }^{\circ}\text{C}$ for 1 h. *S*-Phenyl 4-methylbenzenethiosulfonate (2.33 g, 8.80 mmol) was dissolved in THF (8 mL) and added as a solution to the reaction mixture via syringe. The resulting solution was warmed to $0\text{ }^{\circ}\text{C}$ and stirred for 1h, then further warmed to rt and stirred for 1h. The reaction mixture was quenched with aqueous NH_4Cl (sat.) (20 mL), extracted with Et_2O ($3 \times 20\text{ mL}$), dried (Na_2SO_4), filtered and concentrated under reduced pressure. The crude residue was purified by flash column chromatography (hexane) to afford trimethyl(phenylthioethynyl)silane which was further dissolved in a mixture of CH_2Cl_2 : MeOH (v:v ; 1:1, 16 mL). K_2CO_3 (2.21 g, 16.0 mmol) was added, and the solution was stirred at rt for 16h. H_2O (15 mL) was added, and the product was extracted with CH_2Cl_2 ($3 \times 10\text{ mL}$), dried (Na_2SO_4) and filtered. The solvent was removed under reduced pressure to afford the product

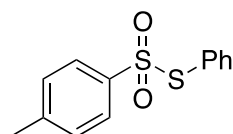
as a yellow oil (862 mg, 80%); **IR (Neat):** $\nu_{\text{max}}/\text{cm}^{-1}$ 3287, 2046, 1582, 1479, 1442, 1085, 1023, 737, 686; **$^1\text{H NMR}$** (300 MHz, CDCl_3) δ 7.46 – 7.40 (m, 2H), 7.35 – 7.29 (m, 2H), 7.26 – 7.19 (m, 1H), 3.23 (s, 1H); **HRMS** (ASAP+) m/z : [M] Calcd for $\text{C}_8\text{H}_6\text{S}$ 134.0190; Found 134.0187. Data matches that reported in the literature.⁶⁴

S-Methyl 4-methylbenzenethiosulfonate



The title compound was prepared according to a literature procedure.⁹⁹ Sodium *p*-toluenesulfinate (8.70 g, 43.0 mmol) and dimethyl disulfide (1.33 mL, 15.0 mmol) were dissolved in CH_2Cl_2 (400 mL) in a round-bottom flask. The solution was stirred vigorously at rt and iodine (3.80 g, 29.9 mmol) was added to the solution. The reaction was stirred for 20 h at rt. $\text{Na}_2\text{S}_2\text{O}_3$ (1 M, aq.) was added to the solution with stirring until the solution turned colourless. The organic layer was washed with H_2O (3 \times 50 mL), dried (Na_2SO_4), filtered and the solvent was removed under reduced pressure to afford the product as an off-white amorphous solid (3.56 g, 59%); **IR (Neat):** $\nu_{\text{max}}/\text{cm}^{-1}$ 2924, 1591, 1328, 1293, 1138, 1074, 809, 699, 653; **$^1\text{H NMR}$** (400 MHz, CDCl_3) δ 7.81 (d, J = 8.4 Hz, 2H), 7.35 (d, J = 8.0 Hz, 2H), 2.50 (s, 3H), 2.45 (s, 3H). Data matches that reported in the literature.⁹⁹

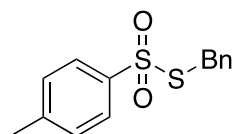
330: S-Phenyl 4-methylbenzenethiosulfonate



Compound **330** was prepared according to a literature procedure.⁹⁹ Sodium *p*-toluenesulfinate (5.77 g, 32.4 mmol) and diphenyl disulfide (2.36 g, 10.8 mmol) were

dissolved in CH₂Cl₂ (290 mL) in a round-bottom flask. The solution was stirred vigorously at rt and iodine (5.48 g, 21.6 mmol) was added to the solution. The reaction was stirred for 20 h at rt. Na₂S₂O₃ (1 M, aq.) was added to the solution with stirring until the solution turned colourless. The organic layer was washed with water (3 × 30 mL), dried (Na₂SO₄), filtered and the solvent was removed under reduced pressure to afford the product as an off-white amorphous solid (2.11 g, 74%); **IR (Neat):** $\nu_{\text{max}}/\text{cm}^{-1}$ 1591, 1327, 1137, 701, 685, 522; **¹H NMR** (400 MHz, CDCl₃) δ 7.49 – 7.41 (m, 3H), 7.40 – 7.31 (m, 4H), 7.20 (d, *J* = 7.9 Hz, 2H), 2.42 (s, 3H); **HRMS** (ASAP+) *m/z*: [M + H] Calcd for C₁₃H₁₃O₂S₂ 265.0357; Found 265.0362. Data matches that reported in the literature.⁹⁹

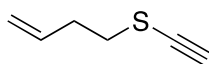
S-Benzyl 4-methylbenzenethiosulfonate



The title compound was prepared according to a literature procedure.¹⁰⁰ Sodium *p*-toluenesulfinate (4.26 g, 23.9 mmol) and dibenzyl disulfide (1.20 g, 4.89 mmol) were dissolved in CH₂Cl₂ (130 mL) in a round-bottom flask. The solution was stirred vigorously at rt and iodine (1.24 g, 9.78 mmol) was added to the solution. The reaction was stirred for 20 h at rt. Na₂S₂O₃ (1 M, aq.) was added to the solution with stirring until the solution turned colourless. The organic layer was washed with H₂O (3 × 20 mL), dried (Na₂SO₄), filtered and the solvent was removed under reduced pressure to afford the product as an off-white amorphous solid (2.11 g, 78%); **IR (Neat):** $\nu_{\text{max}}/\text{cm}^{-1}$ 1594, 1494, 1454, 1321, 1302, 1141, 1070, 776, 701; **¹H NMR** (400 MHz, CDCl₃) δ 7.75 (d, *J* = 8.3 Hz, 2H), 7.30 (dd, *J* = 8.6 and 0.7 Hz, 2H), 7.27 – 7.24 (m, 3H), 7.22 – 7.19 (m, 2H), 4.27 (s, 2H), 2.46 (s, 3H); **HRMS** (ASAP+)

m/z: [M + H] Calcd for C₁₄H₁₅O₂S₂ 279.0513; Found 279.0521. Data matches that reported in the literature.¹⁰¹

332: But-3-en-1-yl(ethynyl)sulfane



Ethynyltrimethylsilane (1.11 mL, 8.00 mmol) was dissolved in THF (40 mL) in a heat-gun dried round-bottom flask under argon and the solution was cooled to $-78\text{ }^{\circ}\text{C}$. n-BuLi (5.50 mL, 8.80 mmol) was added to the solution over 10 min and the solution was stirred at $-78\text{ }^{\circ}\text{C}$ for 1 h. Sulfur (257 mg, 8.00 mmol) was added and the solution turned a deep-red colour. The resulting solution was stirred for 1 h at $-78\text{ }^{\circ}\text{C}$ and was then warmed to $0\text{ }^{\circ}\text{C}$ at which point 4-bromo-1-butene (0.81 mL, 8.00 mmol) was added. The solution was stirred at $0\text{ }^{\circ}\text{C}$ for 2 h and was then allowed to reach rt and stirred for a further 16 h. The reaction mixture was quenched with aqueous NH₄Cl (sat.) (20 mL), extracted with Et₂O (3 × 20 mL), dried (Na₂SO₄), filtered and concentrated under reduced pressure. The crude residue was purified by flash column chromatography (hexane) to afford ((but-3-en-1-ylthio)ethynyl)trimethylsilane which was further dissolved in a mixture of CH₂Cl₂:MeOH (v:v ; 1:1, 16 mL). K₂CO₃ (2.21 g, 16.0 mmol) was added and the solution was stirred at rt for 16 h. H₂O (15 mL) was added and the product was extracted with CH₂Cl₂ (3 × 10 mL), dried (Na₂SO₄) and filtered. The solvent was removed under reduced pressure to afford the product as a yellow oil (486 mg, 54%); **IR (Neat):** $\nu_{\text{max}}/\text{cm}^{-1}$ 3293, 2959, 2930, 2042, 1640, 1436, 1280, 1224, 993, 917, 673; **¹H NMR** (300 MHz, CDCl₃) δ 5.83 (ddt, $J = 16.9, 10.2$ and 6.7 Hz, 1H), 5.18 – 5.05 (m, 2H), 2.82 – 2.76 (m, 2H), 2.54 – 2.47 (m, 2H), 1.55 (s, 1H); **¹³C NMR** (101 MHz, CDCl₃): δ 135.6, 117.1, 82.4,

74.4, 34.4, 33.4; **HRMS** (ES+) m/z : [M + H] Calcd for C₆H₉S 113.0425; Found 113.0421.

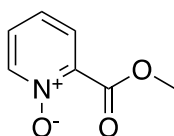
4.7 Pyridine *N*-Oxides

General Procedure 4 (GP4):

Based on an existing literature protocol.¹⁰²

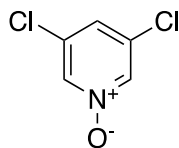
The pyridine or quinoline (1.0 eq) was dissolved in anhydrous CH₂Cl₂ (0.1 – 0.2 M) in a heat-gun dried round-bottom flask under argon and the solution was stirred at 0 °C. *m*CPBA (1.2 eq) was added to the solution portion-wise over 30 min. The reaction was warmed to rt and monitored by TLC. Upon completion, the reaction solution was quenched with aqueous NaHCO₃ (sat.) (~3 mL/mmol) and H₂O (~2 mL/mmol), extracted with CH₂Cl₂ (3 × 3 mL/mmol), dried (Na₂SO₄) and filtered. The solution was concentrated under reduced pressure and the product was purified by flash column chromatography.

451: 2-(Methoxycarbonyl)pyridine *N*-Oxide



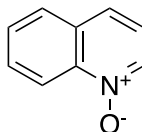
The title compound was prepared according to **GP4** using methyl picolinate (952 mg, 6.90 mmol) and *m*CPBA (1.43 mg, 8.30 mmol) in CH₂Cl₂ (35 mL). The product was purified by flash column chromatography (5% MeOH in EtOAc) to afford the product as an off-white solid (104 mg, 10%); **IR (Neat)**: $\nu_{\max}/\text{cm}^{-1}$ 3079, 2956, 1731, 1604, 1486, 1424, 1309, 1274, 1241, 1131, 1092, 854, 762, 670; **¹H NMR** (300 MHz, CDCl₃) δ 8.26 (ddd, J = 6.5, 1.3 and 0.6 Hz, 1H), 7.61 (dd, J = 7.9 and 2.1 Hz, 1H), 7.40 – 7.22 (m, 2H), 4.00 (s, 3H); **HRMS** (ASAP+) m/z : [M + H] Calcd for C₇H₈NO₃ 154.0504; Found 154.0511. Data matches that reported in the literature.¹⁰³

453: 3,5-Dichloropyridine *N*-Oxide



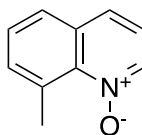
The title compound was prepared according to **GP4** using 3,5-dichloropyridine (592 mg, 4.00 mmol) and *m*CPBA (828 mg, 4.80 mmol) in CH₂Cl₂ (40 mL). The product was purified by flash column chromatography (100% EtOAc) to afford the product as a white amorphous solid (462 mg, 70%); **IR (Neat):** $\nu_{\text{max}}/\text{cm}^{-1}$ 3048, 1585, 1638, 1405, 1271, 1129, 1006, 961, 891, 821, 663; **¹H NMR** (300 MHz, CDCl₃) δ 8.14 (d, *J* = 1.6 Hz, 2H), 7.31 (t, *J* = 1.6 Hz, 1H). Data matches that reported in the literature.¹⁰⁴

454: Quinoline *N*-Oxide



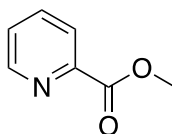
The title compound was prepared according to **GP4** using quinoline (355 mg, 3.00 mmol) and *m*CPBA (621 mg, 3.60 mmol) in CH₂Cl₂ (15 mL). The product was purified by flash column chromatography (5% MeOH in EtOAc) to afford the product as a brown solid (259 mg, 60%); **IR (Neat):** $\nu_{\text{max}}/\text{cm}^{-1}$ 3390, 1571, 1510, 1449, 1393, 1228, 1092, 882, 797, 768, 725; **¹H NMR** (300 MHz, CDCl₃) δ 8.76 (d, *J* = 8.8 Hz, 1H), 8.54 (dd, *J* = 6.0 and 1.0 Hz, 1H), 7.88 (d, *J* = 8.2 Hz, 1H), 7.82 – 7.71 (m, 2H), 7.65 (ddd, *J* = 8.2, 7.0 and 1.3 Hz, 1H), 7.30 (dd, *J* = 8.5 and 6.1 Hz, 1H); **HRMS** (CI⁺) *m/z*: [M + NH₄] Calcd for C₉H₁₁N₂O 163.0871; Found 163.0878. Data matches that reported in the literature.¹⁰⁵

458: 8-Methylquinoline N-Oxide



The title compound was prepared according to **GP4** using 8-methylquinoline (0.67 mL, 5.00 mmol) and *m*CPBA (1.04 mg, 6.00 mmol) in CH₂Cl₂ (50 mL). The product was purified by flash column chromatography (100% EtOAc) to afford the product as a brown oil (357 mg, 45%); **IR (Neat):** $\nu_{\text{max}}/\text{cm}^{-1}$ 2930, 1572, 1416, 1380, 1298, 1219, 1037, 975, 810, 798, 742, 726; **¹H NMR** (300 MHz, CDCl₃) δ 8.39 (d, *J* = 6.1 Hz, 1H), 7.69 – 7.59 (m, 2H), 7.47 – 7.36 (m, 2H), 7.22 – 7.12 (m, 1H), 3.18 (s, 3H). Data matches that reported in the literature.¹⁰⁶

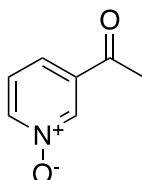
Methyl picolinate



The title compound was prepared according to a literature procedure.¹⁰⁷ Picolinic acid (615 mg, 5.00 mmol) and H₂SO₄ (0.65 mL) were dissolved in MeOH (10 mL) in a round-bottom flask fitted with a reflux condenser. The reaction was stirred and heated at 65 °C. The reaction was left for 24 h and was then cooled to rt. H₂O (10 mL) was added to the solution and K₂CO₃ was then added portion-wise until the reaction no longer effervesced. The product was extracted with EtOAc (3 × 10 mL), dried (Na₂SO₄), filtered and the solvent was removed under reduced pressure to afford the product as a crude oil (549 mg, 80%); **IR (Neat):** $\nu_{\text{max}}/\text{cm}^{-1}$ 2958, 1720, 1583, 1572, 1443, 1431, 1305, 1283, 1125, 745, 705, 696; **¹H NMR** (300 MHz, CDCl₃) δ 8.74 (dd, *J* = 4.7, 1.8 and 0.9 Hz, 1H), 8.13 (dd, *J* = 7.9 and 1.3 Hz, 1H), 7.84 (dt, *J* = 7.7 and 1.8 Hz, 1H), 7.47 (ddd, *J* = 7.6, 4.7 and 1.2 Hz, 1H), 4.00 (s, 3H);

HRMS (ES+) *m/z*: [M + H] Calcd for C₇H₈NO₂ 138.0555; Found 138.0565. Data matches that reported in the literature.¹⁰⁷

452: 3-Acetylpyridine *N*-Oxide

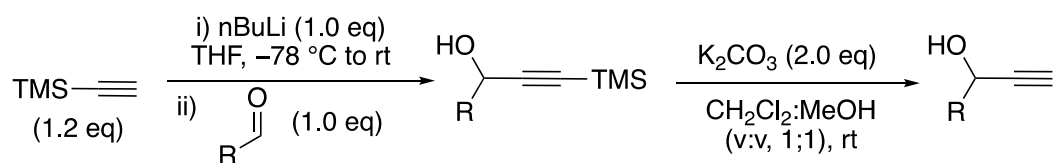


3-Acetylpyridine (0.88 mL, 8.00 mmol) was dissolved in CH₃Cl (80 mL) in a round-bottom flask fitted with a reflux condenser. *m*CPBA (3.40 g, 16.0 mmol) was added to the solution and the reaction was warmed gently to 60 °C over 1h, whilst stirring vigorously. The reaction was stirred for a further 2 h at 60 °C and was then allowed to cool to rt. The solution was then quenched with aqueous NaHCO₃ (sat.) (15 mL) and H₂O (15 mL), extracted with CH₂Cl₂ (2 × 15 mL) and dried (Na₂SO₄). The solvent was removed under reduced pressure and the product was purified by flash column chromatography (10% MeOH in EtOAc) to afford the product as a white solid (620 mg, 64%); **IR (Neat)**: $\nu_{\text{max}}/\text{cm}^{-1}$ 3026, 2923, 1687, 1561, 1418, 1276, 1215, 1010, 919, 812, 680; **¹H NMR** (300 MHz, CDCl₃) δ 8.72 (t, *J* = 1.7 Hz, 1H), 8.35 (ddd, *J* = 6.4, 1.8 and 1.1 Hz, 1H), 7.77 (dt, *J* = 8.0 and 1.2 Hz, 1H), 7.40 (dd, *J* = 8.0 and 6.5 Hz, 1H), 2.61 (s, 3H). Data matches that reported in the literature.¹⁰⁸

4.8 Propargyl Alcohols

General Procedure 5 (GP5):

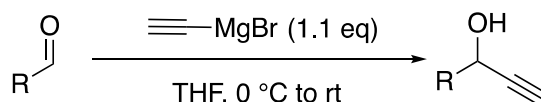
Based on an existing literature protocol.¹⁰⁹



Ethynyltrimethylsilane (1.2 eq) was dissolved in THF (1 M) in a heat-gun dried round-bottom flask under argon and the solution was cooled to $-78\text{ }^{\circ}\text{C}$. n-BuLi (1.0 eq) was added to the solution over 10 min and the solution was stirred at $-78\text{ }^{\circ}\text{C}$ for 2 h. The aldehyde (1.0 eq) was added to the solution and the reaction mixture was allowed to warm to rt. The reaction was monitored by TLC and upon completion the reaction mixture was quenched with aqueous NH_4Cl (sat.) ($\sim 2\text{ mL}/\text{mmol}$), extracted with Et_2O ($3 \times 2\text{ mL}/\text{mmol}$), dried (Na_2SO_4), filtered and concentrated under reduced pressure. The crude residue was purified by flash column chromatography and the resulting product was further dissolved in a mixture of CH_2Cl_2 :MeOH (v:v ; 1:1, 0.5 M). K_2CO_3 (2.0 eq) was added and the solution was stirred at rt for 16 h. H_2O (15 mL) was added and the product was extracted with CH_2Cl_2 ($3 \times 10\text{ mL}$), dried (Na_2SO_4), filtered and the solvent was removed under reduced pressure. The resulting residue was purified by flash column chromatography to afford the desired product.

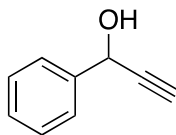
General Procedure 6 (GP6):

Based on an existing literature protocol.¹¹⁰



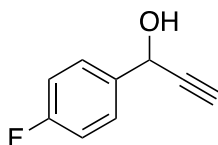
The aldehyde (1.0 eq) was dissolved in THF (0.5 M) in a heat-gun dried round-bottom flask and the solution was cooled to $0\text{ }^{\circ}\text{C}$. Ethynylmagnesium bromide solution (0.5 M in THF, 1.1 eq) was added to the solution and the reaction was stirred at $0\text{ }^{\circ}\text{C}$. The reaction was monitored by TLC and upon completion the reaction was quenched with aqueous NH_4Cl (sat.) ($\sim 2\text{ mL}/\text{mmol}$), extracted with EtOAc ($3 \times 2\text{ mL}/\text{mmol}$), dried (Na_2SO_4) and filtered. The solution was concentrated under a reduced pressure and the product was purified by flash column chromatography.

342: 1-Phenylprop-2-yn-1-ol



The title compound was prepared according to **GP5** using ethynyltrimethylsilane (0.83 mL, 6.00 mmol), n-BuLi (3.13 mL, 5.00 mmol) and benzaldehyde (0.51 mL, 5.00 mmol) in THF (5 mL). Column chromatography (10% EtOAc in hexane) afforded the TMS protected alkyne, which was deprotected with K₂CO₃ (1.38 g, 10.0 mmol). The resulting residue was further purified by column chromatography (10% EtOAc in hexane) to afford the product as a clear oil (536 mg, 81%); **IR (Neat):** $\nu_{\text{max}}/\text{cm}^{-1}$ 3288 (br, OH stretch), 2119, 1493, 1454, 1015, 944, 737, 696; **¹H NMR** (300 MHz, CDCl₃) δ 7.54 – 7.43 (m, 2H), 7.37 – 7.21 (m, 3H), 5.42 (dd, *J* = 6.1 and 2.2 Hz, 1H), 3.37 (d, *J* = 6.1 Hz, 1H), 2.60 (d, *J* = 2.2 Hz, 1H). Data matches that reported in the literature.¹¹¹

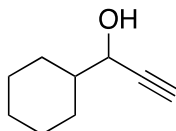
344: 1-(4-Fluorophenyl)prop-2-yn-1-ol



The title compound was prepared according to **GP5** using ethynyltrimethylsilane (2.50 mL, 18.0 mmol), n-BuLi (9.40 mL, 15.0 mmol) and 4-fluorobenzaldehyde (1.60 mL, 15.00 mmol) in THF (15 mL). Column chromatography (10% EtOAc in hexane) afforded the TMS protected alkyne which was deprotected with K₂CO₃ (4.14 g, 30.0 mmol). The resulting residue was further purified by column chromatography (10% EtOAc in hexane) to afford the product as a yellow oil (1.80 mg, 80%); **IR (Neat):** $\nu_{\text{max}}/\text{cm}^{-1}$ 3298 (br, OH stretch), 1604, 1508, 1222, 1158,

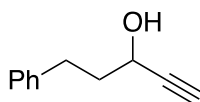
1013, 948, 834, 821, 772; **¹H NMR** (300 MHz, CDCl₃) δ 7.54 (dd, *J* = 8.3 and 5.2 Hz, 2H), 7.07 (*app. t*, *J* = 8.7 Hz, 2H), 5.46 (dd, *J* = 6.1 and 2.2 Hz, 1H), 2.69 (d, *J* = 2.2 Hz, 1H), 2.24 (d, *J* = 6.1 Hz, 1H). Data matches that reported in the literature.¹¹⁰

345: 1-Cyclohexylprop-2-yn-1-ol



The title compound was prepared according to **GP6** using cyclohexanecarbaldehyde (1.82 mL, 15.0 mmol) and ethynylmagnesium bromide (33.0 mL, 16.5 mmol) in THF (30 mL). Column chromatography (10% EtOAc in hexane) afforded the product as a yellow oil (1.64 g, 79%); **IR (Neat)**: $\nu_{\text{max}}/\text{cm}^{-1}$ 3309 (br, OH stretch), 2924, 2852, 1450, 1023, 980, 892; **¹H NMR** (400 MHz, CDCl₃) δ 4.16 (dd, *J* = 6.1 and 2.2 Hz, 1H), 2.46 (d, *J* = 2.2 Hz, 1H), 1.98- 1.83 (m, 2H), 1.82 – 1.74 (m, 3H), 1.72 – 1.63 (m, 1H), 1.62 – 1.52 (m, 1H), 1.30 – 1.01 (m, 5H). Data matches that reported in the literature.¹¹²

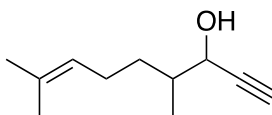
346: 5-Phenylpent-1-yn-3-ol



The title compound was prepared according to **GP6** using 3-phenylpropanal (1.06 mL, 8.00 mmol) and ethynylmagnesium bromide (17.6 mL, 8.80 mmol) in THF (16 mL). Column chromatography (10% EtOAc in hexane) afforded the product as an orange oil (938 mg, 73%); **IR (Neat)**: $\nu_{\text{max}}/\text{cm}^{-1}$ 3290 (br, OH stretch), 3062, 3027, 2926, 2863, 1603, 1496, 1454, 1040, 111, 744, 697; **¹H NMR** (400 MHz, CDCl₃) δ 7.33 – 7.25 (m, 2H), 7.24 – 7.16 (m, 3H), 4.36 (*app. qd*, *J* = 6.6 and 2.1 Hz, 1H), 2.80

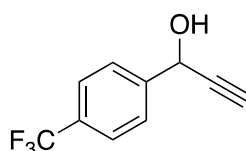
(t, $J = 7.8$ Hz, 2H), 2.50 (d, $J = 2.1$ Hz, 1H), 2.14 – 1.99 (m, 2H). Data matches that reported in the literature.¹¹³

347: 4,8-Dimethylnon-7-en-1-yn-3-ol



The title compound was prepared according to **GP6** using 2,6-dimethyl-5-heptenal (1.32 mL g, 8.00 mmol) and ethynylmagnesium bromide (17.6 mL, 8.80 mmol) in THF (16 mL). Column chromatography (10% EtOAc in hexane) afforded the product as a clear oil (1.03 g, 77%) as a mixture of diastereoisomers; **IR (Neat):** $\nu_{\text{max}}/\text{cm}^{-1}$ 3309 (br, OH stretch), 2966, 2917, 2857, 1452, 1377, 1082, 1035, 984, 742; **¹H NMR** (400 MHz, CDCl₃) δ (all distinct resonances for both isomers) 5.15 – 5.07 (m, 1H), 4.32 – 4.24 (m, 1H), 2.45 (*app.* t, $J = 2.4$ Hz, 1H), 2.15 – 1.90 (m, 2H), 1.82 – 1.73 (m, 1H), 1.69 (s, 3H), 1.61 (s, 3H), 1.64 – 1.50 (m, 1H), 1.33 – 1.19 (m, 1H), 1.02 and 1.01 (d, $J = 3.2$ Hz, 3H, 2 \times CH₃ from different diastereomers); **¹³C NMR** (101 MHz, CDCl₃) δ (all distinct resonances for both isomers) 131.93, 131.87, 124.5, 124.4, 84.1, 83.5, 74.0, 73.7, 66.9, 66.8, 38.9, 38.7, 32.7, 32.0, 25.9, 25.6, 25.5, 17.83, 17.82, 14.9, 14.4; **HRMS** (EI+) m/z : [M] Calcd for C₁₁H₁₈O 166.1358; Found 166.1358.

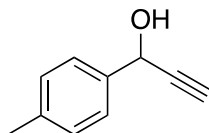
348: 1-(4-(Trifluoromethyl)phenyl)prop-2-yn-1-ol



The title compound was prepared according to **GP6** using 4-(trifluoromethyl)benzaldehyde (1.09 mL g, 8.00 mmol) and ethynylmagnesium bromide (17.6 mL, 8.80 mmol) in THF (16 mL). Column chromatography (10% EtOAc in hexane) afforded the product as an orange solid (1.48 g, 92%);

IR (Neat): $\nu_{\text{max}}/\text{cm}^{-1}$ 3308 (br, OH stretch), 1622, 1416, 1325, 1166, 1125, 1112, 1068, 1018, 948, 849; **$^1\text{H NMR}$** (300 MHz, CDCl_3) δ 7.73 – 7.61 (m, 4H), 5.53 (dd, $J = 6.1$ and 2.2 Hz, 1H), 2.71 (d, $J = 2.2$ Hz, 1H), 2.33 (d, $J = 6.1$ Hz, 1H). Data matches that reported in the literature.¹¹⁰

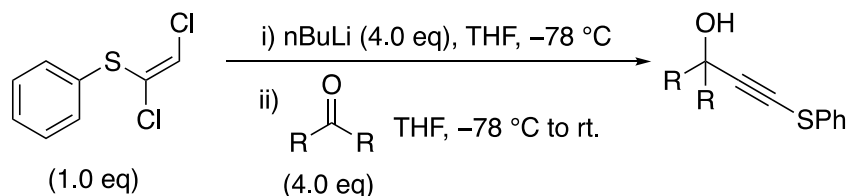
349: 1-(*p*-Tolyl)prop-2-yn-1-ol



The title compound was prepared according to **GP6** using *p*-tolualdehyde (0.95 mL, 8.00 mmol) and ethynylmagnesium bromide (17.6 mL, 8.80 mmol) in THF (16 mL). Column chromatography (10% EtOAc in hexane) afforded the product as a pale orange oil (910 mg, 78%); **IR (Neat):** $\nu_{\text{max}}/\text{cm}^{-1}$ 3288 (br, OH stretch), 1614, 1513, 1179, 1013, 944, 815, 760; **$^1\text{H NMR}$** (400 MHz, CDCl_3) δ 7.44 (d, $J = 8.0$ Hz, 2H), 7.20 (d, $J = 8.0$ Hz, 2H), 5.44 (dd, $J = 6.1$ and 2.3 Hz, 1H), 2.66 (d, $J = 2.2$ Hz, 1H), 2.36 (s, 3H), 2.18 (dd, $J = 6.1$ Hz, 1H); **HRMS** (EI+) m/z : [M] Calcd for $\text{C}_{10}\text{H}_{10}\text{O}$ 146.0732; Found 146.0743. Data matches that reported in the literature.¹¹⁴

4.9 Sulfenylated Propargyl Alcohols

General Procedure 7 (GP7):

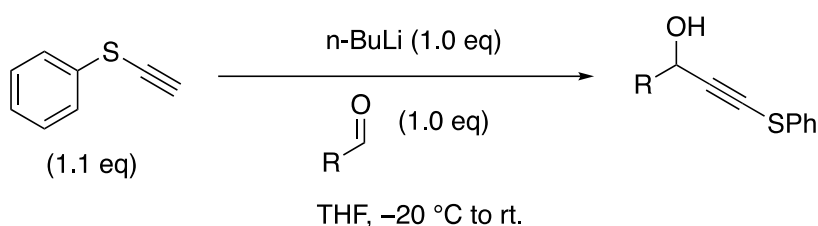


(*E*)-(1,2-Dichlorovinyl)(phenyl)sulfane **319** (1.0 eq) was dissolved in THF (0.2 M) in a heat-gun dried round-bottom flask and the solution was cooled to -78 °C. *n*-BuLi (4.0 eq) was added to the solution dropwise over 10 min and the reaction was stirred

at $-78\text{ }^{\circ}\text{C}$ for 1 h. The aldehyde or ketone (4.0 eq) was added to the solution and the reaction mixture was left to reach rt and stirred for 16 h. The reaction mixture was quenched with aqueous NH_4Cl (sat.) ($\sim 5\text{ mL}/\text{mmol}$), extracted with EtOAc ($3 \times 5\text{ mL}/\text{mmol}$), dried (Na_2SO_4), filtered, concentrated under reduced pressure and purified by flash column chromatography.

General Procedure 8 (GP8):

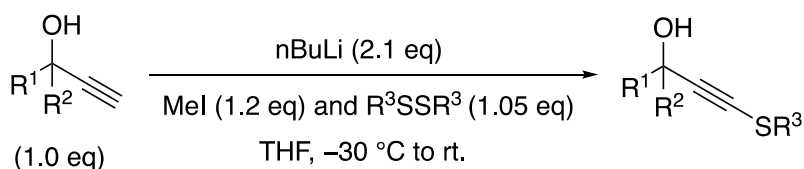
Based on an existing literature protocol.⁶⁵



Ethynyl(phenyl)sulfane **320** (1.1 eq) was stirred in THF (0.5 M) in a heat-gun dried round-bottom flask at $-20\text{ }^{\circ}\text{C}$. $n\text{-BuLi}$ (1.0 eq) was added to the solution dropwise over 10 min and the solution was stirred for 1 h at $-20\text{ }^{\circ}\text{C}$. The aldehyde was added to the reaction mixture and the solution was stirred at $-20\text{ }^{\circ}\text{C}$. The reaction was monitored by TLC. Upon completion, the reaction mixture was quenched with NH_4Cl ($\sim 2\text{ mL}/\text{mmol}$), extracted with EtOAc ($3 \times 2\text{ mL}/\text{mmol}$), dried (Na_2SO_4), filtered, concentrated under reduced pressure and purified by flash column chromatography.

General Procedure 9 (GP9):

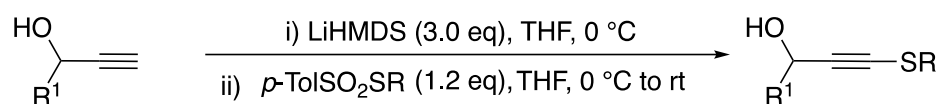
Based on an existing literature protocol.⁶⁸



The disulfide (1.05 eq) was dissolved in THF (0.5 M) in a heat-gun dried round-bottom flask under argon. Methyl iodide (1.2 eq) was added and the solution was stirred at rt

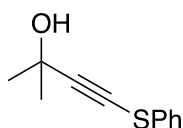
for 2 h. In a separate heat-gun dried round-bottom flask, the propargyl alcohol (1.0 eq) was stirred in THF (0.5 M) at $-30\text{ }^{\circ}\text{C}$. $n\text{-BuLi}$ (2.1 eq) was added to the solution of propargyl alcohol and the reaction mixture was stirred for 30 min at $-30\text{ }^{\circ}\text{C}$. The solution of disulfide and methyl iodide was transferred to the solution of propargyl alcohol at $-30\text{ }^{\circ}\text{C}$ via syringe, and the resulting solution was warmed to rt and stirred. The reaction was monitored by TLC. Upon completion, the reaction mixture was quenched with aqueous NH_4Cl (sat.) ($\sim 2\text{ mL}/\text{mmol}$), extracted with EtOAc ($3 \times 2\text{ mL}/\text{mmol}$), dried (Na_2SO_4), filtered, concentrated under reduced pressure and purified by flash column chromatography.

General Procedure 10 (GP10):



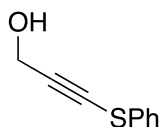
The propargyl alcohol (1.0 eq) was stirred in THF (0.5 M) in a heat-gun dried round-bottom flask at $0\text{ }^{\circ}\text{C}$. LiHMDS (1 M in THF, 3.0 eq) was added to the solution dropwise over 5 minutes. The solution was stirred at $0\text{ }^{\circ}\text{C}$ for 1 h. The thiosulfonate (1.2 – 1.5 eq) was added to the reaction mixture as a solution in THF (0.5 M). The reaction mixture was then warmed to rt and stirred. After 2-3 h an aliquot was taken of the reaction mixture for ^1H NMR spectroscopic analysis. If any propargyl alcohol starting material was present in the ^1H NMR spectrum, the solution was cooled down to $0\text{ }^{\circ}\text{C}$ and more LiHMDS was added (0.5 eq each time). The solution was warmed to rt and stirred for a further 2-3 h. This process was repeated until the propargyl alcohol was consumed. Upon completion, the reaction mixture was quenched with NH_4Cl ($\sim 2\text{ mL}/\text{mmol}$), extracted with EtOAc ($3 \times 2\text{ mL}/\text{mmol}$), dried (Na_2SO_4), filtered, concentrated under reduced pressure and purified by flash column chromatography.

323: 2-Methyl-4-(phenylthio)but-3-yn-2-ol

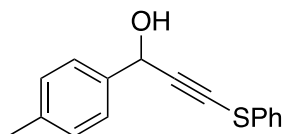


The title compound was prepared according to **GP7** using (*E*)-(1,2-Dichlorovinyl)(phenyl)sulfane **319** (1.03 g, 5.00 mmol), n-BuLi (12.5 mL, 20.0 mmol) and acetone (1.42 mL, 20.0 mmol) in THF (25 mL). Column chromatography (10% EtOAc in hexane) afforded the product as a clear oil (818 mg, 85%); **IR (Neat)**: $\nu_{\text{max}}/\text{cm}^{-1}$ 3360 (br, OH stretch), 2982, 1585, 1479, 1441, 1162, 929, 738; **¹H NMR** (300 MHz, CDCl₃) δ 7.44 – 7.40 (m, 2H), 7.39 – 7.34 (m, 2H), 7.22 (tt, $J = 7.5$ and 1.5 Hz, 1H), 2.00 (s, br, 1H), 1.62 (s, 6H); **HRMS** (ASAP+) m/z : [M + H] Calcd for C₁₁H₁₃OS: 193.0687, found 193.0690. Data matches that reported in the literature.¹¹⁵

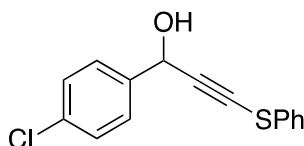
324: 3-(Phenylthio)prop-2-yn-1-ol



The title compound was prepared according to **GP7** using (*E*)-(1,2-dichlorovinyl)(phenyl)sulfane **319** (381 mg, 1.87 mmol), n-BuLi (4.70 mL, 7.48 mmol) and paraformaldehyde (224 mg, 7.48 mmol) in THF (9.4 mL). Column chromatography (10% EtOAc in hexane) afforded the product as a clear oil (277 mg, 88%); **¹H NMR** (300 MHz, CDCl₃) δ 7.46 – 7.40 (m, 2H), 7.38 – 7.30 (m, 2H), 7.27 – 7.20 (m, 1H), 4.51 (s, 2H); **HRMS** (ES+) m/z : [M + H] Calcd for C₉H₉OS 165.0374; Found 165.0371. Data matches that reported in the literature.¹¹⁶

325: 3-(Phenylthio)-1-(*p*-tolyl)prop-2-yn-1-ol

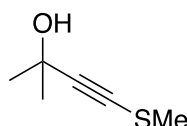
The title compound was prepared according to **GP8** using ethynyl(phenyl)sulfane **320** (355 mg, 2.64 mmol), *n*-BuLi (1.47 mL, 2.36 mmol) and *p*-tolualdehyde (278 μ L, 2.36 mmol) in THF (5.2 mL). Column chromatography (10% EtOAc in hexane) afforded the product as a red oil (322 mg, 54%); **IR (Neat)**: $\nu_{\text{max}}/\text{cm}^{-1}$ 3335 (br, OH stretch), 2919, 2183, 1581, 1478, 1441, 1062, 1023, 978, 818, 736, 686; **$^1\text{H NMR}$** (400 MHz, CDCl_3) δ 7.46 (d, $J = 8.1$ Hz, 2H), 7.44 – 7.40 (m, 2H), 7.33 (*app. t*, $J = 7.7$ Hz, 2H), 7.26 – 7.18 (m, 3H), 5.66 (s, 1H), 2.38 (s, 3H); **$^{13}\text{C NMR}$** (101 MHz, CDCl_3) δ 138.6 (C), 137.5 (C), 132.4 (C), 129.5 (CH), 129.4 (CH), 126.82 (CH), 126.75 (CH), 126.6 (CH), 98.6 (C), 73.9 (C), 65.6 (CH), 21.3 (CH_3); **HRMS** (CI+) m/z : [M] Calcd for $\text{C}_{16}\text{H}_{14}\text{OS}$ 254.0765; Found 254.0771.

331: 1-(4-Chlorophenyl)-3-(phenylthio)prop-2-yn-1-ol

The title compound was prepared according to **GP8** using ethynyl(phenyl)sulfane **320** (402 mg, 3.00 mmol), *n*-BuLi (1.88 mL, 2.73 mmol) and 4-chlorobenzaldehyde (384 mg, 2.73 mmol) in THF (6 mL). Column chromatography (10% EtOAc in hexane) afforded the product as a red oil (637 mg, 85%); **IR (Neat)**: $\nu_{\text{max}}/\text{cm}^{-1}$ 3059 (br, OH stretch), 2959, 2868, 2182, 1582, 1478, 1244, 1066, 998, 802, 776, 736; **$^1\text{H NMR}$** (400 MHz, CDCl_3) δ 7.51 (d, $J = 8.8$ Hz, 2H), 7.44 – 7.31 (m, 6H), 7.28 – 7.22 (tt, $J = 7.2$ and 2.0 Hz, 1H), 5.67 (s, 1H); **$^{13}\text{C NMR}$** (101 MHz, CDCl_3) δ 138.8 (C), 134.5

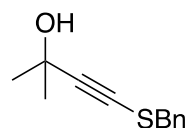
(C), 132.1 (C), 129.5 (CH), 129.0 (CH), 128.1 (CH), 127.0 (CH), 126.7 (CH), 97.8 (C), 74.8 (C), 64.9 (CH); **HRMS** (ASAP+) m/z: [M – OH] Calcd for C₁₅H₁₀SCI 257.0192; Found 257.0198.

335: 2-Methyl-4-(methylthio)but-3-yn-2-ol



The title compound was prepared according to **GP9** using 2-methyl-3-butyn-2-ol (0.58 mL, 6.00 mmol), n-BuLi (7.90 mL, 12.6 mmol), dimethyl disulfide (0.56 mL, 6.30 mmol) and methyl iodide (0.45 mL, 7.20 mmol) in THF (12 mL + 12 mL). Column chromatography (20% EtOAc in hexane) afforded the product as a clear oil (571 mg, 73%); **IR (Neat):** $\nu_{\text{max}}/\text{cm}^{-1}$ 3353 (br, OH stretch), 2980, 2172, 1495, 1455, 1363, 1221, 1160, 978, 926, 806, 765, 697; **¹H NMR** (400 MHz, CDCl₃) δ 2.36 (s, 3H), 1.52 (s, 6H); **¹³C NMR** (101 MHz, CDCl₃) δ 97.0 (C), 74.2 (C), 66.1 (C), 31.5 (CH₃), 19.3 (CH₃); **HRMS** (CI+) m/z: [M + H] Calcd for C₆H₁₁OS 131.0531; Found 131.0528.

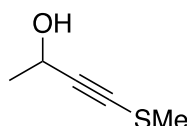
336: 4-(Benzylthio)-2-methylbut-3-yn-2-ol



The title compound was prepared according to **GP9** using 2-methyl-3-butyn-2-ol (0.34 mL, 3.50 mmol), n-BuLi (2.94 mL, 7.35 mmol), dibenzyl disulfide (904 mg, 3.68 mmol) and methyl iodide (261 μ L, 4.20 mmol) in THF (7 mL + 7 mL). Column chromatography (20% EtOAc in hexane) afforded the product as a clear oil (519 mg, 72%); **IR (Neat):** $\nu_{\text{max}}/\text{cm}^{-1}$ 3367 (br, OH stretch), 2980, 2930, 1495, 1455, 1363, 1221, 1161, 979, 927, 806, 765, 698; **¹H NMR** (400 MHz, CDCl₃) δ 7.39 – 7.26

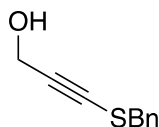
(m, 5H), 3.90 (s, 2H), 1.46 (s, 6H); ^{13}C NMR (101 MHz, CDCl_3) δ 136.7 (C), 129.3 (CH), 128.7 (CH), 127.9 (CH), 100.1 (C), 72.3 (C), 66.0 (C), 40.1 (CH_2), 31.4 (CH_3); **HRMS** (Cl^+) m/z : $[\text{M} + \text{NH}_4]$ Calcd for $\text{C}_{12}\text{H}_{18}\text{NOS}$ 224.1109; Found 224.1097.

337: 4-(Methylthio)but-3-yn-2-ol



The title compound was prepared according to **GP9** using 3-butyn-2-ol (0.63 mL, 8.00 mmol), $n\text{-BuLi}$ (10.5 mL, 16.8 mmol), dimethyl disulfide (0.75 mL, 8.40 mmol) and methyl iodide (0.53 mL, 8.40 mmol) in THF (16 mL + 16 mL). Column chromatography (20% EtOAc in hexane) afforded the product as a pale yellow oil (376 mg, 41%); **IR** (Neat): $\nu_{\text{max}}/\text{cm}^{-1}$ 3334 (br, OH stretch), 2982, 2930, 2182, 1421, 1370, 1313, 1123, 1075, 1048, 959, 860; ^1H NMR (400 MHz, CDCl_3) δ 4.60 (q, $J = 6.6$ Hz, 1H), 2.37 (s, 3H), 1.92 (s, br, 1H), 1.45 (d, $J = 6.6$ Hz, 3H); ^{13}C NMR (101 MHz, CDCl_3) δ 94.6 (C), 76.3 (C), 59.3 (CH), 24.4 (CH_3), 19.2 (CH_3); **HRMS** (EI^+) m/z : $[\text{M}]$ Calcd for $\text{C}_5\text{H}_8\text{OS}$ 116.0296; Found 116.0312.

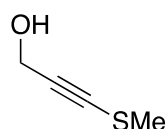
338: 3-(Benzylthio)prop-2-yn-1-ol



The title compound was prepared according to **GP9** using 2-propyn-1-ol (289 μL , 5.00 mmol), $n\text{-BuLi}$ (4.30 mL, 10.5 mmol), dibenzyl disulfide (1.30 g, 5.25 mmol) and methyl iodide (374 μL , 6.00 mmol) in THF (10 mL + 10 mL). Column chromatography (20% EtOAc in hexane) afforded the product as an orange oil (79.0 mg, 9%); **IR** (Neat): $\nu_{\text{max}}/\text{cm}^{-1}$ 3334 (br, OH stretch), 3062, 2183, 1495, 1454, 1237, 1060, 989, 765, 696, 660; ^1H NMR (400 MHz, CDCl_3) δ 7.38 – 7.27 (m, 5H),

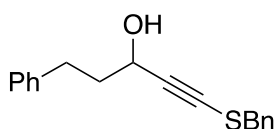
4.32 (s, 2H), 3.94 (s, 2H); $^{13}\text{C NMR}$ (101 MHz, CDCl_3) δ 136.6 (C), 129.2 (CH), 128.7 (CH), 127.9 (CH), 94.1 (C), 76.7 (C), 52.1 (CH_2), 40.3 (CH_2); **HRMS** (CI+) m/z : [M] Calcd for $\text{C}_{10}\text{H}_{10}\text{OS}$ 178.0452; Found 178.0455.

339: 3-(Methylthio)prop-2-yn-1-ol



The title compound was prepared according to **GP9** using 2-propyn-1-ol (0.35 mL, 6.00 mmol), $n\text{-BuLi}$ (7.90 mL, 12.6 mmol), dimethyl disulfide (0.56 mL, 6.30 mmol) and methyl iodide (0.45 mL, 7.20 mmol) in THF (12 mL + 12 mL). Column chromatography (10% EtOAc in hexane) afforded the product as an orange oil (410 mg, 66%); $^1\text{H NMR}$ (300 MHz, CDCl_3) δ 4.36 (d, $J = 4.6$ Hz, 2H), 2.39 (s, 3H), 1.60 (s, br, 1H). Data matches that reported in the literature.¹¹⁷

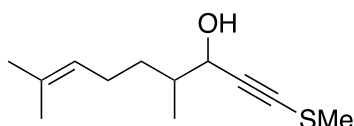
340: 1-(Benzylthio)-5-phenylpent-1-yn-3-ol



The title compound was prepared according to **GP9** using 5-phenylpent-1-yn-3-ol **346** (240 mg, 1.50 mmol), $n\text{-BuLi}$ (2.62 mL, 4.20 mmol), dibenzyl disulfide (590 mg, 2.40 mmol) and methyl iodide (149 μL , 2.40 mmol) in THF (3 mL + 3 mL). Column chromatography (10% EtOAc in hexane) afforded the product as yellow oil (310 mg, <73%); **IR (Neat)**: $\nu_{\text{max}}/\text{cm}^{-1}$ 3369 (br, OH stretch), 2926, 2175, 1602, 1495, 1454, 1048, 1028, 909, 746, 695; $^1\text{H NMR}$ (400 MHz, CDCl_3) δ 7.39 – 7.25 (m, 6H), 7.24 – 7.12 (m, 4H), 4.40 (td, $J = 6.6$ and 5.3 Hz, 1H) 3.93 (s, 2H), 2.71 (t, $J = 7.9$ Hz, 2H), 2.04 – 1.86 (m, 2H), 1.70 (d, $J = 5.3$ Hz, 1H); $^{13}\text{C NMR}$ (101 MHz,

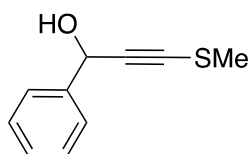
CDCl₃) δ 141.3 (C), 136.6 (C), 129.2 (CH), 128.7 (CH), 128.6 (CH), 128.6 (CH), 128.0 (CH), 126.1 (CH), 96.3 (C), 75.7 (C), 62.8 (CH), 40.2 (CH₂), 39.2 (CH₂), 31.5 (CH₂);
HRMS (CI⁺) m/z: [M + NH₄] Calcd for C₁₈H₂₂NOS 300.1422; Found 300.1412.

341: 4,8-Dimethyl-1-(methylthio)non-7-en-1-yn-3-ol



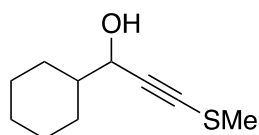
The title compound was prepared according to **GP9** using 4,8-dimethylnon-7-en-1-yn-3-ol **347** (184 mg, 1.10 mmol), n-BuLi (1.45 mL, 2.31 mmol), dimethyl disulfide (108 μ L, 1.21 mmol) and methyl iodide (75.0 μ L, 1.21 mmol) in THF (2.2 mL + 2.2 mL). Column chromatography (10% EtOAc in hexane) afforded the product as a clear oil (157 mg, 67%) as a mixture of diastereoisomers (1:1); **IR (Neat)**: $\nu_{\text{max}}/\text{cm}^{-1}$ 3362 (br, OH stretch), 2965, 2927, 2856, 2176, 1437, 1377, 1313, 1085, 1015, 979, 827, 717; **¹H NMR** (400 MHz, CDCl₃) δ (all distinct resonances for both isomers) 5.16 – 5.05 (m, 1H), 4.41 – 4.30 (m, 1H), 2.38 (s, 3H), 2.12 – 1.92 (m, 2H), 1.78 – 1.70 (m, 1H), 1.69 (s, 3H), 1.65 – 1.46 (m, 1H), 1.61 (s, 3H), 1.29 – 1.19 (m, 1H), 1.01 – 0.97 (m, 3H); **¹³C NMR** (101 MHz, CDCl₃) δ (all distinct resonances for both isomers) 131.9 (C), 131.8 (C), 124.5 (CH), 124.4 (CH), 93.1 (C), 92.5 (C), 77.8 (C), 67.9 (CH), 67.7 (CH), 39.2 (CH), 39.0 (CH), 32.9 (CH₂), 32.2 (CH₂), 25.9 (CH₃), 25.7 (CH₂), 25.6 (CH₂), 19.38 (CH₃), 19.35 (CH₃) 17.8 (CH₃), 15.1 (CH₃) 14.7 (CH₃);
HRMS (CI⁺) m/z: [M] Calcd for C₁₂H₂₀OS 212.1235; Found 212.1228.

343: 3-(Methylthio)-1-phenylprop-2-yn-1-ol



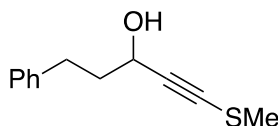
The title compound was prepared according to **GP10** using 1-phenyl-2-propyn-1-ol (330 mg, 2.50 mmol), LiHMDS (7.50 mL, 7.50 mmol), and S-methyl 4-methylbenzenethiosulfonate (759 mg, 3.75 mmol) in THF (5 mL + 5 mL). Column chromatography (0 – 10% EtOAc in hexane) afforded the product as an orange oil (217 mg, 49%); **IR (Neat)**: $\nu_{\text{max}}/\text{cm}^{-1}$ 3293 (br, OH stretch), 2928, 2181, 1493, 1454, 1314, 1191, 1059, 978, 757, 699; **¹H NMR** (400 MHz, CDCl₃) δ 7.56 – 7.49 (m, 2H), 7.43 – 7.29 (m, 3H), 5.56 (d, $J = 6.1$ Hz, 1H), 2.41 (s, 3H), 2.18 (d, $J = 6.1$ Hz, 1H); **¹³C NMR** (101 MHz, CDCl₃) δ 140.6 (C), 128.8 (CH), 128.6 (CH), 126.7 (CH), 92.3 (C), 79.3 (C), 65.6 (CH), 19.2 (CH₃); **HRMS** (ASAP+) m/z : [M – OH] Calcd for C₁₀H₉S 161.0425; Found 161.0431.

350: 1-Cyclohexyl-3-(methylthio)prop-2-yn-1-ol



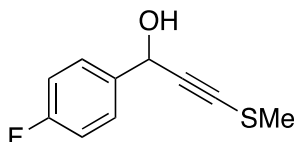
The title compound was prepared according to **GP10** using 1-cyclohexylprop-2-yn-1-ol (252 mg, 1.83 mmol), LiHMDS (5.40 mL, 5.40 mmol) and S-phenyl 4-methylbenzenethiosulfonate (443 mg, 2.19 mmol) in THF (3.6 mL + 3.6 mL). Column chromatography (20% EtOAc in hexane) afforded the product as a clear oil (66.5 mg, <20%); **IR (Neat)**: $\nu_{\text{max}}/\text{cm}^{-1}$ 3370 (br, OH stretch), 2924, 2852, 2179, 1710, 1450, 1312, 1024, 994, 979, 892; **¹H NMR** (400 MHz, CDCl₃) δ 4.23 (d, $J = 5.9$ Hz, 1H), 2.39 (s, 3H), 1.88 – 1.63 (m, 6H), 1.61 – 1.50 (m, 1H), 1.32 – 1.10 (m, 5H); **¹³C NMR** (101 MHz, CDCl₃) δ 93.0 (C), 77.6 (C), 68.2 (CH), 44.4 (CH), 28.7 (CH₂), 28.4 (CH₂), 26.5 (CH₂), 26.03 (CH₂), 26.02 (CH₂), 19.4 (CH₃); **HRMS** (CI+) m/z : [M] Calcd for C₁₀H₁₆OS 184.0922; Found 184.0914.

351: 1-(Methylthio)-5-phenylpent-1-yn-3-ol



The title compound was prepared according to **GP10** using 5-phenylpent-1-yn-3-ol (320 mg, 2.00 mmol), LiHMDS (6.00 mL, 6.00 mmol) and S-methyl 4-methylbenzenethiosulfonate (485 mg, 2.40 mmol) in THF (4 mL + 4 mL). Column chromatography (10% EtOAc in hexane) afforded the product as a yellow oil (410 mg, 34%); **IR (Neat)**: $\nu_{\text{max}}/\text{cm}^{-1}$ 3293 (br, OH stretch), 3027, 2927, 2181, 1496, 1455, 1314, 1049, 1012, 748, 700; **¹H NMR** (400 MHz, CDCl₃) δ 7.32 – 7.26 (m, 2H), 7.24 – 7.17 (m, 3H), 4.46 (td, $J = 6.5$ and 5.3 Hz, 1H), 2.80 (t, $J = 7.8$ Hz, 2H), 2.39 (s, 3H), 2.09 – 1.99 (m, 2H), 1.80 (d, $J = 5.3$ Hz, 1H); **¹³C NMR** (101 MHz, CDCl₃) δ 141.3 (C), 128.64 (CH), 128.59 (CH), 126.2 (CH), 93.6 (C), 77.6 (C), 62.7 (CH), 39.3 (CH₂), 31.6 (CH₂), 19.3 (CH₃); **HRMS** (CI⁺) m/z : [M + NH₄] Calcd for C₁₂H₁₈NOS 224.1109; Found 224.1106.

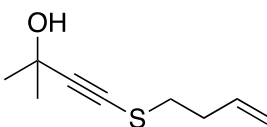
352: 1-(4-Fluorophenyl)-3-(methylthio)prop-2-yn-1-ol



The title compound was prepared according to **GP10** using 1-(4-fluorophenyl)prop-2-yn-1-ol (340 mg, 2.26 mmol), LiHMDS (7.70 mL, 7.70 mmol) and S-methyl 4-methylbenzenesulfonate (574 mg, 2.84 mmol) in THF (5 mL + 5 mL). Column chromatography (20% EtOAc in hexane) afforded the product as an orange oil (319 mg, 72%); **IR (Neat)**: $\nu_{\text{max}}/\text{cm}^{-1}$ 3360 (br, OH stretch), 2929, 2184, 1604, 1507, 1421, 1223, 1157, 1065, 978, 838, 772; **¹H NMR** (400 MHz, CDCl₃) δ 7.50 (dd, $J = 8.3$

and 5.3 Hz, 2H), 7.06 (app. t, $J = 8.7$ Hz, 2H), 5.54 (d, $J = 5.5$ Hz, 1H), 2.41 (s, 3H), 2.20 (d, $J = 5.5$ Hz, 1H); **^{13}C NMR** (101 MHz, CDCl_3) δ 162.8 (d, $^1J_{\text{C-F}} = 247.1$ Hz, C), 136.4 (d, $^4J_{\text{C-F}} = 3.2$ Hz, C), 128.6 (d, $^3J_{\text{C-F}} = 8.4$ Hz, CH), 115.6 (d, $^2J_{\text{C-F}} = 21.7$ Hz, CH), 92.1 (C), 79.6 (C), 64.8 (CH), 19.2 (CH_3); **^{19}F NMR** (376 MHz, CDCl_3): δ -133.8; **HRMS** (EI+) m/z : [M] Calcd for $\text{C}_{10}\text{H}_9\text{OFS}$ 196.0358; Found 196.0367.

333: 4-(But-3-en-1-ylthio)-2-methylbut-3-yn-2-ol

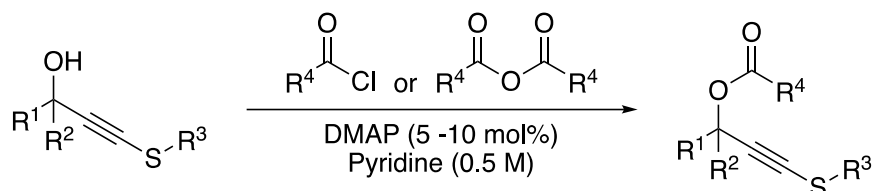


Alkynyl thioether **332** (486 mg, 4.30 mmol) was dissolved in anhydrous THF (21 mL) in a heat-gun dried round-bottom flask under argon and the solution was stirred at -78 °C. $n\text{-BuLi}$ (2.90 mL, 4.70 mmol) was added over 5 min and the reaction was stirred at -78 °C for 2 h. Acetone (0.35 mL, 4.70 mmol) was added and the resulting solution was stirred at -78 °C for 30 min before being warmed to rt and stirred for 12 h. The reaction mixture was quenched with aqueous NH_4Cl (sat.) (~10 mL), extracted with EtOAc (3×10 mL), dried (Na_2SO_4), filtered, concentrated under reduced pressure and purified by flash column chromatography (10% EtOAc in hexane) to afford to product as a clear oil (529 mg, 72%); **IR (Neat)**: $\nu_{\text{max}}/\text{cm}^{-1}$ 3354 (br, OH stretch), 2980, 2931, 2170, 1641, 1442, 1362, 1220, 1160, 979, 920, 807; **^1H NMR** (400 MHz, CDCl_3) δ 5.83 (ddt, $J = 16.9, 10.2$ and 6.6 Hz, 1H), 5.18 – 5.04 (m, 2H), 2.79 – 2.70 (m, 2H), 2.54 – 2.41 (m, 2H), 1.93 (s, br, 1H), 1.52 (s, 6H); **^{13}C NMR** (101 MHz, CDCl_3) δ 135.7, 116.9, 98.7, 72.3, 66.1, 34.6, 33.4, 31.5; **HRMS** (CI+) m/z : [M + H] Calcd for $\text{C}_9\text{H}_{15}\text{OS}$ 171.0844; Found 171.0840.

4.10 Propargyl Carboxylates

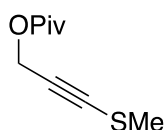
General Procedure 11 (GP11):

Based on an existing literature protocol.⁵³



The propargyl alcohol (1.0 eq) was dissolved in pyridine (0.5 M) in a round-bottom flask. DMAP (5 –10 mol%) was added and the round-bottom flask was sonicated until the DMAP was fully dissolved. The solution was stirred vigorously whilst the acyl chloride or anhydride (3.0 – 5.0 eq) was added to the reaction mixture dropwise over 5 – 10 min (exothermic and effervescent). The reaction mixture was stirred for 16 h at rt and was then quenched with NaHCO₃ (until effervescence was no longer observed upon addition of NaHCO₃), extracted with CH₂Cl₂ (3 × 2 mL/mmol) and dried (Na₂SO₄). The solution was concentrated under reduced pressure and the remaining solution in pyridine was dry-loaded onto a minimum amount of silica. The product was purified by flash column chromatography.

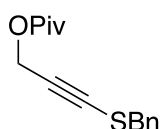
357: 3-(Methylthio)prop-2-yn-1-yl pivalate



The title compound was prepared according to **GP11** using propargyl alcohol **339** (267 mg, 2.61 mmol), DMAP (44.0 mg, 0.37 mmol) and pivaloyl chloride (1.40 mL, 11.3 mmol) in pyridine (7.3 mL). Column chromatography (10% EtOAc in hexane) afforded the product as an orange oil (338 mg, 70%); **IR (Neat):** $\nu_{\text{max}}/\text{cm}^{-1}$ 2974, 2196, 1732 (C=O), 1480, 1278, 1132, 955; **¹H NMR**

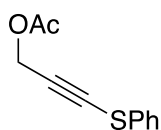
(400 MHz, CDCl₃) δ 4.75 (s, 2H), 2.38 (s, 3H), 1.21 (s, 9H); **¹³C NMR** (101 MHz, CDCl₃) δ 178.0 (C=O), 87.6 (C), 79.3 (C), 53.3 (CH₂), 38.9 (C), 27.2 (CH₃), 19.1 (CH₃); **HRMS** (EI+) m/z: [M] Calcd for C₉H₁₄O₂S 186.0715; Found 186.0720.

358: 3-(Benzylthio)prop-2-yn-1-yl pivalate



DMAP The title compound was prepared according to **GP11** using propargyl alcohol **338** (37.9 mg, 0.21 mmol), DMAP (2.60 mg, 0.02 mmol) and pivaloyl chloride (78.0 μ L, 0.63 mmol) in pyridine (0.41 mL). Column chromatography (10% EtOAc in hexane) afforded the product as a yellow oil (49.0 mg, 89%); **IR (Neat):** $\nu_{\text{max}}/\text{cm}^{-1}$ 2973, 2194, 1730 (C=O), 1455, 1278, 1132, 954, 768, 696; **¹H NMR** (400 MHz, CDCl₃) δ 7.36 – 7.25 (m, 5H), 4.73 (s, 2H), 3.94 (s, 2H), 1.21 (s, 9H); **¹³C NMR** (101 MHz, CDCl₃) δ 178.0 (C=O), 136.6 (C), 129.2 (CH) 128.8 (CH), 127.9 (CH), 90.3 (C), 77.5 (C), 53.2 (CH₂), 40.3 (CH₂), 38.9 (C), 27.2 (CH₃); **HRMS** (CI+) m/z: [M + NH₄] Calcd for C₁₅H₂₂NO₂S 280.1371; Found 280.1372.

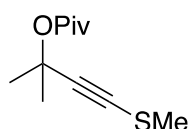
359: 3-(Phenylthio)prop-2-yn-1-yl acetate



The title compound was prepared according to **GP11** using propargyl alcohol **324** (203 mg, 1.24 mmol), DMAP (14.0 mg, 0.12 mmol) and acetic anhydride (0.67 mL, 7.00 mmol) in pyridine (2.4 mL). Column chromatography (10% EtOAc in hexane) afforded the product as a clear oil (208 mg, 81%); **IR (Neat):** $\nu_{\text{max}}/\text{cm}^{-1}$ 3061, 2197, 1743 (C=O), 1582, 1479, 1211, 1074, 1021, 958, 736, 687; **¹H NMR** (400 MHz, CDCl₃) δ 7.46 – 7.40 (m, 2H), 7.35 (t, *J* = 7.5 Hz, 2H), 7.28 – 7.19

(m, 1H), 4.91 (s, 2H), 2.12 (s, 3H); ^{13}C NMR (101 MHz, CDCl_3) δ 170.4 (C=O), 132.1 (C), 129.5 (CH), 127.0 (CH), 126.6 (CH), 93.5 (C), 74.7 (C), 53.2 (CH_2), 20.9 (CH_3); **HRMS** (ES+) m/z : [M + Na] Calcd for $\text{C}_{11}\text{H}_{10}\text{O}_2\text{SNa}$ 229.0284; Found 229.0294.

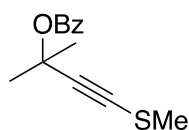
360: 2-Methyl-4-(phenylthio)but-3-yn-2-yl pivalate



The title compound was prepared according to **GP11** using propargyl alcohol **335** (30.0 mg, 0.23 mmol), DMAP (4.40 mg, 0.04 mmol) and pivaloyl chloride (141 μL , 1.15 mmol) in pyridine (0.5 mL). Column chromatography (0 – 10% EtOAc in hexane) afforded the product as a clear oil (15.9 mg, 32%);

IR (Neat): $\nu_{\text{max}}/\text{cm}^{-1}$ 2975, 2931, 2872, 2175, 1733 (C=O), 1250, 1171, 1116, 872; **^1H NMR** (400 MHz, CDCl_3) δ 2.36 (s, 3H), 1.63 (s, 6H), 1.17 (s, 9H); **^{13}C NMR** (101 MHz, CDCl_3) δ 176.8 (C=O), 94.0 (C), 76.2 (C), 72.2 (C), 39.2 (C), 29.0 (CH_3), 27.2 (CH_3), 19.4 (CH_3); **HRMS** (CI+) m/z : [M] Calcd for $\text{C}_{11}\text{H}_{18}\text{O}_2\text{S}$ 214.1028; Found 214.1028.

361: 2-Methyl-4-(methylthio)but-3-yn-2-yl benzoate

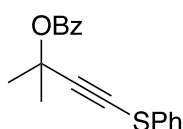


The title compound was prepared according to **GP11** using propargyl alcohol **335** (93.7 mg, 0.72 mmol), DMAP (8.80 mg, 0.07 mmol) and benzoyl chloride (250 μL , 2.15 mmol) in pyridine (1.4 mL). Column chromatography (0 – 10% EtOAc in hexane) afforded the product as a clear oil (43.8 mg, 26%);

IR (Neat): $\nu_{\text{max}}/\text{cm}^{-1}$ 2987, 2930, 2175, 1720 (C=O), 1277, 1094, 708; **^1H NMR** (400 MHz, CDCl_3) δ 8.05 – 7.98 (m, 2H), 7.54 (tt, J = 7.5 and 1.4 Hz, 1H), 7.42 (t, J = 7.5

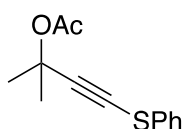
Hz, 2H), 2.38 (s, 3H), 1.80 (s, 6H); ^{13}C NMR (101 MHz, CDCl_3) δ 164.9 (C=O), 132.9 (CH), 131.2 (C), 129.7 (CH), 128.4 (CH), 93.6 (C), 77.1 (C), 73.3 (C), 29.2 (CH_3), 19.4 (CH_3); **HRMS** (CI+) m/z: $[\text{M} + \text{NH}_4]$ Calcd for $\text{C}_{13}\text{H}_{18}\text{NO}_2\text{S}$ 252.1058; Found 252.1055.

362: 2-Methyl-4-(phenylthio)but-3-yn-2-yl benzoate



The title compound was prepared according to **GP11** using propargyl alcohol **323** (135 mg, 0.70 mmol), DMAP (8.50 mg, 0.07 mmol) and benzoyl chloride (0.24 mL, 2.10 mmol) in pyridine (1.4 mL). Column chromatography (10% EtOAc in hexane) afforded the product as a clear oil (185 mg, 89%; purity = 73%; 27% benzoyl chloride impurity determined by ^1H NMR spectroscopy); **IR** (Neat): $\nu_{\text{max}}/\text{cm}^{-1}$ 2937, 1722 (C=O), 1629, 1451, 1282, 1213, 1096, 999, 711; ^1H NMR (400 MHz, CDCl_3) δ 8.06 – 8.01 (m, 2H), 7.55 (tt, $J = 7.4$ and 1.4 Hz, 1H), 7.50 – 7.40 (m, 4H), 7.35 (app. t, $J = 7.8$ Hz, 2H), 7.21 (tt, $J = 7.4$ and 1.1 Hz, 1H), 1.90 (s, 6H); ^{13}C NMR (101 MHz, CDCl_3) δ 165.0 (C=O), 133.0 (CH), 131.0 (C), 129.8 (CH), 129.4 (CH), 128.4 (CH), 126.5 (CH), 126.1 (CH), 100.5 (C), 73.2 (C), 71.8 (C), 29.2 (CH_3), *a quaternary carbon was not observed*; **HRMS** (ES+) m/z: $[\text{M} + \text{Na}]$ Calcd for $\text{C}_{18}\text{H}_{16}\text{O}_2\text{S}$ 296.0871; Found 296.0879.

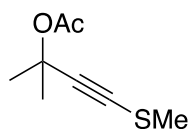
363: 2-Methyl-4-(phenylthio)but-3-yn-2-yl acetate



The title compound was prepared according to **GP11** using propargyl alcohol **323** (817 mg, 4.25 mmol), DMAP (48.9 mg, 0.40 mmol) and acetic anhydride (2.01 mL, 21.3 mmol) in pyridine (7.8 mL). Column chromatography

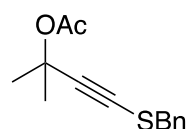
(0 – 10% EtOAc in hexane) afforded the product as a clear oil (731 mg, 73%); **IR (Neat):** $\nu_{\text{max}}/\text{cm}^{-1}$ 2988, 2171, 1736 (C=O), 1583, 1479, 1365, 1236, 1129, 1013, 737; **$^1\text{H NMR}$** (400 MHz, CDCl_3) δ 7.45 (dd, $J = 8.5$ and 1.2 Hz, 2H), 7.34 (*app. t*, $J = 7.8$ Hz, 2H), 7.21 (tt, $J = 8.0$ and 1.2 Hz, 1H), 2.05 (s, 3H), 1.74 (s, 6H); **$^{13}\text{C NMR}$** (101 MHz, CDCl_3) δ 169.6 (C=O), 133.0 (C), 129.4 (CH), 126.5 (CH), 126.0 (CH), 100.5 (C), 72.5 (C), 71.4 (C), 29.0 (CH_3), 22.1 (CH_3); **HRMS** (ES+) m/z : $[\text{M} + \text{Na}]$ Calcd for $\text{C}_{13}\text{H}_{14}\text{O}_2\text{NaS}$ 257.0612; Found 257.0607.

364: 2-Methyl-4-(methylthio)but-3-yn-2-yl acetate



The title compound was prepared according to **GP11** using propargyl alcohol **335** (338 mg, 2.60 mmol), DMAP (42.8mg, 0.35 mmol) and acetic anhydride (1.23 mL, 13.0 mmol) in pyridine (5.2 mL). Column chromatography (0 – 10% EtOAc in hexane) afforded the product as a clear oil (344 mg, 77%); **IR (Neat):** $\nu_{\text{max}}/\text{cm}^{-1}$ 2988, 2931, 2169, 1737 (C=O), 1366, 1238, 1130, 1015, 807, 618; **$^1\text{H NMR}$** (400 MHz, CDCl_3) δ 2.36 (s, 3H), 2.01 (s, 3H), 1.65 (s, 6H); **$^{13}\text{C NMR}$** (101 MHz, CDCl_3) δ 169.5 (C=O), 93.8 (C), 76.7 (C), 72.7 (C), 29.0 (CH_3), 22.1 (CH_3), 19.3 (CH_3); **HRMS** (CI+) m/z : $[\text{M} + \text{NH}_4]$ Calcd for $\text{C}_8\text{H}_{16}\text{NO}_2\text{S}$ 190.0902; Found 190.0905.

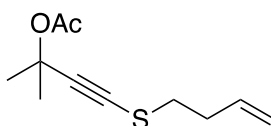
365: 4-(Benzylthio)-2-methylbut-3-yn-2-yl acetate



The title compound was prepared according to **GP11** using propargyl alcohol **336** (519 mg, 2.51 mmol), DMAP (20.0 mg, 0.16 mmol) and acetic anhydride

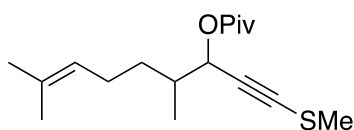
(0.80 mL, 8.47 mmol) in pyridine (5.0 mL). Column chromatography (0 – 10% EtOAc in hexane) afforded the product as a clear oil (295 mg, 47%); **IR (Neat):** $\nu_{\text{max}}/\text{cm}^{-1}$ 2986, 2936, 2166, 1736 (C=O), 1455, 1365, 1237, 1128, 1013, 804, 765, 697; **$^1\text{H NMR}$** (400 MHz, CDCl_3) δ 7.44 – 7.14 (m, 5H), 3.90 (s, 2H), 2.01 (s, 3H), 1.60 (s, 6H); **$^{13}\text{C NMR}$** (101 MHz, CDCl_3) δ 169.5 (C=O), 136.9 (C), 129.4 (CH), 128.6 (CH), 127.8 (CH), 96.7 (C), 74.9 (C), 72.7 (C), 40.3 (CH_2), 29.0 (CH_3), 22.1 (CH_3); **HRMS (CI+)** m/z : [M + H] Calcd for $\text{C}_{14}\text{H}_{15}\text{O}_2\text{S}$ 247.0793; Found 247.0799.

366: 4-(But-3-en-1-ylthio)-2-methylbut-3-yn-2-yl acetate



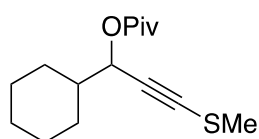
The title compound was prepared according to **GP11** using propargyl alcohol **333** (529 mg, 3.11 mmol), DMAP (33.6 mg, 0.28 mmol) and acetic anhydride (0.78 mL, 8.25 mmol) in pyridine (6.8 mL). Column chromatography (0 – 10% EtOAc in hexane) afforded the product as a clear oil (434 mg, 66%); **IR (Neat):** $\nu_{\text{max}}/\text{cm}^{-1}$ 2988, 2936, 2169, 1737 (C=O), 1366, 1237, 1191, 1129, 1014; **$^1\text{H NMR}$** (400 MHz, CDCl_3) δ 5.83 (ddt, $J = 16.9, 10.2$ and 6.7 Hz, 1H), 5.17 – 5.04 (m, 2H), 2.74 (t, $J = 7.3$ Hz, 2H), 2.49 (*app.* q, $J = 7.4$ Hz, 2H), 2.01 (s, 3H), 1.65 (s, 6H); **$^{13}\text{C NMR}$** (101 MHz, CDCl_3) δ 169.5 (C=O), 135.9 (CH), 116.9 (CH_2), 95.4 (C), 74.8 (C), 72.7 (C), 34.7 (CH_2), 33.3 (CH_2), 29.1 (CH_3), 22.1 (CH_3); **HRMS (CI+)** m/z : [M + NH_4] Calcd for $\text{C}_{11}\text{H}_{20}\text{NO}_2\text{S}$ 230.1215; Found 230.1219.

367: 4,8-Dimethyl-1-(methylthio)non-7-en-1-yn-3-yl pivalate



The title compound was prepared according to **GP11** using propargyl alcohol **341** (125 mg, 0.59 mmol), DMAP (7.2 mg, 0.06 mmol) and pivaloyl chloride (0.22 mL, 1.77 mmol) in pyridine (1.2 mL). Column chromatography (10% EtOAc in hexane) afforded the product as a clear oil (122 mg, 70%) as a mixture of diastereoisomers; **IR (Neat):** $\nu_{\text{max}}/\text{cm}^{-1}$ 2968, 2930, 2185, 1732 (C=O), 1280, 1143, 1030, 968; **¹H NMR** (400 MHz, CDCl₃) δ (all distinct resonances for both isomers) 5.36 (dd, $J = 10.4$ and 4.9 Hz, 1H), 5.13 – 5.01 (m, 1H), 2.37 (s, 3H), 2.11 – 1.90 (m, 2H), 1.88 – 1.80 (m, 1H), 1.68 (s, 3H), 1.60 (s, 3H), 1.58 – 1.47 (m, 1H), 1.32 – 1.19 (m, 1H), 1.21 (s, 9H), 1.01 (d, $J = 4.3$ Hz, 3H, CH₃ of one diastereoisomer), 1.00 (d, $J = 4.3$ Hz, 3H, CH₃ of one diastereoisomer); **¹³C NMR** (101 MHz, CDCl₃) δ (all distinct resonances for both isomers) 177.5 (C=O), 174.1 (C=O), 132.0 (C), 131.8 (C), 124.3 (CH), 124.2 (CH), 89.9 (C), 89.4 (C), 78.1 (C), 77.8 (C), 68.8 (CH), 68.5 (CH), 39.02 (C), 38.98 (C), 37.4 (CH), 37.1 (CH), 32.9 (CH₂), 32.5 (CH₂), 27.2 (CH₃), 26.6 (CH₃), 25.8 (CH₃), 25.6 (CH₂), 25.5 (CH₂), 19.4 (CH₃), 19.3 (CH₃), 17.8 (CH₃), 15.6 (CH₃), 15.1 (CH₃); **HRMS** (CI⁺) m/z : [M + NH₄] Calcd for C₁₇H₃₂NO₂S 314.2154; Found 314.2162.

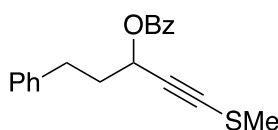
368: 1-Cyclohexyl-3-(methylthio)prop-2-yn-1-yl pivalate



The title compound was prepared according to **GP11** using propargyl alcohol **350** (33.0 mg, 0.18 mmol), DMAP (2.10 mg, 0.02 mmol) and pivaloyl chloride (70.0 μL , 0.57 mmol) in pyridine (1.8 mL). Column chromatography (10% EtOAc in hexane) afforded the product as a clear oil (38.1 mg, 79%); **IR (Neat):** $\nu_{\text{max}}/\text{cm}^{-1}$ 2929, 2855, 2184, 1732 (C=O), 1479, 1451, 1281, 1148, 972; **¹H NMR**

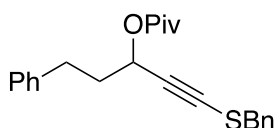
(400 MHz, CDCl₃) δ 5.25 (d, J = 6.0 Hz, 1H), 2.37 (s, 3H), 1.88 – 1.62 (m, 7H), 1.32 – 1.01 (m, 4H), 1.22 (s, 9H); ¹³C NMR (101 MHz, CDCl₃) δ 177.6 (C=O), 89.9 (C), 77.8 (C), 68.9 (CH), 42.2 (CH), 39.0 (C), 28.7 (CH₂), 28.6 (CH₂), 27.3 (CH₃), 27.1 (CH₂) 26.4 (CH₂), 25.9 (CH₂), 19.4 (CH₃); **HRMS** (EI⁺) m/z : [M] Calcd for C₁₅H₂₄O₂S 268.1497; Found 268.1488.

369: 1-(Methylthio)-5-phenylpent-1-yn-3-yl benzoate



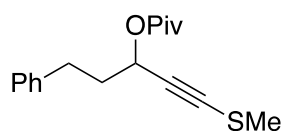
The title compound was prepared according to **GP11** using propargyl alcohol **351** (48.0 mg, 0.23 mmol), DMAP (2.80 mg, 0.02 mmol) and benzoyl chloride (80.0 μ L, 0.69 mmol) in pyridine (0.5 mL). Column chromatography (10% EtOAc in hexane) afforded the product as a clear oil (61.0 mg, 85%); **IR (Neat)**: $\nu_{\max}/\text{cm}^{-1}$ 3027, 2929, 2177, 1718 (C=O), 1451, 1261, 1094, 1069, 1024, 710, 698; **¹H NMR** (400 MHz, CDCl₃) δ 8.04 (d, J = 7.7 Hz, 2H), 7.58 (tt, J = 7.4 and 1.3 Hz, 1H), 7.45 (t, J = 7.8 Hz, 2H), 7.32 – 7.26 (m, 2H), 7.24 – 7.17 (m, 3H), 5.70 (t, J = 6.5 Hz, 1H), 2.86 (t, J = 7.9 Hz, 2H), 2.40 (s, 3H), 2.35 – 2.16 (m, 2H); **¹³C NMR** (101 MHz, CDCl₃) δ 165.6 (C=O), 140.9 (C), 133.3 (CH), 129.9 (CH), 128.7 (CH), 128.6 (CH), 128.5 (CH), 126.3 (CH), 90.2 (C), 78.8 (C), 65.0 (CH), 36.5 (CH₂), 31.6 (CH₂), 19.3 (CH₃) *a quaternary carbon was not observed*; **HRMS** (CI⁺) m/z : [M + NH₄] Calcd for C₁₉H₂₂NO₂S 328.1371; Found 328.1376.

370: 1-(Benzylthio)-5-phenylpent-1-yn-3-yl pivalate



The title compound was prepared according to **GP11** using propargyl alcohol **340** (129 mg, 0.46 mmol), DMAP (5.5 mg, 0.05 mmol) and pivaloyl chloride (170 μ L, 1.38 mmol) in pyridine (0.9 mL). Column chromatography (10% EtOAc in hexane) afforded the product as a clear oil (108 mg, 64%); **IR (Neat):** $\nu_{\text{max}}/\text{cm}^{-1}$ 2932, 2175, 1728 (C=O), 1601, 1495, 1454, 1277, 1141, 1030, 767, 748, 696; **$^1\text{H NMR}$** (400 MHz, CDCl_3) δ 7.36 – 7.23 (m, 7H), 7.24 – 7.17 (m, 1H), 7.16 – 7.11 (m, 2H), 5.39 (t, J = 6.5 Hz, 1H), 3.92 (d, J = 3.2 Hz, 2H), 2.67 (t, J = 8.0 Hz, 2H), 2.14 – 1.89 (m, 2H), 1.20 (s, 9H); **$^{13}\text{C NMR}$** (101 MHz, CDCl_3) δ 177.4 (C=O), 140.9 (C), 136.7 (C), 129.2 (CH), 128.7 (CH), 128.6 (CH), 128.5 (CH), 127.9 (CH), 126.3 (CH), 93.1 (C), 76.3 (C), 64.2 (CH), 40.2 (CH_2), 38.9 (C), 36.4 (CH_2), 31.4 (CH_2), 27.3 (CH_3); **HRMS** (CI+) m/z : [M + NH_4] Calcd for $\text{C}_{23}\text{H}_{30}\text{NO}_2\text{S}$ 384.1997; Found 384.2002.

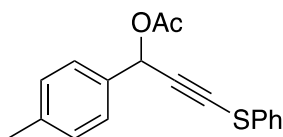
371: 1-(Methylthio)-5-phenylpent-1-yn-3-yl pivalate



The title compound was prepared according to **GP11** using propargyl alcohol **351** (92.0 mg, 0.45 mmol), DMAP (5.5 mg, 0.05 mmol) and pivaloyl chloride (166 μ L, 1.35 mmol) in pyridine (0.9 mL). Column chromatography (10% EtOAc in hexane) afforded the product as a clear oil (108 mg, 83%); **IR (Neat):** $\nu_{\text{max}}/\text{cm}^{-1}$ 2971, 2931, 2179, 1730 (C=O), 1455, 1276, 1140, 1080, 747, 698; **$^1\text{H NMR}$** (400 MHz, CDCl_3) δ 7.33 – 7.25 (m, 2H), 7.24 – 7.14 (m, 3H), 5.43 (t, J = 6.5 Hz, 1H), 2.75 (t, J = 7.9 Hz, 2H), 2.38 (s, 3H), 2.19 – 1.98 (m, 2H), 1.22 (s, 9H); **$^{13}\text{C NMR}$** (101 MHz, CDCl_3) δ 177.5 (C=O), 141.0 (C), 128.6 (CH), 128.5 (CH), 126.3

(CH), 90.4 (C), 78.1 (C), 64.2 (CH), 38.9 (C), 36.5 (CH₂), 31.5 (CH₂), 27.2 (CH₃), 19.3 (CH₃); **HRMS** (CI+) m/z: [M + NH₄] Calcd for C₁₇H₂₆NO₂S 308.1684; Found 308.1696.

372: 3-(Phenylthio)-1-(*p*-tolyl)prop-2-yn-1-yl acetate



The title compound was prepared according to **GP11** using propargyl alcohol **325** (322 mg, 1.27 mmol), DMAP (15.4 mg, 0.13 mmol) and acetic anhydride (0.50 mL, 5.29 mmol) in pyridine (2.5 mL). Column chromatography (0 – 10% EtOAc in hexane) afforded the product as an orange oil (205 mg, 55%);

IR (Neat): $\nu_{\max}/\text{cm}^{-1}$ 1659 (C=O), 1592, 1578, 1450, 1210, 1175, 875, 717, 642;

¹H NMR (400 MHz, CDCl₃) δ 7.47 – 7.38 (m, 4H), 7.33 (*app. t*, $J = 8.0$ Hz, 2H), 7.27 –

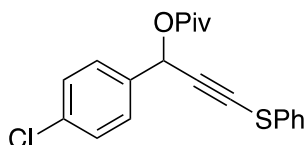
7.18 (m, 3H), 6.62 (s, 1H), 2.38 (s, 3H), 2.12 (s, 3H); **³C NMR** (101 MHz, CDCl₃) δ

170.0 (C=O), 139.2 (C), 133.8 (C), 132.3 (C), 129.6 (CH), 129.4 (CH), 127.9 (CH),

126.9 (CH), 126.5 (CH), 95.8 (C), 75.0 (C), 66.5 (CH), 21.4 (CH₃), 21.3 (CH₃); **HRMS**

(EI+) m/z: [M] Calcd for C₁₈H₁₆O₂S 296.0871; Found 296.0861.

373: 1-(4-Chlorophenyl)-3-(phenylthio)prop-2-yn-1-yl pivalate

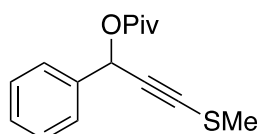


The title compound was prepared according to **GP11** using propargyl alcohol **331** (459 mg, 1.67 mmol), DMAP (20.0 mg, 0.17 mmol) and pivaloyl chloride (0.63 mL, 5.10 mmol) in pyridine (3.4 mL). Column chromatography (0 – 10% EtOAc in hexane) afforded the product as an orange oil (536 mg, 89%);

IR (Neat): $\nu_{\max}/\text{cm}^{-1}$ 2974, 1735 (C=O), 1479, 1273, 1137, 1093, 738, 687;

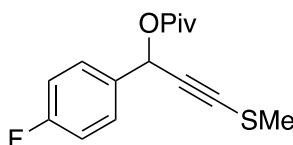
¹H NMR (400 MHz, CDCl₃) δ 7.46 (d, *J* = 8.3 Hz, 2H), 7.41 – 7.29 (m, 6H), 7.27 – 7.21 (m, 1H), 6.59 (s, 1H), 1.22 (s, 9H); **¹³C NMR** (101 MHz, CDCl₃) δ 177.3 (C=O), 135.7 (C), 134.9 (C), 132.1 (C), 129.5 (CH), 129.1 (CH), 128.9 (CH), 126.9 (CH), 126.5 (CH), 95.3 (C), 75.3 (C), 65.7 (CH), 39.0 (C), 27.1 (CH₃); **HRMS** (EI+) *m/z*: [M] Calcd for C₂₀H₁₉ClO₂S 358.0794; Found 358.0801.

374: 3-(Methylthio)-1-phenylprop-2-yn-1-yl pivalate



The title compound was prepared according to **GP11** using propargyl alcohol **343** (217 mg, 1.22 mmol), DMAP (14.6 mg, 0.12 mmol) and pivaloyl chloride (0.45 mL, 3.66 mmol) in pyridine (2.5 mL). Column chromatography (0 – 5% EtOAc in hexane) afforded the product as a yellow oil (266 mg, 83%); **IR** (**Neat**): $\nu_{\max}/\text{cm}^{-1}$ 2973, 2931, 2189, 1733 (C=O), 1479, 1271, 1140, 765, 698; **¹H NMR** (400 MHz, CDCl₃) δ 7.51 – 7.43 (m, 2H), 7.42 – 7.30 (m, 3H), 6.52 (s, 1H), 2.40 (s, 3H), 1.21 (s, 9H); **¹³C NMR** (101 MHz, CDCl₃) δ 177.4 (C=O), 137.5 (C), 128.8 (CH), 128.7 (CH), 127.4 (CH), 89.6 (C), 79.8 (C), 66.3 (CH), 38.9 (C), 27.2 (CH₃), 19.2 (CH₃); **HRMS** (CI+) *m/z*: [M + NH₄] Calcd for C₁₅H₂₂NO₂S 280.1371; Found 280.1369.

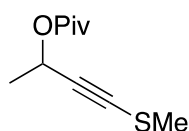
375: 1-(4-Fluorophenyl)-3-(methylthio)prop-2-yn-1-yl pivalate



The title compound was prepared according to **GP11** using propargyl alcohol **352** (319 mg, 1.62 mmol), DMAP (18.3 mg, 0.15 mmol) and pivaloyl chloride (0.56 mL, 4.50 mmol) in pyridine (3.0 mL). Column chromatography

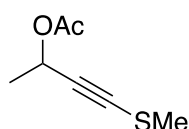
(10% EtOAc in hexane) afforded the product as a yellow oil (376 mg, 83%); **IR (Neat):** $\nu_{\text{max}}/\text{cm}^{-1}$ 2974, 2933, 2874, 2192, 1731 (C=O), 1605, 1509, 1225, 1134, 835; **$^1\text{H NMR}$** (400 MHz, CDCl_3) δ 7.45 (dd, $J = 8.4$ and 5.2 Hz, 2H), 7.05 (t, $J = 8.7$ Hz, 2H), 6.49 (s, 1H), 2.40 (s, 3H), 1.20 (s, 9H); **$^{13}\text{C NMR}$** (101 MHz, CDCl_3) δ 177.3 (C=O), 162.9 (d, $^1J_{\text{C-F}} = 247.5$ Hz, C), 133.4 (d, $^4J_{\text{C-F}} = 3.2$ Hz, C), 129.4 (d, $^3J_{\text{C-F}} = 8.4$ Hz, CH), 115.7 (d, $^3J_{\text{C-F}} = 21.7$ Hz, CH), 89.3 (C), 80.2 (C), 65.6 (CH), 38.9 (C), 27.1 (CH_3), 19.2 (CH_3); **$^{19}\text{F NMR}$** (376 MHz, CDCl_3): δ -113.0; **HRMS** (CI+) m/z : $[\text{M} + \text{NH}_4]$ Calcd for $\text{C}_{15}\text{H}_{21}\text{NO}_2\text{SF}$ 298.1277 ; Found 298.1287.

376: 4-(Methylthio)but-3-yn-2-yl pivalate



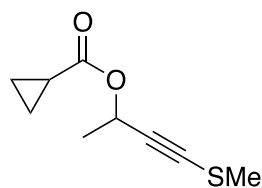
The title compound was prepared according to **GP11** using propargyl alcohol **337** (116 mg, 1.00 mmol), DMAP (12.0 mg, 0.10 mmol) and pivaloyl chloride (0.37 mL, 3.00 mmol) in pyridine (2.0 mL). Column chromatography (10% EtOAc in hexane) afforded the product as a clear oil (131 mg, 65%); **IR (Neat):** $\nu_{\text{max}}/\text{cm}^{-1}$ 2975, 2933, 2874, 2170, 1728 (C=O), 1277, 115, 1131, 1039, 955, 855, 771; **$^1\text{H NMR}$** (400 MHz, CDCl_3) δ 5.50 (q, $J = 6.7$ Hz, 1H), 2.37 (s, 3H), 1.46 (d, $J = 6.7$ Hz, 3H), 1.20 (s, 9H); **$^{13}\text{C NMR}$** (101 MHz, CDCl_3) δ 177.6 (C=O), 91.5 (C), 77.0 (C), 61.0 (CH) 38.8 (C), 27.2 (CH_3), 21.3 (CH_3), 19.2 (CH_3); **HRMS** (CI+) m/z : $[\text{M} + \text{NH}_4]$ Calcd for $\text{C}_{10}\text{H}_{20}\text{NO}_2\text{S}$ 218.1215; Found 218.1207.

377: 4-(Methylthio)but-3-yn-2-yl acetate



The title compound was prepared according to **GP11** using propargyl alcohol **337** (166 mg, 1.42 mmol), DMAP (17.4 mg, 0.14 mmol) and acetic anhydride (0.40 mL, 4.26 mmol) in pyridine (2.8 mL). Column chromatography (40% CH₂Cl in hexane) afforded the product as a clear oil (111 mg, 50%); **IR (Neat):** $\nu_{\max}/\text{cm}^{-1}$ 2990, 2932, 2174, 1734 (C=O), 1371, 1231, 1195, 1138, 1231, 1042, 962; **¹H NMR** (400 MHz, CDCl₃) δ 5.52 (q, J = 6.7 Hz, 1H), 2.38 (s, 3H), 2.07 (s, 3H), 1.49 (d, J = 6.7 Hz, 3H); **¹³C NMR** (101 MHz, CDCl₃) δ 170.1 (C=O), 91.3 (C), 77.6 (C), 61.2 (CH), 21.4 (CH₃), 21.3 (CH₃), 19.2 (CH₃); **HRMS** (CI⁺) m/z : [M] Calcd for C₇H₁₀O₂S 158.0402; Found 158.0400.

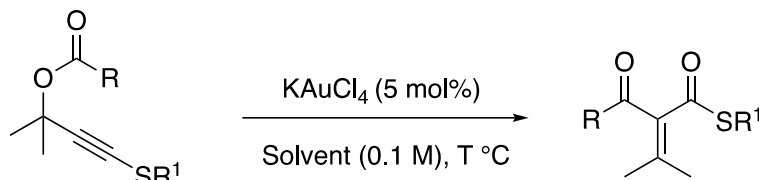
378: 4-(Methylthio)but-3-yn-2-yl cyclopropanecarboxylate



The title compound was prepared according to **GP11** using propargyl alcohol **337** (348 mg, 3.00 mmol), DMAP (36.6 mg, 0.30 mmol) and cyclopropanecarbonyl chloride (0.85 mL, 9.00 mmol) in pyridine (6.0 mL). Column chromatography (10% EtOAc in hexane) afforded the product as a clear oil (520 mg, 94%, purity = 75% determined by ¹H NMR spectroscopy); **IR (Neat):** $\nu_{\max}/\text{cm}^{-1}$ 2990, 2934, 2182, 1727 (C=O), 1390, 1195, 1165, 1134, 1030, 932, 835, 747; **¹H NMR** (400 MHz, CDCl₃) δ 5.57 (q, J = 6.7 Hz, 1H), 2.40 (s, 3H), 1.69 – 1.58 (m, 1H), 1.51 (d, J = 6.7 Hz, 3H), 1.12 – 0.98 (m, 2H), 0.95 – 0.84 (m, 2H); **¹³C NMR** (101 MHz, CDCl₃) δ 173.9 (C=O), 91.4 (C), 77.4 (C), 61.2 (CH), 21.5 (CH₃), 19.2 (CH₃), 13.1 (CH), 8.8 (CH₂); **HRMS** (EI⁺) m/z : [M] Calcd for C₉H₁₂O₂S 184.0558; Found 184.0564.

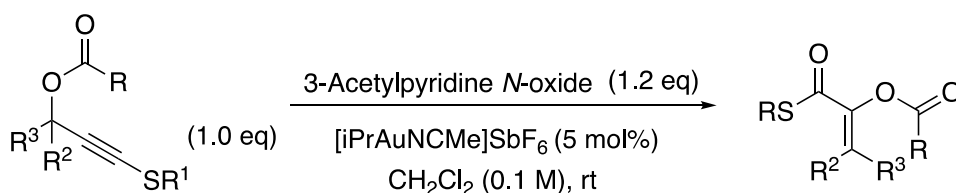
4.11 Products from Propargyl Carboxylate Catalysis

General Procedure GP12:

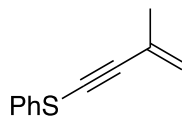


The propargyl carboxylate (1.0 eq) was dissolved in CH₂Cl₂ or toluene (0.1 M) in a glass vial. KAuCl₄ (5 mol%) was added to solution and the reaction mixture was stirred at T °C. The reaction was monitored by TLC. Upon completion, the reaction mixture was filtered through a short pad of celite at rt and the celite was washed with EtOAc (~3 × 1 mL). The solution was concentrated under reduced pressure and the product was purified by flash column chromatography.

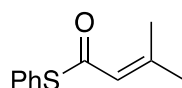
General Procedure GP13:



The propargyl carboxylate (1.0 eq) and 3-acetylpyridine *N*-oxide (1.2 eq) were dissolved in anhydrous CH₂Cl₂ (0.1 M) in a heat-gun dried Schlenk tube under argon. [iPrAuNCMe]SbF₆ (5 mol%) was added to the solution under a positive pressure of argon and the reaction mixture was stirred at rt. The reaction was monitored by TLC. Upon completion, the reaction mixture was filtered through a short pad of celite at rt and the celite was washed with EtOAc (~3 × 1 mL/mmol). The solution was concentrated under reduced pressure and the product was purified by flash column chromatography.

388: (3-Methylbut-3-en-1-yn-1-yl)(phenyl)sulfane

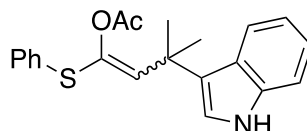
Propargyl acetate **363** (23.8 mg, 0.10 mmol) and SPhosAuNTf₂ (2.20 mg, 2.5 mol%) were stirred in toluene (1 mL) at 50 °C for 1 h in a glass vial. The solution was concentrated under reduced pressure and the product was purified by flash column chromatography (hexane) to afford the product as a clear oil (8.00 mg, 46%); **IR (Neat):** $\nu_{\text{max}}/\text{cm}^{-1}$ 2921, 1582, 1479, 1441, 1024, 897, 737, 687; **¹H NMR** (400 MHz, CDCl₃) δ 7.45 – 7.40 (m, 2H), 7.34 (t, $J = 8.0$ Hz, 2H), 7.22 (tt, $J = 7.3$ and 1.2 Hz, 1H), 5.37 (dq, $J = 2.0$ and 1.0 Hz, 1H), 5.29 – 5.26 (m, 1H), 1.98 (dd, $J = 1.6$ and 1.0 Hz, 3H); **¹³C NMR** (101 MHz, CDCl₃) δ 132.5 (C), 129.4 (CH), 126.7 (C), 126.6 (CH), 126.2 (CH), 121.9 (CH₂), 99.7 (C), 74.7 (C), 23.4 (CH₃); **HRMS** (Cl⁺) m/z : [M + H] Calcd for C₁₁H₁₁S 175.0581; Found 175.0584.

389: S-Phenyl 3-methylbut-2-enethioate

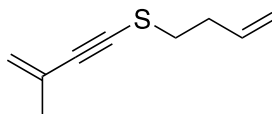
Propargyl acetate **363** (23.4 mg, 0.10 mmol), KAuCl₄ (1.90 mg, 5 mol%) and indole (23.4 mg, 0.20 mmol) were stirred at rt in anhydrous CH₂Cl₂ (1 mL) in a heat-gun dried Schlenk tube under argon for 22 h. The reaction mixture was filtered through a pad of celite and the celite was washed with EtOAc (~3 × 1 mL). The solution was concentrated under reduced pressure and the product was purified by flash column chromatography (0 – 10% EtOAc in hexane) to afford the product as a clear oil (9.00 mg, 46%); **IR (Neat):** $\nu_{\text{max}}/\text{cm}^{-1}$ 2925, 1687 (C=O), 1625, 1439, 1085, 999, 838, 786, 742, 688; **¹H NMR** (400 MHz, CDCl₃) δ 7.47 – 7.38 (m, 5H), 6.10 – 6.07 (m, 1H),

2.15 (d, $J = 1.2$ Hz, 3H), 1.92 (d, $J = 1.2$ Hz, 3H); $^{13}\text{C NMR}$ (101 MHz, CDCl_3) δ 187.4 (C=O), 155.9 (C), 134.8 (CH), 129.3 (CH), 129.2 (CH), 128.6 (C), 122.3 (CH), 27.5 (CH₃), 21.5 (CH₃); **HRMS** (ASAP+) m/z : [M + H] Calcd for C₁₁H₁₃OS 193.0687; Found 193.0688. Data matches that reported in the literature.¹¹⁸

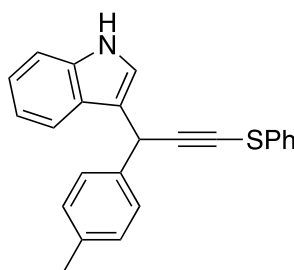
398: 3-(1H-Indol-3-yl)-3-methyl-1-(phenylthio)but-1-en-1-yl acetate



Propargyl acetate **363** (47.0 mg, 0.20 mmol) was dissolved in anhydrous toluene (1 mL) in a heat-gun dried Schlenk tube under argon. Indole (46.8 mg, 0.40 mmol) and KAuCl_4 (3.80 mg, 5 mol%) were added to the reaction mixture and the solution was stirred at rt for 24 h. The reaction mixture was filtered through a pad of celite and the celite was washed with EtOAc ($\sim 3 \times 1$ mL). The solution was concentrated under reduced pressure and the product was purified by flash column chromatography (10% EtOAc in hexane) to afford the product as a brown viscous oil (16.4 mg, 23%); **R_f**: 0.15 (10% EtOAc in hexane, visualisation UV and KMnO_4); **IR (Neat)**: $\nu_{\text{max}}/\text{cm}^{-1}$ 3409 (br, NH stretch), 2924, 1744 (C=O), 1458, 1367, 1188, 1057, 737, 689; **$^1\text{H NMR}$** (400 MHz, CDCl_3) δ 7.99 (s, br, 1H), 7.93 (d, $J = 7.5$ Hz, 1H), 7.36 (dd, $J = 7.3$ and 1.6 Hz, 1H), 7.24 – 7.08 (m, 7H), 7.07 (d, $J = 2.5$ Hz, 1H), 5.81 (s, 1H), 2.23 (s, 3H), 1.62 (s, 6H); **$^{13}\text{C NMR}$** (101 MHz, CDCl_3) δ 168.2 (C=O), 156.3 (C), 137.2 (C), 135.9 (C), 128.9 (CH), 128.8 (CH), 126.2 (CH), 125.8 (C), 122.2 (CH), 122.1 (CH), 121.8 (C), 121.4 (CH), 119.5 (CH), 111.4 (CH), 110.6 (CH), 41.0 (C), 27.1 (CH₃), 20.8 (CH₃); **HRMS** (ES+) m/z : [M + Na] Calcd for C₂₁H₂₁NO₂NaS 374.1191, found 374.1194.

401: But-3-en-1-yl(3-methylbut-3-en-1-yn-1-yl)sulfane

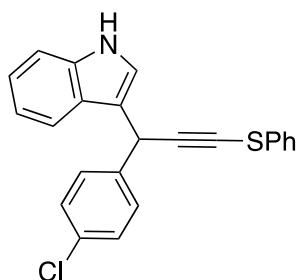
Propargyl acetate **363** (21.3 mg, 0.10 mmol), SPhosAuCl (3.20 mg, 5 mol%) and AgNTf₂ (2.90 mg, 7.5 mol%) were stirred in toluene (1 mL) at 50 °C for 2.5 h in a glass vial. The solution was concentrated under reduced pressure and the product was purified by flash column chromatography (hexane) to afford the product as a clear oil (4.10 mg, 31%); **IR (Neat)**: $\nu_{\text{max}}/\text{cm}^{-1}$ 2926, 1436, 1366, 1193, 1240, 1131, 1011, 803, 616; **¹H NMR** (400 MHz, CDCl₃) δ 5.85 (ddt, $J = 17.0, 10.2$ and 6.7 Hz, 1H), 5.26 – 5.01 (m, 4H), 2.78 (t, $J = 7.3$ Hz, 2H), 2.58 – 2.43 (m, 2H), 1.89 (*app.* t, $J = 1.1$ Hz, 3H); **¹³C NMR** (101 MHz, CDCl₃) δ 135.8 (CH), 127.0 (C), 120.7 (CH₂), 116.9 (CH₂), 95.1 (C), 78.4 (C), 35.0 (CH₂), 33.5 (CH₂), 23.5 (CH₃); **HRMS** (ASAP+) m/z : [M] Calcd for C₉H₁₂S 193.0687; Found 193.0688.

408: 3-(3-(Phenylthio)-1-(*p*-tolyl)prop-2-yn-1-yl)-1H-indole

Propargyl acetate **372** (59.2 mg, 0.20 mmol), indole (25.7 mg, 0.22 mmol) and KAuCl₄ (3.80 mg, 5 mol%) were stirred in toluene (2 mL) at rt for 48 h in a glass vial. The reaction mixture was filtered through a pad of celite and the celite was washed with EtOAc (~3 × 1 mL). The solution was concentrated under reduced pressure and the product was purified by flash column chromatography (10% EtOAc in hexane) to afford the product as a red oil (48.8 mg, 69%); **R_f**: 0.20 (10% EtOAc in hexane, visualisation

UV and KMnO_4); **IR (Neat)**: $\nu_{\text{max}}/\text{cm}^{-1}$ 3412 (br, NH stretch), 2921, 2853, 1510, 1456, 1439, 1022, 736, 687; **$^1\text{H NMR}$** (400 MHz, CDCl_3) δ 7.88 (s, br, 1H), 7.44 (d, $J = 8.0$ Hz, 1H), 7.32 – 7.19 (m, 5H), 7.18 – 7.10 (m, 2H), 7.11 – 6.97 (m, 5H), 6.95 (ddd, $J = 8.0, 7.0$ and 1.0 Hz, 1H), 5.35 (s, 1H), 2.21 (s, 3H); **$^{13}\text{C NMR}$** (101 MHz, CDCl_3) δ 137.9 (C), 136.8 (C), 136.7 (C), 133.7 (C), 129.4 (CH), 129.2 (CH), 127.9 (CH), 126.3 (CH), 126.08 (C), 126.05 (CH), 122.7 (CH), 122.4 (CH), 119.8 (CH), 119.7 (CH), 116.8 (C), 111.4 (CH), 100.2 (C), 68.3 (C), 36.1 (CH), 21.2 (CH_3); **HRMS (ES $^+$)** m/z : $[\text{M} + \text{H}]$ Calcd for $\text{C}_{24}\text{H}_{20}\text{NS}$ 354.1316; Found 354.1326.

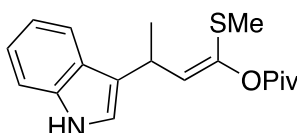
409: 3-(1-(4-Chlorophenyl)-3-(phenylthio)prop-2-yn-1-yl)-1H-indole



Propargyl pivalate **373** (70.0 mg, 0.20 mmol), indole (25.7 mg, 0.22 mmol) and KAuCl_4 (3.80 mg, 5 mol%) were stirred in CH_2Cl_2 (2 mL) at rt for 16 h in a glass vial. The reaction mixture was filtered through a pad of celite and the celite was washed with EtOAc ($\sim 3 \times 1$ mL). The solution was concentrated under reduced pressure and the product was purified by flash column chromatography (10% EtOAc in hexane) to afford the product as a brown oil (10.0 mg, 13%); **R_f**: 0.10 (10% EtOAc in hexane, visualisation UV and KMnO_4); **IR (Neat)**: $\nu_{\text{max}}/\text{cm}^{-1}$ 3415 (br, NH stretch), 3057, 2924, 1580, 1488, 1456, 1090, 1014, 737, 688; **$^1\text{H NMR}$** (400 MHz, CDCl_3) δ 8.08 (s, br, 1H), 7.49 (d, $J = 8.0$ Hz, 1H), 7.43 (d, $J = 8.4$ Hz, 2H), 7.39 – 7.35 (m, 3H), 7.32 – 7.14 (m, 7H), 7.07 (ddd, $J = 8.0, 7.0$ and 1.1 Hz, 1H), 5.47 (s, 1H); **$^{13}\text{C NMR}$** (101 MHz, CDCl_3) δ 139.4 (C), 136.8 (C), 133.3 (C), 132.9 (C), 129.4 (CH), 129.3 (CH), 128.8

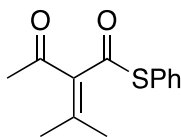
(CH), 126.4 (CH), 126.1 (CH), 125.9 (C), 122.8 (CH), 122.6 (CH), 119.9 (CH), 119.5 (CH), 116.0 (C), 111.5 (CH), 99.2 (C), 69.3 (C), 35.9 (CH); **HRMS** (EI+) m/z: [M] Calcd for C₂₃H₁₆NSCl 373.0692; Found 373.0689.

412: 3-(1H-Indol-3-yl)-1-(methylthio)but-1-en-1-yl pivalate



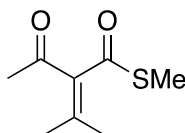
Propargyl pivalate **376** (21.0 mg, 0.10 mmol) was dissolved in toluene (1 mL). Indole (11.7 mg, 0.10 mmol) and KAuCl₄ (1.90 mg, 5 mol%) were added to the reaction mixture and the solution was stirred at 50 °C for 4.5 h. The reaction mixture was filtered through a pad of celite and the celite was washed with EtOAc (~3 × 1 mL). The solution was concentrated under reduced pressure and the product was purified by flash column chromatography (10% EtOAc in hexane) to afford the product as a clear oil (11.5 mg, <36%; product contains minor impurities); **R_f**: 0.10 (10% EtOAc in hexane, visualisation UV and KmnO₄); **IR (Neat)**: $\nu_{\text{max}}/\text{cm}^{-1}$ 3354 (br, NH stretch), 2967, 2927, 1712 (C=O), 1456, 1283, 1120, 1009, 992, 908, 741; **¹H NMR** (400 MHz, CDCl₃) δ 7.98 (s, br, 1H), 7.74 (d, *J* = 7.8 Hz, 1H), 7.35 (d, *J* = 8.0 Hz, 1H), 7.24 – 7.07 (m, 2H), 7.04 (dd, *J* = 2.5, 1.0 Hz, 1H), 5.65 (d, *J* = 9.9 Hz, 1H), 4.26 (dq, *J* = 9.9 and 7.0 Hz, 1H), 2.29 (s, 3H), 1.53 (d, *J* = 7.0 Hz, 3H), 1.28 (s, 9H); **¹³C NMR** (101 MHz, CDCl₃) δ 176.8 (C=O), 141.7 (C), 136.7 (C), 131.2 (CH), 126.8 (C), 122.2 (CH), 120.5 (CH), 120.3 (C), 119.8 (CH), 119.4 (CH), 111.3 (CH), 39.2 (C), 31.1 (CH), 27.3 (CH₃), 21.1 (CH₃), 15.7 (CH₃); **HRMS** (ES+) m/z: [M + H] Calcd for C₁₈H₂₄NO₂S 318.1528; Found 318.1530.

390: S-Phenyl 2-acetyl-3-methylbut-2-enethioate



The title compound was prepared according to **GP12** using propargyl acetate **363** (23.4 mg, 0.10 mmol) and KAuCl_4 (1.70 mg, 5 mol%) in CH_2Cl_2 (1 mL) at rt. The reaction was left for 18 h. Column chromatography (10% EtOAc in hexane) afforded the product as a yellow oil (20.6 mg, 88%). The title compound was also prepared in a separate reaction according to **GP12** using propargyl acetate **363** (208 mg, 0.89 mmol) and KAuCl_4 (8.40 mg, 2.5 mol%) in toluene (9 mL) at rt. The reaction was left for 18 h. Column chromatography (10% EtOAc in hexane) afforded the product as a yellow oil (154 mg, 74%); **R_f**: 0.30 (10% EtOAc in hexane, visualisation UV and KMnO_4); **IR (Neat)**: $\nu_{\text{max}}/\text{cm}^{-1}$ 2918, 1682 (C=O), 1600, 1441, 1956, 1261, 1202, 1137, 809, 745, 688; **¹H NMR** (400 MHz, CDCl_3) δ 7.46 (s, Br, 5H), 2.35 (s, 3H), 2.12 (s, 3H), 2.04 (s, 3H); **¹³C NMR** (101 MHz, CDCl_3) δ 196.0 (C=O), 193.6 (C=O), 153.0 (C), 138.8 (C), 134.4 (CH), 129.9 (CH), 129.6 (CH), 127.5 (C), 30.6 (CH_3), 24.4 (CH_3), 23.0 (CH_3); **HRMS** (ES+) m/z: [M + Na] Calcd for $\text{C}_{13}\text{H}_{14}\text{O}_2\text{NaS}$ 257.0612; Found 257.0613.

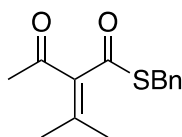
399: S-Methyl 2-acetyl-3-methylbut-2-enethioate



The title compound was prepared according to **GP12** using propargyl acetate **364** (37.3 mg, 0.22 mmol), KAuCl_4 (4.10 mg, 5 mol%) in toluene (2 mL) at 50 °C. The reaction was left for 2.5 h. Column chromatography (10% EtOAc in hexane) afforded the product as a clear oil (30.3 mg, 81%); **R_f**: 0.25 (10% EtOAc in hexane, visualisation

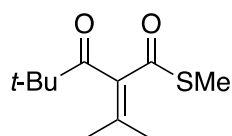
UV and KMnO_4); **IR (Neat)**: $\nu_{\text{max}}/\text{cm}^{-1}$ 2930, 1685 (C=O), 1427, 1357, 1263, 1204, 1144, 1060, 829; **$^1\text{H NMR}$** (400 MHz, CDCl_3) δ 2.41 (s, 3H), 2.25 (s, 3H), 2.06 (s, 3H), 1.93 (s, 3H); **$^{13}\text{C NMR}$** (101 MHz, CDCl_3) δ 196.6 (C=O), 195.5 (C=O), 151.9 (C), 139.2 (C), 30.4 (CH_3), 24.1 (CH_3), 22.9 (CH_3), 12.5 (CH_3); **HRMS (ES $^+$)** m/z : [M + Na] Calcd for $\text{C}_8\text{H}_{12}\text{O}_2\text{SNa}$ 195.0456; Found 195.0457.

415: S-Benzyl 2-acetyl-3-methylbut-2-enethioate



The title compound was prepared according to **GP12** using propargyl acetate **365** (54.8 mg, 0.22 mmol) and KAuCl_4 (4.20 mg, 5 mol%) in toluene (2 mL) at 60 °C. The reaction was left for 2.5 h. Column chromatography (10% EtOAc in hexane) afforded the product as a clear oil (47.2 mg, 86%); **R_f**: 0.20 (10% EtOAc in hexane, visualisation UV and KMnO_4); **IR (Neat)**: $\nu_{\text{max}}/\text{cm}^{-1}$ 2919, 1687 (C=O), 1671 (C=O), 1601, 1496, 1454, 1356, 1263, 1203, 1141, 1058, 976, 887, 824, 701; **$^1\text{H NMR}$** (400 MHz, CDCl_3) δ 7.35 – 7.22 (m, 5H), 4.23 (s, 2H), 2.19 (s, 3H), 2.06 (s, 3H), 1.91 (s, 3H); **$^{13}\text{C NMR}$** (101 MHz, CDCl_3) δ 196.3, 194.3, 152.4, 138.8, 137.2, 128.9, 128.8, 127.6, 34.2, 30.4, 24.1, 22.9; **HRMS (CI $^+$)** m/z : [M + Na] Calcd for $\text{C}_{14}\text{H}_{16}\text{O}_2\text{SNa}$ 271.0769; Found 271.0775.

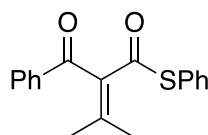
416: S-Methyl 4,4-dimethyl-3-oxo-2-(propan-2-ylidene)pentanethioate



The title compound was prepared according to **GP12** using propargyl pivalate **360** (30.5 mg, 0.14 mmol) and KAuCl_4 (2.10 mg, 5 mol%) in toluene (1 mL) at rt. The

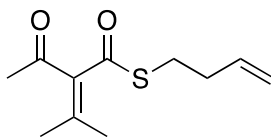
reaction was left for 21 h. Column chromatography (10% EtOAc in hexane) afforded the product as a clear oil (25.3 mg, 83%); **R_f**: 0.30 (10% EtOAc in hexane, visualisation UV and KMnO₄); **IR (Neat)**: $\nu_{\text{max}}/\text{cm}^{-1}$ 2926, 2858, 1750 (C=O), 1668 (C=O), 1279, 1119, 1031, 891; **¹H NMR** (400 MHz, CDCl₃) δ 2.35 (s, 3H), 1.96 (s, 3H), 1.73 (s, 3H), 1.18 (s, 9H); **¹³C NMR** (101 MHz, CDCl₃) δ 211.4 (C=O), 190.7 (C=O), 145.0 (C), 139.7 (C), 46.2 (C), 27.3 (CH₃), 23.7 (CH₃), 21.9 (CH₃), 12.3 (CH₃); **HRMS** (CI⁺) *m/z*: [M + NH₄] Calcd for C₁₁H₂₂NO₂S 232.1371; Found 232.1365.

417: S-Phenyl 2-benzoyl-3-methylbut-2-enethioate



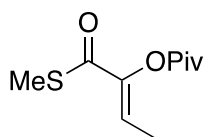
The title compound was prepared according to **GP12** using propargyl benzoate **362** (24.8 mg, 0.08 mmol, purity = 73%; 27% benzyl chloride impurity determined by ¹H NMR spectroscopy) and KAuCl₄ (1.70 mg, 5 mol%) in toluene (1 mL) at 60 °C. The reaction was left for 5 h. Column chromatography (10% EtOAc in hexane) afforded the product as a yellow oil (20.4 mg, 91% wrt true amount of **362** in substrate); **R_f**: 0.25 (10% EtOAc in hexane, visualisation UV and KMnO₄); **IR (Neat)**: $\nu_{\text{max}}/\text{cm}^{-1}$ 2916, 1659 (C=O), 1595, 1440, 1268, 1227, 977, 809, 745, 687; **¹H NMR** (400 MHz, CDCl₃) δ 8.02 (dd, *J* = 8.4 and 1.4 Hz, 2H), 7.63 (tt, *J* = 7.5 and 1.3 Hz, 1H), 7.51 (t, *J* = 7.6 Hz, 2H), 7.42 – 7.34 (m, 3H), 7.34 – 7.28 (m, 2H), 2.20 (s, 3H), 1.80 (s, 3H); **¹³C NMR** (101 MHz, CDCl₃) δ 195.2 (C=O), 188.0 (C=O), 151.3 (C), 137.3 (C), 136.9 (C), 134.7 (CH), 134.1 (CH), 129.8 (CH), 129.7 (CH), 129.3 (CH), 129.1 (CH), 127.6 (C), 24.1 (CH₃), 23.0 (CH₃); **HRMS** (CI⁺) *m/z*: [M + H] Calcd for C₁₈H₁₇O₂S 297.0949; Found 297.0923.

400: S-(But-3-en-1-yl) 2-acetyl-3-methylbut-2-enethioate



The title compound was prepared according to **GP12** using propargyl acetate **366** (21.2 mg, 0.10 mmol) and KAuCl₄ (1.90 mg, 5 mol%) in toluene (1 mL) at 50 °C. The reaction was left for 18 h. Column chromatography (10% EtOAc in hexane) afforded the product as a clear oil (18.6 mg, 88%); **R_f**: 0.34 (10% EtOAc in hexane, visualisation UV and KMNO₄); **IR (Neat)**: $\nu_{\text{max}}/\text{cm}^{-1}$ 2923, 1688 (C=O), 1670 (C=O), 1601, 1436, 1356, 1262, 1203, 1142, 916, 886, 824, 619; **¹H NMR** (400 MHz, CDCl₃) δ 5.79 (ddt, $J = 16.9, 10.2$ and 6.7 Hz, 1H), 5.13 – 5.02 (m, 2H), 3.06 (t, $J = 7.2$ Hz, 2H), 2.39 (app. q, $J = 7.1$ Hz, 2H), 2.25 (s, 3H), 2.06 (s, 3H), 1.93 (s, 3H); **¹³C NMR** (101 MHz, CDCl₃) δ 196.4 (C=O), 195.0 (C=O), 151.9 (C), 139.2 (C), 135.9 (CH), 117.0 (CH₂), 33.5 (CH₂), 30.4 (CH₃), 29.0 (CH₂), 24.1(CH₃), 22.9 (CH₃); **HRMS** (ASAP+) m/z : [M + H] Calcd for C₁₁H₁₇O₂S 213.0949; Found 213.0944.

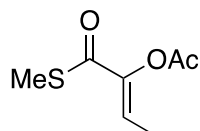
457: 1-(Methylthio)-1-oxobut-2-en-2-yl pivalate



The title compound was prepared according to **GP13** using propargyl pivalate **376** (19.5 mg, 0.10 mmol), 3-acetylpyridine *N*-oxide (16.5 mg, 0.12 mmol) and [IPrAuNCMe]SbF₆ (4.20 mg, 5 mol%) in CH₂Cl₂ (1 mL). The reaction was complete after 4 h. Flash column chromatography (40% CH₂Cl₂ in hexane) afforded the product as a clear oil (15.4 mg, 71%); **R_f**: 0.25 (40% CH₂Cl₂ in hexane, visualisation UV and vanillin); **IR (Neat)**: $\nu_{\text{max}}/\text{cm}^{-1}$ 2975, 2932, 1756 (C=O), 1676 (C=O), 1480, 1271, 1199,

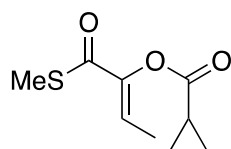
1115, 1090, 1032, 878, 674; **¹H NMR** (400 MHz, CDCl₃) δ 6.61 (q, *J* = 7.2 Hz, 1H), 2.33 (s, 3H), 1.69 (d, *J* = 7.2 Hz, 3H), 1.36 (s, 9H); **¹³C NMR** (101 MHz, CDCl₃) δ 187.7 (C=O), 175.8 (C=O), 144.9 (C), 124.1 (CH), 39.2 (C), 27.2 (CH₃), 11.6 (CH₃), 11.5 (CH₃); **HRMS** (CI+) *m/z*: [M + NH₄] Calcd for C₁₀H₂₀NO₃S 234.1164; Found 234.1160.

459: 1-(Methylthio)-1-oxobut-2-en-2-yl acetate



The title compound was prepared according to **GP13** using propargyl acetate **377** (21.6 mg, 0.14 mmol), 3-acetylpyridine *N*-oxide (27.5 mg, 0.18 mmol) and [IPrAuNCMe]SbF₆ (6.20 mg, 5 mol%) in CH₂Cl₂ (1.5 mL). The reaction was complete after 5 h. Flash column chromatography (40% CH₂Cl₂ in hexane) afforded the product as a clear oil (15.3 mg, 63%); **R_f**: 0.25 (40% CH₂Cl₂ in hexane, visualisation UV and vanillin); **IR (Neat)**: *v*_{max}/cm⁻¹ 1170 (C=O), 1671 (C=O), 1370, 1196, 1026; **¹H NMR** (400 MHz, CDCl₃) δ 6.63 (q, *J* = 7.2 Hz, 1H), 2.34 (s, 3H), 2.29 (s, 3H), 1.73 (d, *J* = 7.2 Hz, 3H); **¹³C NMR** (101 MHz, CDCl₃) δ 187.5 (C=O), 168.4 (C=O), 144.8 (C), 124.7 (CH), 20.5 (CH₃), 11.8 (CH₃), 11.5 (CH₃); **HRMS** (EI+) *m/z*: [M] Calcd for C₇H₁₀O₃S 174.0351; Found 174.0351.

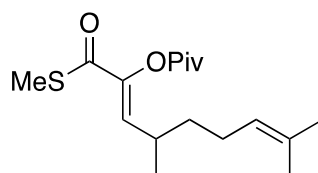
460: 1-(Methylthio)-1-oxobut-2-en-2-yl cyclopropanecarboxylate



The title compound was prepared according to **GP13** using propargyl carboxylate **378** (55.2 mg, 0.30 mmol, purity = 75%), 3-acetylpyridine *N*-oxide (49.0 mg, 0.36 mmol) and [IPrAuNCMe]SbF₆ (12.0 mg, 5 mol%) in CH₂Cl₂ (3 mL). The reaction was complete

after 4 h. Flash column chromatography (10% EtOAc in hexane) afforded the product as a clear oil (28.5 mg, 57% wrt true amount of **378** in substrate); **R_f**: 0.40 (10% EtOAc in hexane, visualisation UV and vanillin); **IR (Neat)**: $\nu_{\text{max}}/\text{cm}^{-1}$ 2929, 1751 (C=O), 1671 (C=O), 1386, 1201, 1131, 1089, 879, 866; **¹H NMR** (400 MHz, CDCl₃) δ 6.61 (q, $J = 7.2$ Hz, 1H), 2.33 (s, 3H), 1.84 (tt, $J = 8.0$ and 4.6 Hz, 1H), 1.72 (d, $J = 7.2$ Hz, 3H), 1.23 – 1.16 (m, 2H), 1.07 – 0.99 (m, 2H); **¹³C NMR** (101 MHz, CDCl₃) δ 187.6 (C=O), 172.3 (C=O), 144.6 (C), 124.5 (CH), 12.7 (CH), 11.8 (CH₃), 11.5 (CH₃), 9.4 (CH₂); **HRMS** (CI⁺) m/z : [M + NH₄] Calcd for C₉H₁₆NO₃S 218.0851; Found 218.0860.

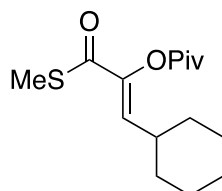
461: 4,8-Dimethyl-1-(methylthio)-1-oxonona-2,7-dien-2-yl pivalate



The title compound was prepared according to **GP13** using propargyl pivalate **367** (58.0 mg, 0.20 mmol), 3-acetylpyridine *N*-oxide (32.9 mg, 0.24 mmol) and [IPrAuNCMe]SbF₆ (8.40 mg, 5 mol%) in CH₂Cl₂ (2 mL). The reaction was left to stir for 15 h. Flash column chromatography (10% EtOAc in hexane) afforded the product as a clear oil (38.0 mg, 61%); **R_f**: 0.40 (10% EtOAc in hexane, visualisation UV and vanillin); **IR (Neat)**: $\nu_{\text{max}}/\text{cm}^{-1}$ 2968, 2929, 1758 (C=O), 1672 (C=O), 1480, 1269, 1148, 1101, 1030; **¹H NMR** (400 MHz, CDCl₃) δ 6.33 (d, $J = 10.3$ Hz, 1H), 5.04 (tt, $J = 7.1$, 1.4 Hz, 1H), 2.42 – 2.31 (m, 1H), 2.33 (s, 3H), 2.06 – 1.85 (m, 2H), 1.66 (d, $J = 1.3$ Hz, 3H), 1.58 (s, 3H), 1.44 – 1.35 (m, 2H), 1.35 (s, 9H), 1.02 (d, $J = 6.7$ Hz, 3H); **¹³C NMR** (101 MHz, CDCl₃) δ 188.0 (C=O), 176.1 (C=O), 143.3 (C), 134.3 (CH), 132.2 (C), 124.0 (CH), 39.2 (C), 36.5 (CH₂), 30.9 (CH), 27.2 (CH₃), 25.91 (CH₂), 25.87 (CH₃), 19.6

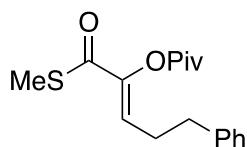
(CH₃), 17.8 (CH₃), 11.5 (CH₃); **HRMS** (EI⁺) m/z: [M] Calcd for C₁₇H₂₈O₃S 312.1759; Found 312.1760.

462: 1-Cyclohexyl-3-(methylthio)-3-oxoprop-1-en-2-yl pivalate



The title compound was prepared according to **GP13** using propargyl pivalate **368** (18.1 mg, 0.07 mmol), 3-acetylpyridine *N*-oxide (12.3 mg, 0.09 mmol) and [IPrAuNCMe]SbF₆ (4.20 mg, 5 mol%) in CH₂Cl₂ (0.7 mL). The reaction was left to stir for 18 h. Flash column chromatography (10% EtOAc in hexane) afforded the product as a clear oil (14.0 mg, 70%); **R_f**: 0.30 (10% EtOAc in hexane, visualisation UV and KMNO₄); **IR (Neat)**: $\nu_{\text{max}}/\text{cm}^{-1}$ 2927, 2853, 1758 (C=O), 1671 (C=O), 1480, 1450, 1138, 1096; **¹H NMR** (400 MHz, CDCl₃) δ 6.39 (d, *J* = 9.7 Hz, 1H), 2.32 (s, 3H), 2.24 – 2.12 (m, 1H), 1.82 – 1.60 (m, 6H), 1.35 (s, 9H), 1.31 – 1.09 (m, 4H); **¹³C NMR** (101 MHz, CDCl₃) δ 188.1 (C=O), 176.3 (C=O), 142.6 (C), 133.6 (CH), 39.2 (C), 35.9 (CH), 31.7 (CH₂), 27.2 (CH₃), 25.9 (CH₂), 25.6 (CH₂), 11.5 (CH₃); **HRMS** (CI⁺) m/z: [M + NH₄] Calcd for C₁₅H₂₈NO₃S 302.1790; Found 302.1778.

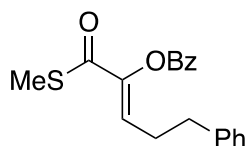
463: 1-(Methylthio)-1-oxo-5-phenylpent-2-en-2-yl pivalate



The title compound was prepared according to **GP13** using propargyl pivalate **371** (59.0 mg, 0.20 mmol), 3-acetylpyridine *N*-oxide (33.0 mg, 0.24 mmol) and [IPrAuNCMe]SbF₆ (8.40 mg, 5 mol%) in CH₂Cl₂ (2 mL). The reaction was complete after 5 h. Flash column chromatography (0 – 10% EtOAc in hexane) afforded the

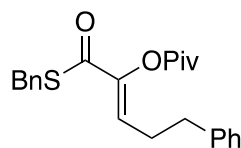
product as a clear oil (42.9 mg, 70%); **R_f**: 0.50 (10% EtOAc in hexane, visualisation UV and vanillin); **IR (Neat)**: $\nu_{\text{max}}/\text{cm}^{-1}$ 2973, 1756 (C=O), 1671 (C=O), 1479, 1145, 1100, 1030, 937, 747, 698; **¹H NMR** (400 MHz, CDCl₃) δ 7.33 – 7.26 (m, 2H), 7.25 – 7.14 (m, 3H), 6.56 (t, *J* = 7.6 Hz, 1H), 2.75 (t, *J* = 7.7 Hz, 2H), 2.37 (*app. q*, *J* = 7.7 Hz, 2H), 2.33 (s, 3H), 1.34 (s, 9H); **¹³C NMR** (101 MHz, CDCl₃) δ 187.8 (C=O), 176.0 (C=O), 144.2 (C), 140.7 (C), 128.7 (CH), 128.4 (CH), 127.7 (CH), 126.4 (CH), 39.2 (C), 34.3 (CH₂), 28.0 (CH₂), 27.2 (CH₃), 11.5 (CH₃); **HRMS** (EI+) *m/z*: [M] Calcd for C₁₇H₂₂O₃S 306.1290; Found 306.1302.

464: 1-(Methylthio)-1-oxo-5-phenylpent-2-en-2-yl benzoate



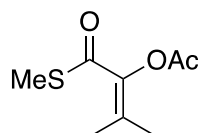
The title compound was prepared according to **GP13** using propargyl benzoate **369** (31.0 mg, 0.10 mmol), 3-acetylpyridine *N*-oxide (16.5 mg, 0.12 mmol) and [IPrAuNCMe]SbF₆ (4.20 mg, 5 mol%) in CH₂Cl₂ (1 mL). The reaction was complete after 6 h. Flash column chromatography (0 – 10% EtOAc in hexane) afforded the product as a clear oil (20.0 mg, 61%); **R_f**: 0.45 (10% EtOAc in hexane, visualisation UV and vanillin); **IR (Neat)**: $\nu_{\text{max}}/\text{cm}^{-1}$ 3029, 2929, 1739 (C=O), 1669 (C=O), 1452, 1236, 1055, 1024, 746, 698; **¹H NMR** (400 MHz, CDCl₃) δ 8.15 (dd, *J* = 8.3 and 1.4 Hz, 2H), 7.65 (t, *J* = 7.5 Hz, 1H), 7.51 (t, *J* = 7.8 Hz, 2H), 7.33 – 7.25 (m, 2H), 7.23 – 7.12 (m, 3H), 6.69 (t, *J* = 7.5 Hz, 1H), 2.80 (t, *J* = 7.7 Hz, 2H), 2.49 (*app. q*, *J* = 7.7 Hz, 2H), 2.34 (s, 3H); **¹³C NMR** (101 MHz, CDCl₃) δ 187.8 (C=O), 164.1 (C=O), 144.0 (C), 140.6 (C), 134.1 (CH), 130.6 (CH), 128.8 (CH), 128.7 (CH), 128.5 (CH), 128.3 (CH), 126.4 (CH), 34.3 (CH₂), 28.2 (CH₂), 11.5 (CH₃); **HRMS** (CI+) *m/z*: [M + NH₄] Calcd for C₁₉H₂₂NO₃S 344.1320; Found 344.1328.

465: 1-(Benzylthio)-1-oxo-5-phenylpent-2-en-2-yl pivalate



The title compound was prepared according to **GP13** using propargyl pivalate **370** (53.0 mg, 0.14 mmol), 3-acetylpyridine *N*-oxide (24.7 mg, 0.18 mmol) and [IPrAuNCMe]SbF₆ (6.20 mg, 5 mol%) in CH₂Cl₂ (1.5 mL). The reaction was left to stir for 14 h. Flash column chromatography (0 – 10% EtOAc in hexane) afforded the product as a yellow oil (39.9 mg, 75%); **R_f**: 0.40 (10% EtOAc in hexane, visualisation UV and KMNO₄); **IR (Neat)**: $\nu_{\text{max}}/\text{cm}^{-1}$ 2974, 1755 (C=O), 1669 (C=O), 1479, 1146, 1102, 1086, 907, 729, 697, 673; **¹H NMR** (400 MHz, CDCl₃) δ 7.31 – 7.17 (m, 8H), 7.16 – 7.11 (m, 2H), 6.55 (t, *J* = 7.6 Hz, 1H), 4.14 (s, 2H), 2.71 (t, *J* = 7.7 Hz, 2H), 2.34 (app. q, *J* = 7.7 Hz, 2H), 1.30 (s, 9H); **¹³C NMR** (101 MHz, CDCl₃) δ 186.8 (C=O), 175.9 (C=O), 144.0 (C), 140.7 (C), 137.0 (C), 129.1 (CH), 128.9 (CH), 128.7 (CH), 128.42 (CH), 128.36 (CH), 127.5 (CH), 126.4 (CH), 39.2 (C), 34.2 (CH₂), 33.2 (CH₂), 28.1 (CH₂), 27.2 (CH₃), a quaternary carbon was not observed; **HRMS** (EI+) *m/z*: [M] Calcd for C₂₃H₂₆O₃S 382.1603; Found 382.1597.

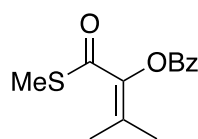
466: 3-Methyl-1-(methylthio)-1-oxobut-2-en-2-yl acetate



The title compound was prepared according to **GP13** using propargyl acetate **364** (18.9 mg, 0.11 mmol), 3-acetylpyridine *N*-oxide (16.4 mg, 0.12 mmol) and [IPrAuNCMe]SbF₆ (4.20 mg, 5 mol%) in CH₂Cl₂ (1 mL). The reaction was complete after 4 h. Flash column chromatography (5% EtOAc in hexane) afforded the product

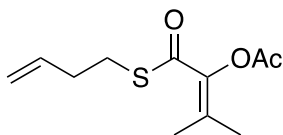
as a clear oil (8.50 mg, 41%); **R_f**: 0.20 (5% EtOAc in hexane, visualisation UV and KMNO₄); **IR (Neat)**: $\nu_{\text{max}}/\text{cm}^{-1}$ 2928, 1772 (C=O), 1671 (C=O), 1371, 1195, 1169, 1131, 973, 813; **¹H NMR** (400 MHz, CDCl₃) δ 2.28 (s, 6H), 2.23 (s, 3H), 1.75 (s, 3H); **¹³C NMR** (101 MHz, CDCl₃) δ 188.2 (C=O), 169.3 (C=O), 138.6 (C), 138.3 (C), 21.1 (CH₃), 20.8 (CH₃), 19.8 (CH₃), 11.5 (CH₃); **HRMS** (CI⁺) *m/z*: [M + NH₄] Calcd for C₈H₁₆NO₃S 206.0851; Found 206.0860.

467: 3-Methyl-1-(methylthio)-1-oxobut-2-en-2-yl benzoate



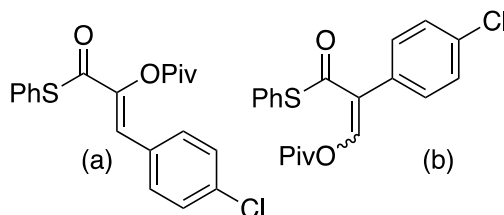
The title compound was prepared according to **GP13** using propargyl benzoate **361** (25.0 mg, 0.11 mmol), 3-acetylpyridine *N*-oxide (17.8 mg, 0.13 mmol) and [IPrAuNCMe]SbF₆ (4.50 mg, 5 mol%) in CH₂Cl₂ (1.3 mL). The reaction was complete after 6 h. Flash column chromatography (10% EtOAc in hexane) afforded the product as a clear oil (17.1 mg, 62%); **R_f**: 0.30 (10% EtOAc in hexane, visualisation UV and KMNO₄); **IR (Neat)**: $\nu_{\text{max}}/\text{cm}^{-1}$ 2927, 1741 (C=O), 1670 (C=O), 1451, 1240, 1128, 1052, 811, 704; **¹H NMR** (400 MHz, CDCl₃) δ 8.21 (dd, *J* = 8.4 and 1.3 Hz, 2H), 7.66 (t, *J* = 7.4 Hz, 1H), 7.53 (tt, *J* = 7.7 and 1.3 Hz, 2H), 2.31 (s, 3H), 2.26 (s, 3H), 1.80 (s, 3H); **¹³C NMR** (101 MHz, CDCl₃) δ 188.3 (C=O), 164.8 (C=O), 138.9 (C), 138.4 (C), 134.0 (CH), 130.5 (CH), 128.9 (C), 128.8 (CH), 21.2 (CH₃), 19.9 (CH₃), 11.5 (CH₃); **HRMS** (CI⁺) *m/z*: [M + H] Calcd for C₁₃H₁₅O₃S 251.0742; Found 251.0740.

468: 1-(But-3-en-1-ylthio)-3-methyl-1-oxobut-2-en-2-yl acetate



The title compound was prepared according to **GP13** using propargyl acetate **366** (32.0 mg, 0.15 mmol), 3-acetylpyridine *N*-oxide (24.7 mg, 0.18 mmol) and [IPrAuNCMe]SbF₆ (6.20 mg, 5 mol%) in CH₂Cl₂ (1.5 mL). The reaction was left to stir for 12 h. Flash column chromatography (10% EtOAc in hexane) afforded the product as a clear oil (17.5 mg, 51%); **R_f**: 0.20 (10% EtOAc in hexane, visualisation UV and KMNO₄); **IR (Neat)**: $\nu_{\text{max}}/\text{cm}^{-1}$ 2925, 1773 (C=O), 1671 (C=O), 1371, 1195, 1167, 1131, 970, 812; **¹H NMR** (400 MHz, CDCl₃) δ 5.79 (ddt, *J* = 16.9, 10.2 and 6.6 Hz, 1H), 5.15 – 4.97 (m, 2H), 2.92 (t, *J* = 7.4 Hz, 2H), 2.32 (*app.* q, *J* = 7.4 Hz, 2H), 2.27 (s, 3H), 2.22 (s, 3H), 1.75 (s, 3H); **¹³C NMR** (101 MHz, CDCl₃) δ 187.6 (C=O), 169.3 (C=O), 138.7 (C), 138.3 (C), 136.3 (CH), 116.5 (CH₂), 33.5 (CH₂), 27.9 (CH₂), 21.1 (CH₃), 20.8 (CH₃), 19.8 (CH₃); **HRMS** (CI⁺) *m/z*: [M + NH₄] Calcd for C₁₁H₂₀NO₃S 246.1164; Found 246.1176.

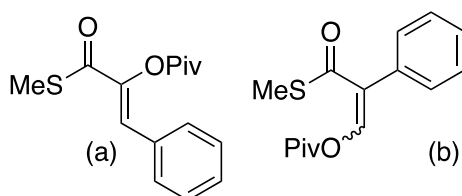
443: 1-(4-Chlorophenyl)-3-oxo-3-(phenylthio)prop-1-en-2-yl pivalate



The title compound was prepared according to **GP13** using propargyl pivalate **373** (99.0 mg, 0.28 mmol), 3-acetylpyridine *N*-oxide (45.2 mg, 0.33 mmol) and [IPrAuNCMe]SbF₆ (12.0 mg, 5 mol%) in CH₂Cl₂ (3 mL). The reaction was left to stir for 24 h. Flash column chromatography (10% EtOAc in hexane) afforded the product as

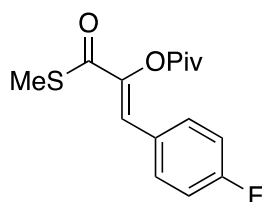
a yellow solid (20.9 mg, 20%) as a mixture of regioisomers (3.0:1, **443a:443b**); **R_f**: 0.30 (5% EtOAc in hexane, visualisation UV and KMNO₄); **mp**: 46 – 50 °C; **IR (Neat)**: $\nu_{\max}/\text{cm}^{-1}$ 2967, 1760 (C=O), 1670 (C=O), 1477, 1440, 1265, 1151, 1085, 1012, 950, 818, 746, 687; **¹H NMR** (400 MHz, CDCl₃) δ 7.52 (d, *J* = 8.5 Hz, 2H), 7.49 – 7.42 (m, 5H), 7.37 (d, *J* = 8.5 Hz, 2H), 7.35 (s, 1H), 1.39 (s, 9H); **¹³C NMR** (101 MHz, CDCl₃) δ 186.2 (C=O), 175.5 (C=O), 143.1 (C), 136.1 (C), 135.2 (CH), 131.5 (CH), 130.5 (C), 129.9 (CH), 129.5 (CH), 129.2 (CH), 126.5 (C), 124.9 (CH), 39.3 (C) 27.3 (CH₃); **HRMS** (Cl⁺) *m/z*: [M + NH₄] Calcd for C₂₀H₂₃O₃SCl 392.1087; Found 392.1096.

445: 3-(Methylthio)-3-oxo-1-phenylprop-1-en-2-yl pivalate



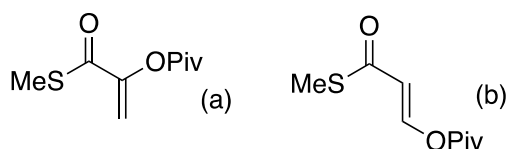
The title compound was prepared according to **GP13** using propargyl pivalate **374** (39.0 mg, 0.15 mmol), 3-acetylpyridine *N*-oxide (24.7 mg, 0.18 mmol) and [IPrAuNCMe]SbF₆ (6.20 mg, 5 mol%) in CH₂Cl₂ (1.5 mL). The reaction was left to stir for 24 h. Flash column chromatography (0 -10% EtOAc in hexane) afforded the product as a yellow solid (14.0 mg, 34%) as a mixture of regioisomers (11:1, **445a:445b**); **R_f**: 0.55 (10% EtOAc in hexane, visualisation UV and KMNO₄); **mp**: 75 – 79 °C; **IR (Neat)**: $\nu_{\max}/\text{cm}^{-1}$ 2976, 2931, 1758 (C=O), 1665 (C=O), 1632, 1480, 1296, 1155, 1090, 951, 767, 753, 692; **¹H NMR** (400 MHz, CDCl₃) δ 7.58 – 7.52 (m, 1H), 7.42 – 7.34 (m, 4H), 7.33 (s, 1H), 2.40 (s, 3H), 1.39 (s, 9H); **¹³C NMR** (101 MHz, CDCl₃) δ 188.5 (C=O), 175.8 (C=O), 143.0 (C), 132.0 (C), 130.3 (CH), 130.0 (CH), 128.8 (CH), 125.1 (CH), 39.3 (C), 27.3 (CH₃), 11.9 (CH₃); **HRMS** (Cl⁺) *m/z*: [M] Calcd for C₁₅H₁₈O₃S 278.0977; Found 278.0979.

446: 1-(4-Fluorophenyl)-3-(methylthio)-3-oxoprop-1-en-2-yl pivalate



The title compound was prepared according to **GP13** using propargyl pivalate **375** (56.0 mg, 0.20 mmol), 3-acetylpyridine *N*-oxide (33.0 mg, 0.22 mmol) and [IPrAuNCMe]SbF₆ (8.20 mg, 5 mol%) in CH₂Cl₂ (2 mL). The reaction was left to stir for 24 h. Flash column chromatography (10% EtOAc in hexane) afforded the product as white needles (19.2 mg, 32%); **R_f**: 0.55 (10% EtOAc in hexane, visualisation UV and KMNO₄); **mp**: 88 – 92 °C; **IR (Neat)**: $\nu_{\text{max}}/\text{cm}^{-1}$ 2929, 1759 (C=O), 1670 (C=O), 1596, 1506, 1158, 1081, 952, 816, 796; **¹H NMR** (400 MHz, CDCl₃) δ 7.55 (dd, *J* = 9.6 and 5.4 Hz, 2H), 7.29 (s, 1H), 7.06 (*app. t*, *J* = 8.7 Hz, 2H), 2.40 (s, 3H), 1.39 (s, 9H); **¹³C NMR** (101 MHz, CDCl₃) δ 188.4 (C=O), 175.7 (C=O), 163.47 (d, ¹*J*_{C-F} = 251.6 Hz, C), 142.8 (C), 132.3 (d, ³*J*_{C-F} = 8.6 Hz, CH), 128.2 (d, ⁴*J*_{C-F} = 3.3 Hz, C), 123.9 (CH), 116.0 (d, ²*J*_{C-F} = 21.7 Hz, CH), 39.3 (C), 27.3 (CH₃), 11.9 (CH₃); **¹⁹F NMR** (376 MHz, CDCl₃): δ -109.5; **HRMS** (ES+) *m/z*: [M + Na] Calcd for C₁₅H₁₇O₃NaSF 319.0780; Found 319.0787.

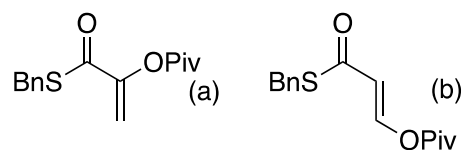
470: 3-(Methylthio)-3-oxoprop-1-en-2-yl pivalate



The title compound was prepared according to **GP13** using propargyl pivalate **357** (32.1 mg, 0.17 mmol), 3-acetylpyridine *N*-oxide (28.0 mg, 0.20 mmol) and [IPrAuNCMe]SbF₆ (6.90 mg, 5 mol%) in CH₂Cl₂ (1.7 mL). The reaction was left to stir

for 24 h. Flash column chromatography (5% EtOAc in hexane) afforded the product as a clear oil (22.5 mg, 37% **470a+b**) as a mixture of products (3.3:1:1, **367:470a:470b**); **R_f**: 0.20 (5% EtOAc in hexane, visualisation UV and KMNO₄); **IR (Neat)**: $\nu_{\max}/\text{cm}^{-1}$ 2930, 1764 (C=O), 1673 (C=O), 1481, 1160, 1119, 1084, 1019, 894, 821; **¹H NMR** (400 MHz, CDCl₃) δ (all distinct resonances for both isomers) 8.32 (d, $J = 12.4$ Hz, 1H), 6.09 (d, $J = 12.4$ Hz, 1H), 6.04 (d, $J = 2.3$ Hz, 1H), 5.34 (d, $J = 2.3$ Hz, 1H), 2.37 (s, 3H), 2.36 (s, 3H), 1.33 (s, 9H), 1.27 (s, 9H); **¹³C NMR** (101 MHz, CDCl₃) δ (all distinct resonances for both isomers) 189.5 (C=O), 188.0 (C=O), 176.2 (C=O), 174.6 (C=O), 149.6 (C), 146.9 (CH), 112.8 (CH), 110.4 (CH₂), 39.2 (C), 38.9 (C), 27.1 (CH₃), 26.9 (CH₃), 19.1 (CH₃), 11.6 (CH₃); **HRMS** (CI+) m/z : [M + H] Calcd for C₉H₁₅O₃S 203.0742; Found 203.0733.

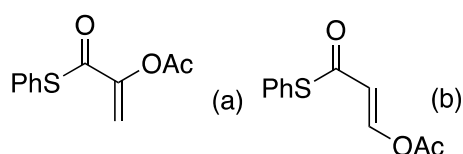
471: 3-(Benzylthio)-3-oxoprop-1-en-2-yl pivalate



The title compound was prepared according to **GP13** using propargyl pivalate **358** (28.0 mg, 0.10 mmol), 3-acetylpyridine *N*-oxide (16.5 mg, 0.12 mmol) and [IPrAuNCMe]SbF₆ (4.10 mg, 5 mol%) in CH₂Cl₂ (1 mL). The reaction was left to stir for 24 h. Flash column chromatography (5% EtOAc in hexane) afforded the product as a clear oil (17.3 mg, 42% of **471a+b**) as a mixture of products (4.7:1.4:1, **358:471a:471b**); **R_f**: 0.40 (5% EtOAc in hexane, visualisation UV and KMNO₄); **IR (Neat)**: $\nu_{\max}/\text{cm}^{-1}$ 2975, 2931, 1759 (C=O), 1671 (C=O), 1631, 1480, 1455, 1256, 1161, 1105, 1014, 996, 966, 892, 819, 700; **¹H NMR** (400 MHz, CDCl₃) δ (all distinct resonances for both regioisomers) 8.35 (d, $J = 12.4$ Hz, 1H), 7.36 – 7.21 (m, 5H), 6.03 (d, $J = 12.4$ Hz, 1H), 6.01 (d, $J = 2.3$ Hz, 1H), 5.33 (d, $J = 2.3$ Hz, 1H), 4.17 (s, 2H),

4.15 (s, 2H), 1.28 (s, 9H), 1.22 (s, 9H); ^{13}C NMR (101 MHz, CDCl_3) δ (all distinct resonances for both isomers) 188.4 (C=O), 187.0 (C=O), 176.2 (C=O), 174.5 (C=O), 149.4 (C), 147.4 (CH), 137.6 (C), 136.8 (C), 129.1 (CH), 129.0 (CH), 128.79 (CH), 128.75 (CH), 127.6 (CH), 127.5 (CH), 112.6 (CH), 110.9 (CH_2), 39.2 (C), 39.1 (C), 33.4 (CH_2), 33.2 (CH_2), 27.1 (CH_3) 26.9 (CH_3); **HRMS** (CI+) m/z: [M + H] Calcd for $\text{C}_{15}\text{H}_{19}\text{O}_3\text{S}$ 279.1055: Found 279.1047.

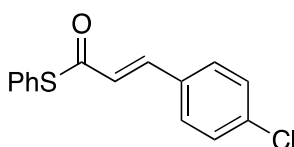
472: 3-Oxo-3-(phenylthio)prop-1-en-2-yl acetate



Propargyl acetate **359** (43.0 mg, 0.21 mmol) and 3-acetylpyridine *N*-oxide (34.3 mg, 0.25 mmol) were dissolved in anhydrous CHCl_3 (3 mL) in a heat-gun dried Schlenk tube under argon. $[\text{IPrAuNCMe}]\text{SbF}_6$ (9.00 mg, 5 mol%) was added to the solution under a positive pressure of argon and the reaction mixture was stirred at 50 °C for 14 h. The reaction mixture was filtered through a short pad of celite at rt and the celite was washed with EtOAc ($\sim 3 \times 1$ mL/mmol). The solution was concentrated under reduced pressure and the product was purified by flash column chromatography (10% EtOAc in hexane) to afford the product as a yellow oil (4.70 mg, 10%) as a mixture of regioisomers (1.5:1, **472a:472b**); **R_f**: 0.40 (10% EtOAc in hexane, visualisation UV and KMnO_4); **IR (Neat)**: $\nu_{\text{max}}/\text{cm}^{-1}$ 3062, 1772 (C=O), 1686 (C=O), 1633, 1370, 1187, 1018, 949, 898, 747, 689; ^1H NMR (400 MHz, CDCl_3) δ (all distinct resonances for both regioisomers) 8.37 (d, $J = 12.4$ Hz, 1H), 7.50 – 7.36 (m, 5H), 6.12 (d, $J = 12.4$ Hz, 1H), 6.13 (d, $J = 2.5$ Hz, 1H), 5.49 (d, $J = 2.6$ Hz, 1H), 2.28 (s, 3H), 2.24 (s, 3H); ^{13}C NMR (101 MHz, CDCl_3) δ (all distinct resonances for both isomers) 187.4 (C=O), 185.7 (C=O), 168.5 (C=O), 166.9 (C=O), 149.1 (C), 147.2 (CH), 135.0

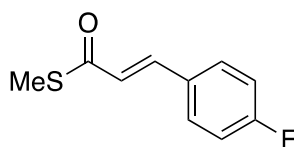
(CH), 134.8 (CH), 130.0 (CH), 129.7 (CH), 129.5 (CH), 129.4 (CH), 127.3 (C), 126.3 (C), 112.3 (CH), 112.1 (CH₂), 20.6 (CH₃), 20.7 (CH₃); **HRMS** (EI+) m/z: [M] Calcd for C₁₁H₁₀O₃S 222.0351; Found 222.0357.

444: S-Phenyl (E)-3-(4-chlorophenyl)prop-2-enethioate



Propargyl pivalate **373** (35.8 mg, 0.10 mmol) and 3,5-dichloropyridine *N*-oxide (18.9 mg, 0.11 mmol) were dissolved in toluene (1 mL) in a glass vial. XPhosAuNTf₂ (4.30 mg, 5 mol%) was added to the solution and the reaction mixture was stirred at 50 °C for 3 h. The reaction mixture was filtered through a short pad of celite at rt and the celite was washed with EtOAc (~3 × 1 mL/mmol). The solution was concentrated under reduced pressure and the product was purified by flash column chromatography (10% EtOAc in hexane) to afford the product as a yellow solid (20.7 mg, 76%); **IR (Neat)**: $\nu_{\text{max}}/\text{cm}^{-1}$ 2924, 1685 (C=O), 1615, 1590, 1491, 1090, 1029, 813, 779, 746, 689; **¹H NMR** (400 MHz, CDCl₃) δ 7.62 (d, *J* = 15.8 Hz, 1H), 7.53 – 7.42 (m, 7H), 7.41 – 7.35 (m, 2H), 6.76 (d, *J* = 15.8 Hz, 1H); **HRMS** (ASAP+) m/z: [M + H] Calcd for C₁₅H₁₂OSCl 275.0297; Found 275.0303. Data matches that reported in the literature.¹¹⁹

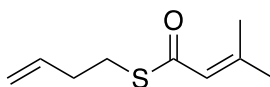
450: S-Methyl (E)-3-(4-fluorophenyl)prop-2-enethioate



Propargyl pivalate **375** (28.3 mg, 0.10 mmol) and 2-(methoxycarbonyl)pyridine *N*-oxide (17.0 mg, 0.11 mmol) were dissolved in CH₂Cl₂ (1 mL) in a glass vial.

[IPrAuNCMe]SbF₆ (4.50 mg, 5 mol%) was added to the solution and the reaction mixture was stirred at rt for 18 h. The reaction mixture was filtered through a short pad of celite at rt and the celite was washed with EtOAc (~3 × 1 mL/mmol). The solution was concentrated under reduced pressure and the product was purified by flash column chromatography (30% toluene in hexane) to afford the product as white needles (6.70 mg, 34%); **IR (Neat):** $\nu_{\text{max}}/\text{cm}^{-1}$ 2936, 1659 (C=O), 1615, 1599, 1588, 1512, 1233, 1165, 1046, 830, 823, 744; **¹H NMR** (400 MHz, CDCl₃) δ 7.58 (d, J = 15.8 Hz, 1H), 7.55 – 7.51 (m, 2H), 7.09 (*app. t*, J = 8.6 Hz, 2H), 6.66 (dd, J = 15.8 Hz, 1H), 2.43 (s, 3H); **¹³C NMR** (400 MHz, CDCl₃) δ 190.3 (C=O), 164.2 (d, $^1J_{\text{C-F}}$ = 252.1 Hz, C), 139.1 (CH), 130.4 (d, $^3J_{\text{C-F}}$ = 8.5 Hz, CH), 124.7 (CH), 116.3 (d, $^2J_{\text{C-F}}$ = 22.0 Hz, CH), 11.8 (CH₃), *a quaternary carbon was not observed*; **HRMS** (EI+) m/z : [M] Calcd for C₁₀H₉OFS 196.0358; Found 196.0355.

469: S-(but-3-en-1-yl) 3-methylbut-2-enethioate



The title compound was prepared according to **GP13** using propargyl acetate **366** (32.0 mg, 0.15 mmol), 3-acetylpyridine *N*-oxide (24.7 mg, 0.18 mmol) and [IPrAuNCMe]SbF₆ (6.20 mg, 5 mol%) in CH₂Cl₂ (1.5 mL). Flash column chromatography (10% EtOAc in hexane) afforded the product as a clear oil (6.91 mg, 27%); **IR (Neat):** $\nu_{\text{max}}/\text{cm}^{-1}$ 2919, 2857, 1681 (C=O), 1627, 1443, 1259, 1017, 795; **¹H NMR** (400 MHz, CDCl₃) δ 6.00 – 5.97 (m, 1H), 5.81 (ddt, J = 16.9, 10.2 and 6.6 Hz, 1H), 5.13 – 5.00 (m, 2H), 2.96 (t, J = 7.3 Hz, 2H), 2.39 – 2.30 (m, 2H), 2.16 (d, J = 1.3 Hz, 3H), 1.87 (d, J = 1.3 Hz, 3H); **¹³C NMR** (101 MHz, CDCl₃) δ 189.3 (C=O), 153.7

(C), 136.5 (CH), 123.5 (CH), 116.4 (CH₂), 34.0 (CH₂), 28.1 (CH₂), 27.4 (CH₃), 21.3 (CH₃); **HRMS** (CI+) m/z: [M + H] Calcd for C₉H₁₅OS 171.0844; Found 171.0840.

5 Appendix

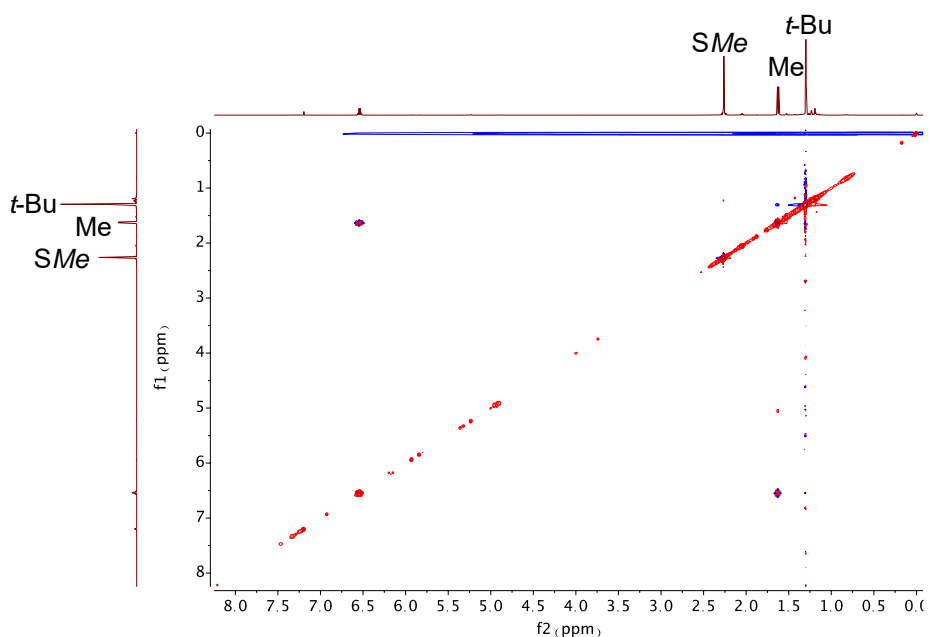
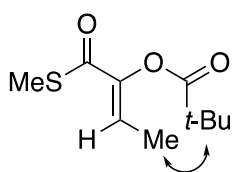
For all relevant spectra for “Chapter 2 : Gold-catalysed oxyarylation of alkynes with benzothiophene S-oxides” please see the supplementary information of our published paper “Gold-Catalyzed Intermolecular Alkyne Oxyarylation for C3 Functionalization of Benzothiophenes”²⁹

Link to supplementary information:

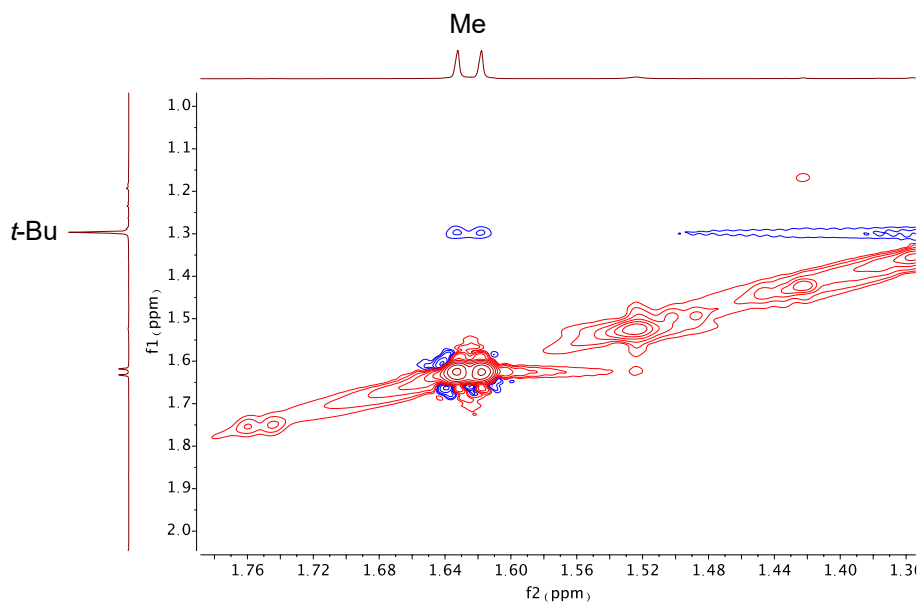
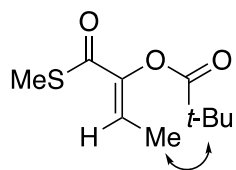
<https://pubs.acs.org/doi/10.1021/acs.orglett.0c03596>

5.1 NOESY Spectra for Stereochemical Assignment of Captodative Olefins

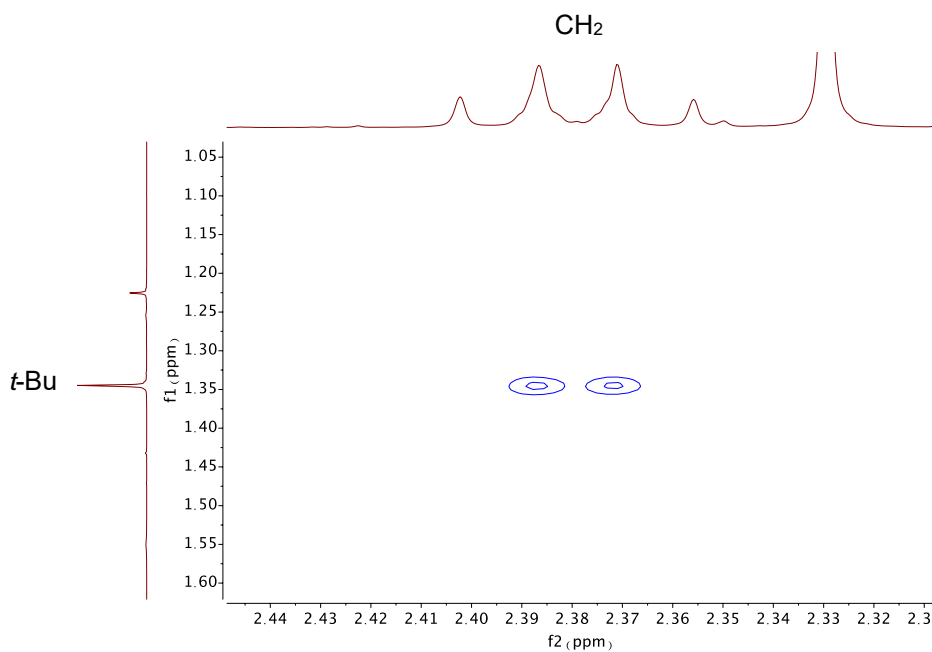
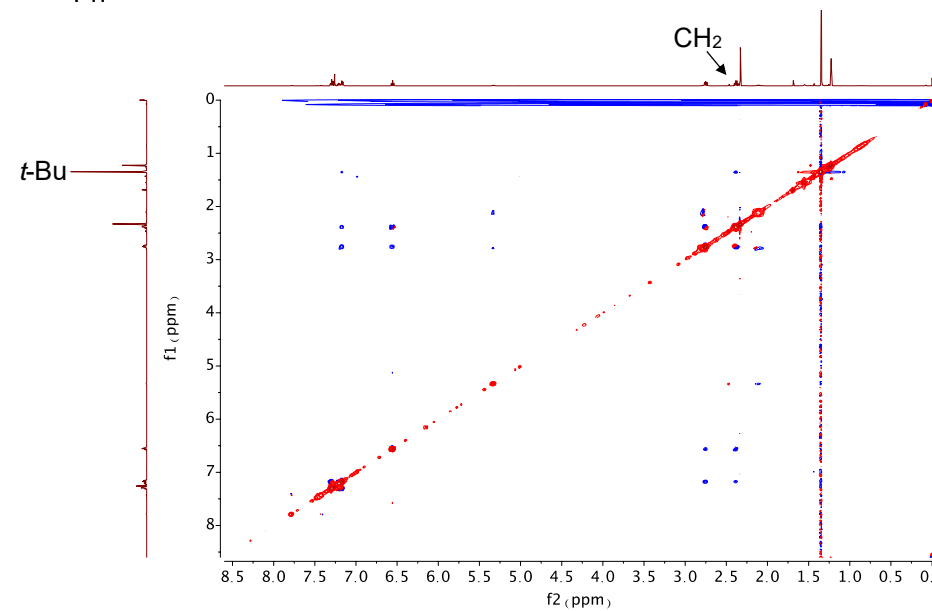
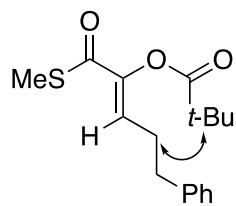
NOESY of compound 457 (CDCl₃, 500 MHz)



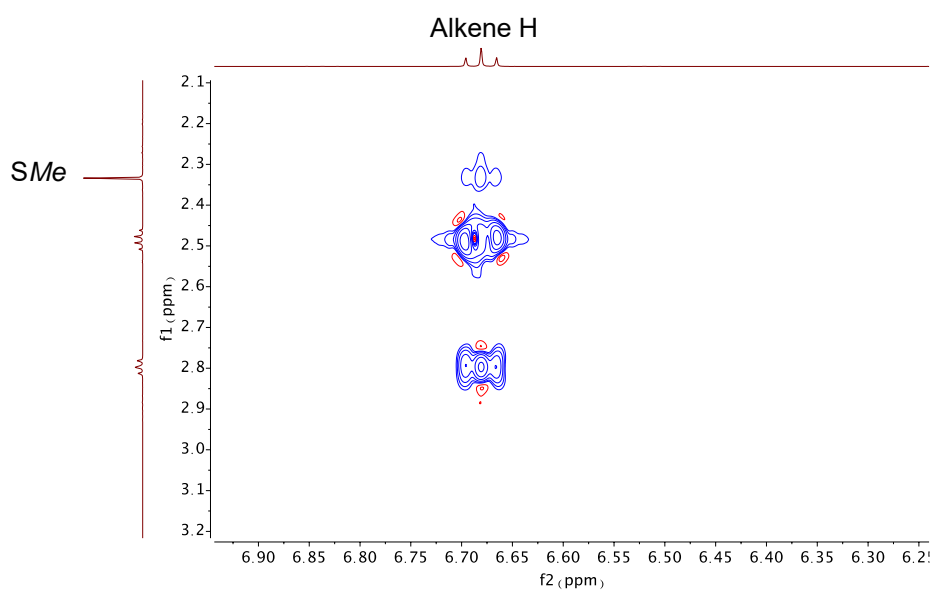
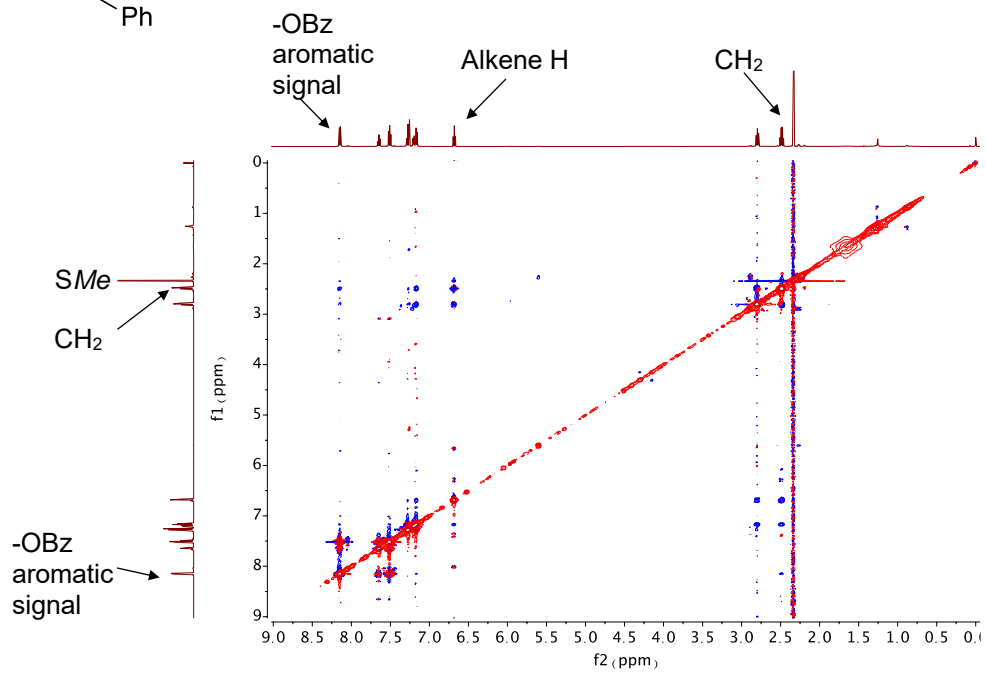
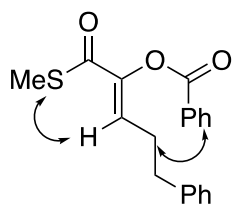
NOESY expansion of compound 457 (CDCl₃, 500 MHz)

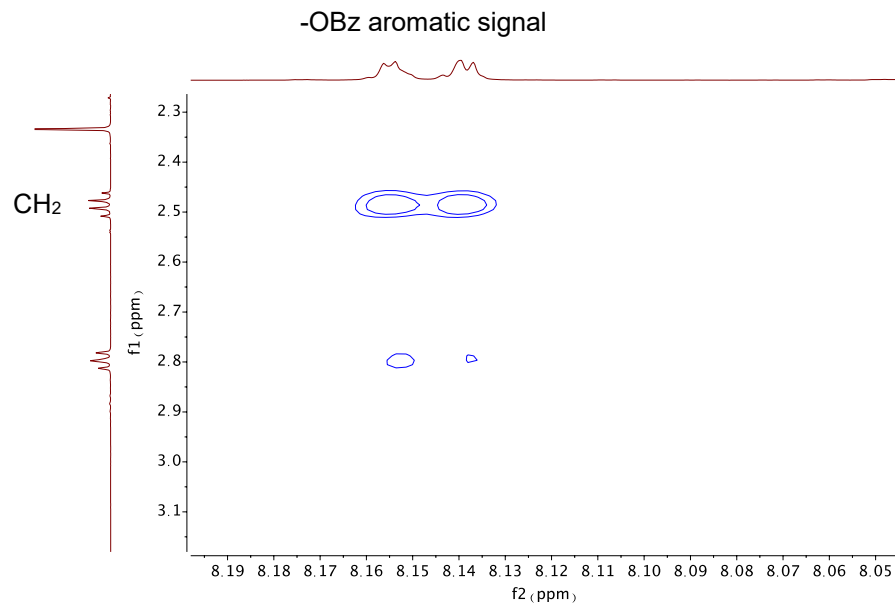
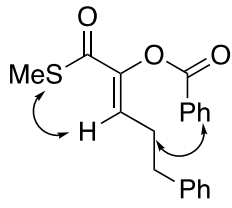


NOESY and NOSEY expansion of compound 463 (CDCl₃, 400 MHz)

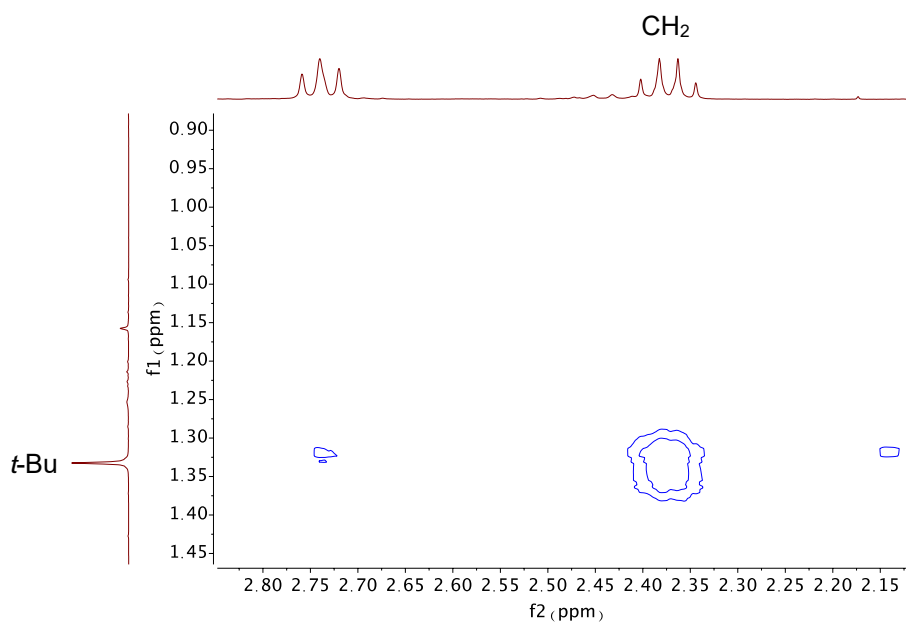
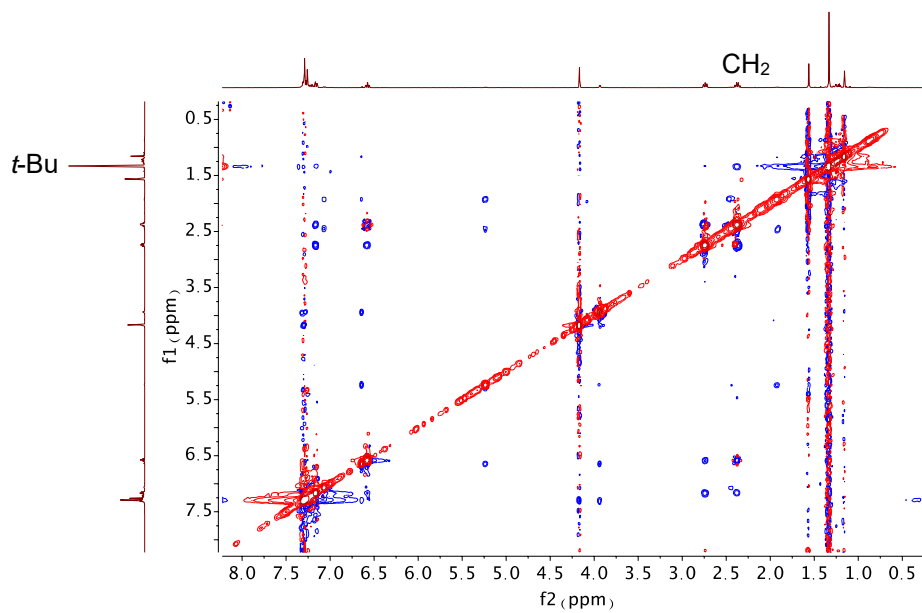
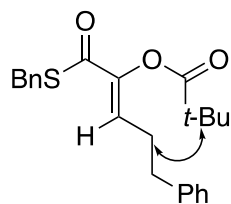


NOESY and NOESY expansions of compound (CDCl₃, 400 MHz)

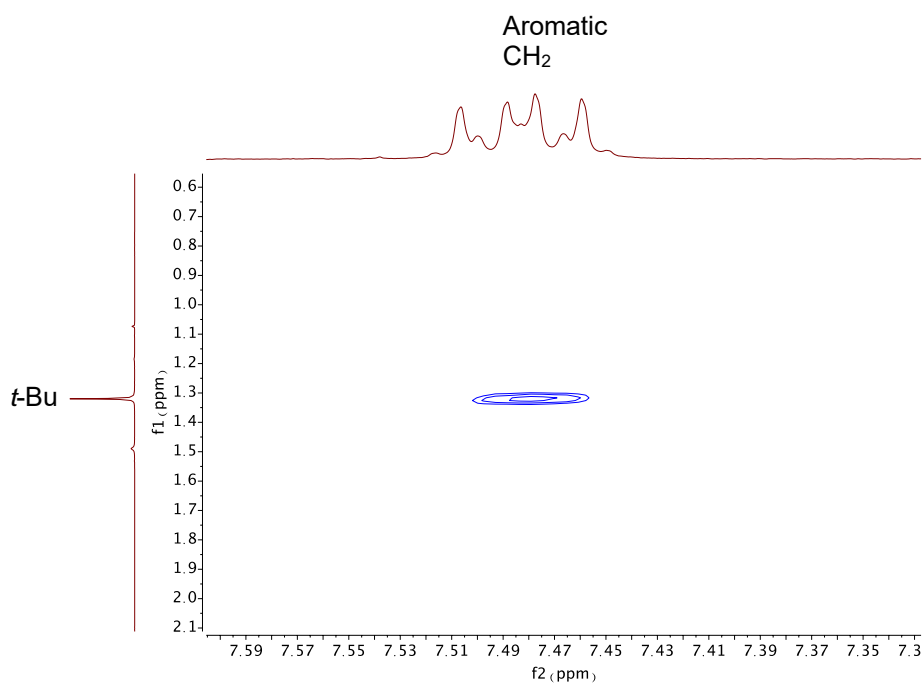
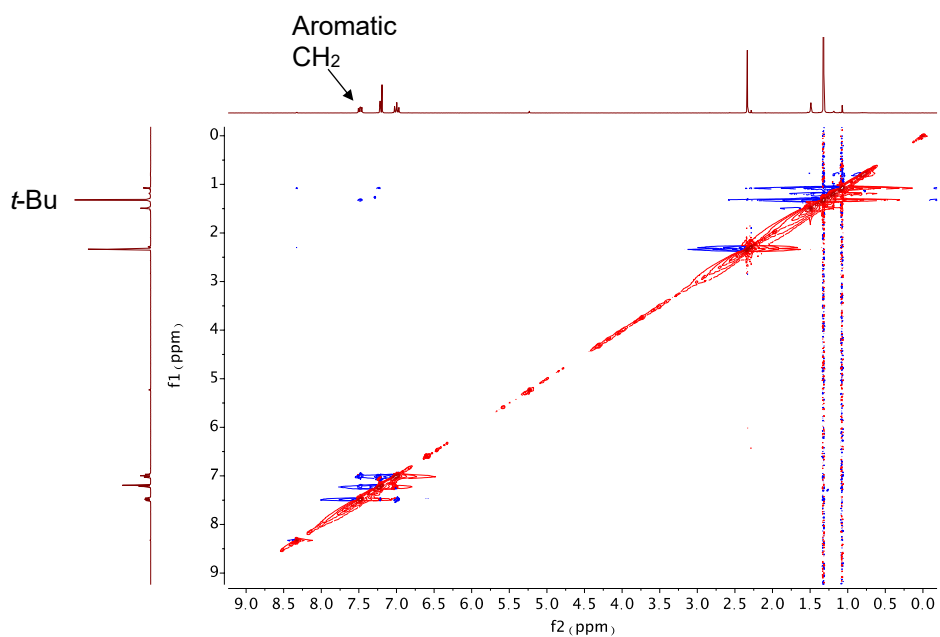
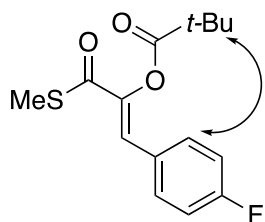




NOESY and NOESY expansion of compound 465 (CDCl₃, 400 MHz)



NOESY and NOESY expansion of compound 446 (CDCl₃, 500 MHz)



5.2 Crystal Data and Structure Refinement for 412

Empirical formula	C ₁₈ H ₂₃ NO ₂ S
Formula weight	317.43
Temperature/K	100(2)
Crystal system	monoclinic
Space group	P2 ₁ /c
a/Å	12.7478(6)
b/Å	13.4259(6)
c/Å	10.4584(5)
α/°	90
β/°	104.619(5)
γ/°	90
Volume/Å ³	1732.01(14)
Z	4
ρ _{calc} /cm ³	1.217
μ/mm ⁻¹	1.705
F(000)	680.0
Crystal size/mm ³	0.216 × 0.155 × 0.127
Radiation	Cu Kα (λ = 1.54184)
2θ range for data collection/°	7.166 to 145.81
Index ranges	-15 ≤ h ≤ 12, -11 ≤ k ≤ 16, -11 ≤ l ≤ 12
Reflections collected	6710
Independent reflections	3360 [R _{int} = 0.0257, R _{sigma} = 0.0321]
Data/restraints/parameters	3360/0/208
Goodness-of-fit on F ²	1.046
Final R indexes [I ≥ 2σ (I)]	R ₁ = 0.0409, wR ₂ = 0.0997
Final R indexes [all data]	R ₁ = 0.0490, wR ₂ = 0.1062
Largest diff. peak/hole / e Å ⁻³	0.63/-0.45

Notes

The structure occupies a centrosymmetric space group and is thus an exact 50:50 mixture of enantiomers. In half of cases, C(1) is *S* and in the other half C(1) is *R*. In all cases, the relative stereochemistry is the same.

The hydrogen atom bonded to N(1) was located in the electron density and freely refined. The remaining hydrogen atoms were fixed as riding models and the isotropic thermal parameters (*U*_{iso}) were based on the *U*_{eq} of the parent atom. Hydrogen bonding is detailed in Table 6 of the PAR1053_Tables.html document.

Tables in the report entitled PAR1053_Tables.html give experimental details, bond lengths, angles, torsion angles and hydrogen bonding with standard deviations given in brackets.

Table 2 Fractional Atomic Coordinates ($\times 10^4$) and Equivalent Isotropic Displacement Parameters ($\text{\AA}^2 \times 10^3$) for PAR1053. U_{eq} is defined as 1/3 of the trace of the orthogonalised U_{ij} tensor.

Atom	x	y	z	U(eq)
C1	1333.7(14)	6155.2(13)	5527.9(16)	19.9(3)
C2	1675.1(13)	5838.3(13)	6961.8(16)	20.1(3)
C3	1972.6(15)	6436.8(14)	8045.1(17)	25.0(4)
C4	2124.3(13)	4879.7(13)	8835.2(16)	20.4(3)
C5	1775.6(13)	4833.1(13)	7438.4(16)	18.2(3)
C6	1575.6(13)	3901.2(13)	6829.3(17)	21.4(4)
C7	1717.8(15)	3058.6(14)	7607.1(18)	26.1(4)
C8	2054.1(14)	3122.5(14)	8992.4(18)	26.2(4)
C9	2264.3(14)	4028.8(14)	9625.7(17)	24.3(4)
C10	735.3(14)	7156.4(13)	5357.6(18)	25.3(4)
C11	2339.8(14)	6217.3(13)	5017.7(16)	20.0(3)
C12	2590.9(13)	5637.4(13)	4123.5(16)	21.1(4)
C13	800.8(15)	5206.5(15)	2010.2(18)	28.5(4)
C14	3751.5(14)	6076.7(13)	2764.9(16)	22.5(4)
C15	4909.0(14)	6014.9(15)	2636.2(18)	28.1(4)
C16	5001.5(17)	6588(2)	1409(2)	45.7(6)
C17	5167.8(17)	4907.1(18)	2501(2)	40.1(5)
C18	5686.0(16)	6447.8(18)	3875(2)	37.8(5)
N1	2246.2(13)	5869.2(12)	9176.3(15)	26.3(3)
O1	2979.9(9)	6386.3(9)	1939.2(11)	23.0(3)
O2	3659.6(10)	5731.9(11)	3944.8(11)	27.8(3)
S1	1840.3(4)	4625.0(3)	3295.6(4)	27.90(14)

Table 3 Anisotropic Displacement Parameters ($\text{\AA}^2 \times 10^3$) for PAR1053. The Anisotropic displacement factor exponent takes the form: $-2\pi^2[h^2a^*2U_{11}+2hka^*b^*U_{12}+\dots]$.

Atom	U_{11}	U_{22}	U_{33}	U_{23}	U_{13}	U_{12}
C1	22.4(8)	21.1(8)	17.3(8)	-1.0(6)	7.1(6)	-0.4(7)
C2	21.9(8)	21.7(8)	18.6(8)	-1.4(7)	8.5(6)	-0.7(7)
C3	33.5(10)	22.3(9)	20.8(8)	-0.1(7)	10.0(7)	-1.5(7)
C4	18.4(8)	25.4(9)	18.4(8)	-0.3(7)	6.3(6)	-0.7(7)
C5	15.8(8)	23.2(8)	16.9(8)	0.8(6)	6.3(6)	0.3(6)
C6	21.6(8)	22.6(8)	20.3(8)	-2.4(7)	5.6(7)	-0.2(7)
C7	27.9(9)	21.8(9)	28.8(9)	-1.6(7)	7.5(7)	-0.6(7)
C8	25.8(9)	25.9(9)	28.1(9)	8.9(8)	8.9(7)	2.5(7)
C9	21.4(9)	33.3(10)	19.1(8)	4.9(7)	6.8(7)	0.8(7)
C10	25.5(9)	23.5(9)	26.8(9)	-1.8(7)	6.2(7)	0.9(7)
C11	22.8(8)	21.6(8)	15.1(8)	4.0(6)	3.7(6)	-1.1(7)
C12	19.4(8)	26.5(9)	17.6(8)	5.2(7)	5.4(6)	3.3(7)
C13	25.1(9)	32.5(10)	29.6(10)	-3.1(8)	9.6(8)	-4.2(8)
C14	24.8(9)	27.6(9)	16.2(8)	0.1(7)	7.5(7)	0.5(7)
C15	20.7(9)	43.7(11)	21.1(9)	1.8(8)	7.5(7)	3.4(8)
C16	28.2(11)	78.6(17)	34.3(11)	16.9(11)	15.4(9)	2.7(11)
C17	27.9(10)	54.0(14)	40.8(11)	-7.2(10)	13.1(9)	8.7(10)
C18	24.0(10)	58.3(14)	31.3(10)	-7.4(10)	7.6(8)	-3.3(9)
N1	37.4(9)	26.8(8)	15.9(7)	-4.2(6)	8.8(6)	-4.1(7)
O1	20.9(6)	30.2(7)	17.2(6)	3.0(5)	3.8(5)	2.5(5)

Atom	U ₁₁	U ₂₂	U ₃₃	U ₂₃	U ₁₃	U ₁₂
O2	19.7(6)	46.6(8)	18.5(6)	8.1(6)	7.0(5)	7.4(6)
S1	41.9(3)	21.0(2)	22.4(2)	1.07(17)	11.14(19)	1.15(18)

Table 4 Bond Lengths for PAR1053.

Atom	Atom	Length/Å	Atom	Atom	Length/Å
C1	C2	1.513(2)	C8	C9	1.379(3)
C1	C10	1.534(2)	C11	C12	1.317(2)
C1	C11	1.511(2)	C12	O2	1.427(2)
C2	C3	1.362(2)	C12	S1	1.7591(18)
C2	C5	1.433(2)	C13	S1	1.8092(19)
C3	N1	1.376(2)	C14	C15	1.517(2)
C4	C5	1.417(2)	C14	O1	1.207(2)
C4	C9	1.395(2)	C14	O2	1.350(2)
C4	N1	1.374(2)	C15	C16	1.527(3)
C5	C6	1.398(2)	C15	C17	1.538(3)
C6	C7	1.378(2)	C15	C18	1.532(3)
C7	C8	1.406(3)			

Table 5 Bond Angles for PAR1053.

Atom	Atom	Atom	Angle/°	Atom	Atom	Atom	Angle/°
C2	C1	C10	111.83(14)	C12	C11	C1	126.76(16)
C11	C1	C2	107.95(13)	C11	C12	O2	116.86(16)
C11	C1	C10	110.63(14)	C11	C12	S1	127.36(14)
C3	C2	C1	127.47(16)	O2	C12	S1	115.02(12)
C3	C2	C5	106.53(15)	O1	C14	C15	126.18(15)
C5	C2	C1	125.98(15)	O1	C14	O2	121.92(15)
C2	C3	N1	110.20(16)	O2	C14	C15	111.89(14)
C9	C4	C5	122.32(16)	C14	C15	C16	109.29(15)
N1	C4	C5	107.21(15)	C14	C15	C17	107.27(16)
N1	C4	C9	130.44(16)	C14	C15	C18	109.87(15)
C4	C5	C2	107.11(15)	C16	C15	C17	110.26(17)
C6	C5	C2	133.98(16)	C16	C15	C18	110.42(18)
C6	C5	C4	118.88(15)	C18	C15	C17	109.67(17)
C7	C6	C5	118.95(16)	C4	N1	C3	108.94(15)
C6	C7	C8	121.23(17)	C14	O2	C12	117.14(13)
C9	C8	C7	121.37(17)	C12	S1	C13	103.75(8)
C8	C9	C4	117.24(16)				

Table 6 Hydrogen Bonds for PAR1053.

D	H	A	d(D-H)/Å	d(H-A)/Å	d(D-A)/Å	D-H-A/°
N1	H1A	O1 ¹	0.84(2)	2.05(2)	2.8882(19)	170(2)

Table 7 Torsion Angles for PAR1053.

A	B	C	D	Angle/°	A	B	C	D	Angle/°
C1	C2	C3	N1	-178.92(16)	C10	C1	C2	C3	-32.6(2)
C1	C2	C5	C4	179.41(15)	C10	C1	C2	C5	149.24(16)

A	B	C	D	Angle/°	A	B	C	D	Angle/°
C1	C2	C5	C6	-2.9(3)	C10	C1	C11	C12	-124.79(19)
C1	C11	C12	O2	-170.39(15)	C11	C1	C2	C3	89.3(2)
C1	C11	C12	S1	-0.9(3)	C11	C1	C2	C5	-88.8(2)
C2	C1	C11	C12	112.56(19)	C11	C12	O2	C14	-114.79(18)
C2	C3	N1	C4	-0.2(2)	C11	C12	S1	C13	79.90(17)
C2	C5	C6	C7	-177.14(18)	C15	C14	O2	C12	-172.55(15)
C3	C2	C5	C4	0.94(19)	N1	C4	C5	C2	-1.05(18)
C3	C2	C5	C6	178.66(18)	N1	C4	C5	C6	-179.18(15)
C4	C5	C6	C7	0.4(2)	N1	C4	C9	C8	178.44(17)
C5	C2	C3	N1	-0.5(2)	O1	C14	C15	C16	10.8(3)
C5	C4	C9	C8	0.3(2)	O1	C14	C15	C17	-108.7(2)
C5	C4	N1	C3	0.77(19)	O1	C14	C15	C18	132.1(2)
C5	C6	C7	C8	0.3(3)	O1	C14	O2	C12	7.2(3)
C6	C7	C8	C9	-0.6(3)	O2	C12	S1	C13	-110.50(12)
C7	C8	C9	C4	0.3(3)	O2	C14	C15	C16	-169.44(17)
C9	C4	C5	C2	177.43(15)	O2	C14	C15	C17	71.02(19)
C9	C4	C5	C6	-0.7(2)	O2	C14	C15	C18	-48.1(2)
C9	C4	N1	C3	-177.55(18)	S1	C12	O2	C14	74.46(17)

Table 8 Hydrogen Atom Coordinates ($\text{\AA} \times 10^4$) and Isotropic Displacement Parameters ($\text{\AA}^2 \times 10^3$) for PAR1053.

Atom	x	y	z	U(eq)
H1	840.97	5635.9	5012.98	24
H3	1988.81	7143.88	8022.72	30
H6	1345.25	3849.48	5894.25	26
H7	1586.28	2422.73	7199.43	31
H8	2138.11	2529.02	9502.84	31
H9	2495.01	4071.89	10561.51	29
H10A	97.75	7107.74	5717.19	38
H10B	504.74	7325.01	4416.47	38
H10C	1220.85	7676.36	5830.37	38
H11	2843.63	6727.65	5379.41	24
H13A	1131	5495.23	1344.28	43
H13B	445.44	5733.1	2396.08	43
H13C	263.03	4705.99	1593.9	43
H16A	4498.4	6304.82	626.44	69
H16B	5744.68	6537.5	1312.49	69
H16C	4820.82	7289.66	1499.23	69
H17A	5097.26	4546.32	3289.75	60
H17B	5910.73	4839.74	2409.06	60
H17C	4660.38	4629.17	1718.46	60
H18A	5507.42	7149.35	3969.95	57
H18B	6432.81	6395.76	3791.67	57
H18C	5614.61	6075.11	4653.86	57
H1A	2466(18)	6090(18)	9950(20)	35(6)

6 References

- 1) (a) Hashmi, A. S. K., Homogeneous gold catalysis and alkynes: A successful liaison. *Gold Bull.* **2003**, *36*, 3-9. (b) Jiménez-Núñez, E.; Echavarren, A. M., Molecular diversity through gold catalysis with alkynes. *Chem. Commun.* **2007**, 333-346. (c) Shahzad, S. A.; Sajid, M. A.; Khan, Z. A.; Canseco-Gonzalez, D., Gold catalysis in organic transformations: A review. *Synth. Commun.* **2017**, *47*, 735-755.
- 2) (a) Echavarren, A. M., Carbene or cation? *Nat. Chem.* **2009**, *1*, 431-433. (b) Wang, Y.; Muratore, M. E.; Echavarren, A. M., Gold Carbene or Gold Carbenoid: Is There a Difference. *Chem. Eur. J.* **2015**, *21*, 7332-7339. (c) Hashmi, A. S. K., "High Noon" in Gold Catalysis: Carbene versus Carbocation intermediates. *Angew. Chem. Int. Ed.* **2008**, *57*, 6754-6756.
- 3) Seidel, G.; Fürstner, A., Structure of a Reactive Gold Carbenoid. *Angew. Chem. Int. Ed.* **2014**, *53*, 4807-4811.
- 4) Hussong, M. W.; Rominger, D. F.; Krämer, P.; Straub, B. F., Isolierung eines nicht-Heteroatom-stabilisierten Goldcarbens. *Angew. Chem.* **2014**, *125*, 9526-9529.
- 5) Benitez, D.; Shapiro, N. D.; Tkatchouk, E.; Wang, Y.; Goddard, W. A.; Toste, F. D., A bonding model for gold(I) carbene complexes. *Nat. Chem.* **2009**, *1*, 482-486.
- 6) Ford, A.; Miel, H.; Ring, A.; Slattery, C. N.; Maguire, A. R.; McKervey, M. A., Modern Organic Synthesis with α -Diazocarbonyl Compounds. *Chem. Rev.* **2015**, *115*, 9981-10080.
- 7) (a) Shapiro, N. D.; Toste, F. D., Rearrangement of Alkynyl Sulfoxides Catalyzed by Gold(I) Complexes. *J. Am. Chem. Soc.* **2007**, *129*, 4160-4161. (b) Li, G.; Zhang, L., Gold-Catalyzed Intramolecular Redox Reaction of Sulfinyl Alkynes: Efficient Generation of α -Oxo Gold Carbenoids and Application in Insertion into R-CO Bonds. *Angew. Chem. Int. Ed.* **2007**, *46*, 5156-5159.
- 8) (a) Bhunia, S.; Ghosh, P.; Patra, S. R., Gold-Catalyzed Oxidative Alkyne Functionalization by N-O/S-O/C-O Bond Oxidants. *Adv. Synth. Catal.* **2020**, *362*, 3664-3708. (b) Zhang, L., A Non-Diazo Approach to α -Oxo Gold Carbenes via Gold-Catalyzed Alkyne Oxidation. *Acc. Chem. Res.* **2014**, *47*, 877-888.
- 9) Davies, P. W.; Albrecht, S. J. C., Gold- or Platinum-Catalyzed Synthesis of Sulfur Heterocycles: Access to Sulfur Ylides without Using Sacrificial Functionality. *Angew. Chem. Int. Ed.* **2009**, *48*, 8372-8375.
- 10) Kaur, P. H.; Davies, P. W., Gold-Catalysed Cycloisomerisation of Ynamides To Access 2,2- Disubstituted Tetrahydrothiophene Motifs. *Synlett* **2021**, *32*, 897-900.
- 11) Cuenca, A. B.; Montserrat, S.; Hossain, K. M.; Mancha, G.; Lledós, A.; Medio-Simón, M.; Ujaque, G.; Asensio, G., Gold(I)-Catalyzed Intermolecular Oxyarylation of Alkynes: Unexpected Regiochemistry in the Alkylation of Arenes. *Org. Lett.* **2009**, *11*, 4906-4909.
- 12) Lu, B.; Li, Y.; Wang, Y.; Aue, D. H.; Luo, Y.; Zhang, L., [3,3]-Sigmatropic Rearrangement versus Carbene Formation in Gold-Catalyzed Transformations of Alkynyl Aryl Sulfoxides: Mechanistic Studies and Expanded Reaction Scope. *J. Am. Chem. Soc.* **2013**, *135*, 8512-8524.
- 13) (a) Ye, L.; He, W.; Zhang, L., Gold-Catalyzed One-Step Practical Synthesis of Oxetan-3-ones from Readily Available Propargylic Alcohols. *J. Am. Chem. Soc.* **2010**, *132*, 8550-8551. (b) Ye, L.; He, W.; Zhang, L., A Flexible and Stereoselective Synthesis of Azetidion-3-ones through Gold-Catalyzed Intermolecular Oxidation of Alkynes. *Angew. Chem. Int. Ed.* **2011**, *50*,

3236-3239. (c) Ye, L.; Cui, L.; Zhang, G.; Zhang, L., Alkynes as Equivalents of α -Diazo Ketones in Generating α -Oxo Metal Carbenes: A Gold-Catalyzed Expedient Synthesis of Dihydrofuran-3-ones. *J. Am. Chem. Soc.* **2010**, *132*, 3258-3259. (d) Davies, P. W.; Cremonesi, A.; Martin, N., Site-specific introduction of gold-carbenoids by intermolecular oxidation of ynamides or ynol ethers. *Chem. Commun.* **2011**, *47*, 379-381. (e) Bhunia, S.; Ghorpade, S.; Huple, D. B.; Liu, R.-S., Gold-Catalyzed Oxidative Cyclizations of cis-3-En-1-ynes To Form Cyclopentenone Derivatives. *Angew. Chem. Int. Ed.* **2012**, *51*, 2939-2942. (f) Lu, B.; Li, C.; Zhang, L., Gold-Catalyzed Highly Regioselective Oxidation of C–C Triple Bonds without Acid Additives: Propargyl Moieties as Masked α,β -Unsaturated Carbonyls. *J. Am. Chem. Soc.* **2010**, *132*, 14070-14072.

14) Barrett, M. J.; Davies, P. W.; Grainger, R. S., Regioselective functionalisation of dibenzothiophenes through gold-catalysed intermolecular alkyne oxyarylation. *Org. Biomol. Chem.* **2015**, *13*, 8676-8686.

15) Peng, B.; Huang, X.; Xie, L.-G.; Maulide, N., A Brønsted Acid Catalyzed Redox Arylation. *Angew. Chem. Int. Ed.* **2014**, *53*, 8718-8721.

16) (a) Baldassari, L. L.; Mantovani, A. C.; Senoner, S.; Maryasin, B.; Maulide, N.; Lüdtke, D. S., Redox-Neutral Synthesis of Selenoesters by Oxyarylation of Selenoalkynes under Mild Conditions. *Org. Lett.* **2018**, *20*, 5881-5885. (b) Hu, L.; Gui, Q.; Chen, X.; Tan, Z.; Zhu, G., HOTf-Catalyzed, Solvent-Free Oxyarylation of Ynol Ethers and Thioethers. *J. Org. Chem.* **2016**, *81*, 4861-4868. (c) Kaiser, D.; Veiros, L. F.; Maulide, N., Brønsted Acid-Mediated Hydrative Arylation of Unactivated Alkynes. *Chem. Eur. J.* **2016**, *22*, 4727-4732.

17) (a) Takimiya, K.; Shinamura, S.; Osaka, I.; Miyazaki, E., Thienoacene-Based Organic Semiconductors. *Adv. Mater.* **2011**, *23*, 4347-4370. (b) Ruzié, C.; Karpinska, J.; Laurent, A.; Sanguinet, L.; Hunter, S.; Anthopoulos, T. D.; Lemaur, V.; Cornil, J.; Kennedy, A. R.; Fenwick, O.; Samorì, P.; Schweicher, G.; Chattopadhyay, B.; Geerts, Y. H., Design, synthesis, chemical stability, packing, cyclic voltammetry, ionisation potential, and charge transport of [1]benzothieno[3,2-b][1]benzothiophene derivatives. *J. Mater. Chem. C* **2016**, *4*, 4863-4879. (c) Usta, H.; Kim, D.; Ozdemir, R.; Zorlu, Y.; Kim, S.; Ruiz Delgado, M. C.; Harbuzaru, A.; Kim, S.; Demirel, G.; Hong, J.; Ha, Y.-G.; Cho, K.; Facchetti, A.; Kim, M.-G., High Electron Mobility in [1]Benzothieno[3,2-b][1]benzothiophene-Based Field-Effect Transistors: Toward n-Type BTBTs. *Chem. Mater.* **2019**, *31*, 5254-5263. (d) Chapman, N. B.; Scrowston, R. M.; Westwood, R., Pharmacologically active benzo[b]thiophen derivatives. Part VIII. Benzo[b]thiophen analogues of tryptophan and α -methyltryptophan, and some of their 5-substituted derivatives. *J. Chem. Soc. C* **1969**, 1855-1858. (e) Keri, R. S.; Chand, K.; Budagumpi, S.; Balappa Somappa, S.; Patil, S. A.; Nagaraja, B. M., An overview of benzo[b]thiophene-based medicinal chemistry. *Eur. J. Med. Chem.* **2017**, *138*, 1002-1033. (f) Muchmore, D. B., Raloxifene: A selective estrogen receptor modulator (SERM) with multiple target system effects. *Oncologist* **2000**, *5*, 388-392. (g) Croxtall, J. D.; Plosker, G. L., Sertaconazole: a review of its use in the management of superficial mycoses in dermatology and gynaecology. *Drugs* **2009**, *69*, 339-359.

18) (a) Morgan, D.; Yarwood, S. J.; Barker, G., Recent Developments in C–H Functionalisation of Benzofurans and Benzothiophenes. *Eur. J. Org. Chem.* **2021**, *2021*, 1072-1102. (b) Bheeter, C. B.; Chen, L.; Soulé, J.-F.; Doucet, H., Regioselectivity in palladium-catalysed direct arylation of 5-membered ring heteroaromatics. *Catal. Sci. Technol.* **2016**, *6*, 2005-2049.

- 19) Ueda, K.; Yanagisawa, S.; Yamaguchi, J.; Itami, K., A General Catalyst for the β -Selective C–H Bond Arylation of Thiophenes with Iodoarenes. *Angew. Chem. Int. Ed.* **2010**, *49*, 8946-8949.
- 20) Funaki, K.; Sato, T.; Oi, S., Pd-Catalyzed β -Selective Direct C–H Bond Arylation of Thiophenes with Aryltrimethylsilanes. *Org. Lett.* **2012**, *14*, 6186-6189.
- 21) Tang, D.-T. D.; Collins, K. D.; Glorius, F., Completely Regioselective Direct C–H Functionalization of Benzo[b]thiophenes Using a Simple Heterogeneous Catalyst. *J. Am. Chem. Soc.* **2013**, *135*, 7450-7453.
- 22) Tang, D.-T. D.; Collins, K. D.; Ernst, J. B.; Glorius, F., Pd/C as a Catalyst for Completely Regioselective C-H Functionalization of Thiophenes under Mild Conditions. *Angew. Chem. Int. Ed.* **2014**, *53*, 1809-1813.
- 23) Yuan, K.; Doucet, H., Benzenesulfonyl chlorides: new reagents for access to alternative regioisomers in palladium-catalysed direct arylations of thiophenes. *Chem. Sci.* **2014**, *5*, 392-396.
- 24) Colletto, C.; Islam, S.; Juliá-Hernández, F.; Larrosa, I., Room-Temperature Direct β -Arylation of Thiophenes and Benzo[b]thiophenes and Kinetic Evidence for a Heck-type Pathway. *J. Am. Chem. Soc.* **2016**, *138*, 1677-1683.
- 25) Shrives, H. J.; Fernández-Salas, J. A.; Hedtke, C.; Pulis, A. P.; Procter, D. J., Regioselective synthesis of C3 alkylated and arylated benzothiophenes. *Nat. Commun.* **2017**, *8*, 14801.
- 26) Martínez, A.; Vázquez, M.-V.; Luis Carreón-Macedo, J.; Sansores, L. E.; Salcedo, R., Benzene fused five-membered heterocycles. A theoretical approach. *Tetrahedron* **2003**, *59*, 6415-6422.
- 27) Pouzet, P.; Erdelmeier, I.; Ginderow, D.; Mornon, J.-P.; Dansette, P.; Mansuy, D., Thiophene S-oxides: convenient preparation, first complete structural characterization and unexpected dimerization of one of them, 2,5-diphenylthiophene-1-oxide. *J. Chem. Soc., Chem. Commun.* **1995**, 473-474.
- 28) (a) He, Z.; Biremond, T.; Perry, G. J. P.; Procter, D. J., Para-coupling of phenols with C2/C3-substituted benzothiophene S-oxides. *Tetrahedron* **2020**, *76*, 131315. (b) Šiaučiulis, M.; Ahlsten, N.; Pulis, A. P.; Procter, D. J., Transition-Metal-Free Cross-Coupling of Benzothiophenes and Styrenes in a Stereoselective Synthesis of Substituted (E,Z)-1,3-Dienes. *Angew. Chem. Int. Ed.* **2019**, *58*, 8779-8783.
- 29) Rist, P. A.; Grainger, R. S.; Davies, P. W., Gold-Catalyzed Intermolecular Alkyne Oxyarylation for C3 Functionalization of Benzothiophenes. *Org. Lett.* **2021**, *23*, 642-646.
- 30) He, Z.; Shrives, H. J.; Fernández-Salas, J. A.; Abengózar, A.; Neufeld, J.; Yang, K.; Pulis, A. P.; Procter, D. J., Synthesis of C2 Substituted Benzothiophenes via an Interrupted Pummerer/[3,3]-Sigmatropic/1,2-Migration Cascade of Benzothiophene S-Oxides. *Angew. Chem. Int. Ed.* **2018**, *57*, 5759-5764.
- 31) (a) Riley, K. E.; Hobza, P., On the Importance and Origin of Aromatic Interactions in Chemistry and Biodisciplines. *Acc. Chem. Res.* **2013**, *46*, 927-936. (b) Waters, M. L., Aromatic interactions in model systems. *Curr. Opin. Chem. Biol.* **2002**, *6*, 736-741.
- 32) Burés, J., Variable Time Normalization Analysis: General Graphical Elucidation of Reaction Orders from Concentration Profiles. *Angew. Chem. Int. Ed.* **2016**, *55*, 16084-16087.
- 33) Blackmond, D. G., Kinetic Profiling of Catalytic Organic Reactions as a Mechanistic Tool. *J. Am. Chem. Soc.* **2015**, *137*, 10852-10866.

- 34) (a) Kumar, M.; Jasinski, J.; Hammond, G. B.; Xu, B., Alkyne/Alkene/Allene-Induced Disproportionation of Cationic Gold(I) Catalyst. *Chem. Eur. J.* **2014**, *20*, 3113-3119. (b) Cai, R.; Lu, M.; Aguilera, E. Y.; Xi, Y.; Akhmedov, N. G.; Petersen, J. L.; Chen, H.; Shi, X., Ligand-Assisted Gold-Catalyzed Cross-Coupling with Aryldiazonium Salts: Redox Gold Catalysis without an External Oxidant. *Angew. Chem. Int. Ed.* **2015**, *127*, 8896-8900. (c) Brooner, R. E. M.; Brown, T. J.; Widenhoefer, R. A., Synthesis and Study of Cationic, Two-Coordinate Triphenylphosphine–Gold– π Complexes. *Chem. Eur. J.* **2013**, *19*, 8276-8284.
- 35) Marion, N.; Nolan, S. P., Propargylic Esters in Gold Catalysis: Access to Diversity. *Angew. Chem. Int. Ed.* **2007**, *46*, 2750-2752.
- 36) (a) Ghosh, N.; Nayak, S.; Prabagar, B.; Sahoo, A. K., Regioselective Hydration of Terminal Halo-Substituted Propargyl Carboxylates by Gold Catalyst: Synthesis of α -Acyloxy α' -Halo Ketones. *J. Org. Chem.* **2014**, *79*, 2453-2462. (b) Huang, X.; de Haro, T.; Nevado, C., Gold-Catalyzed Stereocontrolled Synthesis of 2,3-Bis(acetoxy)-1,3-dienes. *Chem. Eur. J.* **2009**, *15*, 5904-5908. (c) Wang, Y.; Lu, B.; Zhang, L., The use of Br/Cl to promote regioselective gold-catalyzed rearrangement of propargylic carboxylates: an efficient synthesis of (1Z, 3E)-1-bromo/chloro-2-carboxy-1,3-dienes. *Chem. Commun.* **2010**, *46*, 9179-9181.
- 37) Correa, A.; Marion, N.; Fensterbank, L.; Malacria, M.; Nolan, S. P.; Cavallo, L., Golden Carousel in Catalysis: The Cationic Gold/Propargylic Ester Cycle. *Angew. Chem. Int. Ed.* **2008**, *47*, 718-721.
- 38) Mauleón, P.; Krinsky, J. L.; Toste, F. D., Mechanistic Studies on Au(I)-Catalyzed [3,3]-Sigmatropic Rearrangements using Cyclopropane Probes. *J. Am. Chem. Soc.* **2009**, *131*, 4513-4520.
- 39) Li, G.; Zhang, G.; Zhang, L., Au-Catalyzed Synthesis of (1Z,3E)-2-Pivaloxy-1,3-Dienes from Propargylic Pivalates. *J. Am. Chem. Soc.* **2008**, *130*, 3740-3741.
- 40) Mamane, V.; Gress, T.; Krause, H.; Fürstner, A., Platinum- and Gold-Catalyzed Cycloisomerization Reactions of Hydroxylated Enynes. *J. Am. Chem. Soc.* **2004**, *126*, 8654-8655.
- 41) Fürstner, A.; Hannen, P., Platinum- and Gold-Catalyzed Rearrangement Reactions of Propargyl Acetates: Total Syntheses of (-)- α -Cubebene, (-)-Cubebol, Sesquicarene and Related Terpenes. *Chem. Eur. J.* **2006**, *12*, 3006-3019.
- 42) Buzas, A.; Gagosz, F., Gold(I) Catalyzed Isomerization of 5-en-2-yn-1-yl Acetates: An Efficient Access to Acetoxy Bicyclo[3.1.0]hexenes and 2-Cycloalken-1-ones. *J. Am. Chem. Soc.* **2006**, *128*, 12614-12615.
- 43) Shi, X.; Gorin, D. J.; Toste, F. D., Synthesis of 2-Cyclopentenones by Gold(I)-Catalyzed Rautenstrauch Rearrangement. *J. Am. Chem. Soc.* **2005**, *127*, 5802-5803.
- 44) Zhang, L.; Wang, S., Efficient Synthesis of Cyclopentenones from Enynyl Acetates via Tandem Au(I)-Catalyzed 3,3-Rearrangement and the Nazarov Reaction. *J. Am. Chem. Soc.* **2006**, *128*, 1442-1443.
- 45) Lemière, G.; Gandon, V.; Cariou, K.; Fukuyama, T.; Dhimane, A.-L.; Fensterbank, L.; Malacria, M., Tandem Gold(I)-Catalyzed Cyclization/Electrophilic Cyclopropanation of Vinyl Allenes. *Org. Lett.* **2007**, *9*, 2207-2209.
- 46) Zhang, L., Tandem Au-Catalyzed 3,3-Rearrangement–[2 + 2] Cycloadditions of Propargylic Esters: Expedient Access to Highly Functionalized 2,3-Indoline-Fused Cyclobutanes. *J. Am. Chem. Soc.* **2005**, *127*, 16804-16805.

- 47) Marion, N.; Díez-González, S.; de Frémont, P.; Noble, A. R.; Nolan, S. P., Au-Catalyzed Tandem [3,3] Rearrangement–Intramolecular Hydroarylation: Mild and Efficient Formation of Substituted Indenes. *Angew. Chem. Int. Ed.* **2006**, *45*, 3647-3650.
- 48) Johansson, M. J.; Gorin, D. J.; Staben, S. T.; Toste, F. D., Gold(I)-Catalyzed Stereoselective Olefin Cyclopropanation. *J. Am. Chem. Soc.* **2005**, *127*, 18002-18003.
- 49) Gorin, D. J.; Watson, I. D. G.; Toste, F. D., Fluorenes and Styrenes by Au(I)-Catalyzed Annulation of Enynes and Alkynes. *J. Am. Chem. Soc.* **2008**, *130*, 3736-3737.
- 50) Amijs, C. H. M.; López-Carrillo, V.; Echavarren, A. M., Gold-Catalyzed Addition of Carbon Nucleophiles to Propargyl Carboxylates. *Org. Lett.* **2007**, *9*, 4021-4024.
- 51) (a) Peng, Y.; Cui, L.; Zhang, G.; Zhang, L., Gold-Catalyzed Homogeneous Oxidative C–O Bond Formation: Efficient Synthesis of 1-Benzoxyvinyl Ketones. *J. Am. Chem. Soc.* **2009**, *131*, 5062-5063. (b) Witham, C. A.; Mauleón, P.; Shapiro, N. D.; Sherry, B. D.; Toste, F. D., Gold(I)-Catalyzed Oxidative Rearrangements. *J. Am. Chem. Soc.* **2007**, *129*, 5838-5839. (c) Ji, K.; Nelson, J.; Zhang, L., Gold-catalyzed regioselective oxidation of propargylic carboxylates: a reliable access to α -carboxy- α,β -unsaturated ketones/aldehydes. *Beilstein J. Org. Chem.* **2013**, *9*, 1925-1930.
- 52) Li, C.-W.; Pati, K.; Lin, G.-Y.; Md, S.; Sohel, A.; Hung, H.-H.; Liu, R.-S., Gold-Catalyzed Oxidative Ring Expansions and Ring Cleavages of Alkynylcyclopropanes by Intermolecular Reactions Oxidized by Diphenylsulfoxide. *Angew. Chem. Int. Ed.* **2010**, *49*, 9891 - 9894.
- 53) Wang, S.; Zhang, L., A Highly Efficient Preparative Method of α -Ylidene- β -Diketones via Au(III)-Catalyzed Acyl Migration of Propargylic Esters. *J. Am. Chem. Soc.* **2006**, *128*, 8414-8415.
- 54) Wang, L.-J.; Zhu, H.-T.; Wang, A.-Q.; Qiu, Y.-F.; Liu, X.-Y.; Liang, Y.-M., Gold-Catalyzed Tandem [3,3]-Propargyl Ester Rearrangement Leading to (E)-1H-Inden-1-ones. *J. Org. Chem.* **2014**, *79*, 204-212.
- 55) (a) Liu, J.; Chen, M.; Zhang, L.; Liu, Y., Gold(I)-Catalyzed 1,2-Acyloxy Migration/[3+2] Cycloaddition of 1,6-Diynes with an Ynamide Propargyl Ester Moiety: Highly Efficient Synthesis of Functionalized Cyclopenta[b]indoles. *Chem. Eur. J.* **2015**, *21*, 1009-1013. (b) Heffernan, S. J.; Beddoes, J. M.; Mahon, M. F.; Hennessy, A. J.; Carbery, D. R., Gold-catalysed cascade rearrangements of ynamide propargyl esters. *Chem. Commun.* **2013**, *49*, 2314-2316.
- 56) Arce, E. M.; Lamont, S. G.; Davies, P. W., Sulfenyl Ynamides in Gold Catalysis: Synthesis of Oxo-functionalised 4-aminoimidazolyl Fused Compounds by Intermolecular Annulation Reactions. *Adv. Synth. Catal.* **2020**, *362*, 2503-2509.
- 57) (a) Xie, L.-G.; Shaaban, S.; Chen, X.; Maulide, N., Metal-Free Synthesis of Highly Substituted Pyridines by Formal [2+2+2] Cycloaddition under Mild Conditions. *Angew. Chem. Int. Ed.* **2016**, *55*, 12864-12867. (b) Ye, X.; Wang, J.; Ding, S.; Hosseyni, S.; Wojtas, L.; Akhmedov, N. G.; Shi, X., Investigations on Gold-Catalyzed Thioalkyne Activation Toward Facile Synthesis of Ketene Dithioacetals. *Chem. Eur. J.* **2017**, *23*, 10506-10510. (c) Baldassari, L. L.; Mantovani, A. C.; Jardim, M.; Maryasin, B.; Lüdtkke, D. S., Meyer–Schuster-type rearrangement for the synthesis of α -selanyl- α,β -unsaturated thioesters. *Chem. Commun.* **2021**, *57*, 117-120. (d) Xie, L.-G.; Niyomchon, S.; Mota, A. J.; González, L.; Maulide, N., Metal-free intermolecular formal cycloadditions enable an orthogonal access to nitrogen heterocycles. *Nat. Commun.* **2016**, *7*, 10914.
- 58) Reddy, R. J.; Ball-Jones, M. P.; Davies, P. W., Alkynyl Thioethers in Gold-Catalyzed Annulations To Form Oxazoles. *Angew. Chem. Int. Ed.* **2017**, *56*, 13310-13313.

- 59) Ding, S.; Jia, G.; Sun, J., Iridium-Catalyzed Intermolecular Azide–Alkyne Cycloaddition of Internal Thioalkynes under Mild Conditions. *Angew. Chem. Int. Ed.* **2014**, *53*, 1877-1880.
- 60) (a) Nitsch, D.; Bach, T., Bismuth(III) Triflate-Catalyzed Synthesis of Substituted 2-Alkenylfurans. *J. Org. Chem.* **2014**, *79*, 6372-6379. (b) Kikuchi, J.; Takano, K.; Ota, Y.; Umemiya, S.; Terada, M., Chiral Brønsted Acid Catalyzed Enantioconvergent Propargylic Substitution Reaction of Racemic Secondary Propargylic Alcohols with Thiols. *Chem. Eur. J.* **2020**, *26*, 11124-11128. (c) Nitsch, D.; Huber, S. M.; Pöthig, A.; Narayanan, A.; Olah, G. A.; Prakash, G. K. S.; Bach, T., Chiral Propargylic Cations as Intermediates in SN1-Type Reactions: Substitution Pattern, Nuclear Magnetic Resonance Studies, and Origin of the Diastereoselectivity. *J. Am. Chem. Soc.* **2014**, *136*, 2851-2857. (d) Kita, Y.; Iio, K.; Kawaguchi, K.-i.; Fukuda, N.; Takeda, Y.; Ueno, H.; Okunaka, R.; Higuchi, K.; Tsujino, T.; Fujioka, H.; Akai, S., Total Synthesis of the Antitumor Antibiotic (±)-Fredericamycin A by a Linear Approach. *Chem. Eur. J.* **2000**, *6*, 3897-3905.
- 61) (a) Sharma, P.; Singh, R. R.; Giri, S. S.; Chen, L.-Y.; Cheng, M.-J.; Liu, R.-S., Gold-Catalyzed Oxidation of Thioalkynes To Form Phenylthio Ketene Derivatives via a Noncarbene Route. *Org. Lett.* **2019**, *21*, 5475-5479. (b) Cossu, S.; De Lucchi, O.; Peluso, P.; Volpicelli, R., IMPROVED SELECTIVE SYNTHESIS OF (Z)- AND (E)-1,2-BIS(PHENYLSULFONYL)-CHLOROETHYLENE. *Synth. Commun.* **2001**, *31*, 27-32.
- 62) Mansfield, S. J.; Campbell, C. D.; Jones, M. W.; Anderson, E. A., A robust and modular synthesis of ynamides. *Chem. Commun.* **2015**, *51*, 3316-3319.
- 63) Matsui, Y.; Mochida, K., Binding Forces Contributing to the Association of Cyclodextrin with Alcohol in an Aqueous Solution. *Bull. Chem. Soc. Jpn.* **1979**, *52*, 2808-2814.
- 64) Miura, K.; Saito, H.; Fujisawa, N.; Wang, D.; Nishikori, H.; Hosomi, A., Homolytic Carbostannylation of Alkenes and Alkynes with Tributylstannyl Enolates. *Org. Lett.* **2001**, *3*, 4055-4057.
- 65) Yoshimatsu, M.; Otani, T.; Matsuda, S.; Yamamoto, T.; Sawa, A., Scandium-Catalyzed Carbon–Carbon Bond-Forming Reactions of 3-Sulfanyl- and 3-Selanylpropargyl Alcohols. *Org. Lett.* **2008**, *10*, 4251-4254.
- 66) Barrett, M. J.; Khan, G. F.; Davies, P. W.; Grainger, R. S., Alkynyl sulfoxides as α -sulfinyl carbene equivalents: gold-catalysed oxidative cyclopropanation. *Chem. Commun.* **2017**, *53*, 5733-5736.
- 67) Brandsma, L.; Wijers, H. E.; Jonker, C., Chemistry of acetylenic ethers 70: Preparation of 1-alkynyl thioethers and 1-alkynyl selenoethers from sodium alkynylides, sulphur or selenium and alkyl halides. *Recueil des Travaux Chimiques des Pays-Bas* **1964**, *83*, 208-216.
- 68) Kaiser, D.; Veiros, L. F.; Maulide, N., Redox-Neutral Arylations of Vinyl Cation Intermediates. *Adv. Synth. Catal.* **2017**, *359*, 64-77.
- 69) Kanemoto, K.; Yoshida, S.; Hosoya, T., Synthesis of Alkynyl Sulfides by Copper-Catalyzed Thiolation of Terminal Alkynes Using Thiosulfonates. *Org. Lett.* **2019**, *21*, 3172-3177.
- 70) Gorin, D. J.; Dubé, P.; Toste, F. D., Synthesis of Benzenorcaradienes by Gold(I)-Catalyzed [4+3] Annulation. *J. Am. Chem. Soc.* **2006**, *128*, 14480-14481.
- 71) Engel, D. A.; Dudley, G. B., The Meyer–Schuster rearrangement for the synthesis of α,β -unsaturated carbonyl compounds. *Org. Biomol. Chem.* **2009**, *7*, 4149-4158.
- 72) Ramón, R. S.; Marion, N.; Nolan, S. P., [(NHC)AuCl]-catalyzed Meyer–Schuster rearrangement: scope and limitations. *Tetrahedron* **2009**, *65*, 1767-1773.

- 73) Yu, M.; Li, G.; Wang, S.; Zhang, L., Gold-Catalyzed Efficient Formation of α,β -Unsaturated Ketones from Propargylic Acetates. *Adv. Synth. Catal.* **2007**, *349*, 871-875.
- 74) Khatik, G. L.; Sharma, G.; Kumar, R.; Chakraborti, A. K., Scope and limitations of $\text{HClO}_4\text{-SiO}_2$ as an extremely efficient, inexpensive, and reusable catalyst for chemoselective carbon–sulfur bond formation. *Tetrahedron* **2007**, *63*, 1200-1210.
- 75) Sharma, B. M.; Rathod, J.; Gonnade, R. G.; Kumar, P., Harnessing Nucleophilicity of Allenol Ester with p-Quinone Methides via Gold Catalysis: Application to the Synthesis of Diarylmethine-Substituted Enones. *J. Org. Chem.* **2018**, *83*, 9353-9363.
- 76) Georgy, M.; Boucard, V.; Campagne, J.-M., Gold(III)-Catalyzed Nucleophilic Substitution of Propargylic Alcohols. *J. Am. Chem. Soc.* **2005**, *127*, 14180-14181.
- 77) Sanz, R.; Miguel, D.; Martínez, A.; Gohain, M.; García-García, P.; Fernández-Rodríguez, M. A.; Álvarez, E.; Rodríguez, F., Brønsted Acid Catalyzed Alkylation of Indoles with Tertiary Propargylic Alcohols: Scope and Limitations. *Eur. J. Med. Chem.* **2010**, *2010*, 7027-7039.
- 78) (a) Gohain, M.; Marais, C.; Bezuidenhout, B. C. B., An $\text{Al}(\text{OTf})_3$ -catalyzed environmentally benign process for the propargylation of indoles. *Tetrahedron Lett.* **2012**, *53*, 4704-4707. (b) Silveira, C. C.; Mendes, S. R.; Wolf, L.; Martins, G. M., Anhydrous CeCl_3 catalyzed C3-selective propargylation of indoles with tertiary alcohols. *Tetrahedron Lett.* **2010**, *51*, 4560-4562.
- 79) (a) Jones, G., The Knoevenagel Condensation. In *Organic Reactions*, pp 204-599. (b) van Beurden, K.; de Koning, S.; Molendijk, D.; van Schijndel, J., The Knoevenagel reaction: a review of the unfinished treasure map to forming carbon–carbon bonds. *Green. Chem. Lett. Rev.* **2020**, *13*, 349-364.
- 80) (a) Hayashi, Y.; Miyamoto, Y.; Shoji, M., β -Ketothioester as a reactive Knoevenagel donor. *Tetrahedron. Lett.* **2002**, *43*, 4079-4082. (b) Inokuchi, T.; Kawafuchi, H., E- or Z-Selective Knoevenagel Condensation of Acetoacetic Derivatives: Effect of Acylated Substituent, that is, TEMPO and Amines, as an Auxiliary, and New Accesses to Trisubstituted E- and Z-2-Alkenals and Furans. *J. Org. Chem.* **2006**, *71*, 947-953.
- 81) (a) Sanabria, R.; Herrera, R.; Aguilar, R.; González-Romero, C.; Jiménez-Vázquez, H. A.; Delgado, F.; Söderberg, B. C. G.; Tamariz, J., Reactivity and Selectivity of Captodative Olefins as Dienes in Hetero-Diels–Alder Reactions. *Helv. Chim. Acta* **2008**, *91*, 1807-1827. (b) Mertes, J.; Mattay, J., Captodative olefins in normal and inverse Diels–Alder Reactions. *Helv. Chim. Acta.* **1988**, *71*, 742-748. (c) Herrera, R.; Nagarajan, A.; Morales, M. A.; Méndez, F.; Jiménez-Vázquez, H. A.; Zepeda, L. G.; Tamariz, J., Regio- and Stereoselectivity of Captodative Olefins in 1,3-Dipolar Cycloadditions. A DFT/HSAB Theory Rationale for the Observed Regiochemistry of Nitrones. *J. Org. Chem.* **2001**, *66*, 1252-1263. (d) Fuentes, A.; Martínez-Palou, R.; Jiménez-Vázquez, H. A.; Delgado, F.; Reyes, A.; Tamariz, J., Diels–Alder Reactions of 2-Oxazolidinone Dienes in Polar Solvents Using Catalysis or Non-conventional Energy Sources. *Monatsh. Chem.* **2005**, *136*, 177-192. (e) Ardecky, R. J.; Dominguez, D.; Cava, M. P., 3-(Acyloxy)-3-buten-2-ones as dienophiles in anthracyclinone synthesis. An efficient route to 4-demethoxy-7-deoxydaunomycinone derivatives. *J. Org. Chem.* **1982**, *47*, 409-412.
- 82) Aguilar, R.; Benavides, A.; Tamariz, J., Friedel–Crafts Reaction of Activated Benzene Rings with Captodative and Electron-Deficient Alkenes. A One-Step Synthesis of the Natural Product Methyl 3-(2,4,5-Trimethoxyphenyl)propionate. *Synth. Commun.* **2004**, *34*, 2719-2735.

- 83) Villar, L.; Bullock, J. P.; Khan, M. M.; Nagarajan, A.; Bates, R. W.; Bott, S. G.; Zepeda, G.; Delgado, F.; Tamariz, J., Highly stereoselective palladium-catalyzed coupling reactions of captodative olefins acetylvinyln arenecarboxylates. *J. Organomet. Chem.* **1996**, *517*, 9-17.
- 84) (a) Sun, T.; Zhang, X., A Simple Synthetic Route to Enantiopure α -Hydroxy Ketone Derivatives by Asymmetric Hydrogenation. *Adv. Synth. Catal.* **2012**, *354*, 3211-3215. (b) Bartels, A.; Mahrwald, R.; Müller, K., On the Palladium(II)-Catalysed Oxidative Rearrangement of Propargylic Acetates. *Adv. Synth. Catal.* **2004**, *346*, 483-485.
- 85) (a) Hirschbeck, V.; Bödl, M.; Gehrtz, P. H.; Fleischer, I., Tandem Acyl Substitution/Michael Addition of Thioesters with Vinylmagnesium Bromide. *Org. Lett.* **2019**, *21*, 2578-2582. (b) Liebeskind, L. S.; Srogl, J., Thiol Ester-Boronic Acid Coupling. A Mechanistically Unprecedented and General Ketone Synthesis. *J. Am. Chem. Soc.* **2000**, *122*, 11260-11261. (c) Gehrtz, P. H.; Kathe, P.; Fleischer, I., Nickel-Catalyzed Coupling of Arylzinc Halides with Thioesters. *Chem. Eur. J.* **2018**, *24*, 8774-8778. (d) Fausett, B. W.; Liebeskind, L. S., Palladium-Catalyzed Coupling of Thiol Esters with Aryl and Primary and Secondary Alkyl Organoindium Reagents. *J. Org. Chem.* **2005**, *70*, 4851-4853.
- 86) Nishikawa, D.; Hirano, K.; Miura, M., Asymmetric Synthesis of α -Aminoboronic Acid Derivatives by Copper-Catalyzed Enantioselective Hydroamination. *J. Am. Chem. Soc.* **2015**, *137*, 15620 - 15623.
- 87) Picher, M.; Plietker, B., Fe-Catalyzed Selective Cyclopropanation of Enynes under Photochemical or Thermal Conditions. *Org. Lett.* **2020**, *22*, 340 - 344.
- 88) Xu, C.; Du, W.; Zeng, Y.; Dai, B.; Guo, H., Reactivity Switch Enabled by Counterion: Highly Chemoselective Dimerization and Hydration of Terminal Alkynes. *Org. Lett.* **2014**, *16*, 948 - 951.
- 89) González-Cantalapiedra, E.; de Frutos, Ó.; Atienza, C.; Mateo, C.; Echavarren, A. M., Synthesis of the Benzo[b]fluorene Core of the Kinamycins by Arylalkyne-Allene and Arylalkyne-Alkyne Cycloadditions. *Eur. J. Org. Chem.* **2006**, 1430 - 1443.
- 90) Kasten, K.; Slawin, A. M. Z.; Smith, A. D., Enantioselective Synthesis of β -Fluoro- β -aryl- α -aminopentenamides by Organocatalytic [2,3]-Sigmatropic Rearrangement. *Org. Lett.* **2017**, *19*, 5182 - 5185.
- 91) Beshai, M.; Dhudshia, B.; Mills, R.; Thadani, A. N., Terminal alkynes from aldehydes via dehydrohalogenation of (Z)-1-iodo-1-alkenes with TBAF. *Tetrahedron Lett.* **2008**, *49*, 6794-6796.
- 92) Niu, H.; Lu, L.; Shi, R.; Chiang, C.-W.; Lei, A., Catalyst-free *N*-methylation of amines using CO₂. *Chem, Commun.* **2017**, *53*, 1148-1151.
- 93) Marshall, R. J.; Griffin, S. L.; Wilson, C.; Forgan, R. S., Stereoselective Halogenation of Integral Unsaturated C-C Bonds in Chemically and Mechanically Robust Zr and Hf MOFs. *Chem. Eur. J.* **2016**, *22*, 4870 - 4877.
- 94) Fang, Z.; Song, Y.; Sarkar, T.; Hamel, E.; Fogler, W. E.; Agoston, G. E.; Fanwick, P. E.; Cushman, M., Stereoselective Synthesis of 3,3-Diarylacrylonitriles as Tubulin Polymerization Inhibitors. *J. Org. Chem.* **2008**, *73*, 4241 - 4244.
- 95) Spielmann, K.; Xiang, M.; Schwartz, L. A.; Krische, M. J., Direct Conversion of Primary Alcohols to 1,2-Amino Alcohols: Enantioselective Iridium-Catalyzed Carbonyl Reductive Coupling of Phthalimido-Allene via Hydrogen Auto-Transfer. *J. Am. Chem. Soc.* **2019**, *141*, 14136 - 14141.

- 96) Panda, S.; Jadav, A.; Panda, N.; Mohapatra, S., A Novel Carbon quantum dot-based fluorescent nanosensor for selective detection of flumioxazin in real samples. *New. J. Chem.* **2018**, *42*, 2074-2080.
- 97) Pérez-Gálan, P.; Waldmann, H.; Kumar, K., Building polycyclic indole scaffolds via gold(I)-catalyzed intra- and inter-molecular cyclization reactions of 1,6-enynes. *Tetrahedron* **2016**, *72*, 3647-3652.
- 98) Chandanshive, J. Z.; Bonini, B. F.; Gentili, D.; Fochi, M.; Bernardi, L.; Franchini, M. C., Regiocontrolled Synthesis of Ring-Fused Thieno[2,3-c]pyrazoles through 1,3-Dipolar Cycloaddition of Nitrile Imines with Sulfur-Based Acetylenes. *Eur. J. Org. Chem* **2010**, *2010*, 6440-6447.
- 99) Bulman Page, P. C.; Goodyear, R. L.; Horton, A. E.; Chan, Y.; Karim, R.; O'Connell, M. A.; Hamilton, C.; Slawin, A. M. Z.; Buckley, B. R.; Allin, S. M., Formal Total Synthesis of (+)-C9-Deoxyomuralide from L-Leucine Using a Double Sacrificial Chirality Transfer Approach. *J. Org. Chem.* **2017**, *82*, 12209-12223.
- 100) Zhang, Y.; Ji, P.; Hu, W.; Wei, Y.; Huang, H.; Wang, W., Organocatalytic Transformation of Aldehydes to Thioesters with Visible Light. *Chem. Eur. J.* **2019**, *25*, 8225-8228.
- 101) Peng, Z.; Zheng, X.; Zhang, Y.; An, D.; Dong, W., H₂O₂-mediated metal-free protocol towards unsymmetrical thiosulfonates from sulfonyl hydrazides and disulfides in PEG-400. *Green Chem.* **2018**, *20*, 1760-1764.
- 102) Schießl, J.; Stein, P. M.; Stirn, J.; Emler, K.; Rudolph, M.; Rominger, F.; Hashmi, A. S. K., Strategic Approach on N-Oxides in Gold Catalysis – A Case Study. *Adv. Synth. Catal.* **2019**, *361*, 725-738.
- 103) Yang, K.; Qiu, Y.; Li, Z.; Wang, Z.; Jiang, S., Ligands for Copper-Catalyzed C–N Bond Forming Reactions with 1 Mol% CuBr as Catalyst. *J. Org. Chem.* **2011**, *76*, 3151-3159.
- 104) D. Chambers, R.; W. Hall, C.; Hutchinson, J.; W. Millar, R., Polyhalogenated heterocyclic compounds. Part 42.1 Fluorinated nitrogen heterocycles with unusual substitution patterns. *J. Chem. Soc.* **1998**, 1705-1714.
- 105) Palav, A.; Misal, B.; Ernolla, A.; Parab, V.; Waske, P.; Khandekar, D.; Chaudhary, V.; Chaturbuj, G., The m-CPBA–NH₃(g) System: A Safe and Scalable Alternative for the Manufacture of (Substituted) Pyridine and Quinoline N-Oxides. *Org. Process Res. Dev.* **2019**, *23*, 244-251.
- 106) Henrion, G.; Chavas, T. E. J.; Le Goff, X.; Gagosz, F., Biarylphosphonite Gold(I) Complexes as Superior Catalysts for Oxidative Cyclization of Propynyl Arenes into Indan-2-ones. *Angew. Chem. Int. Ed.* **2013**, *52*, 6277-6282.
- 107) Gross, U.; Koos, P.; O'Brien, M.; Polyzos, A.; Ley, S. V., A General Continuous Flow Method for Palladium Catalysed Carbonylation Reactions Using Single and Multiple Tube-in-Tube Gas-Liquid Microreactors. *Eur. J. Org. Chem.* **2014**, *2014*, 6418-6430.
- 108) Roudesly, F.; Veiros, L. F.; Oble, J.; Poli, G., Pd-Catalyzed Direct C–H Alkenylation and Allylation of Azine N-Oxides. *Org. Lett.* **2018**, *20*, 2346-2350.
- 109) Gan, X.; Fu, Z.; Liu, L.; Yan, Y.; Chen, C.; Zhou, Y.; Dong, J., Phosphorous acid promoted isomerization of propargyl alcohols to α,β -unsaturated carbonyl compounds. *Tetrahedron Lett.* **2019**, *60*, 150906.
- 110) Petrone, D. A.; Isomura, M.; Franzoni, I.; Rössler, S. L.; Carreira, E. M., Allenylic Carbonates in Enantioselective Iridium-Catalyzed Alkylations. *J. Am. Chem. Soc.* **2018**, *140*, 4697-4704.

- 111) Eccleshare, L.; Lozada-Rodríguez, L.; Cooper, P.; Burroughs, L.; Ritchie, J.; Lewis, W.; Woodward, S., Diversification of ortho-Fused Cycloocta-2,5-dien-1-one Cores and Eight- to Six-Ring Conversion by σ Bond C–C Cleavage. *Chem. Eur. J.* **2016**, *22*, 12542-12547.
- 112) Ishizawa, K.; Majima, S.; Wei, X.-F.; Mitsunuma, H.; Shimizu, Y.; Kanai, M., Copper(I)-Catalyzed Stereodivergent Propargylation of *N*-Acetyl Mannosamine for Protecting Group Minimal Synthesis of C3-Substituted Sialic Acids. *J. Org. Chem.* **2019**, *84*, 10615-10628.
- 113) Ziffle, V. E.; Cheng, P.; Clive, D. L. J., Conversion of 1,4-Diketones into para-Disubstituted Benzenes. *J. Org. Chem.* **2010**, *75*, 8024-8038.
- 114) Silvestri, A. P.; Oakdale, J. S., Intermolecular cyclotrimerization of haloketoalkynes and internal alkynes: facile access to arenes and phthalides. *Chem. Commun.* **2020**, *56*, 13417-13420.
- 115) Lopes, E. F.; Dalberto, B. T.; Perin, G.; Alves, D.; Barcellos, T.; Lenardão, E. J., Synthesis of Terminal Ethynyl Aryl Selenides and Sulfides Based on the Retro-Favorskii Reaction of Hydroxypropargyl Precursors. *Chem. Eur. J.* **2017**, *23*, 13760-13765.
- 116) Huang, K.-H.; Isobe, M., Highly Regioselective Hydrosilylation of Unsymmetric Alkynes Using a Phenylthio Directing Group. *Eur. J. Org. Chem.* **2014**, *2014*, 4733-4740.
- 117) Heaps, N. A.; Poulter, C. D., Type-2 Isopentenyl Diphosphate Isomerase: Evidence for a Stepwise Mechanism. *J. Am. Chem. Soc.* **2011**, *133*, 19017-19019.
- 118) Dawson, M. I.; Hobbs, P. D.; Derdzinski, K.; Chan, R. L. S.; Gruber, J.; Chao, W.; Smith, S.; Thies, R. W.; Schiff, L. J., Conformationally restricted retinoids. *J. Med. Chem.* **1984**, *27*, 1516-1531.
- 119) Xia, Z.; Lv, X.; Wang, W.; Wang, X., Regioselective addition of thiophenol to α,β -unsaturated *N*-acylbenzotriazoles. *Tetrahedron Lett.* **2011**, *52*, 4906-4910.